OPTIMIZATION OF POWER SYSTEM PERFORMANCE USING FACTS DEVICES

A Thesis
Presented to
The Academic Faculty

by

Yamille E. del Valle

In Partial Fulfillment
of the Requirements for the Degree
Doctor of Philosophy in the
School of Electrical and Computer Engineering

Georgia Institute of Technology
August 2009

OPTIMIZATION OF POWER SYSTEM

PERFORMANCE USING FACTS DEVICES

Approved by:

Dr. Ronald Harley, Advisor
School of Electrical and Computer Engineering
Georgia Institute of Technology

Dr. Bonnie Heck-Ferri
School of Electrical and Computer Engineering
Georgia Institute of Technology

Dr. Miroslav Begovic
School of Electrical and Computer Engineering
Georgia Institute of Technology

Dr. Ganesh K. Venayagamoorthy
School of Electrical and Computer Engineering
Missouri University of Science and Technology

Dr. Deepak Divan
School of Electrical and Computer Engineering
Georgia Institute of Technology

Date Approved: June 22, 2009

To my wonderful family, I love you with all my heart

Para mi maravillosa familia, los amo con todo mi corazón

ACKNOWLEDGEMENTS

Several individuals deserve my thanks for their help with this research. First, I would like to express my gratitude to Dr. Ronald G. Harley for all his support during all these years of study: *"Dear Dr. Harley, I truly do not have enough words to thank you for all your dedicated work throughout my thesis, and most importantly, for always caring and looking for the best opportunities for me during my time here at Georgia Tech."*

I would like express my appreciation to my thesis committee: Dr. Miroslav Begovic, Dr. Deepak Divan, Dr. Bonnie Heck, and Dr. Kumar Venayagamoorthy for their valuable contributions, help, and suggestions for this research.

In addition, I am deeply appreciative for the funds provided by the Electrical and Computer Engineering Department at Georgia Tech, "Beca de doctorado en el extranjero por gestión propia" provided by Comisión Nacional de Investigación Científica y Tecnológica (CONICYT), Chile, and the Intelligent Power Infrastructure Consortium (IPIC) at Georgia Tech. Last but not least, my sincere gratitude to the National Electric Energy Testing, Research, and Applications Center (NEETRAC), especially to Rick Hartlein and Nigel Hampton, for giving me the opportunity to work, and keep working, with them, so I can enrich my knowledge with practical applications within the power industry.

Many thanks to my colleagues in the power group, especially the Fall 2003 generation, and to Dr. Salman Mohagheghi for his friendship and support during all the struggles that came with this research.

More personally, I wish to express my respect, gratitude, and deep admiration to "my boys," my brother, Dr. Harjeet Johal (Monkey), and Dr. Jean Carlos Hernandez (J.C.), and to my very best friend Mabel Munoz (Nany) for all the wonderful moments we have shared, and because, even though I have done nothing to deserve all your love, you have given it to me constantly and without hesitation during all the good and bad moments. This gratitude also extends to Dr. Marcos Orchard (Toto) for 13 years of constant love and support that I will always keep in my heart. I could have not done without you, and my gratitude will last a lifetime.

Finally I would like to thank and dedicate this work to my family: mama, papa, Ilennita, abuelita Blanca, Sra. Berta, and especially to my Josh and Elizabeth

To my parents, Dr. Yamille Kessra and Dr. Julio del Valle, for always loving and supporting me and for giving me all I needed to be here today: *"Mamita, eres el ejemplo al que siempre aspirare convertirme, profesional, madre y por sobre todo amiga," "Papun, gracias por ponerme las metas más altas, ha sido siempre mi dulce placer demostrarte que puedo lograrlas."*

To the most beautiful, smartest, wisest, and funniest sister ever, Ilenne (not yet a doctor but I'm sure you will be): *"Pepom, eres la mejor, gracias por siempre confiar en mi y apoyarme en todas las batallas. Siempre has sido una fuente de alegría e inspiración para mí y te debo mucho más de lo que puedes imaginar."*

To Dr. Joshua Perkel and our sweet Elizabeth: *"You are my reasons for living, the reasons to impatiently await the dawn of every day and the reasons to calmly say thanks every night. For being the source of all my happiness, thank you…always."*

TABLE OF CONTENTS

LIST OF TABLES

LIST OF FIGURES

LIST OF ABBREVIATIONS

AC: alternating current

ACD: adaptive critic design

ADACD: action dependent ACD design

ADHDP: action dependent heuristic dynamic programming

AI: artificial intelligence

AVR: automatic voltage regulator

B&B: branch and bound

BFA: bacterial foraging algorithm

CA: cellular automata

CCT: critical clearing time

CP: candidate problem

CPF: continuation power flow

DP: dynamic programming

DSSC: distributes static series compensator

EP: evolutionary programming

ES: evolution strategies

FACTS: flexible AC transmission systems

FIPS: fully informed particle swarm

GA: genetic algorithm

IEEE: institute of electrical and electronics engineers

IP: integer programming

LIB: limit-induced bifurcation

LP: linear programming

LUF: line utilization factor

MATLAB: matrix laboratory

MIP: mixed integer programming

MILP: mixed integer linear programming

MINLP: mixed integer non linear programming

MVA: mega volt-ampere

NLP: non linear programming

OPF: optimal power flow

P.I.: real power performance index

POD: power oscillation damper

PSAT: power system analysis toolbox

PSO: particle swarm optimization

PSS: power system stabilizer

QP: quadratic programming

SA: simulating annealing

SCOPF: security constrained optimal power flow

SNB: saddle-node bifurcation

SSO: sub-synchronous oscillations

SSR: sub-synchronous resonance

SSSA: small signal stability analysis

SSSC: static synchronous series compensator

STATCOM: static compensator

SVC: static var compensator

TCSC: thyristor controlled series compensator

TS: tabu search

TTC: total transfer capability

UPFC: unified power flow controller

WAC: wide area control

Note about nomenclature:

The word “method”, as in “optimization method”, refers to a way of doing things or procedure. The word “technique”, as in “evolutionary computation technique”, has the same meaning. Along this research, the words “method” and “technique” are interchangeable.

The same definition is also associated to the word “algorithm”, which can replace either “method” or “technique”. The word “algorithm” is use along this research to slightly emphasize the implementation of a particular optimization method. Nevertheless, the reader should not be concern in finding any specific meanings for these words beyond what it is stated in this note.

SUMMARY

The object of this research is to optimize the overall power system performance using FACTS devices. Particularly, it is intended to improve the reliability, and the performance of the power system considering steady state operating condition as well as the system subjected to small and large disturbances.

The methodology proposed to achieve this goal corresponds to an enhanced particle swarm optimizer (Enhanced-PSO) that is proven in this work to have several advantages, in terms of accuracy and computational effort, as compared with other existing methods.

Once the performance of the Enhanced PSO is verified, a multi-stage PSO-based optimization framework is proposed for optimizing the power system reliability (N-1 contingency criterion). The algorithm finds optimal settings for present infrastructure (generator outputs, transformers tap ratios and capacitor banks settings) as well as optimal control references for distributed static series compensators (DSSC) and optimal locations, sizes and control settings for static compensator (STATCOM) units.

Finally, a two-stage optimization algorithm is proposed to improve the power system performance in steady state conditions and when small and large perturbations are applied to the system. In this case, the algorithm provides optimal control references for DSSC modules, optimal location and sizes for capacitor banks, and optimal location, sizes and control parameters for STATCOM units (internal and external controllers), so that the loadability and the damping of the system are maximized at minimum cost.

Simulation results throughout this research show a significant improvement of the power system reliability and performance after the system is optimized.

CHAPTER 1

INTRODUCTION AND OBJECTIVE OF RESEARCH

1.1 Problem statement

At the present time, power systems are forced to operate at almost full capacity. More and more often, generation patterns result in heavy flows that tend to incur greater losses as well as threatening stability and security of the system. This ultimately creates undesirably increased risk of power outages of different levels of severity. For this reason, there is a general consensus that the power grid has to be reinforced, to make it smart and aware, fault tolerant and self-healing, and dynamically and statically controllable.

A traditional alternative to reinforce the power network consists of upgrading the electrical transmission system infrastructure through the addition of new transmission lines, substations, and associated equipment. However, the process to permit, site, and construct new transmission lines has become difficult, expensive, time consuming, and many times even controversial.

The utilization of the existing power system can be improved through the application of advanced power electronics technologies. Flexible AC Transmission Systems (FACTS) provide technical solutions to address the new operating challenges being presented today. Devices, such as a STATCOM, SVC, SSSC, and UPFC, can be connected in series or shunt (or a combination of the two) to achieve numerous control functions, including voltage regulation, power flow control, and system damping. In this

way, the system performance can be considerably improved by controlling the power flows without generation rescheduling or topological changes. Furthermore, the thermal limits are not violated, losses are minimized, and the stability margin is increased.

The potential benefits of FACTS equipment are nowadays widely recognized by the power systems engineering community, however, the current challenge is now to obtain the maximum benefit from these devices at minimum cost.

This optimization problem includes basically three aspects: finding the optimal location of the device in the network, finding its optimal size, and optimizing its controller parameters such that the maximum benefit can be obtained in both steady state and transient operation.

Considering these three aspects, the problem becomes a multi-objective optimization problem which involves a very complex formulation and it is certainly difficult to solve in an efficient manner.

On the one hand, the power system itself is a highly nonlinear and non-stationary system, subject to noise and uncertainties.

On the other hand, the operation of the FACTS devices is quite difficult to optimize because of the complexity in the control schemes, particularly if adaptability or intelligent techniques are considered. From the optimization perspective, the inclusion of multiple objectives, discontinuous and discrete domain variables, the existence of a non-convex feasible region, and multiple local minima, all make it difficult to find a suitable algorithm with the ability to pursue the global optimum with reasonable computational effort.

1.2 Proposed method

Many areas in power systems, including the FACTS devices placement, sizing and control, require solving one or more nonlinear, multi-objective optimization problems. While analytical methods might suffer from slow convergence and the curse of dimensionality, heuristics based evolutionary computation techniques can be an efficient alternative to solve these complex optimization problems.

Particle swarm optimization (PSO) is an evolutionary computation technique developed by Russell Eberhart and James Kennedy in 1995, which is inspired by the social behavior of bird flocking and fish schooling. PSO has its roots in artificial life and social psychology as well as in engineering and computer science. It utilizes a "population" of particles that fly through the problem hyperspace with given velocities. At each iteration, the velocities of the individual particles are stochastically adjusted according to the historical best position for the particle itself and the neighborhood best position. Both the particle best and the neighborhood best are derived according to a user defined fitness function. The movement of each particle naturally evolves to an optimal or near-optimal solution.

PSO is known to effectively solve large scale nonlinear optimization problems. It is not largely affected by the size and nonlinearity of the problem, and can converge to the optimal solution in many problems where most analytical methods fail to converge. It can therefore be effectively applied to optimal location, sizing and control of FACTS devices in the power systems. Moreover, PSO has some advantages over other similar

optimization techniques since: (i) it is easier to implement and there are few parameters to adjust, (ii) it has an effective memory capability, therefore it is able to perform an efficient search of the problem hyperspace, and (iii) PSO maintains the diversity of the particles (more similar to the ideal social interaction in a community), thus it is capable to avoid getting trapped in local minima. In particular, this research proposed an enhanced particle swarm optimizer that improves even further the previously stated PSO advantages.

1.3 Research contributions

The contributions of the proposed research are: (i) the development of a comprehensive and complete formulation of the problem of optimizing the power system performance using FACTS devices and (ii) the development of a mathematical algorithm, called Enhanced-PSO, capable of pursuing global minimization, with desired accuracy and reasonable computational time.

The achievement of the previous global objectives requires the consideration of the following specific tasks:

- Theoretical study and comparison of various optimizations methods including classical approaches and evolutionary computation techniques. The problem of improving the voltage profile using shunt compensation is used as an illustrative example of a power system problem. The efficiency of each optimization technique is evaluated based on its capability of achieving global optimality and corresponding computational effort. Statistical analysis is additionally used to assess the

performance of stochastic based search algorithms, in particular their capability of converging into feasible regions and the accuracy in finding the global optimum of the problem.

- Development of a comprehensive problem formulation and optimization framework for improvement of power system reliability using distributed series compensation and shunt compensation. The improvement of the power system reliability is approached from the perspective of satisfying the N-1 contingency criterion using existing network resources and new FACTS installments. The optimization framework is a multistage process, which considers security constrained optimal power flow, optimal global control settings of distributed static series compensators (DSSC) and optimal global control settings of static compensator (STATCOM).
- Development of a comprehensive problem formulation and optimization framework for optimization of power system performance under steady state and transient conditions using series and shunt FACTS devices. The technical parameters to optimize, in steady state conditions, are the voltage profile, system loadability, transmission losses, and line utilization factor of the system. In the case of transient behavior, system damping and eigenvalue analysis are considered. In addition, economic criteria.

1.4 Organization of the chapters

A brief description of the problem to be solved, proposed approach, and main contributions of this research are described in this chapter. The rest of the thesis is

divided in four parts: (i) theoretical background, (ii) validation of the Enhanced-PSO method, (iii) optimization of power system reliability using PSO, and (iv) optimization of power system performance using PSO. A diagram of the thesis is presented in Figure 1.1.

Part I, theoretical background, consists in two chapters. Chapter 2 provides a literature survey on essential topics of this research. It starts with a general overview of optimization techniques for solving complex optimization problems, followed by specific methods to solve the problem of optimal allocation of FACTS devices in the power network. Chapter 3 focuses on the proposed PSO method. The theory and mathematical formulation of this method is explained together with the discrete PSO variant which is used when some or all the decision variables are integer numbers. Additionally, the concept of the proposed enhanced particle swarm optimizer is described in this chapter.

Part II, validation of the proposed Enhanced-PSO method, studies the performance of the proposed enhanced particle swarm optimizer and compares it with other optimization techniques to corroborate its advantages.

In particular, chapter 4 introduces the optimization problem to be solved, which consists in the optimal allocation of multiple STATCOM units in a 45 bus system, part of the Brazilian power network. An exhaustive search is carried out in this problem to have a certainty of the global optimal solution.

Chapter 5 describes the implementation of different optimization methods, including the canonical and Enhanced-PSO, genetic algorithm (GA), bacterial foraging algorithm (BFA), Bender's decomposition and Branch-and-Bound (B&B).

Chapter 6 discusses and compares the results of the different optimization techniques and validates the superior performance of the proposed enhanced particle

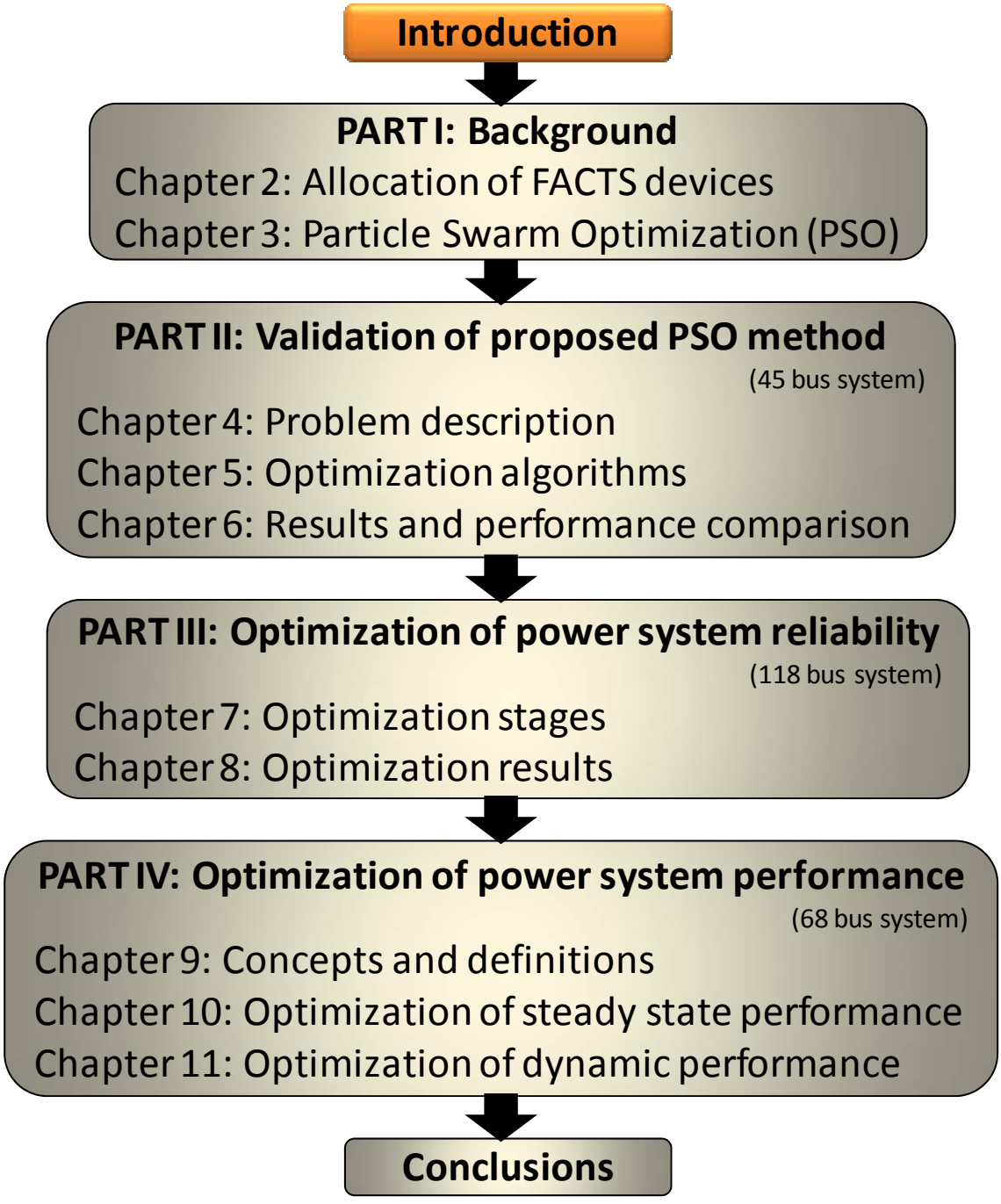

Figure 1.1: Organization of contents

swarm optimizer. Specifically, the technical discussion focuses in aspects such as convergence into feasible regions, global optimality and computational effort. In addition, the issue of the scalability of the proposed technique to solve problem in large power system is studied.

Part III, optimization of power system reliability using PSO, includes two chapters. Chapter 7, presents basic concepts of reliability of the power system, introduces the problem to be solved and describes in detail a proposed multistage PSO-based optimization framework. In particular, the description of each stage includes a brief background, objective function formulation, and definition of feasible region.

Chapter 8 discusses the results obtained by the proposed optimization process in the IEEE 118 bus system. Specifically, the focus of discussion is the dramatic improvement of the reliability achieved by the optimization of existing infrastructure and installation of distributed static series compensators (DSSC) and static compensator (STATCOM) units.

Finally, part IV, optimization of power system reliability using PSO, applies the proposed Enhanced-PSO method to two optimization stages: (i) the improvement of power system steady state performance and (ii) the improvement of the power system performance under small and large disturbances.

Chapter 9 provides a background of techniques and tools to evaluate power system performance under steady state and dynamic conditions. It also presents the problem to be solved, in this case the improvement of the performance of a 16 machine, 68 bus system using both series and shunt FACTS devices.

Chapter 10 focuses in the optimization of steady state performance using DSSC modules and capacitor banks while chapter 11, concentrates in the improvement of the behavior of the power system under small and large disturbances using STATCOM devices. In both chapters, the description of each stage includes objective function formulation and definition of feasible region. Simulation results are also discussed from the perspective of the power system performance and the usefulness of the solution to the utilities and system operators. The proposed PSO-based optimization frameworks can be used as an effective planning tool that provides optimal location, ratings and control parameters of series and shunt FACTS devices, considering technical as well as economical constraints.

As a final point, a chapter that summarizes the concluding remarks of the research as well as the suggested future work is presented to close this research work. The remaining portion of this document corresponds to reference list and FACTS models and system data, the latter presented as a series of appendices.

PART I: THEORETICAL BACKGROUND

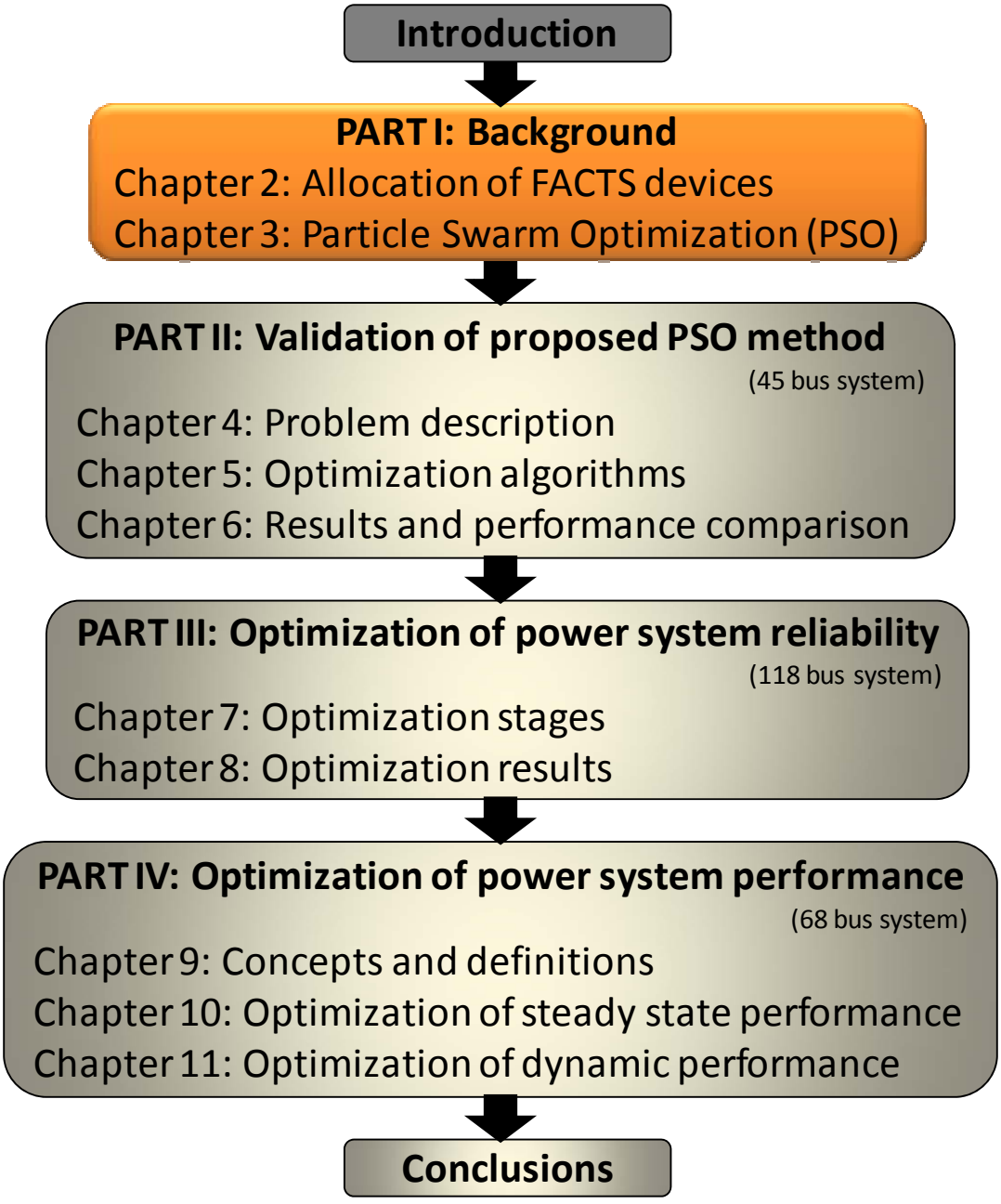

CHAPTER 2

BACKGROUND ON OPTIMAL ALLOCATION OF FACTS DEVICES

2.1 Introduction

The purpose of this chapter is to present some general background on optimization theory and the current optimization methods to solve the problem of optimal allocation of FACTS devices in the power system.

The overview on optimization theory includes two parts: (i) classical optimization methods and (ii) evolutionary computation techniques (ECTs). The first part provides definition of different techniques such as linear programming (LP), non linear programming (NLP), quadratic programming (QP), integer and mixed integer programming (IP and MIP respectively), and dynamic programming (DP). The second part introduces general descriptions of ECTs, such as genetic algorithm (GA), evolutionary programming (EP), tabu search (TS), simulating annealing (SA), and particle swarm optimization (PSO) are described. The type of problems that can be solved with these methods, together with the advantages and advantages and disadvantages of each method are discussed in this section.

The optimization techniques applied to the problem of optimal allocation of FACTS devices can be separated in three main groups: (i) classical optimization algorithms, (ii) allocation of devices based on technical criteria, and (iii) ECTs. All three groups are discussed in detail, different problem formulations, simulation results and

concluding remarks provide a comprehensive view of the current research effort in this area.

2.2 Methods for solving complex optimization problems

The electric power grid is the largest man-made machine in the world. It consists of synchronous generators, transformers, transmission lines, switches and relays, active/reactive compensators and controllers. Various control objectives, operation actions and/or design decisions in such a system require solving an optimization problem. For such a nonlinear non-stationary system with possible noise and uncertainties, as well as various design/operational constraints, the solution to the optimization problem is by no means trivial. Moreover, the following issues need attention: (i) an appropriate optimization technique has to be selected that suits the nature of the problem best, (ii) all the system constraints should be correctly addressed, and (iii) a comprehensive yet not too complicated objective function should be defined [1].

Various methods exist in the literature that address optimization problems subject to varying conditions. In its simplest form, any problem can be expressed as:

$$Min \quad f(\underline{x}) : A \rightarrow R$$

Subject to:

$$g_i(\underline{x}) = 0 \qquad i = 1,\ldots,k$$

$$h_j(\underline{x}) \leq 0 \qquad j = 1,\ldots,m$$

Different optimization methods are classified based on the type of the search space $A \subseteq R^n$ and the objective (cost) function f. The simplest technique is linear programming (LP) that concerns the case where the objective function f is linear and the set A is specified using only linear equality and inequality constraints [2]. In general the objective function or the constraints or both contain nonlinearities, raising the concept of nonlinear programming (NLP) [3].

Because NLP is a difficult field, researchers have identified special cases for study. A particularly well studied case is the one where the objective function f is nonlinear but all the constraints g and h are linear. This problem is referred to as linearly constrained optimization, if in addition to linear constraints, the objective function is quadratic then the optimization problem is called quadratic programming (QP).

In general, for a simple case where the possible decisions (potential solutions) can be parameterized by finite-dimensional vectors and the quality of these decisions can be characterized by a finite set of computable criteria, the solution of the Karush-Kuhn-Tucker system of equations and inequalities provides all optimal solutions to a nonlinear problem. However, to solve this system in an analytical fashion is not always possible, so that numerical routines (algorithms that numerically approximate the solutions of the problem) are needed [4].

The numerical routines in NLP can be classified according to the type of local information that they need. From this point of view, the methods are divided into: (i) zero-order routines using only values of the objective function and the constraints and not using their derivatives; (ii) first-order routines using the values and the gradients of the objective function and constraints; (iii) second-order routines using the values, the

gradients and the Hessians (i.e. matrices of the second order derivatives) of the objective function and the constraints. In principle it could be possible to use higher order derivatives, however these are not used in practice because of the difficulties in programming, computational time, and memory required [4].

In addition to nonlinear conditions, often some or all variables are constrained to take on integer values, and the technique is then referred to as mixed integer programming (MIP) or strictly integer programming (IP). MIP and IP problems are difficult to solve, in fact, no efficient general algorithm is known for their solution. There are three main categories of algorithms that can be applied to this type of problem [5]: (i) exact algorithms that are guaranteed to find an optimal solution but may take an exponential number of iterations, (ii) approximation algorithms that provide in polynomial time a suboptimal solution, and (iii) heuristic algorithms that provide a suboptimal solution relatively fast, but without a guarantee on its quality.

While deterministic optimization problems are formulated with known parameters, real world problems almost invariably include some unknown parameters. This necessitates the introduction of stochastic programming models that incorporate the probability distribution functions of various variables into the problem formulation. In its most general case, the method is referred to as dynamic programming (DP).Although the DP has been mathematically proven to find an optimal solution; it has its own disadvantages. Solving the dynamic programming algorithm in most of the cases is not feasible. Even a numerical solution requires overwhelming computational effort, which increases exponentially as the size of the problem increases (curse of dimensionality).

These restrictive conditions lead the solution to a suboptimal control scheme with limited look-ahead policies [6]. The complexity level is even further exacerbated when moving from finite horizon to infinite horizon problems, while also considering the stochastic effects, model imperfections and the presence of the external disturbances.

Computational intelligence based techniques, such as GA, evolutionary programming (EP), tabu search (TS), simulating annealing (SA), and PSO can be solutions to the above problems.

Computational intelligence combines elements of learning, adaptation, and biological evolution to create methods that are, in some sense, intelligent [7]. GA, EP, TS, SA and PSO, are a subset of computational intelligence, and generic population-based metaheuristic algorithms for global optimization applications [8].

Candidate solutions to the optimization problem play the role of individuals in a population, and the cost function determines the environment where the solutions exist. Evolution of the population then takes place after the repeated application of operators such as inheritance, mutation, natural selection and crossover for evolutionary biologically inspired algorithms, or social communication and cultural learning for those methods based on swarm intelligence [9].

Evolutionary computation algorithms consistently perform well to approximate solutions to all types of problems because they do not make any assumption about the underlying fitness landscape. They are not largely affected by the size and nonlinearity of the problem, and they can perform well in highly constrained and integer (or mixed integer) optimization problems.

2.3 Current methods for solving the FACTS allocation problem

Since 1995, researchers have investigated the effects of FACTS devices in the power system. Steady state performance as well as dynamic and transient stability have been focus areas of study, but mainly for the purpose of finding appropriate controllers for these equipments.

The problem of optimal allocation of FACTS devices, considering technical criteria and cost functions, is still in a relatively early stage of investigation. Frequently, only technical criteria have been considered and the solutions found are not proven to be the global optimum.

This section presents current methods for allocating FACTS devices in the power system. These methods can be separated in three distinctive groups: (i) classical optimization methods (section 2.3.1), (ii) methods based on technical criteria (section 2.3.2), and (iii) evolutionary computation techniques (section 2.3.3).

In the literature, classical optimization methods have been applied to the optimal allocation of FACTS devices, mixed integer linear programming (MILP) [10]-[12], mixed integer non linear programming (MINLP) [13]-[16], and sensitivity analysis [17]-[24]. In the last case, the analysis often differs from classical optimization theory leading to a combination of technical parameters upholding mild optimization conditions.

Considering purely technical criteria, modal analysis [25], [26], constitutes the basic approach for this type of problem when dynamic and transient conditions are taken into account.

Finally, evolutionary computation techniques have been extensively applied including: (i) GA [14], [15], [27]-[39], (ii) PSO [38], [40], [41], (iii) SA [39], [42], (iv) TS [42], [43], and (v) EP [45], [46].

Other methods present in the literature include evolution strategies (ES) [47], artificial intelligence (AI) [48], frequency response [49], sequence component [50], sequential number [51], stability index [52], and voltage phasor [53].

2.3.1 Classical optimization methods

Classical optimization theory has been applied in the literature to the FACTS allocation problem in the form of MILP and MINLP.

In the MILP formulation, the approach is based on DC power flow that allows the power system to be represented in a linear manner [10]-[12]. The performance of the system is analyzed in steady state conditions considering maximum loadability of the system [10]-[12] and total transfer capability (TTC) [10]. The algorithms considered in solving the MILP problem are B&B, Gomory cuts [10], [11], and Bender's decomposition [12].

The concluding remarks of the MILP approach indicate that the optimization process is performed in an efficient manner. However DC power flow is not suitable for performing transient analysis, therefore AC models should be considered and then the problem becomes non linear.

For the formulation based on MINLP, the optimal allocation of FACTS devices is determined using, as main criteria, the power price in deregulated markets [13], optimal economic dispatch and transmission losses [16], and security enhancement [14], [15].

Particularly in the case of security enhancement, the complexity of the problem is exacerbated since several states are defined to describe the operation of the power system (normal, collapse, corrective, and preventive). These states occur as a consequence of stochastic events (failures, topological changes), therefore there are certain probabilities associated with each one of them. Additionally, the feasibility of the problem must be guaranteed by considering load shedding as a last resort solution to avoid voltage collapse.

In all the studies reported in literature, the algorithm used to solve the optimization problem is the Bender's decomposition that consists of separating the main problem into multiple subproblems that are simpler to solve. However, in the case where security enhancement is considered, the complexity of the problem requires the optimization process to be aided by GA [14], [15].

The main conclusions about the MINLP formulation indicate that the size and the nonconvexity of the problem, which depend on the system parameters, are critical issues that may cause a convergence problem in the algorithm. Authors have proposed the investigation of modern heuristics methods to address the nonconvex cases [14].

2.3.2 Methods based on technical criteria

Another group of methods that the literature have presented to solve the allocation of FACTS devices correspond to those based on pure technical criteria, in particular, sensitivity analysis for steady state performance and modal analysis for transient and dynamic conditions of the power system.

2.3.2.1 Sensitivity analysis

Sensitivity analysis is a widely used terminology to describe the analysis based on the evaluation of the rate of change of one group of variables in a system with respect to another group. There are many different ways to perform the analysis depending on the selected variables and methodologies used to calculate the sensitivities.

On the one hand, from the perspective of the classical optimization theory, the sensitivities can be calculated using the Lagrange multipliers [24], which provide the rate of change of the quantity being optimized as a function of the specific constraint variable.

On the other hand, technically speaking, different rates of change may be of interest depending on the application, therefore many performance indexes can be defined such as the real power performance index [17], [18], [21], [22]. For example, this index considers the derivatives of the power flow equations with respect to the steady state representation of the FACTS devices. Another such index is the single contingency sensitivity index [19]; this index considers the percentage of overload in the system's branches for different contingencies and assigns a probability of occurrence to each of them.

For transient stability, a sensitivity analysis based on critical clearing time (CCT) is proposed for optimal allocation of a TCSC in a 10 bus system [20]. The FACTS devices are located in those lines where the CCT has its maximum improvement.

All the indices defined above, with the exception of the Lagrange multipliers, constitute a methodology for evaluating the impact of FACTS devices in the system. However, to find the best location for each device an exhaustive evaluation of all possible locations is required. Therefore, the basis of these methodologies is deficient in the formulation and implementation of an appropriate search process to avoid the exhaustive search and corresponding computational burden. In addition, these methodologies evaluate the sensitivity indices independently for each FACTS device. In this way it is not possible to evaluate the combined effect of several of these devices installed in the system.

2.3.2.2 Modal analysis

Modal analysis is the technical method most commonly used to allocate FACTS devices when the dynamic and transient conditions for the power system are considered.

Since modal analysis includes the calculation of the eigenvalues and eigenvectors, the method is not suitable for large power systems. The Extended Phillips-Heffron method, proposed in [25], is able to handle larger power systems by reducing the order of the matrix to a number no larger the number of the machines in the system. However this method is validated using a very small power system of 5 buses and 3 machines.

Another method proposed in literature defines a controllability index as a measurement of the damping of inter-area modes of oscillation [26]. This controllability

index is based on the relative participation of the parameters of each FACTS device to the critical mode. Additionally, in this study a steady state criterion, based on sensitivity indices, is applied to also find the optimal locations of the FACTS devices. The result of this last search process is different than the case where the controllability indices are used.

In general, from the perspective of finding the optimal location of FACTS devices, the modal analysis method offers technical feasibility but no guarantee about the optimality of the solution. Moreover, there is a discrepancy when both steady state and transient analysis are considered that makes the method not suitable for multi-objective optimization.

2.3.3 Evolutionary computation techniques

A third group of methods to address the problem of optimally allocate FACTS devices corresponds to ECTs. In this case, the main objective is to find the optimal types, number, sizes, and locations for the FACTS devices in the system. To achieve this goal, several criteria are considered such as maximum loadability, minimum cost (installation and maintenance), transmission loss minimization, improvement of security margin, and maximization of TTC. Some studies also include N-1 contingency analysis [31] and the power generation and dispatch problem in deregulated markets [32].

The investigation mostly limited to steady state conditions; just two cases consider dynamic analysis of the power system. In one of these cases ([33]), the transient analysis is not used to allocate the FACTS device but to determine optimal control

settings for power system stabilizers (PSS). The other study ([34]) uses small signal analysis in order to determine the optimal location and types of FACTS devices. The objective function is formulated based on three measurements: overshoot coefficient, damping ratio, and a penalty term for those unstable eigenvalues aligned in the right hand side plane.

The results obtained for steady state analysis [14], [15], [27]-[32], [35]-[46], are satisfactory in finding global optimum in reasonable computational time; however there is no clear indication that one algorithm outperforms all others.

Several evolutionary computation techniques and hybrid versions can be used to address power system problems but the results are highly dependent on the nature of the problem and the implementation of the algorithm. In terms of transient analysis, results reported considering eigenvalue analysis are promising for small power systems (IEEE 14 bus system) [34].

In general the evolutionary computation techniques perform well in solving mixed integer non linear problems. However the scalability of these methods as well as their applications to dynamic and transient analysis requires further investigation.

2.4 Summary

This chapter presents a general overview on optimization techniques and more specific details on those methods that have been applied to solve the specific problem of optimal allocation of FACTS devices in a power system.

The work published by others indicates that there are some disadvantages in using classical optimization theory, particularly considering the size of the system and non-convexity problems. In addition, there are a number of techniques for allocating FACTS devices that are based on technical criteria. In these cases, technical feasibility is considered, and despite that there is an improvement in the power system performance, it is not possible to evaluate the degree of optimality of the solution provided by these methods.

Finally, stochastic search based algorithms, like ECTs, have gained the interest of many researchers because of the simplicity in their implementation and their capability of handling highly non-linear systems and finding optimal solutions in a reasonable amount of computational time.

CHAPTER 3

BACKGROUND ON PARTICLE SWARM OPTIMIZATION (PSO)

3.1 Introduction

This chapter presents the basic theory of the PSO method and introduces the concept of a new enhanced particle swarm optimizer that is proposed in this research to improve the performance of the canonical PSO formulation.

The theoretical background includes a detailed description of the PSO in the real number space with its corresponding mathematical equations, different configurations of the swarm (including the *gbest* and *lbest* topologies), and an explanation of the PSO parameters.

Additionally, the integer PSO variant that is used when some (or all) the decision variables are integer numbers is fully described together with the theory of the proposed enhanced particle swarm optimizer.

3.2 PSO Background

The canonical PSO formulation is based on two fundamental disciplines: social science and computer science. In addition, PSO uses the swarm intelligence concept, which is the property of a system whereby, the collective behaviors of unsophisticated agents that are interacting locally with their environment create coherent global functional patterns. Therefore, the cornerstones of PSO can be described as:

- Social concepts [54]: It is known that “human intelligence results from social interaction”. Evaluation, comparison and imitation of others, as well as learning from experience allow humans to adapt to the environment and determine optimal patterns of behavior. In addition, a second fundamental social concept indicates that “culture and cognition are inseparable consequences of human sociality”. Culture is generated when individuals become more similar because of the mutual social learning. The sweep of culture allows individuals to move towards more adaptive patterns of behavior.
- Swarm intelligence principles [54] -[58]: swarm intelligence can be described by considering five fundamental principles: (i) proximity principle: the population should be able to carry out simple space and time computations, (ii) quality principle: the population should be able to respond to quality factors in the environment, (iii) diverse response principle: the population should not commit its activity along excessively narrow channels, (iv) stability principle: the population should not change its mode of behavior every time the environment changes, and (v) adaptability principle: the population should be able to change its behavior mode when it is worth the computational price.
- Computational characteristics [54]: swarm intelligence provides a useful paradigm for implementing adaptive systems. It is an extension of evolutionary computation and includes the softening parameterization of logical operators like AND, OR and NOT. In particular, PSO is an extension, and a potentially important incarnation of cellular automata (CA). The particle swarm can be conceptualized as cells in CA, whose states change in many dimensions simultaneously. Both PSO and CA share the

following computational attributes: (i) individual particles (cells) are updated in parallel, (ii) each new value depends only on the previous value of the particle (cell) and its neighbors, and (iii) updates are performed according to the same rules.

3.2.1 PSO in real number space

In the real number space, each individual possible solution can be modeled as a particle that moves through the problem hyperspace. The position of each particle is determined by the vector $x_i \in R^n$ and its movement by the velocity of the particle $v_i \in R^n$ [59], as shown in (3.1).

$$\vec{x}_i(t) = \vec{x}_i(t-1) + \vec{v}_i(t) \tag{3.1}$$

The information available for each individual is based on its own experience (the decisions that it has made so far and the success of each decision) and the knowledge of the performance of other individuals in its neighborhood. Since the relative importance of these two factors can vary from one decision to another, it is reasonable to apply random weights to each factor, and therefore the velocity will be determined by:

$$\vec{v}_i(t) = \vec{v}_i(t-1) + \varphi_1 \cdot rand_1 \cdot (\vec{p}_i - \vec{x}_i(t-1)) + \varphi_2 \cdot rand_2 \cdot (\vec{p}_g - \vec{x}_i(t-1)) \tag{3.2}$$

where:

φ_1, φ_2 are two positive numbers, called acceleration constants,

$rand_1$, $rand_2$ are two random numbers with uniform distribution in the range of [0.0, 1.0].

p_i is the best position that the corresponding particle has found so far,

p_g is the best position of the entire swarm.

The velocity update equation in (3.2) has three major components [60]:

- The first component is sometimes referred to as "inertia", "momentum" or "habit". It models the tendency of the particle to continue in the same direction it has been traveling. This component can be scaled by a constant as in the modified versions of PSO.
- The second component is a linear attraction towards the best position ever found by the given particle: p_i (whose corresponding fitness value is called the particle's best: *pbest*), scaled by a random weight $\varphi_1 \cdot rand_1$. This component is referred to as "memory", "self-knowledge", "nostalgia" or "remembrance".
- The third component of the velocity update equation is a linear attraction towards the best position found by any particle: p_g (whose corresponding fitness value is called global best: *gbest*), scaled by another random weight $\varphi_2 \cdot rand_2$. This component is referred to as "cooperation", "social knowledge", "group knowledge" or "shared information".

According to the formulation above, the following procedure can be used for implementing the PSO algorithm [61].

1) Initialize the swarm by assigning a random position in the problem hyperspace to each particle,
2) Evaluate the fitness function for each particle,
3) For each individual particle, compare the particle's fitness value with its *pbest*. If the current value is better than the *pbest* value, then set this value as the *pbest* and the current particle's position, x_i, as p_i,
4) Identify the particle that has the best fitness value. The value of its fitness function is identified as *gbest* and its position as p_g,
5) Update the velocities and positions of all the particles using (3.1) and (3.2),
6) Repeat steps 2-5 until a stopping criterion is met (e.g. maximum number of iterations or a sufficiently good fitness value).

3.2.1.1 Topology of the swarm

Particles have been studied in two general types of neighborhoods: (i) global best (*gbest*) and (ii) local best (*lbest*) [54]. In the *gbest* neighborhood the particles are attracted to the best solution found by any member of the swarm. This represents a fully connected network where each particle has access to the information of all other members in the community (Figure 3.1(a)). However, in the case of using the local best approach, each particle has access to the information corresponding to its immediate neighbors, according to a certain swarm topology. The two most common topologies are the ring topology, where each particle is connected with two neighbors (Figure 3.1(b)), and the wheel topology (typical for highly centralized business organizations), where the

individuals are isolated from one another and all the information is communicated to a focal individual (Figure 3.1(c)).

Kennedy [62] suggested that the *gbest* version (Figure 3.1(a)) converges fast but may be trapped in a local minimum, while the *lbest* networks have more chances to find an optimal solution, although with slower convergence.

Kennedy and Mendes [63] have evaluated all the topologies in Figure 1 as well as the case of random neighbors. In their investigations with a total number of 20 particles, they found that the best performance occurred in a randomly generated neighborhood with an average size of 5 particles.

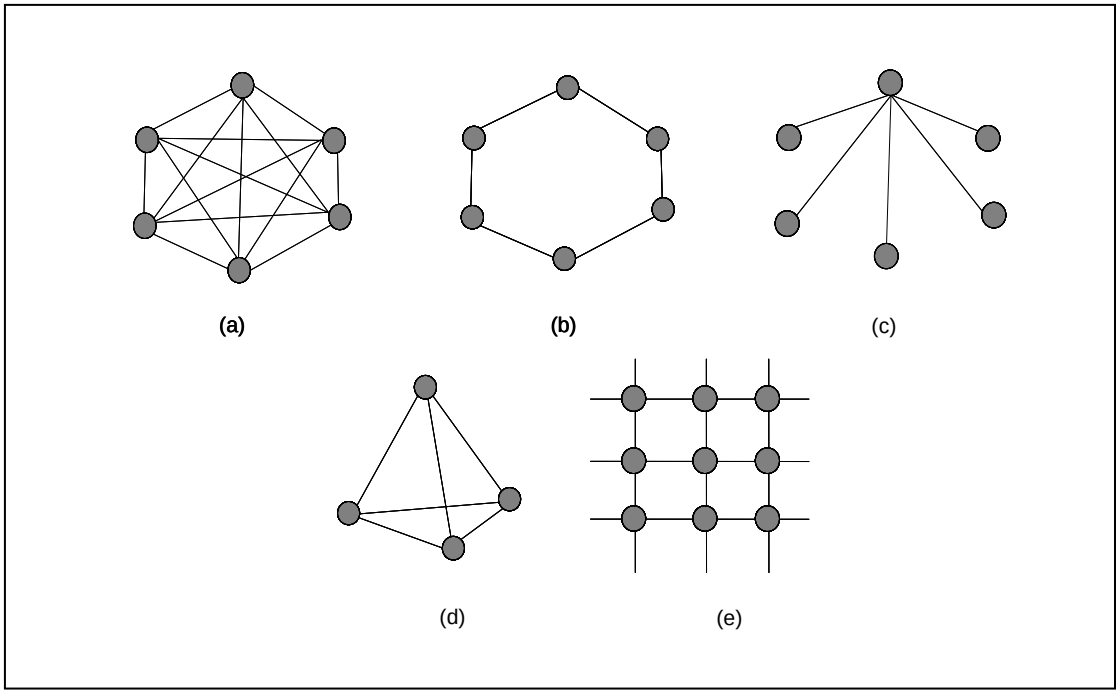

Figure 3.1: Swarm topologies: (a) global best, (b) ring topology, (c) wheel topology, (d) pyramid topology, (e) Von Neumann topology

They [63] have also suggested that the Von Neumann configuration may perform better than other topologies including the *gbest* version. Nevertheless, selecting the most efficient neighborhood structure in general depends on the type of problem. One structure may perform more effectively for certain types of problems, yet have a lower performance for other problems.

Additionally, the authors proposed a fully informed particle swarm (FIPS), where each individual is influenced by the successes of all its neighbors, rather than just the best one and itself [64]. Therefore, instead of adding two terms to the velocity (attraction to the individual and global (or local best) and dividing the acceleration constant between them, the FIPS distributes the weight of the acceleration constant φ equally across the entire neighborhood [64].

3.2.1.2 PSO Parameters

When implementing the particle swarm algorithm, several issues must be taken into account to facilitate the convergence and prevent an "explosion" of the swarm. These considerations include limiting the maximum velocity, selecting acceleration constants, and the constriction factor or the inertia constant.

Selection of maximum velocity

At each iteration step, the algorithm proceeds by adjusting the distance (velocity) that each particle moves in every dimension of the problem hyperspace. The velocity of the particle is a stochastic variable and is therefore subject to creating an uncontrolled

trajectory, causing the particle to follow wider cycles in the problem space [65], [66]. To damp these oscillations, upper and lower limits can be defined for the velocity v_i [54].

Most of the time, the value of the maximum velocity, v_{max}, is selected empirically according to the characteristics of the problem. Generally, if the value of this parameter is too high then the particles may move erratically. On the other hand, if v_{max} is too small then the particle's movement is limited and the optimal solution may not be reached.

Selection of acceleration constants

Acceleration constants φ_1 and φ_2 in (3.2) control the movement of each particle towards its individual and global best position respectively. Small values limit the movement of the particles, while large numbers may cause the particles to diverge. Ozcan and Mohan [54], [67] conducted several experiments for the special case of a single particle in a one dimensional problem space to examine the effect of a deterministic acceleration constant. In this particular case, the two acceleration constants were considered as a single acceleration constant $\varphi = \varphi_1 + \varphi_2$, since the individual and global best positions are the same. The authors concluded that by an increase in the value of the acceleration constant, the frequency of the oscillations around the optimal point increases.

For smaller values of φ , the pattern of the trajectory is similar to a sinusoidal waveform; however, if the value is increased the complex paths of interwoven cyclic trajectories appear. The trajectory goes to infinity for values of φ greater than 4.0.

The effect of considering a random value for the acceleration constant helps to create an uneven cycling for the trajectory of the particle when it is searching around the

optimal value. Since the acceleration parameter controls the strength of "*(p – x)*" terms in (3.2), a small value will lead to a weak effect; and the particles will follow a wide path and will be pulled back only after a large number of iterations. If the acceleration constant is too high then the steps will be limited by v_{max}.

In general, the maximum value for this constant should be $\varphi = 4.0$, or accordingly, $\varphi_1 + \varphi_2 = 4$. A good starting point has been proposed [54], [67] to be $\varphi_1 = \varphi_2 = 2$. It is important to note that φ_1 and φ_2, should not necessarily be equal since the "weights" for individual and group experience can vary according to the characteristics of the problem.

Selection of constriction factor or inertia constant

Empirical studies performed on PSO indicate that even when the maximum velocity and acceleration constants are correctly defined, the particles may still diverge. Two methods are proposed in the literature to control this "explosion": constriction factor [68]-[70] and inertia constant [71], [72].

Constriction factor

The first method to control the "explosion" of the swarm was developed by Clerc and Kennedy [68]. It introduces a constriction coefficient that in the simplest case is called "Type 1" (χ) [54]. In general when several particles are considered in a multi-dimensional problem space, Clerc's method leads to the following update rule [65]:

$$\vec{v}_i(t) = \chi \cdot \left\{ \vec{v}_i(t-1) + \varphi_1 \cdot rand_1 \cdot (\vec{p}_i - \vec{x}_i(t-1)) + \varphi_2 \cdot rand_2 \cdot (\vec{p}_g - \vec{x}_i(t-1)) \right\} \qquad (3.3)$$

where:

$$\chi = \frac{2}{\left|2 - \varphi - \sqrt{\varphi^2 - 4\varphi}\right|}, \quad \varphi_1 + \varphi_2 = \varphi > 4.0 \tag{3.4}$$

Typically, when this method is used, φ is set to 4.1 and the constant χ is thus 0.729. This results in the previous velocity being multiplied by 0.729 and each of the two *"(p – x)"* terms being multiplied by 1.49.

In general, the constriction factor improves the convergence of the particle over time by damping the oscillations once the particle is focused on the best point in an optimal region. The main disadvantage of this method is that the particles may follow wider cycles and may not converge when the individual best performance p_i is far from the neighborhood's best performance p_g (two different regions).

Inertia constant

The second method (proposed by Shi and Eberhart [71], [72]) suggests a new parameter that will only multiply the velocity at the previous time step, i.e., $v_i(t\text{-}1)$, instead of having one parameter multiplying the whole right hand side as in (3.3). This parameter can be interpreted as an inertia constant (φ_{ic}), that results in the modified equation for the velocity of the particle [54] presented in (3.5).

$$\vec{v}_i(t) = \phi_{ic} \cdot \vec{v}_i(t-1) + \phi_1 \cdot rand_1 \cdot (\vec{p}_i - \vec{x}_i(t-1)) + \phi_2 \cdot rand_2 \cdot (\vec{p}_g - \vec{x}_i(t-1)) \tag{3.5}$$

The inertia constant can be either implemented as a fixed value or can be dynamically changing [65], [69], [73]. Essentially, this parameter controls the exploration of the search space, therefore an initially higher value for φ_{ic} (typically 0.9) allows the particles to move freely to find the global optimum neighborhood fast. Once the optimal region is found, the value of the inertia constant can be decreased (usually to 0.4) to narrow the search, shifting from an exploratory mode to an exploitative mode. Commonly, a linearly decreasing inertia constant (first introduced by Shi and Eberhart [74], [75]) has produced good results in many applications; however, the main disadvantage of this method is that, once the inertia constant is decreased, the swarm loses its ability to search new areas because it is not able to recover its exploration mode (which does not happen with Clerc's constriction coefficient [68]).

3.2.2 Discrete particle swarm optimization

The general concepts behind optimization techniques initially developed for problems defined over real-valued vector spaces, such as particle swarm optimization, can also be applied to discrete-valued search spaces where either binary or integer variables have to be arranged into particles. In general, when integer solutions are needed, the positions of the particles can be determined by rounding off the real values to the nearest integer [76]. Equations (3.1) and (3.2), developed for a real number space, are used to determine the new position for each particle. Once $x_i(t) \in \Re^n$ is determined, its value in the d^{th} dimension is rounded to the nearest integer value using (3.6).

$$\mathrm{X}_{id}(t) = \left[x_{id}(t) \right], \quad d : 1 \to n, \; x_{id}(t) \in \Re \; and \; \mathrm{X}_{id}(t) \in \mathrm{Z} \tag{3.6}$$

The results presented by Laskari et al. [77] using integer PSO indicate that the performance of the method is not affected when the real values of the particles are truncated. Moreover, integer PSO has a high success rate in solving integer programming problems even when other methods, such as branch-and-bound, fail [77].

3.3 Proposed enhanced particle swarm optimizer

As part of this research, an enhanced particle swarm optimizer is proposed. The canonical PSO algorithm, described previously in section 3.2, is enhanced by adding a basic logic to the particles to facilitate the search through the problem hyperspace.

The additional logic in each individual is defined by the following rules:

- If the corresponding particle's *pbes*t and the *gbest* positions are both feasible solutions (i.e. solutions that satisfy all the constraints of the problem), then the velocity update is performed according to (3.5).

- If the particle has not found a feasible solution yet, then the velocity update equation is replaced by:

$$\vec{v}_i(t) = \phi_{ic} \cdot \vec{v}_i(t-1) + \phi \cdot rand \cdot (\vec{p}_g - \vec{x}_i(t-1)) \tag{3.7}$$

where:

φ is a single acceleration constant: $\varphi = \varphi_1 + \varphi_2$,

rand is a random number with uniform distribution in the range of [0, 1].

This means that when the particle has not found a feasible solution by itself then it is better to rely on the social rather than the self knowledge, thus the particle follows the best particle in the swarm.

- If none of the particles have found a feasible solution (the *gbest* value and the *pbest* value are both infeasible) then the velocity of the particles are updated using a random value of the maximum velocity as shown in (3.8).

$$v_i(t) = \left[r_1 \cdot v_{\max}(1) \quad r_2 \cdot v_{\max}(2) \quad \ldots \quad r_D \cdot v_{\max}(D) \right] \tag{3.8}$$

where:

r_h is a random number with uniform distribution in the range of [0, 1], and $h \in \{1, \ldots, D\}$,

$v_{max}(h)$ is the maximum velocity in the h^{th} dimension of the problem hyperspace,

D is dimension of the problem hyperspace.

In this last case, when a feasible solution has not been found by any member of the swarm, the particles may get confused by following the directions represented by the

gbest and *pbest* positions. As a consequence the particles move erratically in the problem hyperspace. Therefore, it is advantageous to assign random values to the velocity component so that only the limits represented by the maximum velocity are considered.

3.4 Summary

This chapter presents the fundamental theory to understand the PSO method that will be used in this research.

The chapter covers the canonical PSO formulation, the integer PSO version that it is used to handle integer variables, and the new Enhanced-PSO method, which is proposed in this study to improve the performance of the PSO algorithm, in particular to aid the initial search for feasible solutions.

The following chapters, corresponding to part II of this research, are dedicated to validate the proposed Enhanced-PSO method as an efficient algorithm for solving the problem of improving the power system performance using FACTS devices.

PART II: VALIDATION OF THE PROPOSED ENHANCED-PSO METHOD

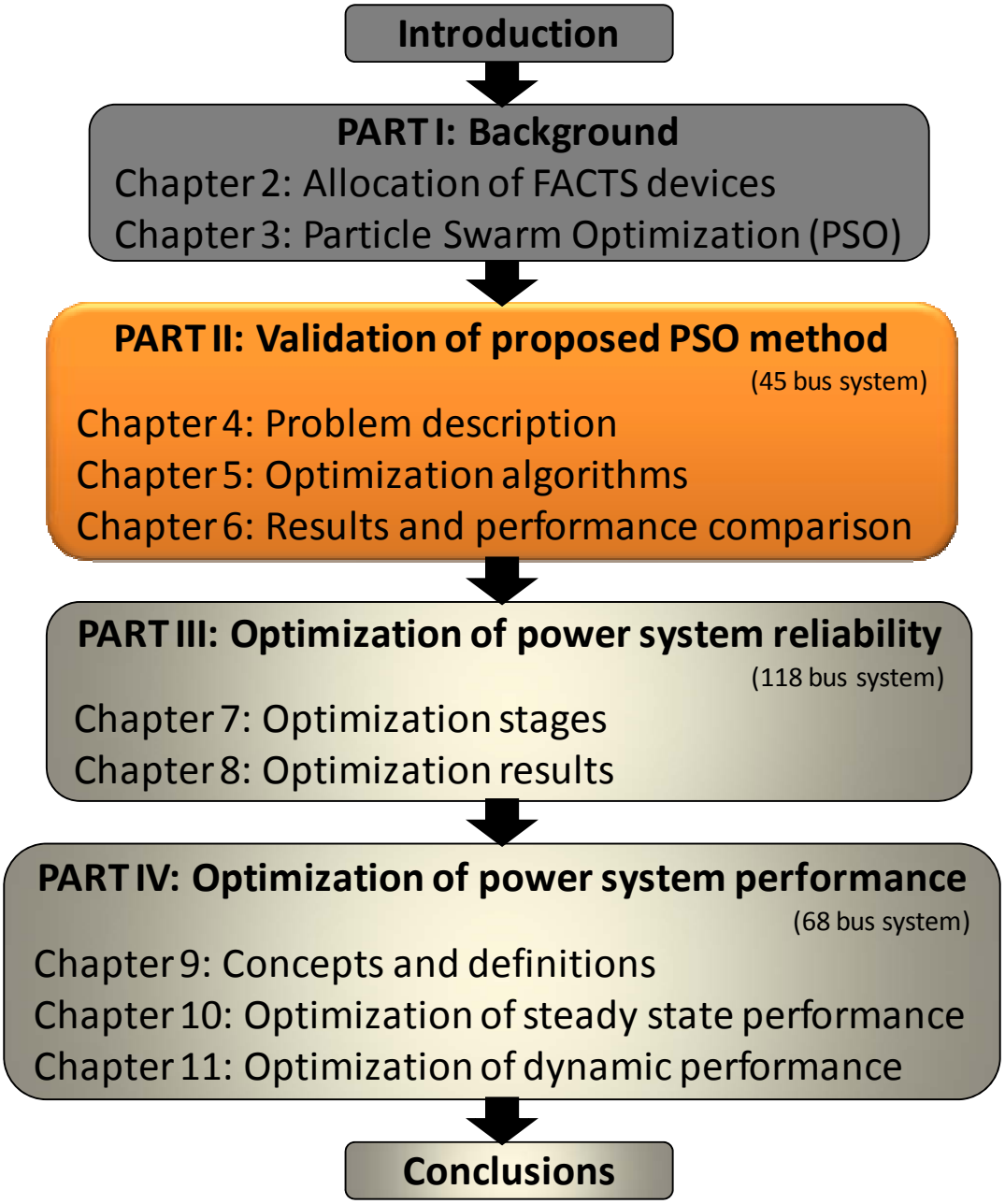

CHAPTER 4

PROBLEM DESCRIPTION AND EXHAUSTIVE SEARCH

4.1 Introduction

Part II of this research, consisting in chapters 4, 5 and 6, focuses on the validation of the superior performance of the proposed Enhanced-PSO formulation (as compare with other optimization techniques) in solving the problem of optimal allocation of FACTS devices in a power system.

This particular chapter presents the details of the problem to be solved: the optimal allocation of multiple STATCOM units in a 45 bus system, part of the Brazilian power network.

Initially, the problem to be solved is described in detail by considering the characteristics of the power system, the objective function and the system constraints (section 4.2). Then, an exhaustive search is performed in order to identify the global optimum of the problem (section 4.3). This exhaustive search also provides useful information about the problem hyperspace, its feasible regions (areas that contain solutions which satisfy all the system constraints), and the total computational effort involved, which can later on be used as a point of comparison for the computational times obtained by the optimization algorithms.

It is important to mention that, in this study, the STATCOM units (model described in Appendix A) are selected as an illustrative example, however the same method can be also applied to SVC devices or capacitor banks.

4.2 Problem statement

The multimachine power system used for this study appears in Figure 4.1 (details of the system data are presented in appendix B). It corresponds to a part of the Brazilian power network and it has two distinct load centers, one of them located among buses 377-380 and the other among buses 430-433. The existence of these two load centers suggests that the voltage support should be done through two STATCOM units.

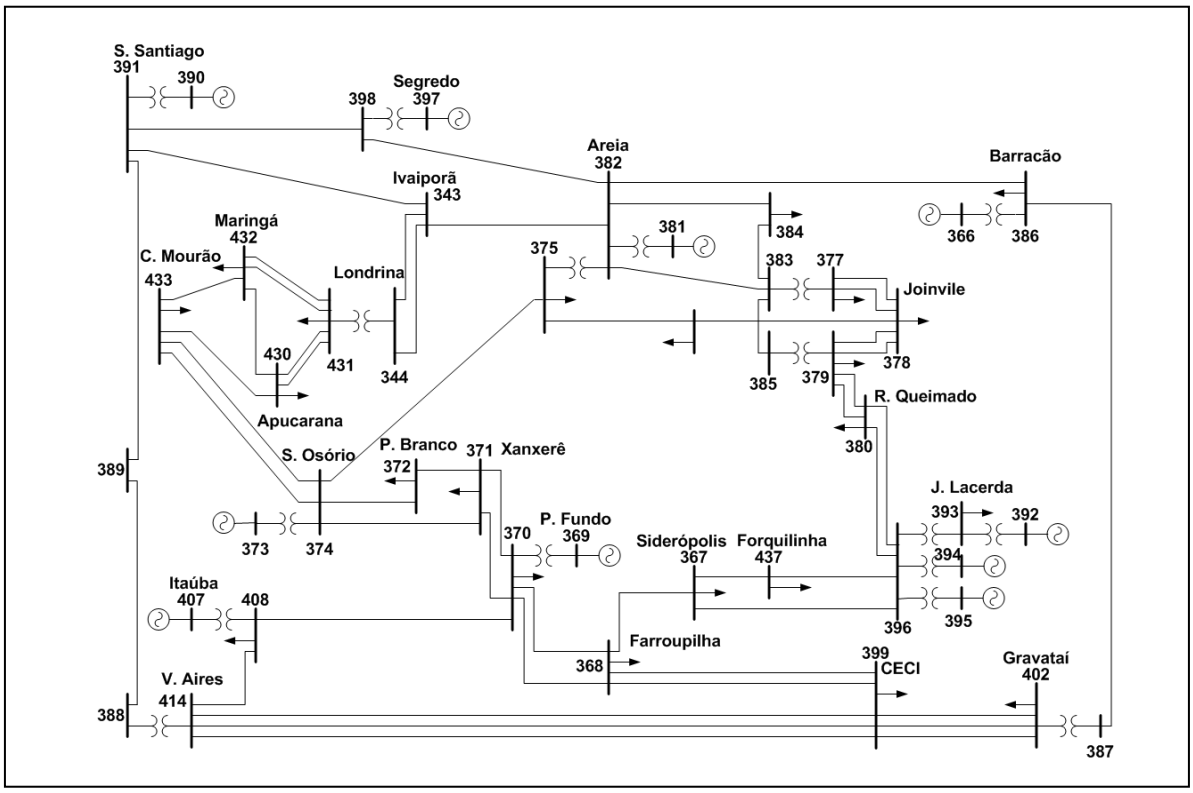

Figure 4.1: One line diagram of the 45 bus system, part of the Brazilian power network.

For implementing the optimization algorithms, two main aspects must be considered in the definition of the problem statement: (i) identify a proper objective function, (ii) characterize the set of feasible solutions (constraints definition).

4.2.1 Objective function

In this case there are two goals that have to be accomplished: (i) minimize the voltage deviations at all the buses in the system and (ii) minimize the STATCOM sizes/ratings. Thus, two metrics J_1 and J_2 are defined as in (4.1) and (4.2).

$$J_1 = \sqrt{\sum_{i=1}^{Nbus} (V_i - 1)^2} \tag{4.1}$$

where:

J_1 is the voltage deviation metric,

V_i is the value of the voltage at bus i in p.u.,

N_{bus} is the total number of buses in the system.

$$J_2 = \sum_{j=1}^{Nunits} \eta_j \tag{4.2}$$

where:

J_2 is the STATCOM size metric,

η_j is the sizes, in MVA, of STATCOM unit j,

N_{units} is the number of STATCOM units to be allocated.

The multi-objective optimization problem can now be defined using the weighted sum of both metrics J_1 and J_2 to create the objective function J shown in (4.3). The best solution is the one for which J is a minimum.

$$J = \omega_1 \cdot J_1 + \omega_2 \cdot J_2 \tag{4.3}$$

where:

J is the overall objective function.

The weight that multiplies each metric is adjusted to reflect the relative importance that each goal has with respect to the other. In this case, it is decided to give equal importance to both metrics, giving values of $\omega_1 = 1$ and $\omega_2 = 1/500$, so that the two terms in the objective function are comparable in magnitude.

4.2.2 Search Space (constraints)

There are several constraints in this problem regarding the characteristics of the power system and the desired voltage profile. Each of these constraints represents a limit in the search space. For instance, the network in Figure 4.1 has 10 generator buses where voltages are regulated by each generator's automatic voltage regulator (AVR). These generator buses do not need a STATCOM and are omitted from the search process, leaving 35 other possible locations for the STATCOM units.

Also, considering the topology of the system, the bus numbers are limited to the range from 1 to 45, thus the constraint shown in (4.4) have to be considered.

$$1 \le \lambda_j \le N_{bus}, \quad j \in \{1, 2, ..., N_{units}\} \tag{4.4}$$

where:

λ_j is the location of STATCOM unit j.

Additionally, the event of having more than one STATCOM unit connected to the same bus is considered infeasible, giving the restriction in (4.5).

$$\lambda_i \neq \lambda_j \qquad \forall i, j \tag{4.5}$$

The desired voltage profile requires 45 restrictions defined as (4.6).

$$0.95 \leq V_i \leq 1.05 \ , \quad i \in \{1, 2, ..., N_{bus}\} \tag{4.6}$$

Each solution that does not satisfy the above restrictions is considered infeasible. Finally, to limit the sizes of the STATCOM units the restrictions in (4.7) are applied.

$$0 \leq \eta_j \leq 250 \ , \quad j \in \{1, 2, ..., N_{units}\} \tag{4.7}$$

4.3 Exhaustive search

The multimachine power system in Figure 4.1 has 10 generators buses. At each of these buses the voltage is regulated by the corresponding generator's AVR and therefore no STATCOM unit is needed. For this reason, the generator buses are omitted from the searching process, leaving 35 possible locations for the STATCOM.

The exhaustive search is performed by running a power flow computation for each possible solution, in other words, for each possible combination of locations and sizes. Considering the total problem hyperspace, for this medium size power system, this search implies a total computational effort of 37,187,500 power flows. This number is calculated considering all possible pairs of locations multiplied by the number of possible combinations of STATCOM sizes.

After the exhaustive search is completed, it is possible to determine the feasible solutions among the total problem hyperspace. The feasible region of the problem is small, scattered and non convex. It is not possible to plot the entire feasible region since the dimensions are greater than three, however for illustrative purposes Figure 4.2 shows the best scenario considering all possible bus locations and maximum STATCOM sizes of 250 MVA for each unit.

The figure shows in black the solutions that are infeasible (solutions that have one or more constraint violations) and in white the solutions that are feasible (solutions that satisfy the problem constraints). The feasible regions (in white) represent a small portion of the total problem hyperspace.

For this simplified version of the problem, where the size of each unit is fixed at a maximum value of 250 MVA, only 15 pairs of locations (λ_1, λ_2) provide feasible solutions of where to place STATCOM units 1 and 2 (white areas in Figure 4.2). This value of 15 corresponds to 2.52% of the 595 total possible combinations as shown in Figure 4.3.a.

In the case where locations and sizes are considered for both STATCOM units, there are 414,750 combinations that meet all constraints, representing just 1.12% of the

total hyperspace of 37,187,500. Figure 4.3.b shows the percentage of the feasible region with respect to the total number of cases.

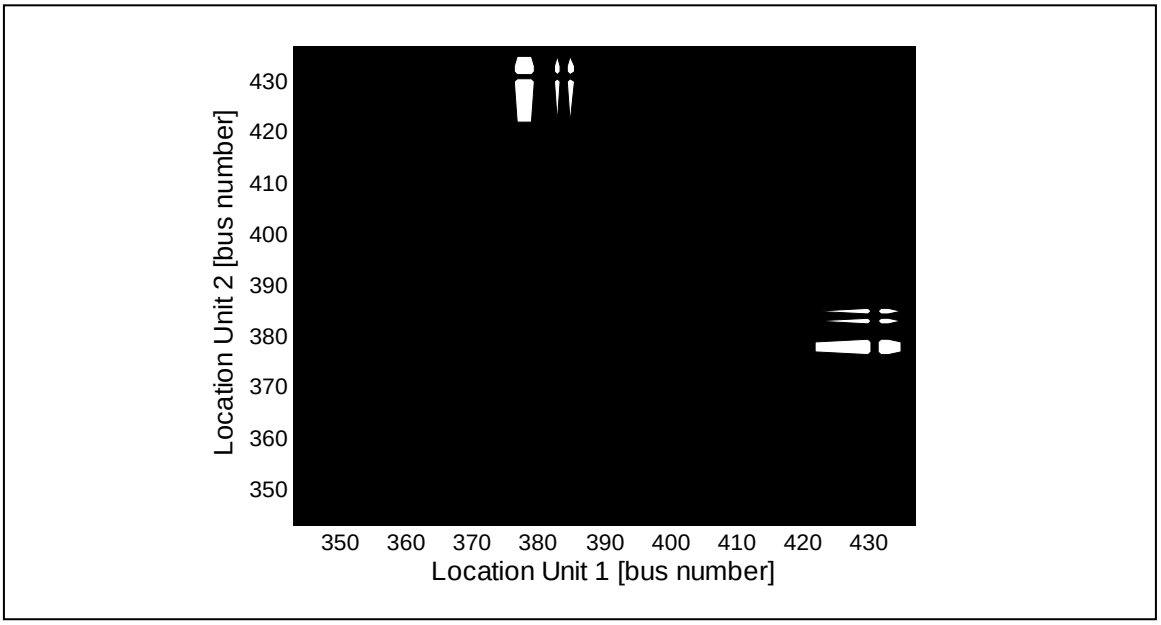

Figure 4.2: Feasible region (white areas) over total problem hyperspace

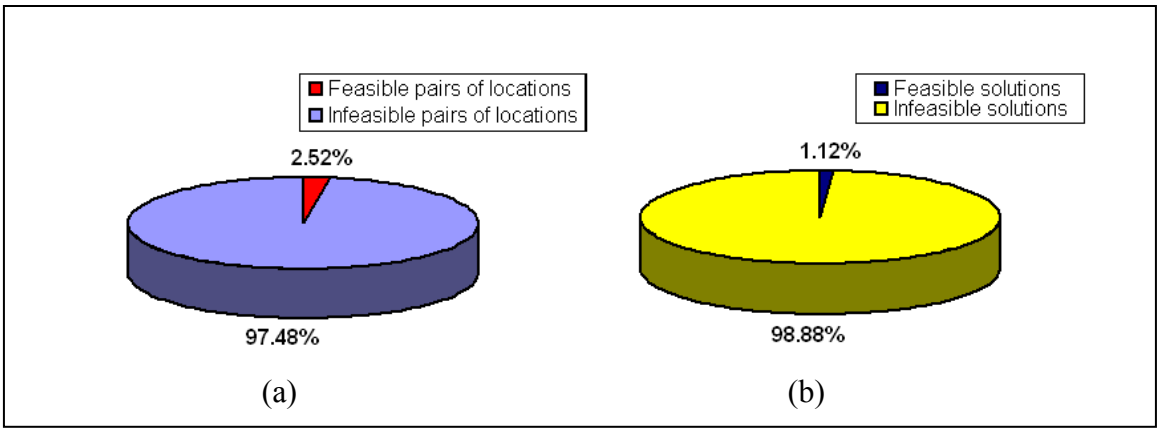

Figure 4.3: (a) Percentage of feasible locations over total possible combinations, (b) percentage of feasible solutions over total problem hyperspace

The global optimal solution is to place one STATCOM unit of 75 MVA at bus 378 and the second unit of 92 MVA at bus 433. The effect of the two STATCOM units is shown in Figure 4.4.

After the devices are optimally placed, all bus voltages are within the desired range of ±5% voltage deviation. Additionally, the voltage deviation metric J_1 improves by 26.5 % from an original value of 0.2482 to 0.1824.

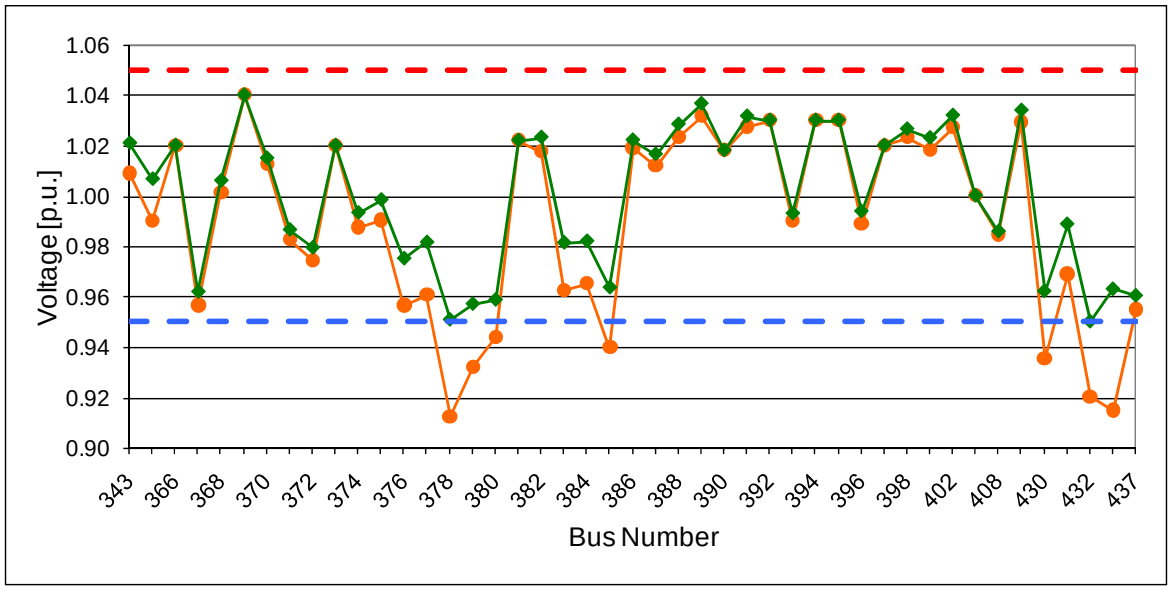

Figure 4.4: Voltage profile without (-•-) and with STATCOM units (-♦-)

4.4 Summary

This chapter presents the description of the problem of optimal allocation of multiple STATCOM units in a 45 bus system, part of the Brazilian power network. The objective function is to improve the voltage profile of the system, by minimize the sum of voltage deviations, at minimum cost (minimum rating for each device).

The system constraints include to keep all bus voltage deviations between ±5% of the corresponding nominal voltage, limit the size of each STATCOM device to a maximum of 250 MVA, exclude the generator buses from the search and avoid multiple units connected to the same bus.

After the problem description, an exhaustive search is performed to investigate the characteristics of the problem hyperspace, calculate the computational effort and ultimately find the global optimal solution to the problem.

The results of the exhaustive search have indicated that only 1.12% of the total possible solutions lead to feasible conditions (all system constraints are satisfied). Moreover, this small percentage of solutions is scattered among the total problem hyperspace making really challenging for an optimization algorithm to converge into a feasible region.

Regarding the computational effort, for this particular problem, an exhaustive search takes 37,187,500 power flows to evaluate all possible solutions and find the global optimum.

Finally, the global optimal solution is to place one STATCOM unit of 75 MVA at bus 378 and the second unit of 92 MVA at bus 433. After the devices are optimally placed, all bus voltages are within the desired range of ±5% voltage deviation, and the voltage deviation metric improves by 26.5 %.

CHAPTER 5

IMPLEMENTATION OF OPTIMIZATION ALGORITHMS

5.1 Introduction

Part II of this research, consisting in chapters 4, 5 and 6, focuses on the validation of the superior performance of the proposed Enhanced-PSO formulation (as compare with other optimization techniques) in solving the problem of optimal allocation of FACTS devices in a power system.

The previous chapter (chapter 4) provides the details of the problem to be solved and the results of an exhaustive search performed to find the global optimal solution to this problem.

This chapter presents the implementation of the Enhanced-PSO and several other optimization methods that are used as points of comparison. In particular, these other optimization methods corresponds to the canonical PSO formulation, genetic algorithm (GA) and bacterial foraging algorithm (BFA), and then Bender's decomposition and Branch-and-Bound (B&B) which are classical optimization methods.

Since the background of PSO, both canonical and Enhanced-PSO formulation, are extensively discussed in chapter 3, this chapter focuses in the implementation of the fitness function, particle definition and search space constraints. Emphasis is given in selecting the optimal PSO parameters: different sets of PSO parameters are tried multiple times and a statistical analysis is used to identify those parameters that produce the best performance of the algorithm.

For the other algorithms, GA, BFA, Bender's decomposition and B&B, which are used to compare the performance of the proposed Enhanced-PSO method, a brief theoretical background, problem formulation, and parameter settings are presented.

5.2 Particle swarm optimization

5.2.1 Theoretical framework

The canonical PSO formulation presented in chapter 3 (sections 3.2 and 3.3) and the proposed enhanced particle swarm optimizer described in section 3.4 of the same chapter are used for solving the problem of optimal allocation of multiple STATCOM units in the power system.

In particular the canonical PSO, considers the mathematical relationships in (3.1), (3.5), and (3.6), and the Enhanced-PSO formulation includes (3.7) and (3.8) in addition to the previous three equations.

5.2.2 Algorithm implementation

To correctly implement the PSO algorithm (canonical and enhanced versions), several aspects have to be considered: (i) define a proper fitness function to evaluate the performance of each individual in the population, (ii) define the particle vector such that each individual represents a potential solution to the optimization problem, (iii) characterize the search space taking into account feasible solutions and discarding

infeasible ones, and (iv) tune parameters, such as inertia and acceleration constants, to achieve optimal performance of the algorithm (less computational effort, more accuracy, etc.).

i) Fitness function definition

To evaluate each particle's position it is necessary to define a fitness function that can properly take into account the main objectives that are pursued. In this case the fitness function corresponds to the objective function defined in (4.3).

ii) Particle definition

The particle is defined as a vector containing the location (bus number) of the two STATCOM units and their sizes as shown in (5.1).

$$x_i = \begin{bmatrix} \lambda_1 & \eta_1 & \lambda_2 & \eta_2 \end{bmatrix} \tag{5.1}$$

All components of the particle vector (bus numbers and sizes) are integer numbers, thus $x_i \in Z^4$.

iii) Search space definition

The following rules are applied to guarantee that all the particles move only over the feasible region:

- Each time that a particle's new position includes a generator bus, the position is changed to the geographically closest load bus.
- Considering the location constraint presented in (4.4), where all the bus numbers must be between 1 and 45, the algorithm is programmed to re-randomize the value of λ_1 or λ_2 if the corresponding constraint is violated.
- Additionally, it is not permitted to have two STATCOM units connected to the same bus (4.5), so if this event happens, the second STATCOM is relocated to the nearest bus.
- Considering the voltage profile constraint in (4.6), if the solution does not satisfy the maximum voltage deviation for all the buses, then the corresponding fitness function value is set to infinity.
- Finally, if the maximum size of one of the STATCOM units is exceeded or if a negative value is calculated (4.7) then η_1 or η_2 is re-randomized accordingly.

iv) PSO parameters

In the PSO algorithm, there are five different parameters to be tuned for optimal performance: (a) type and value of inertia constant (φ_{ic}), (b) acceleration constants (φ_1 and φ_2), (c) maximum velocity (V_{max}) for each dimension of the problem hyperspace, (d) number of particles in the swarm, and (e) maximum number of iterations.

While the values for acceleration constants, maximum velocity, and inertia constant are mostly related to the nature of the problem (allocation of FACTS devices), the values of the number of particles and maximum number of iterations are associated

with the size of the problem hyperspace, which depends on the size of the power system and the number of units to be allocated.

In this study, a statistical analysis is carried out to determine the optimal values for all five PSO parameters and general guidelines are suggested for setting the values of the first three parameters (acceleration constants, maximum velocity and inertia constant). The different values considered for the PSO parameters are summarized in Table 5.1.

In order to construct some general rules for the selection of the number of particles and the maximum number of iterations, the scalability of the Enhanced-PSO algorithm is studied separately using the previously described 45 bus system as well as the IEEE 118 bus system. The results of that study are presented separately in chapter 6, section 6.4.

a) Regarding the type and value of inertia constant, three approaches are considered: fixed value, linearly decreasing and randomly decreasing inertia constant. In the fixed value approach, the values of 0.5, 0.7 and 0.9 are considered. The linearly decreasing inertia weight improves the convergence of the swarm by reducing the inertia weight from 0.9 to 0.1 in even steps over the maximum number of iterations (5.2). The third method, the randomly decreasing inertia weight, introduces a random factor in the previous approach in order to prevent the swarm from getting trapped in a local minimum (5.3).

$$\varphi_{ic} = 0.9 - 0.8 \cdot \frac{iter - 1}{\max\_iter - 1} \tag{5.2}$$

$$\varphi_{ic} = k \cdot \left(0.9 - 0.8 \cdot \frac{iter - 1}{\max\_iter - 1} \right) \tag{5.3}$$

where:

φ_{ic} is the inertia constant at iteration i,

$iter$ is the iteration number,

max_iter is the maximum number of iterations,

k is a random number between 0 and 1.

b) To evaluate the effect of giving more importance to the individual's best or the swarm's best in finding the optimal solution, a set of three values for the individual acceleration constant are evaluated: $\varphi_1 = \{1.5, 2, 2.5\}$. The value for the social acceleration constant is defined as in all the cases as: $\varphi_2 = 4 - \varphi_1$.

c) Three different values for maximum velocity are considered for each dimension of the problem hyperspace. In the case of the bus location a maximum velocity of 5 (smooth movement), 7 (normal velocity) and 9 (rapid changes allowed) are studied. As for STATCOM sizes, the maximum velocity values correspond to 25, 50, 75 MVA.

d) The values for the maximum number of particles are 15 and 20. As the number of particles increases, the more evaluations of the fitness functions are required, thus the computational effort increases.

e) Finally, maximum numbers of iterations of 50, 75, and 100 are carried out to evaluate the performance of the PSO.

Table 5.1 presents a summary of the values considered in determining the optimal set of parameters for the PSO algorithm (canonical and enhanced versions).

Table 5.1: Tested values for PSO parameters

Parameter	Tested values
Inertia constant	Fixed inertia weight: {0.5, 0.7, 0.9} Linearly decreasing inertia weight Randomly decreasing inertia weight
Individual acceleration constant (c_1)	{1.5, 2.0, 2.5}
Maximum velocity for bus location	{5, 7, 9}
Maximum velocity for STATCOM size	{25, 50, 75}
Number of particles	{15, 20}
Maximum number of iterations	{50, 75, 100}

A total number of 50 trials, per set of parameters, are carried out and a statistical analysis is performed to find the optimal PSO parameters. The performance of the PSO is evaluated in terms of the quality of the solution found (minimum, maximum and mean values), accuracy of the algorithm in finding the optimal solution (standard deviation),

and convergence rate (number of times that the algorithm finds feasible solutions). The optimal values of each of the PSO parameters, determined through this statistical study, are shown in Table 5.2.

Considering the results presented in Table 5.2, the parameter settings of the PSO algorithm, for addressing the problem of optimal allocation of FACTS devices in the power system, can be selected using the following guidelines:

Table 5.2: Optimal PSO parameters (canonical and enhanced versions)

Parameter	Optimal value
Inertia constant	Linearly decreasing
Individual acceleration constant (c_1)	2.5
Social acceleration constant (c_2)	1.5
Maximum velocity for bus location	9
Maximum velocity for STATCOM size	50
Number of particles	20
Maximum number of iterations	100

- Implement a linearly decreasing inertia constant that provides a wide range of movement in the early search and has less influence in the later stages where the search has narrowed in promising areas. A suitable scheme is proposed in (5.2).
- Give more emphasis to the self knowledge as compare to the social information channels. An individual acceleration constant of 2.5 is proposed in this study.
- A maximum velocity for the FACTS location equal to the nearest integer of 25% of the total domain (total number of buses for shunt units or total number of lines for series devices).

- A maximum velocity for the FACTS unit size equals to 20% of the maximum device's rating.

5.3 Genetic algorithm

5.3.1 Theoretical framework

The GA is an evolutionary computation technique that patterns itself after Charles Darwin's "survival of the fittest" concept. Through selection of parents, crossover between members of the current population, and mutation of the offspring, the population evolves and after a number of generations it approaches an optimal fitness [78]-[82].

After the population data is initialized, the fitness of each individual is evaluated through the use of a fitness function. The fitness function value quantitatively compares each individual of the current generation to obtain a fitness ranking (ordering) of all the members. Higher ranking individuals have fitness values that are closer to the optimal fitness value and vice versa for lower ranking individuals. After the fitness of each individual has been assessed, a subgroup of individuals is selected to become the parents for the next generation [78], [82].

There are several ways to determine which members of the population will produce offspring. Tournament selection begins by randomly selecting a group of two or more parents from the population and then choosing the individual within the group with the best fitness value for crossover. Elitism is another selection method that copies the

elite (highest ranking) members of the current population into the new population while the rest of the new population is generated through random selection of parents or any other alternative way. A third method of parent selection is the "roulette wheel", where potential parents are assigned a probability of being selected based on their rank such that higher-ranking individuals receive higher probabilities of being selected.

Once the two parents are chosen, crossover between them will produce two offspring. The crossover operator applies to the parents according to a pre-defined crossover probability [81]. If the crossover is not allowed, then the two offspring will be identical to the parents. On the other hand, if crossover is allowed, a portion of each parent's genes goes to one child and the rest to the other. In this way, two individuals containing the same number of genes are produced.

The split point, or point where the parents' genes are divided in two, can be pre-determined before crossover or chosen randomly for each set of parents.

After crossover, there is a chance that any number of the offspring's genes may be mutated or altered. This probability is generally small to prevent changing the original offspring too much. Each gene of the new individual is given the possibility of mutation, in other words, the genes are treated independently and this results in anywhere from zero to all genes being mutated.

The previous generation is replaced by the new generation and the entire process is repeated until a terminating condition is reached, such as maximum number of generations, satisfying convergence for the population's overall fitness, or minimum improvement of the fitness value from one generation to the next.

5.3.2 Algorithm implementation

The GA requires the following aspects be considered: (i) define a proper fitness function, (ii) define the chromosome's structure, (iii) characterize the search space, (iv) identify the parent selection scheme, and (v) determine parameters, such as number of elite members, crossover probability, split point, mutation probability, number of chromosomes, and maximum number of generations.

i) Fitness function definition

In this case, the same fitness function used in the PSO algorithm, (4.3), is used to evaluate the performance of the chromosomes.

ii) Chromosome structure

The chromosome structure represents a potential solution to the problem and thus, it is defined as the decision vector containing the location of the two STATCOM units as well as their sizes as shown in (5.1).

iii) Search space definition

The same rules described for the PSO method are applied to guarantee that all the particles move only over the feasible region.

iv) Selection method

For this particular application of GA, the roulette wheel method is chosen to

perform the selection of the parents. The parents are selected according to their fitness (rank), the better the fitness value is the higher the chance of the corresponding chromosome being selected.

This process can be visualized as a roulette wheel (pie chart) where all chromosomes in the population are placed according to their normalized fitness. Then a random number is generated to decide the chromosome to be selected. Chromosomes with higher rank are selected more times since they occupy more space on the pie.

v) GA parameters

There are six different parameters to be tuned in GA: (a) percentage of elite members, (b) crossover probability, (c) split point, (d) mutation probability, (e) number of chromosomes, and (f) maximum number of generations. In contrast to the PSO algorithm, where the values of parameters are problem dependant, in GA the performance of the algorithm is not particularly sensitive to these parameters. Literature suggests very narrow ranges for most of the GA parameters based on studies in several fields and applications. As a result, the parameters presented in Table 5.3 are used in the GA search process in this study.

Table 5.3: GA parameters

Parameter	Optimal value
Percentage of elite members	10%
Crossover probability	85%
Mutation probability	5%
Split point	2
Number of chromosomes	20
Maximum number of generations	100

For the parameters shown in Table 5.3, it is important to mention that the number of chromosomes and maximum number of iterations are the same as for the PSO algorithm, so these two evolutionary computation techniques can be compared based on a statistical analysis. Additionally, the parameter called "split point" is fixed at the value of 2 since the solution of the problem corresponds to a "location-size" pairing that is not possible to separate. Therefore a split point equal to 1 or 3 would generate meaningless offspring.

5.4 Bacterial foraging algorithm

5.4.1 Theoretical framework

The BFA is based on the movement patterns of E. coli in the intestines. Each individual, in this case a bacterium, represents a possible solution to the problem. The algorithm considers four successive processes: Chemotaxis, Swarming, Reproduction and Elimination [83]-[85].

a) Chemotaxis: the bacteria move towards better nutrient concentrations avoiding noxious substances, and search for ways out of neutral media. The bacterium takes a tumble followed by a tumble or a tumble followed by a run. For N_c number of chemotactic steps the direction of movement after a tumble is given by (5.4).

$$\theta^i(j+1,k,l) = \theta(j,k,l) + C(i)\cdot\varphi(j) \tag{5.4}$$

where:

C(i) is the step size taken in direction of the tumble,

j is the index for the chemotactic step,

k is the index for the number of reproduction step,

l is the index for the number of elimination-dispersal event,

$\varphi(j)$ is the unit length random direction taken at each step.

If the fitness function value at $\theta^i(j+1, k, l)$ is better than the one corresponding to $\theta^i(j, k, l)$ then the bacterium takes another step of size *C(i)* in that direction. This process continues until the number of repetitions per chemotactic cycle reaches a maximum of N_s.

b) Swarming: in times of stress the bacteria release attractants to signal all bacteria to swarm together. Each bacterium also releases a repellant to signal others to be at a minimum distance from it. Thus all the bacteria will have a cell-to-cell attraction via attractant and cell-to-cell repulsion via repellant.

The equation involved in the process is shown in (5.5).

$$\begin{aligned} J_{cc}(\theta, P(j,k,l)) &= \sum_{i=1}^{S} J_{cc}^{i}(\theta, \theta^{i}(j,k,l)) \\ &= \sum_{i=1}^{S}\left[-d_{attract}\cdot\exp(-w_{attract}\cdot\sum_{m=1}^{p}(\theta_m-\theta_m^i)^2)\right]+ \\ &\quad \sum_{i=1}^{S}\left[h_{repellant}\cdot\exp(-w_{repellant}\cdot\sum_{m=1}^{p}(\theta_m-\theta_m^i)^2)\right] \end{aligned} \tag{5.5}$$

where:

$d_{attract}$ is the depth of the attractant,

$w_{attract}$ is a measure of the width of the attractant,

$h_{repellant}$ is the height of the repellant effect,

$w_{repellant}$ is a measure of the width of the repellant,

p is the number of parameters to be optimized,

S is the number of bacteria.

The bacteria moving towards better nutrient concentrations can be represented by:

$$J(i, j, k, l) + J_{cc}(\theta, P) \tag{5.6}$$

where:

$J(i,j,k,l)$ is the fitness function.

c) Reproduction: after N_c chemotactic steps, the population of bacteria is allowed to reproduce. S_r (S_r=$S/2$) bacteria having the worst fitness function value die and the remaining S_r are allowed to split into two thus keeping the population size constant.

d) Elimination-Dispersal: at an elimination-dispersal event, each bacterium is eliminated with a probability of p_{ed}. This probability p_{ed} should not be large or it can lead to an exhaustive search.

5.4.2 Algorithm implementation

The BFA requires: (i) to define a proper fitness function, (ii) to define the bacterium's position, (iii) characterize the search space, and (iv) determine BFA parameters, such as number of bacteria, number of chemotactic cycles, number of swim steps, number of reproductions, number of elimination-dispersal loops, probability of elimination, maximum distance, attraction coefficients, and repellent coefficients.

i) Fitness function definition

The fitness function in (4.3) is used to evaluate the nutrient concentrations.

Since the BFA search mechanism follows the best nutrient gradient, for this particular case, the voltage profile constraint in (4.6) is incorporated to the main objective function:

$$J_{BFA} = J + \omega_p \cdot \sum_{1}^{45} V_v(i) \tag{5.7}$$

where:

J is the overall objective function as defined in (4.3),

$V_v(i)$ is a voltage violation indicator, which is equals to 1 if the voltage as bus i is either lower than 0.95 or greater than 1.05, and zero otherwise,

ω_p is a penalty weight equals to 1.5.

ii) Bacterium's structure

Analogous to the PSO's particles and GA's chromosomes, the bacteria structures represents potential solutions to the problem. They are defined as the decision vector in (5.1) which contains the location of the two STATCOM units and their sizes.

iii) Search space definition

To ensure that all bacteria move in the feasible region, the following rules are applied:

- If a bacterium's new position corresponds to a generator bus, the position is changed to the geographically closest load bus.
- If the location constraint in (4.4) is violated, then the value of λ_1 or λ_2 is re-randomized.
- If two bacteria's positions concur at the same bus, then the second STATCOM is relocated to the geographically nearest bus.
- If the maximum size of the STATCOM is exceeded (or if a negative value is calculated) then η_1 or η_2 are re-randomized accordingly.

iv) BFA parameters

For this particular study, trial an error is used to find the best parameters for the BFA. A summary of the parameters and their corresponding best values appear in Table 5.4.

Table 5.4: BFA parameters

Parameter	Optimal value
Number of bacteria	20
Number of chemotactic cycles (N_c)	30
Number of swim steps (N_s)	3
Number of reproductions (N_{re})	3
Number of elimination-dispersal loops (N_{ed})	2
Probability of elimination (P_{ed})	0.5
Maximum distance ($C(i)$)	4
Attraction coefficients $d_{attract}$ and $w_{attract}$	0.1
Repellent coefficient d_{repel} and w_{repel}	0.05

5.5 Bender's decomposition

5.5.1 Theoretical framework

Benders' decomposition is a classical optimization technique that is mainly used to solve large scale optimization problems [5], [86]. In basic terms, this technique separates two sets of decisions that are made in two consecutive stages.

In the first stage of the decision making, some of the constraints are delayed to reduce the complexity of the original (master) problem. In the second stage, some of the parameters that influence the decision, whose values were originally uncertain, become known and fixed after the first decision vector is found. Thus the secondary problem is reduced in complexity and in the number of variables [5].

To illustrate the method, the following general formulation of a non linear problem with continuous variables can be considered:

$$
\begin{aligned}
&Min \;\; f(Z) \\
&s.t. \;\; g_i(Z) \le 0, \quad i = 1,..., p \\
&\qquad h_j(Z) = 0 \quad j = 1,..., q
\end{aligned}
$$

The decision vector Z can be separated into vectors X and Y, such that the first stage involves the choice of the decision vector X and then, in the second stage, vector Y is chosen. The objective function is reformulated to consider the first stage decision making. Additionally, the sets of equality and inequality constraints, g_i and h_j are separated, thus the first stage optimization problem corresponds to:

$$
\begin{aligned}
&Min \;\; f^1(X) \\
&s.t. \;\; g_i^1(X) \le 0, \quad i \le p \\
&\qquad h_j^1(X) = 0 \quad j \le q
\end{aligned}
$$

It is assumed that there are K possible scenarios and the best scenario is only revealed after vector X is chosen [86]. Now, assign the index w to the best scenario, then the second stage decision variable becomes Y_w and the corresponding optimization problem can be formulated as:

$$
\begin{aligned}
&Min \;\; f^2(Y_w) \\
&s.t. \;\; g_i^2(Y_w) \le 0, \quad i \le p \\
&\qquad h_j^2(Y_w) = 0 \quad j \le q
\end{aligned}
$$

This problem may then be solved using standard optimization techniques.

5.5.2 Algorithm implementation

In the case of the STATCOM allocation problem, the master problem considers the decision vector Z that consists of selecting the optimal locations, λ_1 and λ_2, and the optimal sizes η_1 and η_2. The natural separation for vectors X and Y_w becomes locations ($X=[\lambda_1, \lambda_2]$) and sizes ($Y_w=[\eta_1, \eta_2]$), and consequently the separation of the constraints can be stated as follows:

1) For the first stage of the decision making: sizes of the STATCOM units become delayed constraints, thus the reactive power limits for these devices are relaxed in the solution of the power flow. The voltage references for the STATCOM units are set to be 1.0 p.u. for each of them. The objective function of the problem corresponds to the voltage deviation metric (J_1) defined in (4.1).

2) For the second stage of the decision making: with the locations of the devices determined, the set of constraints is limited to those related to the maximum size of each unit (4.7). The objective function includes both, the voltage deviation metric and the STATCOM size metric, as in (4.3).

5.6 Branch-and-bound

5.6.1 Theoretical framework

The total enumeration method, also called exhaustive search, evaluates every feasible solution to the problem and selects the best. The computational effort involved is

then reasonable for small problems where the number of solutions is a small finite number, but this is not the case for the vast majority of the real and practical problems. B&B is a classical approach to search for an optimum feasible solution by performing only a partial evaluation of the possible solutions [5], [86], [87].

Considering a general non linear optimization problem:

$$\begin{aligned} &Min \quad f(Z) \\ &s.t. \quad g_i(Z) \le 0, \qquad i = 1,..., p \\ &\qquad h_j(Z) = 0 \qquad j = 1,..., q \end{aligned}$$

Then denote K_0 as the set of feasible solutions to this problem and f_0 as the unknown optimal objective value. The main tools in the algorithm are the following:

- Branching or Partitioning: in the course of applying B&B, K_0 is partitioned into many simpler subsets. Each subset is a set of feasible solutions of a problem called the "candidate problem" (CP), which is the original problem augmented by additional constraints called branching constraints. At each step, one of the promising subsets is chosen and an effort is made to find the best feasible solution from it. If the best feasible solution of that set is found, or the set is empty because all solutions are infeasible, then it is said that the associated candidate problem is "fathomed" and the corresponding set of solutions is no longer considered. If the subset is not fathomed then it is partitioned into simpler subsets and the same procedure is repeated [87].
- Bounding: the algorithm proceeds to find upper and lower bounds for the optimal objective value f_0. There is only one upper bound u at each stage, which corresponds,

at the beginning of the algorithm, to the first feasible solution found. For the next stages, u corresponds to the lowest among the objective values of all the feasible solutions that have appeared so far. The feasible solution whose objective value is the current upper bound is called the "incumbent" at that stage. In the case of the lower bound, there is one per each CP. For each of them, the lower bound, l , is computed by a procedure called "the lower bounding strategy". This procedure is problem dependant and has to satisfy the property that every feasible solution for that CP is greater or equal to l [86], [87].

- Pruning: If at a certain stage one of the CPs has a lower bound greater than the current upper bound, meaning that none of the feasible solutions in that CP are better than the current incumbent, and then the algorithm prunes that CP (the subset is discarded) [87]

  Branching, bounding and pruning are repeated until optimal solution is found.

5.6.2 Algorithm implementation

The objective function is defined in (4.3) and K_0 is defined by the set of constraints in (4.4)-(4.7).

To reduce the number of branches to the minimum possible, a feasibility test is created where each possible combination between two STATCOM locations is tested considering the maximum STATCOM size of 250 MVA for both units. If for a specific pair of locations there is no feasible solution then the corresponding CP is fathomed. The results of the feasibility test indicate that only 15 combinations of STATCOM locations

are able to satisfy the conditions imposed by the constraints of the problem hyperspace. Consequently, there are 15 CPs in the partition of K_0.

The branching strategy used in this application corresponds to the "depth-first search", which implies that, for the first CP, further partitions are going to be performed. This will continue until the best feasible solution is found, and then the same procedure is performed in the second CP and so on, up to the 15^{th} CP.

For each CP the branching strategy starts by defining two sub-problems. The first considers the size of STATCOM 2 fixed in 250 MVA (to allow feasibility), while the size of STATCOM 1 varies from 0 to 250 MVA. The second sub-problem, which is solved sequentially after the first, leaves the size of STATCOM 1 fixed at the optimum value found in the previous step and then varies the size of STATCOM 2 from 0 to 250 MVA.

Further branching in the "depth-first search" is performed by dividing progressively the STATCOM size intervals *[min_size, max_size]* in each sub-problem into four more sub-intervals. In this way the bounding and pruning strategies help to narrow the search until the optimal value is found.

The bounding strategy for the upper bound initially assigns the first feasible solution as an incumbent, later on the value keeps updating by taking the first-in-list feasible solution over the subsets that are not fathomed or pruned. On the other hand, the strategies to find the lower bound consist of successively dividing the promising CP into smaller and smaller intervals until the distance between two consecutive intervals is 1 MVA. At that point the best solution (minimum fitness value in the interval) is found and the CP is fathomed.

At each stage if the lower bound of one sub-interval is greater than the current upper bound then the corresponding sub-interval is pruned. Once there are no more intervals to be pruned or fathomed, the best solution for the CP is said to have been found. Finally, once the best solution for the 15^{th} CP is found the best among all is assigned as the optimal solution for the original problem.

5.7 Summary

This chapter describes the implementation of the canonical and Enhanced-PSO algorithm, GA, BFA, Bender's decomposition and B&B.

PSO background, for both canonical and Enhanced-PSO formulation, has been discussed in chapter 3, therefore this chapter focuses in the implementation of the algorithm so it is capable of solving the problem of optimal allocation of multiple STATCOM devices in a 45 bus system, part of the Brazilian power network.

For all other algorithms, namely GA, BFA, Bender's decomposition and B&B, brief theoretical backgrounds are added to the actual implementation of each method (problem formulation, definition of the decision vector, search space description, and parameter settings).

In the case of the canonical and Enhanced-PSO, the optimal settings of PSO parameters are investigated using statistical analysis. The results of this optimal parameter selection suggest the following guidelines to set the PSO parameters:

- Implement a linearly decreasing inertia constant that provides a wide range of movement in the early search and has less influence in the later stages where the search has narrowed into promising areas. A suitable scheme is proposed in (5.2).
- Give more emphasis to the self knowledge as compared to the social information channels. An individual acceleration constant of 2.5 is proposed in this study.
- A maximum velocity for the FACTS location equals to 25% of the total domain (total number of buses for shunt units or total number of line for series devices).
- A maximum velocity for the FACTS unit size equals to 20% of the maximum device's rating.

The implementation of each algorithm, as discussed in this chapter, leads to the simulation results presented in the next chapter.

CHAPTER 6

DISCUSSION AND VALIDATION OF THE PROPOSED METHOD

6.1 Introduction

This chapter validates the superior performance of the proposed Enhanced-PSO formulation in solving the problem of optimal allocation of FACTS devices in a power system. In particular, the problem of optimal allocation of multiple STATCOM units in a 45 bus system, part of the Brazilian power network described in chapter 4.

The validation of the proposed Enhanced-PSO method considers three important factors: (i) convergence into feasible regions, (ii) analysis of global optimality, and (iii) scalability of the algorithm.

In the first two cases, the performance of the Enhanced-PSO algorithm is compared with other optimization techniques, in particular genetic algorithm (GA), bacterial foraging algorithm (BFA), Bender's decomposition, and Branch-and-Bound (B&B) (detailed implementation in chapter 5).

The Enhanced-PSO method is used to aid the convergence into feasible regions (solutions that satisfy all the constraints of the problem). The performance of the proposed Enhanced-PSO is compared with the canonical PSO formulation, the GA and the BFA using a Weibull analysis (section 6.2).

The assessment of the capability of achieving global optimality is addressed by analyzing how accurately each algorithm finds the global optimal solution versus getting trapped in local minima (section 6.3). The performance of the Enhanced-PSO is

compared with two classical optimization techniques, Benders' decomposition and B&B, and two evolutionary computation techniques, GA and BFA.

Finally, the scalability of the PSO algorithm is analyzed by comparing statistical results for two power system sizes: the Brazilian 45 bus system and the IEEE 118 bus system.

6.2 Convergence into feasible regions

Evolutionary computation techniques, such as PSO, are stochastic search based optimization algorithms. Because of random components that are part of the optimization process, each time that the algorithm is run it may provide a different solution. The quality of the final solution is strictly related to the capability of the algorithm in finding promising feasible regions where, most likely, the global optimal solution can be found. Depending on the type of the problem, finding these feasible regions may become a challenge.

Power system problems are complex from the optimization perspective, since their nature is highly non linear, and therefore it is often difficult to apply traditional optimization algorithms based on convexity assumptions.

The concept of convexity is mostly analyzed in the case of the objective function; however, the convexity assumption also applies to the feasible region. For example, in the case of linear programming problems, the optimum can be found (either by simplex method or interior point method) if the feasible region is a convex set, as shown in Figure 6.1.a (as opposed to Figure 6.1.b) [5].

A worst case is presented in Figure 6.1.c. where the feasible region consists of several small areas (white) scattered among the area limited by the upper and lower bounds of the decision variables, var_1 and var_2 (black area). This type of feasible region, as shown earlier in section 4.2, is typical when technical constraints are imposed in the power system. The optimization algorithms in this case should have efficient exploration mechanisms so that feasible solutions can be found fast and therefore minimum computational effort is wasted wandering around in infeasible areas.

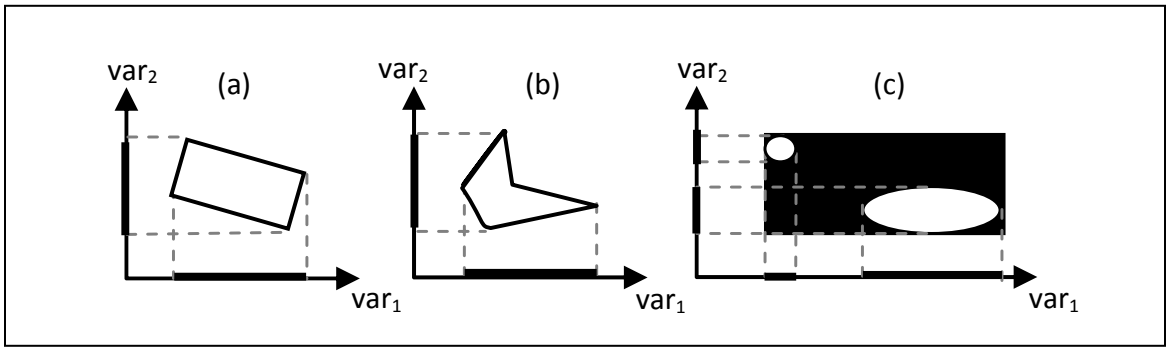

Figure 6.1: Convexity of the feasible region

In this subsection the capability of the proposed Enhanced-PSO is evaluated and compared with other evolutionary computation techniques: canonical PSO formulation, GA and BFA. The problem to be addressed consists of finding the optimal placement (bus number) and power rating (MVA) of multiple STATCOM units in a medium size power system, based on its steady state performance as stated in section 4.2.

In order to evaluate the performance of the optimization algorithms, 150 trials are carried out for each one of them using PSAT software. At each trial, the number of power flow evaluations is recorded until the first feasible solution is found. If no feasible

solution is found, then the algorithms stops automatically when the number of power flow evaluations reaches a maximum number of 2000 power flows. A performance indicator called "Success Rate" is calculated to determine the percentage of time that the algorithm is able to converge into feasible regions.

In order to use statistical parameters to evaluate the performance of each optimization technique, the Anderson-Darling normality test is first performed to measure how likely the data (in this case the number of power flows) comes from a normal distribution [88].

Performing the normality test is necessary in order to determine whether or not the means and standard deviations of these data sets are valid metrics to assess the differences between the techniques. In all cases, the Anderson-Darling p-values are less than 0.005 indicating that, with better than 99.5% certainty, the data are not normally distributed; therefore other statistical distributions have to be used.

6.2.1 Simulation results

Figure 6.2 shows the histogram for each technique. These histograms show the percentage of time in which the first feasible solution is found by the corresponding number of power flows indicated along the x-axis. The percentages on the y-axis are calculated over the total number of trials when each optimization algorithm converges into a feasible region (Success Rate shown in Table 6.1). For example, in the case of GA, the algorithm converged into a feasible region in 45 out of 150 trials (Success Rate equal to 30%). Of those 45 cases, the histogram shows that 5% of the time the first feasible

solution was found in less than 100 power flows, 15% of the time the first feasible solution was found between 100 and 200 power flows and so on.

Based on observation of the histograms, a Weibull distribution is considered appropriate to analyze the data. This distribution is used extensively to study extreme valued data, in this particular case, the number of power flows to find the first feasible solution [89].

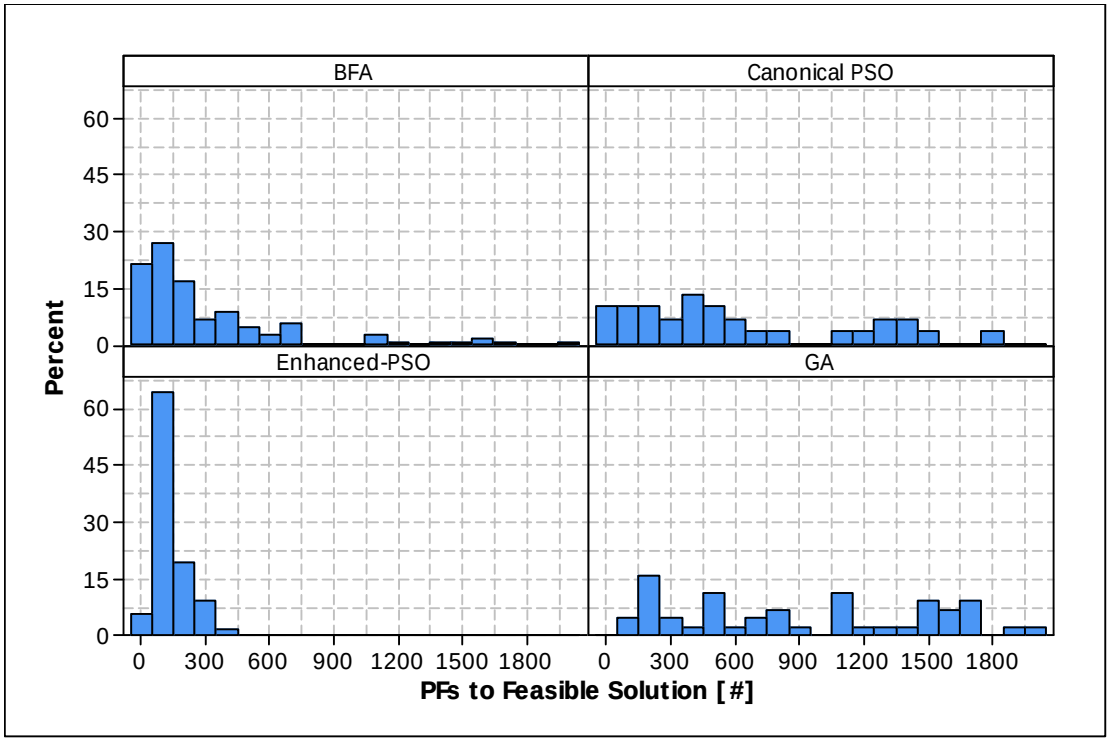

Figure 6.2: Histogram for each evolutionary computation technique

For each of the four datasets that contain the number of power flows until the first feasible solution is found, a two-parameter Weibull distribution, shown in (6.1), is fitted

to each dataset using the standard statistical software package Minitab. In each case, the correlation is greater than 0.95, indicating that the choice of Weibull is suitable.

$$f(x,\alpha,\beta)=\begin{cases}0 & if\ \ x<0\\ \dfrac{\beta}{\alpha}\cdot\left(\dfrac{x}{\alpha}\right)^{\beta-1}\cdot e^{-\left(x/\alpha\right)^{\beta}} & if\ \ x\geq 0\end{cases} \tag{6.1}$$

where:

α is the scale parameter,

β is the shape parameter.

Figure 6.3 shows the resulting probability plots for each technique and Table 6.1 shows the corresponding statistical parameters. The analysis based on Table 6.1 and Figure 6.3 is presented in section 6.2.2.

Table 6.1: Statistical values for a two-parameter Weibull distribution

	Enhanced-PSO	**PSO**	**GA**	**BFA**
Minimum PF	22	28	67	24
Maximum PF	379	1992	1972	1834
Success Rate	100	20.7	30	100
Scale (α)	147	8650	4329	326
Shape (β)	2.5	0.8	1.1	1.2

The columns of Table 6.1 show the results for each optimization algorithm. The rows of this table indicate the minimum number of power flows when the first feasible solution was found (Minimum PF), the maximum number of power flow computations

when the first feasible solution was found (Maximum PF), the Success Rate, defined as the percentage over 150 trial in which the corresponding algorithm actually converged into a feasible region, and finally the scale and shape parameters of the Weibull distribution.

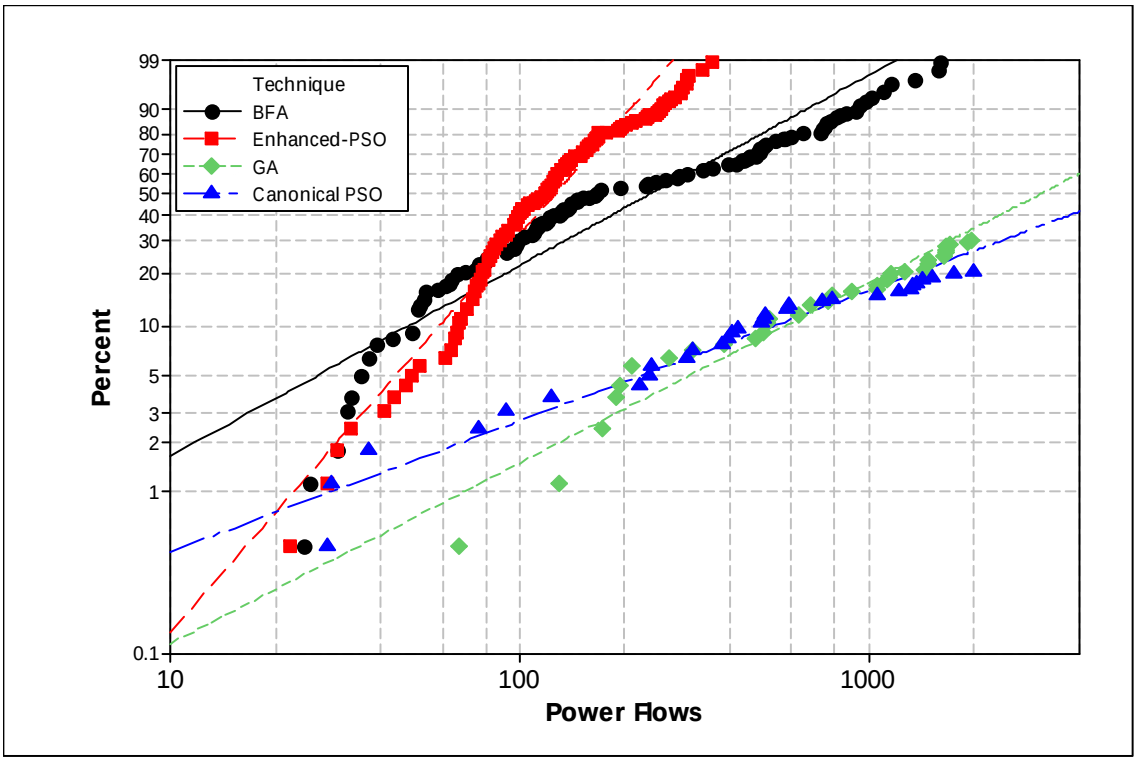

Figure 6.3: Weibull plot for each evolutionary computation technique

6.2.2 Technical discussion

Table 6.1 indicates that, based on the ranges for the number of power flow evaluations, the proposed Enhanced-PSO is faster in finding feasible solutions as compared with all other algorithms. Moreover its Success Rate is 100% versus 20.7% for canonical PSO and 30% in the case of GA.

Additionally, the Weibull parameters, α and β, carry important physical meanings. The scale parameter, α, corresponds to the characteristic time (or number of power flows) to find the first feasible solution. This is defined as the number of power flows needed to obtain a feasible solution in 63.2% of the trials.

The shape parameter, β represents the slope produced by data when plotted on a Weibull plot (Figure 6.3). More interestingly, the shape parameters provide insight into how the algorithms are able to seek out feasible solutions. Shape parameters greater than one imply increasing ability to locate feasible solutions. Enhanced-PSO is the only algorithm that falls into this category. GA and BFA both have shape parameters that are slightly greater than one while canonical PSO is slightly less than one. Clearly, the Enhanced-PSO offers the most efficient means of locating the feasible regions.

Figure 6.3 shows the probability of obtaining a feasible solution in any number of power flows (or less) for each of the techniques. Equally, the probability may be specified and then the maximum number of power flows required may be determined.

In addition, the resulting characteristic time to find a feasible solution was 147 and 326 power flows for Enhanced-PSO and BFA, respectively. The canonical PSO and GA were only able to find feasible solutions in at most 30% of the trials while the rest of the values are censored. This leads to characteristic times (or number of power flows) of 4329 and 8650 for GA and canonical PSO, respectively.

As a summary, the characteristic times to first feasible solution obtained from the Weibull analysis indicate that the Enhanced-PSO offers substantial performance gains as compared to the canonical PSO. Furthermore, its performance is also superior to BFA and GA.

6.3 Global versus local optimality

The improvement of a power system's performance is a complex optimization problem. Its highly non linear nature makes it difficult to find suitable optimization algorithms since many traditional optimization algorithms are based on convexity assumptions.

The concept of convexity is mostly analyzed in the case of the objective function, and if the function is strictly convex a unique optimal solution is guaranteed (Figure 6.4.a).

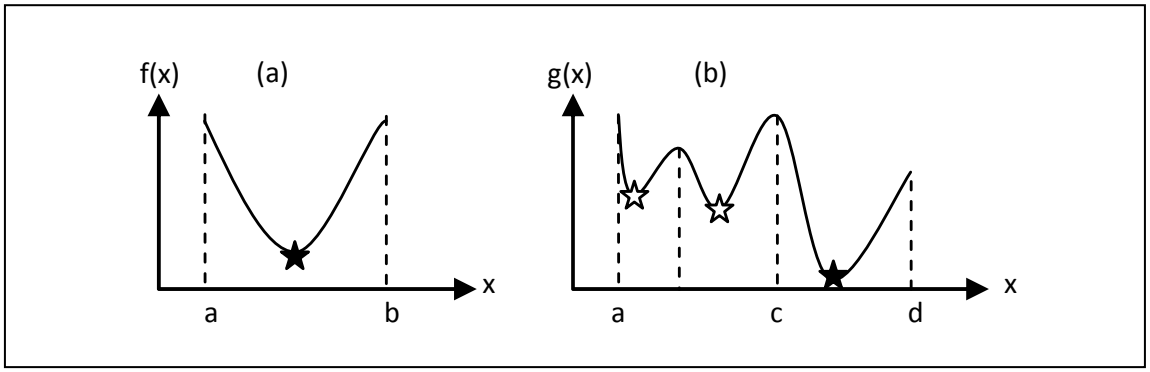

Figure 6.4: Global versus local minima

This characteristic is most desirable but it rarely occurs in power system problems. Most of the time, the plot of the objective function resembles the function in Figure 6.4.b where there are several local minima (white stars) and one true global optimum (black stars). As a result, gradient descent algorithms are prone to getting trapped in local valleys. In these cases, special mechanisms, such as injecting randomness

to the search, must be considered.

The capability of achieving global optimality is addressed in this study by analyzing how accurately the algorithms finds the global optimal solution versus getting trapped in local minima.

The Enhanced-PSO performance is compared with other optimization algorithms, in particular, two classical optimization techniques, Benders' decomposition and B&B, and two evolutionary computation techniques, GA and BFA.

First, classical optimization techniques are compared against evolutionary computation techniques. The parameters considered to evaluate the performance of each method are: (i) the ability of the corresponding algorithm to find the global optimum and (ii) its computational effort.

Second, the three evolutionary computation techniques are compared to validate the superior performance of the proposed Enhanced-PSO method. The parameters for comparison are in this case (i) the accuracy in finding the optimal solution and (ii) the convergence rate.

In the case of evolutionary computation techniques, Enhanced-PSO, GA, and BFA, 50 trials are performed and statistical values are used for comparison. For each algorithm, the Anderson-Darling normality test gives p-values greater than 0.05, indicating that the data have a Normal distribution.

All simulations are carried out using PSAT software.

6.3.1 Simulation results

Enhanced particle swarm optimizer

The Enhanced-PSO algorithm finds, as the optimal solution, to place one STATCOM unit of 75 MVA at bus 378 and the second unit at bus 433 with 92 MVA, which corresponds to the global optimal solution found by the exhaustive search (section.4.3).

Since the Enhanced-PSO method has a stochastic component, the algorithm is run 50 times to calculate minimum, maximum and mean values as well as standard deviation. Additionally, the convergence rate, defined as the percentage of times, over 50 trials, when the algorithm converged into a feasible region is calculated.

The corresponding results are shown in Table 6.2.

Table 6.2: Statistics of Enhanced-PSO for objective function value

Parameter	Value
Minimum objective function value (*J*)	0.51745
Maximum objective function value (*J*)	0.68390
Average objective function value (*J*)	0.58791
Standard deviation objective function value (*J*)	0.04167
Convergence rate (%)	100

In terms of actual time, the Enhanced-PSO algorithm takes 666 seconds for the case where the number of particles is equal to 20 and the maximum number of iterations is 100. However, the computing time depends on the characteristics of the computer, therefore it is preferable to count the number of evaluations of the fitness function (power

flows) that the algorithm requires before its terminating condition is met. This number corresponds to the number of particles multiplied by the maximum number of iterations. For this particular case, this results in 2,000 power flows.

To have a notion of how much computational effort the 2,000 power flows represent, this value can be compared with the computational effort of the exhaustive search, which corresponds to 37,187,500 power flow computations. This comparison of implies that, to find the global optimum, the Enhanced-PSO method takes only 0.005% of computing time as compared with exhaustive search.

A summary of the obtained results is shown in Table 6.3.

Table 6.3: Summary of Enhanced-PSO results

Bus 1	**Size 1 (MVA)**	**Bus 2**	**Size 2 (MVA)**	***J***	**Time (sec)**	**No. of Power flows**
378	75	433	92	0.51745	666	2,000

Genetic algorithm

The GA determines the optimal solution by placing one 75 MVA STATCOM unit at bus 378 and a second unit of 93 MVA at bus 433. This solution is slightly different from the one found by the Enhanced-PSO; the locations are the same for both units but the size of one of them has a 1 MVA difference. In terms, of the fitness value, and the voltage deviation metric the differences of this additional MVA are almost negligible.

Because the GA is a stochastic search method, the algorithm is run 50 times to calculate minimum, maximum and mean values as well as the standard deviation, as

shown in Table 6.4. In addition, the convergence rate, defined as the percentage of times, over 50 trials, when the algorithm converged into a feasible region is presented in this table.

Table 6.4: Statistics of GA for objective function values

Parameter	Value
Minimum objective function value (*J*)	0.51922
Maximum objective function value (*J*)	0.86216
Average objective function value (*J*)	0.68795
Standard deviation objective function value (*J*)	0.10401
Convergence rate (%)	32

Considering the computational effort, the running time of GA is 605 seconds and the number of evaluations of the fitness function is 2,000 power flows (20 chromosomes and 100 generations).

A summary of the previous results is shown in Table 6.5.

Table 6.5: Summary of GA results

Bus 1	Size 1 (MVA)	Bus 2	Size 2 (MVA)	*J*	Time (sec)	No. of Power flows
378	75	433	93	0.51922	605	2,000

Bacterial foraging algorithm

The solution found by the BFA corresponds to locating one 76 MVA STATCOM unit at bus 378 with 76 MVA and the second unit of 95 MVA at bus 437.

This solution is different from the one found by Enhanced-PSO; the location and size of the first unit is almost identical (1 MVA different in the size of the STATCOM) but the second unit is located in a different bus. For this reason, the fitness value is 7% higher than the global optimal solution found by the Enhanced-PSO algorithm.

BFA is also a stochastic search method; therefore the algorithm is run 50 times to calculate some statistical values, as shown in Table 6.7. The convergence rate, defined as the percentage of times, over 50 trials, when the algorithm converged into a feasible region is also presented in this table.

Table 6.6: Statistics of BFA for objective function values

Parameter	Value
Minimum objective function value (*J*)	0.52440
Maximum objective function value (*J*)	0.96422
Average objective function value (*J*)	0.74765
Standard deviation objective function value (*J*)	0.09654
Convergence rate (%)	100

Considering the computational effort, the running time of BFA is 9,454 seconds and the number of evaluations of the fitness function is 2,000 power flows.

A summary of the previous results is presented in Table 6.7.

Table 6.7: Summary of BFA results

Bus 1	Size 1 (MVA)	Bus 2	Size 2 (MVA)	*J*	Time (sec)	No. of Power flows
378	76	437	95	0.55440	9,454	2,000

Bender's decomposition

The Benders' decomposition algorithm finds at its first decision stage that the optimal locations for the STATCOM units correspond to buses 378 and 433. In the second phase, the optimal sizes are found as 75 MVA and 92 MVA respectively. This solution is identical to the one found by the Enhanced-PSO algorithm, thus both algorithms are capable of finding the global optimum.

In terms of the computational effort, the Benders' decomposition algorithm takes 18,611 seconds to run and the number of fitness evaluations corresponds to 63,095 power flows.

The number of power flows is calculated as follows:

1) First stage: the number of possible combinations of two buses among 35 feasible locations is equal to 595 power flows.
2) Second stage: the number of possible combinations of two sizes among 250 feasible values, which corresponds to 62,500 power flows.
3) Total number of fitness evaluations: the summation of computational effort on first and second stage.
4)

A summary of the previous results is shown in Table 6.8.

Table 6.8: Summary of Bender's decomposition results

Bus 1	**Size 1 (MVA)**	**Bus 2**	**Size 2 (MVA)**	***J***	**Time (sec)**	**No. of Power flows**
378	75	433	92	0.51745	18,611	63,095

Branch-and-bound

The solution found by the B&B method consists of placing one STATCOM of 67 MVA at bus 378 and another unit of 150 MVA at bus 430. This solution leads to an objective function (J) of 0.6170 as compared with 0.51745 determined by the Enhanced-PSO and Bender's decomposition algorithms. The voltage deviation metric (J_1) is equal to 0.1819 which is smaller than the previous value of 0.1824 because of the substantial difference in the MVAr injected into the system (50 MVA difference in the sum of the capacities of both STATCOM units). The benefit obtained on the voltage deviation metric clearly does not compensate for the drawback caused by the STATCOM size metric. From the optimization point of view, the B&B algorithm gets trapped in one of the local minima.

The computation time of the algorithm is 846 seconds and the number of fitness evaluations is 2,155 power flows.

The previous number of power flows is computed as follows:

1) Feasibility test: the number of possible combinations of two buses among 35 feasible locations equals to 595 power flows.
2) Branching: the number of branches (feasible solutions) is equal to 15 pairs of locations and there are 2 sub-problems per branch, leading to 30 sub-branches.
3) Pruning: average number of evaluations per sub-problem estimated as 52 power flows.
4) Total number of fitness evaluations: the computational effort in feasibility test plus the multiplication of number of evaluations in both branching and pruning.

A summary of the previous results is shown in Table 6.9.

Table 6.9: Summary of B&B results

Bus 1	Size 1 (MVA)	Bus 2	Size 2 (MVA)	*J*	Time (sec)	No. of Power flows
378	67	430	150	0.6170	847	2,155

6.3.2 Technical discussion

Comparison of classical and evolutionary computation techniques.

Table 6.10 summarizes the overall performance data for each of the algorithms presented.

Table 6.10: Summary of performance date for all algorithms

Method	Bus 1	Size 1 (MVA)	Bus 2	Size 2 (MVA)	J	Time (sec)	No. of Power flows
Enhanced PSO	378	75	433	92	0.5174	666	2,000
GA	378	75	433	93	0.5192	605	2,000
BFA	378	76	437	95	0.5544	9,454	2,000
Benders	378	75	433	92	0.5174	18,611	63,095
B&B	378	67	430	150	0.6170	847	2,155

The parameters considered for evaluating the performance of each method are: (i) the ability of the corresponding algorithm to find the global optimal solution, and (ii) its computational effort.

Considering the ability of the algorithms to find the global optimal solution, it is clear that Enhanced-PSO, GA and Bender's decomposition, are all able to find the correct

solution. In the case of BFA and B&B, both algorithms get trapped in a local minimum and, therefore, are discarded from future comparisons.

From the perspective of the computational effort, the Enhanced-PSO and GA are programmed to compute the same number of power flow evaluations; both of them have very close values for the computational time with a slight advantage for the GA. The number of fitness function evaluations for Benders' decomposition is 31.5 times more than either the Enhanced-PSO or GA methods.

As a conclusion, the evolutionary computation techniques, the Enhanced-PSO and GA, have a superior performance as compared to the classical optimization techniques, Benders' decomposition and B&B, both in terms of the ability to find the optimal solution and the computational effort.

Comparison of evolutionary computation techniques.

The conclusion from the previous section indicates that only Enhanced-PSO and GA are able to find the global optimum solution by avoiding the local minima (just a negligible difference can be perceived because of one additional MVA in STATCOM size 2 in the case of GA). Also, the two algorithms are programmed to have the same number of power flow computations and they perform these in almost the same amount on time (with a minor advantage for GA with respect to the Enhanced- PSO). Therefore, further indicators to compare the performances of both algorithms are needed. These indicators are statistical parameters calculated for both, Enhanced-PSO and GA, over a set of 50 trials which are presented in Table 6.11.

Table 6.11: Summary of Statistical analysis for Enhanced-PSO and GA

Parameter	Enhanced PSO	GA
Minimum objective function value (J)	0.51745	0.51922
Maximum objective function value (J)	0.68390	0.86216
Average objective function value (J)	0.58791	0.68795
Standard deviation objective function value (J)	0.04167	0.10401
Convergence rate (%)	100	32

The information presented in Table 6.11, provides the additional indicators to evaluate the accuracy in finding the optimal solution and the convergence rate (number of time that the algorithm is able to converge to a feasible solution).

The accuracy in finding the optimal solution is considerably better in the case of the Enhanced-PSO algorithm with a standard deviation of 0.04167 as compared with GA that is 2.5 times bigger (0.10401).

In terms of the convergence rate, the difference between the two algorithms is enormous; GA reaches a modest 32% while the Enhanced-PSO achieves 100%. Additionally, maximum and average values of the objective function value (J) indicate a clear advantage for the Enhanced-PSO over the GA.

In terms of the search procedure, Figure 6.5 shows the trajectories of the best members in the populations of the Enhanced-PSO and GA for a random trial.

The best member of the Enhanced-PSO (p_g) is able to locate a feasible solution at a much early stage as compared with the best elite member of GA (infeasible solutions are represented in the figure with an objective value function (J) equal to 1.0). After the first feasible solution is found, both algorithms evolve into better neighborhoods in the

problem hyperspace; however the Enhanced-PSO does it with a faster rate than GA. Finally, the best solution is found by the Enhanced-PSO algorithm.

As an overall conclusion, all previous remarks indicate that the proposed Enhanced-PSO method outperforms GA and all other methods investigated.

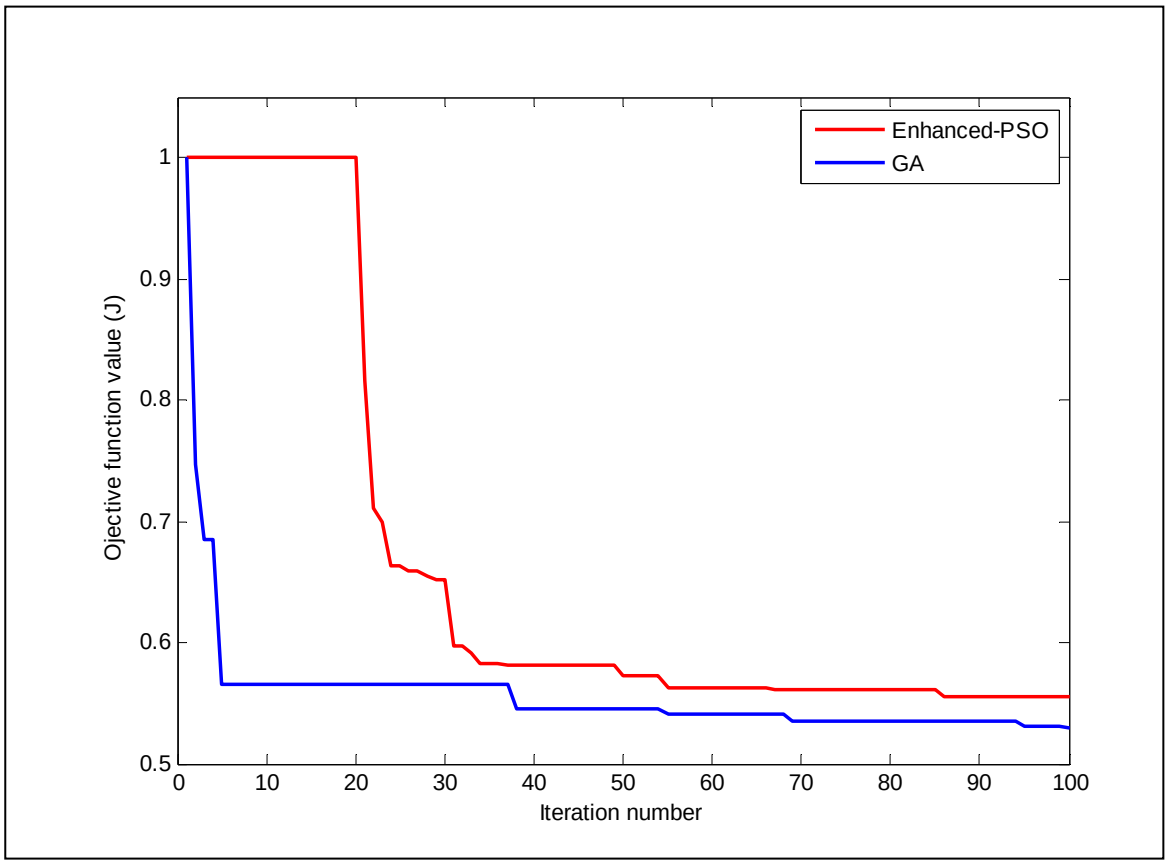

Figure 6.5: Trajectory of best member, Enhanced-PSO vs. GA

Lastly, considering the performance of the Enhanced-PSO algorithm as a stochastic search method, Figure 6.6 shows the degree of sub-optimality in the solutions provided by the Enhanced-PSO algorithm. The degree of sub-optimality, presented along

the x-axis of Figure 6.6, is defined as the difference percentagewise between the solution found by the algorithm and the global optimal solution.

The y-axis of Figure 6.6 corresponds to the percentage of the cases (over a total of 50 trials) when the degree of sub-optimality is lees or equal to the corresponding value along the x-axis.

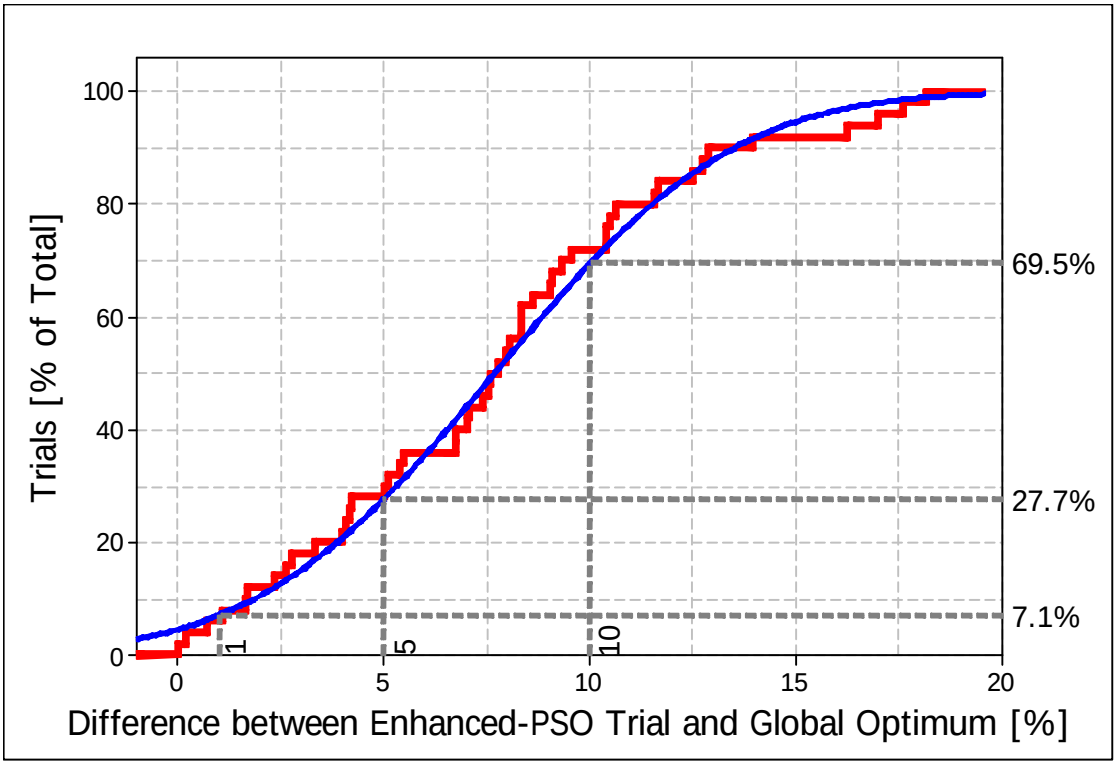

Figure 6.6: Degree of sub-optimality for Enhanced-PSO algorithm

From Figure 6.6, it is possible to note that 69.5% of the time, the solutions found by the Enhanced-PSO algorithm have 10% or less difference with respect to the global optimum. Additionally, the difference does not exceed the value of 20% in any of the trials.

6.4 Scalability of the Enhanced-PSO algorithm

As the previous section demonstrates, the evolutionary computation techniques are able to find solutions in a small fraction of the number of power flows required by the exhaustive search. In particular, since the power flow number is limited to a maximum of 2,000 power flows, the total computational effort for the Enhanced-PSO algorithm corresponds to 0.005% of the total effort spent in the exhaustive search performed in chapter 4, section 4.3.

This maximum number of power flows, is calculated as the number of particles in the swarm, 20 for this study, multiplied by the maximum number of iterations, equals to 100. These values of number of particles and maximum number of iterations were obtained after a statistical study applied to the problem of optimal allocation of FACTS devices in a 45 bus system.

One aspect of concern about the use of the Enhanced-PSO algorithm is its capability to effectively solve optimization problems when the size of the power system is increased. Specifically, how to assign a proper value to the number of particles in the swarm and the maximum number of iterations, so the problem can be solved with high accuracy in finding the global optimal solution but reasonable computational time.

The following guidelines are proposed to set these parameters for this investigation:

- Set the number of particles to be approximately 25% of the total number of possible locations multiplied by the number of units that need to be allocated.

- Use as stopping criteria a minimum value for the improvement of the *gbest*, if the value of the *gbest* has not changed in a certain number of iterations or if it is changing by less that 5% with respect to its previous value, then stop the algorithm. Using these criteria may allow the algorithm to run for a long time, therefore, if the computational time is a constraint, keep the maximum number of iterations to 100.

The Enhanced-PSO algorithm is applied to illustrate how the algorithm performs when the power system is changed from the Brazilian 45 bus system to the IEEE 118 bus network [90]. In both cases the problem to be solved corresponds to the optimal allocation of two STATCOM units in the power system. The detail of the problem corresponds to those presented in chapter 4, section 4.2. The objective function corresponds to (4.3) and the constraints are defined as in (4.4)-(4.7).

The implementation of the Enhanced-PSO algorithm is carried out according to the problem formulation described in chapter 5, section 5.2. Particle and search space definitions are identical in both cases (45 bus system and 118 bus system), while the PSO parameter settings are calculated for the 118 bus system according to the guidelines proposed in this section. Table 6.12 shows the PSO parameters used in the case of the 118 bus system. The simulation results of both systems are obtained using PSAT software.

Figure 6.7 shows the capability of the algorithm to converge into feasible regions using boxplots (the box represents the middle 50% of data).

The y-axis of Figure 6.7 represents the number of power flows when the first feasible solution is found; these values are shown as a percentage of the total number of

power flow computations which is 2,000 in the case of the 45 bus system and 5,000 for the 118 bus system.

Table 6.12: PSO parameters-118 bus system

Parameter	Optimal value
Inertia constant	Linearly decreasing
Individual acceleration constant (c_1)	2.5
Social acceleration constant (c_2)	1.5
Maximum velocity for bus location	9
Maximum velocity for STATCOM size	50
Number of particles	50
Maximum number of iterations	100

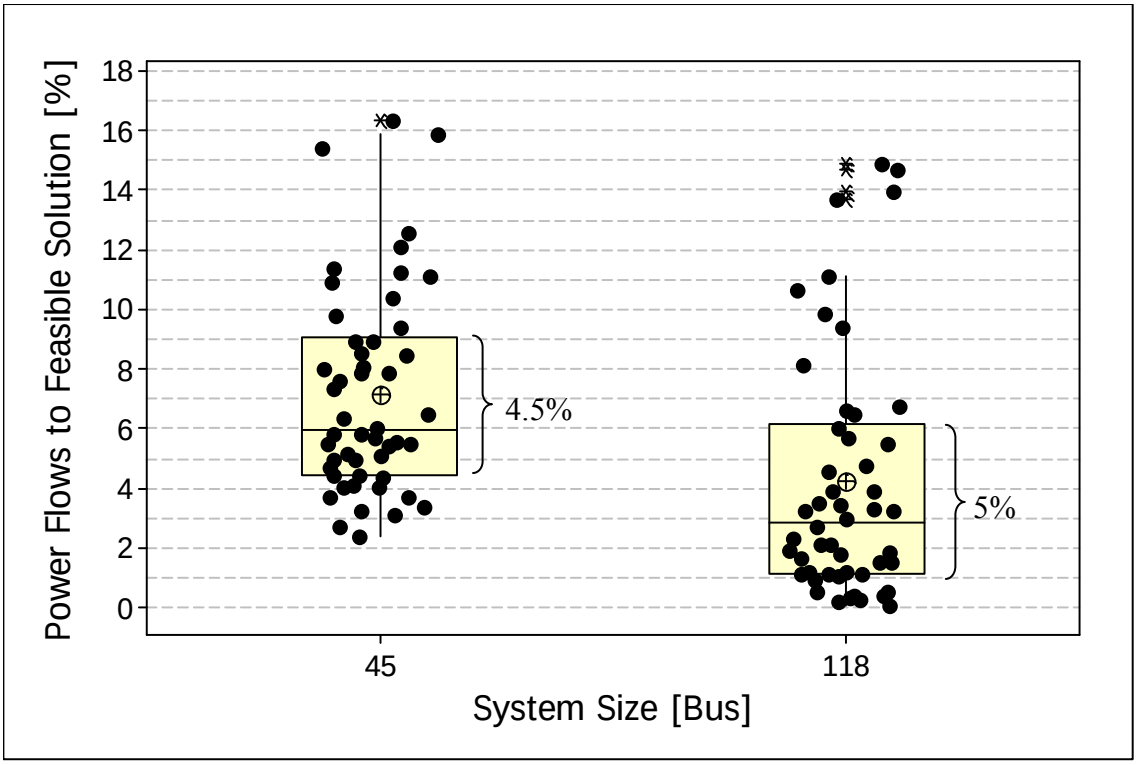

Figure 6.7: Convergence into feasible regions for 45 and 118 bus system

In addition, each dot in Figure 6.7 corresponds to one trial of the algorithm and the total number of trials is equal to 50 for both the 45 and the 118 bus system.

Figure 6.7 provides evidence that the performance of the algorithm, with the proposed parameter settings, is not substantially affected by the size of the system. In both cases, feasible solutions are found in fewer than 17% of the maximum allowed power flow computations and the inter-quartile ranges (difference between the first and third quartile, that spans the middle 50% of the data) are fairly similar (4.5% and 5% for 45 bus and 118 bus systems respectively).

Due to the large number of power flow computations, an exhaustive search is not performed in the case of the 118 bus system. To give an idea of the computational time involved, if one power flow computation takes 125 msec, then the total time to run an exhaustive search for the 45 bus system is 54 days; however for the 118 bus system the total time is 475 days (almost one year and four months). For this reason, the quality of the optimal solutions is assessed only by a statistical analysis over 50 trials.

Table 6.13 shows the results for the 45 bus and 118 bus systems. The maximum, average and standard deviation values of the objective function value are presented as percentages with respect to the minimum objective function value.

Table 6.13: Optimal solutions - 45 and 118 bus systems

Parameter	45 Bus	118 Bus
Minimum objective function value (J)	0.51745	0.4734
Maximum objective function value [%]	132.1	117.0
Average objective function value [%]	113.6	101.4
Standard deviation [%]	4.54	1.17

Comparing the percentages in both columns, it is possible to conclude that there are not significant differences in the performance when the size of the power system is increased.

6.5 Summary

This chapter validates the proposed Enhanced-PSO method as a suitable algorithm for solving the problem of optimal allocation of FACTS devices in the power system.

The followings aspects are considered in the evaluation of the proposed technique: (i) convergence into feasible regions, (ii) capability of achieving global optimality, and (iii) scalability of the Enhanced-PSO algorithm.

The convergence into feasible regions is analyzed by comparing the performance of the Enhanced-PSO algorithm with three other evolutionary computation techniques: canonical PSO formulation, GA, and BFA. A Weibull analysis is used as a statistical tool to assess the performance of each algorithm.

The characteristic times to find the first feasible solution, obtained from the Weibull analysis, indicate that the Enhanced-PSO substantially outperforms all other techniques. Additionally, considering the physical meaning of the Weibull parameters, α and β, the Enhanced-PSO method shows an increasing ability to locate feasible solutions as the number of iterations increases.

With the purpose of investigating the capability of the proposed approach in finding the global optimal solution, two classical optimization techniques (Bender's

decomposition and B&B) and three evolutionary computation techniques (the proposed Enhanced-PSO method, GA, and BFA) are compared.

The parameters considered to evaluate the performance of each technique include the ability of finding the global optimal solution and the computational effort. The Enhanced-PSO, GA, and Bender's decomposition are able to find the global best solution, while BFA and B&B algorithm are trapped in a local minimum and, therefore, did not give the optimal solution.

Considering the computational effort, the Enhanced-PSO and GA have almost identical computational times since the maximum number of power flow computation is set to the same value of 2,000 power flows. Benders' decomposition method is also able to find the correct solution, however it requires excessive computational effort compared to the Enhanced-PSO and GA (31.5 times more power flow evaluations).

In addition, since the previous parameters do not reveal significant differences between the proposed Enhanced-PSO and GA, a statistical analysis is performed where the accuracy in finding the optimal solution and the convergence rates are the focus of interest. The results clearly indicate the superior performance of the proposed Enhanced-PSO method: it is more accurate in finding the global optimal solution because of its small standard deviation and it has 100% convergence rate while GA just delivers a modest 32%.

Finally the scalability of the Enhanced-PSO is studied by analyzing the performance of the algorithm in solving the optimal allocation of multiple STATCOM units in a larger power system, in this case the IEEE 118 bus system.

The following guidelines are proposed for setting the number of particles and maximum number of iterations:

- Set the number of particles to be approximately 25% of the total number of possible locations multiplied by the number of units that need to be allocated.
- Use the following stopping criteria: if the value of the *gbest* has not changed in a certain number of iterations or if it is changing by less that 5% with respect to its previous value, then stop the algorithm. An alternative stooping criterion, that limits the computation effort to a fixed amount, is to keep the maximum number of iterations in a value of 100.

These proposed guidelines are used in the IEEE 118 bus system, and the results are compared with the 45 bus system to assess the difference in the algorithm's performance. Using a statistical analysis it is shown that the performance of the algorithm is not affected by the size of the power system, maintaining similar properties for converging into feasible regions and accurately finding optimal solutions.

In sum, this chapter provides the validation of the Enhanced-PSO method to be used as a suitable algorithm for solving the optimization of power system performance using FACTS devices. In addition, it proposes general guidelines for setting the PSO parameters such as the optimal performance of the algorithm is obtained.

This information represents the base in which the other two parts of this research, part III, optimization of power system reliability, and part IV, optimization of power system performance, are based on.

PART III: OPTIMIZATION OF POWER SYSTEM RELIABILITY USING PSO

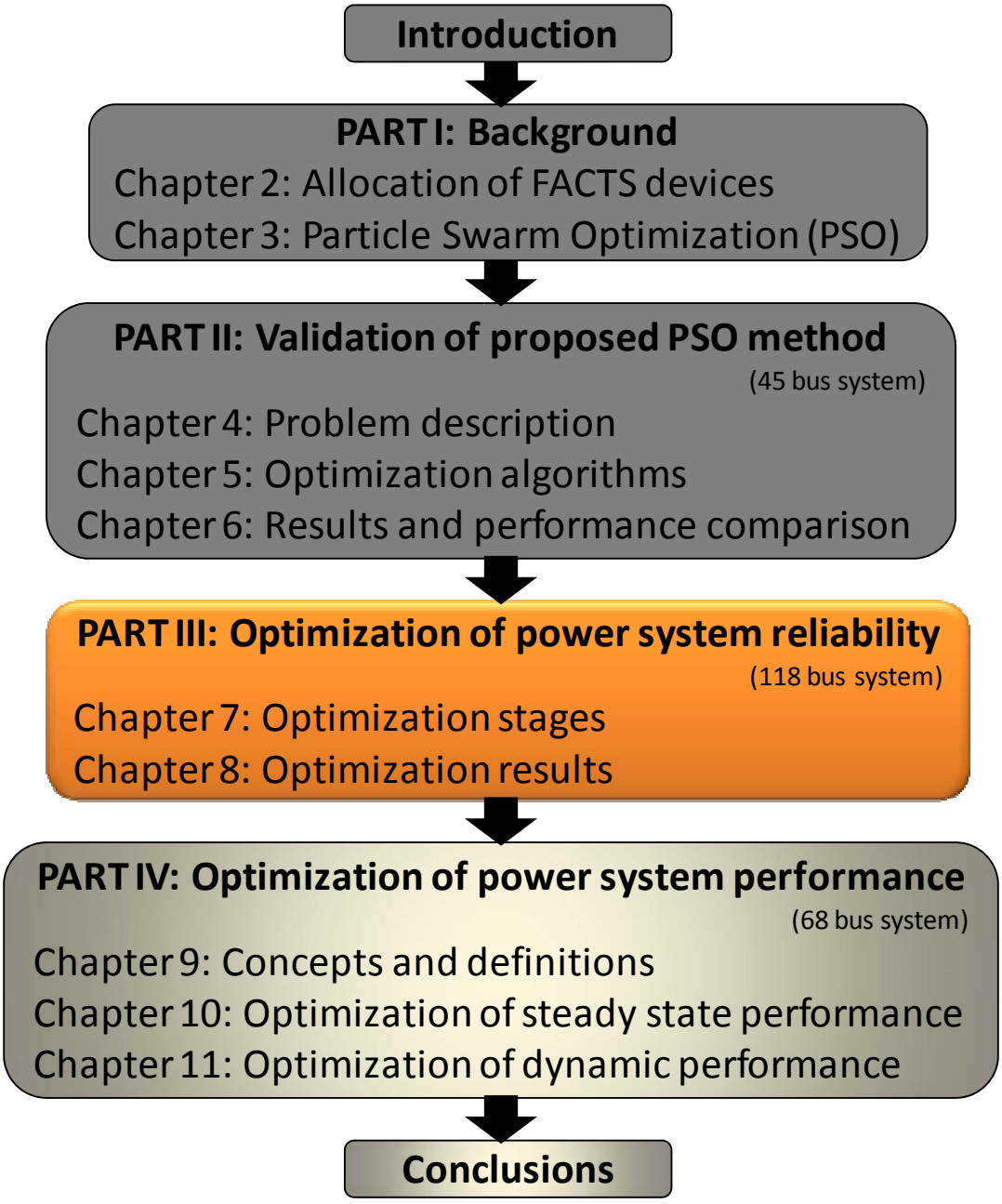

d

CHAPTER 7

PSO-BASED OPTIMIZATION FRAMEWORK

7.1 Introduction

This chapter introduces a multistage PSO-based optimization framework to improve the reliability of the power system using FACTS devices. The objective is to enable the IEEE 118 bus system to satisfy the N-1 security criterion using the existing infrastructure and new FACTS installations, in particular distributed static series compensators (DSSC) and static compensator (STATCOM) units, whose models are described in Appendix A.

The optimization process considers three stages:

(i) Security Constrained Optimal Power Flow (SCOPF) stage: it provides the optimal settings for the present power system infrastructure (optimal generator power output, transformers tap ratios, capacitor banks settings). These settings are found considering the economic dispatch and power system security constraints.

(ii) Series compensation stage: assuming the system to be fully deployed with DSSC units, this stage provides the optimal settings for each DSSC module. In particular, the value of the DSSC control reference is provided by the algorithm, considering global system controllability instead of traditional local control. The optimization objective is to maximize the line utilization factor (LUF) while minimizing the impact

on transmission losses and voltage profile. Emphasis is given to security constraints related to the number of overloaded lines and maximum line loading.

(iii) Shunt compensation stage: this stage provides the optimal number, location, rating, and control references for internal controllers of multiple STATCOM units in the power system. Analogous to the series FACTS devices, the STATCOM control references are provided considering global control, such that the maximum benefit is obtained over the entire power system, instead of focusing on immediate neighborhoods. The objective of this stage is to improve the voltage profile at minimum cost while giving special attention to the mitigation of undesired voltage violations.

7.2 Problem description

In this study, a modified version of the IEEE 118 bus system is used [90]. The one line diagram of the system is shown in Figure 7.1. The corresponding detailed data is presented in Appendix C.

As described above, the main objective is for this system to satisfy the N-1 security criterion using the existing infrastructure and new FACTS device installations.

This system has 186 branches and, therefore, 186 contingencies are considered as part of this study. In addition, the base case, where there is no contingency, is also analyzed.

Table 7.1 shows an example of the system condition for the base case (case 1) and

the first ten contingencies. The columns of Table 7.1 show the case number (#), the voltage deviation metric (V_{dev}), as defined in (4.1), total transmission power losses (P_{loss}), minimum and maximum voltage (V_{min} and V_{max}, respectively), number of overloaded lines (OVL), number of voltage violations ($V_{violations}$), which includes both the number of buses below 0.95 p.u. and the number of buses above 1.05 p.u.

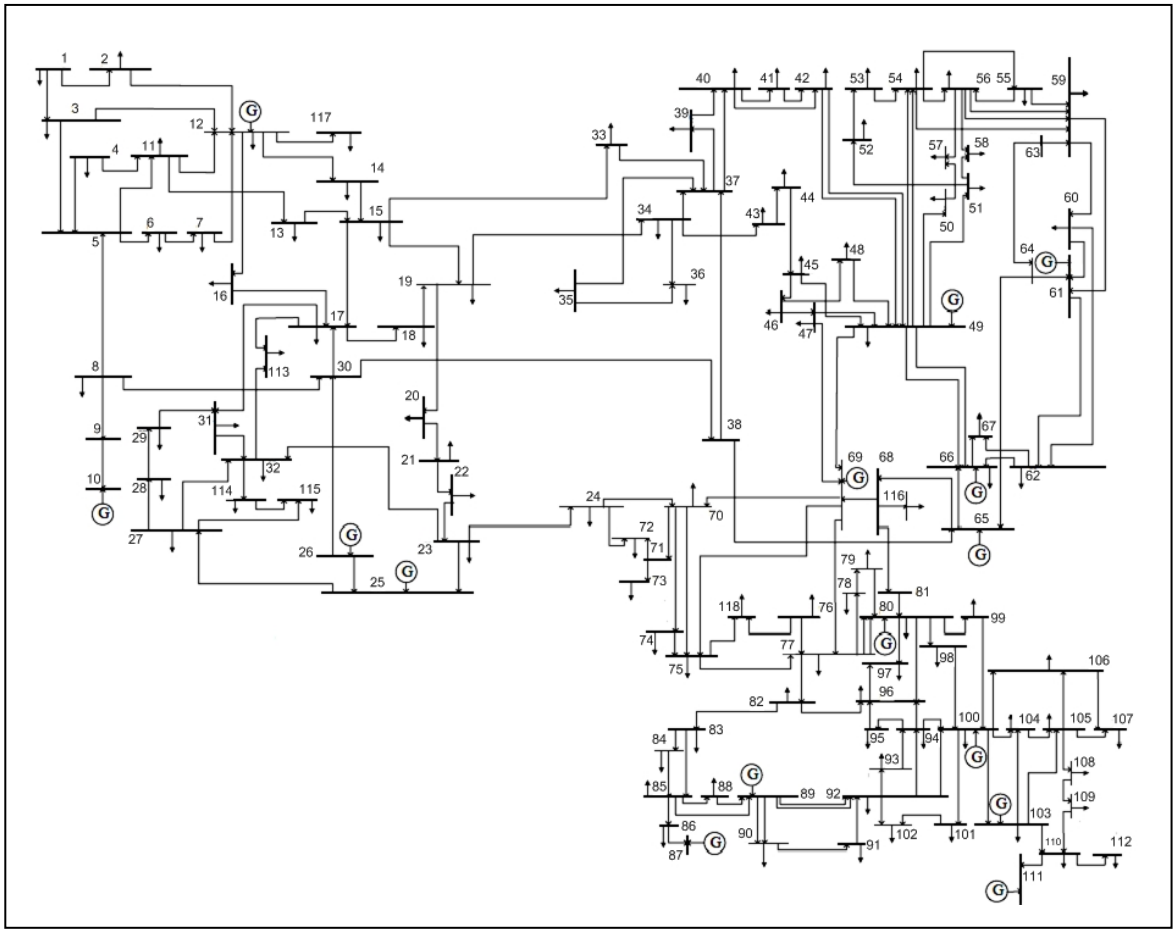

Figure 7.1: One line diagram of the modified IEEE 118 bus system

Table 7.1 shows ten example contingencies as well as the base case (case 1). Each contingency consists of removing a branch between the "From bus" and the "To bus".

Considering these examples, all cases require shunt compensation since the bus voltages exceed the desired limit of ±5% voltage deviation. Additionally, half the cases (4, 5, 6, 8, 9, and 11) require both shunt and series compensation since there is bus voltage violations as well as overloaded lines.

Table 7.1: Example of system condition for base case and 10 contingencies

Case #	From Bus	To Bus	V_{dev}	P_{loss} [W]	V_{min} [p.u.]	V_{max} [p.u.]	OVL	$V_{violations}$
1	-	-	0.309	116.6	0.93	1.05	0	4
2	1	2	0.315	117.0	0.93	1.05	0	6
3	1	3	0.320	118.4	0.91	1.05	0	5
4	4	5	0.311	119.6	0.93	1.05	2	4
5	3	5	0.317	120.1	0.93	1.05	1	6
6	5	6	0.308	119.6	0.93	1.05	1	4
7	6	7	0.311	117.4	0.93	1.05	0	5
8	8	9	0.559	185.9	0.88	1.063	2	36
9	9	10	0.493	179.0	0.89	1.05	1	31
10	4	11	0.309	117.7	0.93	1.05	0	4
11	5	11	0.309	118.0	0.93	1.05	1	4

There are three contingencies in the system that must be analyzed separately. These contingencies are shown in Table 7.2.

Table 7.2: Critical contingencies

Case #	From Bus	To Bus	V_{dev}	P_{loss} [W]	V_{min} [p.u.]	V_{max} [p.u.]	OVL	$V_{violations}$
169	110	112	1.043	115.12	0	1.05	0	4
176	12	117	1.046	115.49	0	1.05	0	5
179	5	8	3.353	798.93	0	1.05	10	44

In case 169, the branch out of service corresponds to the line from bus 110 to bus

112 and since this line is the only one that feeds bus 112 the voltage in that bus goes to zero. A similar situation occurs in case number 176 where the branch out of service corresponds to the one that connects buses 12 and 117. In this case, the voltage at bus 117 also drops to zero. Unfortunately in both cases, 169 and 176, the loads at isolated buses must be disconnected as no amount of compensation will maintain the supply to these buses.

A different situation occurs with case 179, which corresponds to the transformer that connects buses 8 and 5 being out of service. This is a catastrophic event that leads to voltage collapse in several areas of the system.

Considering all contingencies, with the exception of the three previous cases, the summary of the uncompensated system condition for the N-1 contingency analysis is presented in Table 7.3.

Table 7.3: Summary of system condition for N-1 contingency analysis

Max V_{dev}	**Max P_{loss} [MW]**	**V_{min} [p.u.]**	**V_{max} [p.u.]**	**Total OVL**	**Total $V_{violations}$**
1.170	186.83	0.63	1.06	22	1145

As Table 7.3 shows, the contingencies generate numerous violations that must be corrected by DSSC modules and STATCOM units. The optimization objective consists of satisfying the N-1 security criterion. This implies that, for all types of incidents leading to the disconnection of only one element (generator, circuit, line, transformer, etc.), all

bus voltages should remain within desired security limits and there are no overloaded lines in the system [91]. In other words, no single contingency should cause further outages in the system [92].

In order to determine the voltage security limits the Information Technology Industry Council (ITIC) curve, shown in Figure 7.2, is used [93]. As a primary objective, the bus voltages are kept within the range of ±5% voltage deviation; however in some contingencies, where it is not possible to accomplish this goal, the limits of ±10% voltage deviation, suggested by the ITIC curve, are used instead.

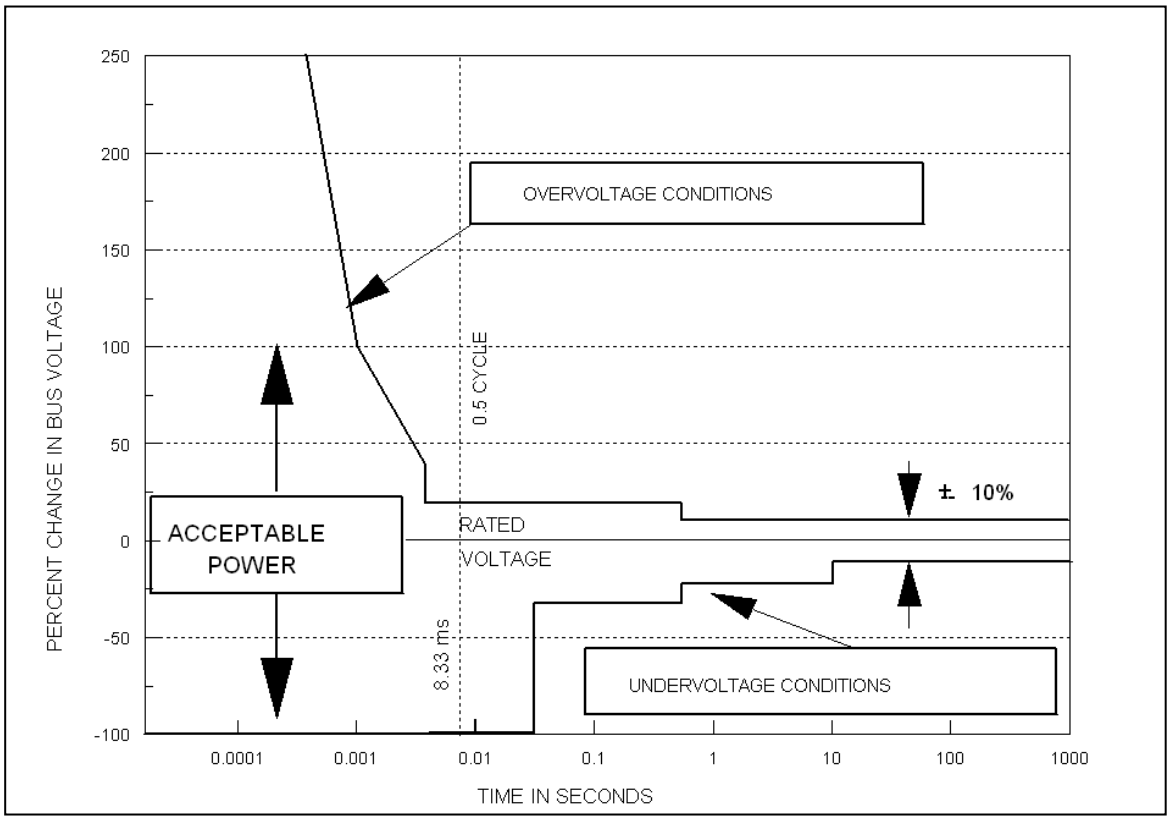

Figure 7.2: Information Technology Industry Council (ITIC) curve

7.3 Optimization stages

The multistage PSO optimization framework proposed in this study consists of three stages: (i) security constrained optimal power flow (SCOPF) stage (section 7.3.1), (ii) series compensation stage (section 7.3.2), and (iii) shunt compensation stage (section 7.3.3), as shown in Figure 7.3.

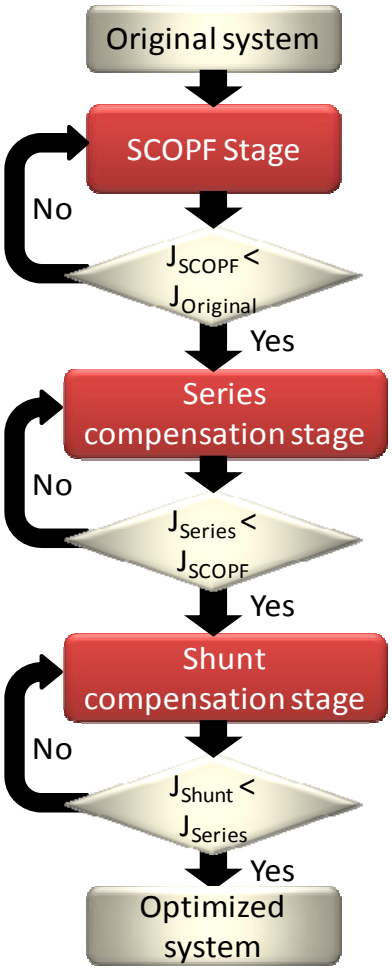

Figure 7.3: Flow chart, optimization of power system reliability

These optimization stages are sequentially applied to the problem. First, as a result of the SCOPF stage, the power system state is improved using the existing infrastructure. Then the overloaded lines are corrected in the series compensation stage using DSSC units. Finally, the shunt compensation stage improves the overall voltage profile and eliminates any undesired bus voltage violations.

The order in which these stages are performed is carefully selected. In order to minimize the cost of new FACTS installations, the available resources of the system are optimized first, and then the control references of the series FACTS devices (DSSCs) are optimally tuned. Since the operation of the DSSC modules may be detrimental to the voltage profile (if the overall inductive compensation is greater than the capacitive compensation) [94], this stage is carried out before shunt compensation is allocated in the system.

Each of these stages is described in detail in the next subsection, objective function, particle definition and search space constraints are comprehensively defined. The models for DSSC modules and STATCOM devices are described in Appendix A.

7.3.1 Security constrained optimal power flow (SCOPF) stage

An optimal power flow (OPF) program minimizes an objective function such as generation costs or transmission losses, by adjusting system variables, such as tap ratios, active and reactive generation, capacitor banks settings, etc. The OPF evaluates the nonlinear power flow equations and limits on bus voltages and line flows, however, the

optimal solution is valid only for the particular system conditions and constraints presented to the OPF [95].

The security constrained optimal power flow SCOPF extends the formulation of the OPF problem to include the effect of contingencies in the system. Particularly, the SCOPF program optimizes the objective function of interest while observing both the pre- and post-contingency system constraints.

Ideally, the control variables that optimize the system in its pre-contingency state remain in effect after any one of the contingencies occurs, in this case the value of the system settings are referred as a "preventive mode" setting. If no such preventive solution exists, the SCOPF program finds the optimal system settings to achieve the feasibility of the system in its post-contingency state [95].

In general, the SCOPF is a nonlinear, nonconvex, static, large-scale optimization problem with both continuous and discrete variables [96], and therefore it is not trivial to find a suitable optimization algorithm to solve it in an efficient manner. In this study, the proposed PSO method is used to solve the SCOPF problem.

The overall progress towards the fully optimized system considering the SCOPF stage is shown in Figure 7.4.

Fitness function definition

In its basic form, the main objective of the optimal power flow (OPF) is to minimize generation costs, which can be done by minimizing the fuel cost while

satisfying the load demand [97]. In this case, since the SCOPF approach is used, the pre- and post-contingency states of the system are also taken into account.

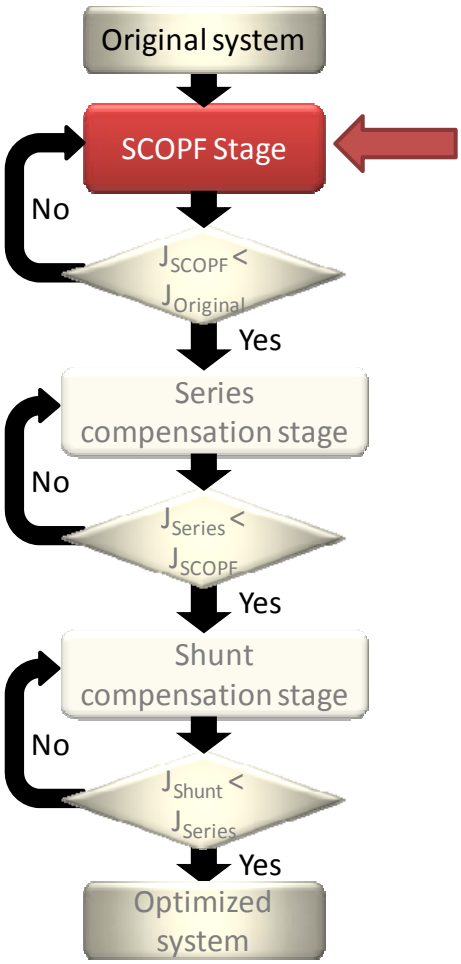

Figure 7.4: Flow chart, overall progress and SCOPF stage

The fuel cost of generating power is defined as follows:

$$FC = \sum_{i=1}^{Ng} \left(a_i \cdot P_{gi}^2 + b_i \cdot P_{gi} + c_i \right) \tag{7.1}$$

where:

FC is the total fuel cost of the system using present settings (potential solution),

N_g is the total number of generators,

P_{gi} is the real power output of generator unit *i,*

a_i, b_i, and c_i are fuel cost coefficients of generator unit *i.*

To use the value of the fuel cost as a metric in the PSO fitness function, it is required to normalize its value:

$$J_1 = FC \big/ FC_0 \tag{7.2}$$

where:

J_1 is the generation cost metric,

FC_0 is the generation cost metric before the system parameters are optimized.

In the case of this study, a modified version IEEE 118 bus system is used. This version includes 15 generators whose cost coefficients are shown in Table 7.4 [98].

In addition to the generation cost, it is desirable to improve the voltage profile of the power system. In this case, the following voltage deviation metric, equivalent to (4.1), is used.

$$V_{dev} = \sqrt{\sum_{i=1}^{Nbus} \left(V_i - 1\right)^2} \tag{7.3}$$

where:

V_{dev} is the voltage deviation metric for the system using present settings (potential solution),

N_{bus} is the total number of buses,

V_i is the value of the voltage at bus i in p.u.

$$J_2 = V_{dev} / V_{dev0} \tag{7.4}$$

where:

J_2 is the normalized voltage deviation metric,

V_{dev0} is the voltage deviation metric before the system parameters are optimized.

Table 7.4: Fuel coefficients for each generator unit

Gen #	Bus	a_i	b_i	c_i
1	10	0.005	2.45	130
2	12	0.007	3.45	70
3	25	0.007	3.45	70
4	26	0.005	1.89	150
5	49	0.0055	2	115
6	61	0.006	3.5	40
7	65	0.005	3.15	122
8	66	0.005	3.05	125
9	69	0.007	2.75	120
10	80	0.005	2.45	130
11	87	0.0045	1.6	200
12	89	0.0055	2.35	135
13	100	0.007	3.45	70
14	103	0.006	3.89	45
15	111	0.0055	3	35

The system security constrains are incorporated using a penalty function when a violation, either a bus voltage or a line overload, occurs. In this way, two metrics ((7.5) and (7.6)) are proposed that consider the violations in line loading: number of overloaded lines (OVL) and maximum loading, and two metrics ((7.7) and (7.8)) that address the bus violations: low voltage violations and high voltage violations.

$$J_3 = \begin{cases} OVL / OVL_0 & if\ OVL_0 > 0 \\ OVL & if\ OVL_0 = 0 \end{cases} \tag{7.5}$$

where:

J_3 is the overloaded lines metric,

OVL is the number of overloaded lines of the system using present settings (potential solution),

OVL_0 is the number of overloaded lines before the system parameters are optimized.

$$J_4 = \begin{cases} 0 & if\ OVL = 0 \\ \dfrac{Max\_loading}{Max\_loading_0} & if\ OVL > 0 \end{cases} \tag{7.6}$$

where:

J_4 is the maximum loading metric,

Max_loading is the maximum load among all overloaded lines for the system using present settings (potential solution),

Max_loading$_0$ is the maximum load among all overloaded lines for the system before its parameters are optimized.

$$J_5 = \begin{cases} Vbus\_low / Vbus\_low_0 & if\ Vbus\_low_0 > 0 \\ Vbus\_low & if\ Vbus\_low_0 = 0 \end{cases} \tag{7.7}$$

where:

J_5 is low voltage violation metric,

Vbus_low is the number of buses with low voltage violation (below 0.95 p.u.) for the system using present settings (potential solution),

Vbus_low$_0$ is the number of buses with low voltage violation for the system before its parameters are optimized.

$$J_6 = \begin{cases} Vbus\_high / Vbus\_high_0 & if\ Vbus\_high_0 > 0 \\ Vbus\_high & if\ Vbus\_high_0 = 0 \end{cases} \tag{7.8}$$

where:

J_6 is high voltage violation metric,

Vbus_high is the number of buses with high voltage violation (above 1.05 p.u.) for the system using present settings (potential solution),

$Vbus\_high_0$ is the number of buses with high voltage violation for the system before its parameters are optimized.

In the same fashion as with the generation metric, the number of overloaded lines, maximum loading, number of low bus voltages, and number of high bus voltages are each normalized with respect to their nominal values. The nominal values are defined as the values for the original system with settings presented in Appendix C.

The benefit of normalizing these metrics is that it allows all the values to have similar magnitudes. Additionally, it is easy to define the performance differences with respect to the base case: if the value of a metric is smaller than one, then there is an improvement. On the other hand, if the value of a metric is greater than one, then the system condition has worsened.

Considering the variables to optimize, namely generation cost and voltage profile, the problem becomes a multi-objective optimization problem. In addition, the security constraints are included in the objective function as penalty functions, giving the following design of the PSO fitness function:

$$J = \omega_1 \cdot J_1 + \omega_2 \cdot J_2 + \omega_{p1} \cdot J_3 + \omega_{p2} \cdot J_4 + \omega_{p3} \cdot J_5 + \omega_{p4} \cdot J_6 \qquad (7.9)$$

where:

J is the overall objective function,

ω_1, ω_2 are weights that reflect the relative importance of each objective (minimization of generation cost and improvement of voltage profile),

ω_{p1}, ω_{p2}, ω_{p3}, ω_{p4} are penalty weights that penalize system violations.

The selection of weights and penalty factors, as well as the cost and technical metrics, depend on the particular interest of the operator or utility. For this study, the following values are used: $\omega_1 = \omega_2 = 1$, $\omega_{p1} = \omega_{p2} = 2$, $\omega_{p3} = 3$, and $\omega_{p4} = 5$ The objective function weights and penalty factors presented here have been heuristically selected to illustrate the performance at each stage. Identical weights are selected for metrics J_1 and J_2, thus both objectives have the same importance in the optimization process.

Regarding penalty weights, lower penalty factors are assigned to line loading violations since the series compensation stage can effectively solve this issue. Following the same logic, the highest penalty factor is given to high voltage violation since they are difficult to resolve.

Particle definition

The system parameters, that represent the decision variables, are the generator's active power output and terminal voltage, transformer tap ratios, transformer phase angle (only one phase shifter transformer in the system), and capacitor banks settings. All these settings are part of the PSO particle definition.

Generator's active power output and voltage

Considering all 15 generator units, the generator's decision vector is defined as:

$$X_g = \begin{bmatrix} P_{g1} & V_1^{ref} & P_{g2} & V_2^{ref} & \dots & P_{gNg} & V_{Ng}^{ref} \end{bmatrix} \tag{7.10}$$

where:

X_g is the vector of generator settings (active power outputs and voltages), where $X_g \in \Re^{30}$,

P_{gh} is the real power output of generator unit h, $h \in \{1, 2, ..., N_g\}$,

V_h^{ref} is voltage regulator reference of generator unit h, $h \in \{1, 2, ..., N_g\}$,

N_g is the total number of generator units.

Transformer tap ratio

There are 8 variable tap transformers, thus the decision vector in this case is:

$$X_t = \begin{bmatrix} tap_1 & tap_2 & \dots & tap_{Nt} \end{bmatrix} \tag{7.11}$$

where:

X_t is the vector containing the tap settings of all 8 transformers, $X_t \in \Re^8$,

N_t is the total number of variable tap ratio transformers.

Transformer phase shift

Since there is one phase shifting transformer, for this particular element the decision vector is:

$$X_{tps} = \begin{bmatrix} tap & angle \end{bmatrix} \tag{7.12}$$

where:

X_{tps} is the vector of the transformer's tap setting and phase angle, $X_{tps} \in \Re^2$

Capacitor bank settings

Finally, the system has 14 capacitor banks, whose reactive power injection can be adjusted. Therefore, the following decision vector is defined:

$$X_{cap} = \begin{bmatrix} Q_1 & Q_2 & \dots & Q_{Ncap} \end{bmatrix} \tag{7.13}$$

where:

X_{cap} is the vector containing the setting for reactive power injection of each capacitor bank, $X_{cap} \in \Re^{14}$,

N_{cap} is the total number of capacitor banks in the system,

Q_i is the reactive power injection of capacitor bank i, $i \in \{1, 2, \dots N_{cap}\}$.

Considering the decision vector of all previous system settings, the PSO particle, x_i, is defined as:

$$x_i = \begin{bmatrix} X_g & X_t & X_{tps} & X_{cap} \end{bmatrix} \tag{7.14}$$

According to the dimension of the system's decision vectors, the resulting dimension of the vector x_i is 54 ($x_i \in \Re^{54}$)

Search space definition

For each of the components of the PSO particle, X_g, X_t, X_{tps} and X_{cap}, the corresponding settings' limits are taken into account, giving the following search space definition.

In the case of X_g, the maximum active power that each generator can deliver and the maximum bus voltage are considered as constraints:

$$P_h^{\min} \le P_h \le P_h^{\max}, \quad h \in \{1, 2, ..., N_g\} \tag{7.15}$$

where:

P_h^{min} is the minimum active power that generator unit h can deliver,

P_h^{max} is the maximum active power that generator unit h can deliver.

$$0.95 \le V_h^{ref} \le 1.05, \quad h \in \{1, 2, ..., N_g\} \tag{7.16}$$

The actual values for the generator active power limits are shown in Appendix C.

Considering the transformer's tap ratio, X_t, the following constraint is defined:

$$0.8 \le tap_j \le 1.2, \quad j \in \{1, 2, ..., N_t\} \tag{7.17}$$

where:

tap_j is the tap setting of transformer unit j.

In the case of the phase shifter transformer, the previous limits, (7.17), apply for the first component of the vector, *tap*. The phase angle is limited by:

$$-15^\circ \le angle \le 15^\circ \tag{7.18}$$

Finally the constraints associated with the capacitor bank settings are as follows:

$$Q_k^{\min} \le Q_k \le Q_k^{\max}, \quad k \in \{1, 2, ..., N_{cap}\} \tag{7.19}$$

where:

Q_k^{min} is the minimum reactive power setting of capacitor bank k.

Q_k is the present reactive power setting of capacitor bank k.

Q_k^{max} is the maximum reactive power setting of capacitor bank k.

The actual limits for the reactive power setting of each capacitor bank are given in Appendix C.

In addition to the limits for each component of the decision vector (PSO particle), the system constraints also define the feasible region of the problem hyperspace. For this particular application, the system constraints that keep all the line flows and bus voltages within limits are incorporated in the main objective function as the penalty functions in (7.5)-(7.8).

Finally the following restriction is applied to the candidate solutions: if the solution of the any particle leads to an objective function value that is worse than the original case, then the objective function value is set to infinity. In other words, this declares this particle as infeasible.

$$J_i = \begin{cases} J_i & if \quad J_i \le J_0 \\ \infty & if \quad J_i > J_0 \end{cases} \tag{7.20}$$

where:

J_i is the objective function value of particle i,

J_0 is the objective function value of the original system (Appendix C).

PSO parameters

The concept of fine tuning the PSO algorithm is introduced at this stage as a tool for finding the optimal values of the system parameters in (7.14).

Since the decision vector in (7.14) considers 54 different settings, it is difficult to find solutions that allow the stable operation of the system. Therefore, the following rules are applied to the PSO algorithm:

- All the particles are randomly initialized except one. This single particle is initialized at the original system settings (shown in Appendix C).
- The maximum PSO velocity is limited in each dimension of the problem hyperspace to be at most 10% of the corresponding particle's limits.

Other PSO parameters are presented in Table 7.5.

Table 7.5: PSO parameters, SCOPF stage

Parameter	Tested values
Inertia constant	Linearly decreased inertia weight
Individual acceleration constant (c_1)	2.5
Maximum velocity	10% of corresponding limits
Number of particles	15
Maximum number of iterations	100

Once the SCOPF stage is performed, the obtained objective function value (J_{SCOPF}) is compared with the one corresponding to the original system settings ($J_{Original}$). If the J_{SCOPF} value results to be better than the original ($J_{SCOPF} < J_{Original}$), then the next optimization stage is performed, otherwise a new trial of the SCOPF routine is carried out.

7.3.2 Series compensation stage

The purpose of this optimization stage is to find the optimal control reference for the DSSC modules. The solution provided by this optimization stage informs the operator of the system the optimal values for all line reactances that need to be achieved by the DSSC modules. These values assure the optimal performance of the overall system considering the line utilization factor, transmission losses and, particularly, security margins. The algorithm provides the solution for the system in its base case (case 1 in Table 7.1) as well as for the different contingencies.

The overall progress towards the fully optimized system considering is shown in Figure 7.5.

In this study the DSSC modules are represented as lumped devices with the capability of changing the line reactance by up to 20% in both directions (increase and decrease). The system is assumed to be fully deployed, meaning that the operator has the capability of controlling all the lines of the system.

The interaction between turbine-generators and the capacitive compensation of DSSC modules, that may potentially lead to sub synchronous oscillations (SSO) [99], is not part of this study, and therefore the phenomenon sub synchronous resonance (SSR) is neglected in the optimization objectives. Nevertheless, the requirement of avoiding SSO can be added in the optimization problem (either as an optimization objective or as a constraint) when turbine-governors and electromagnetic flux dynamics are modeled in the system.

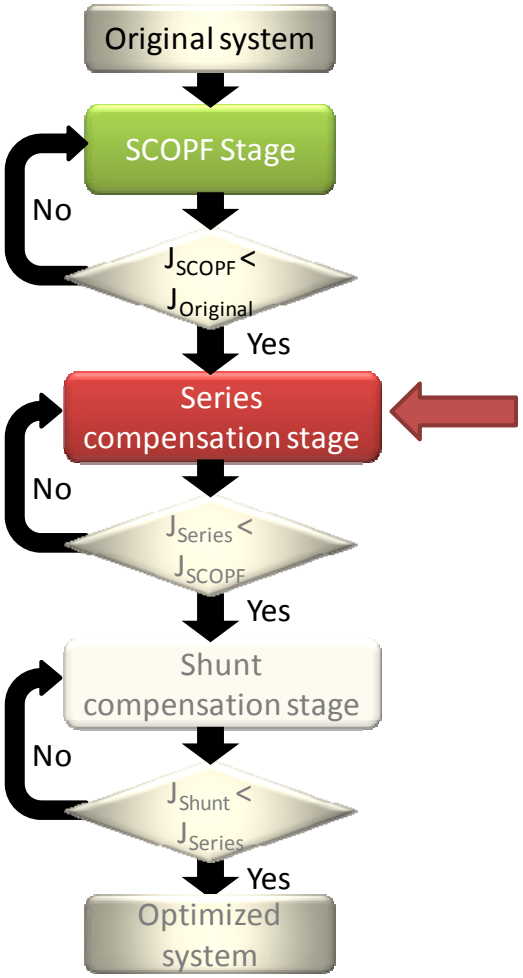

Figure 7.5: Flow chart, overall progress and series compensation stage

Fitness function definition

The objective function considers two goals (multiobjective function) as well as security constraints that are incorporated into the main objective as penalty functions.

The goal is to maximize the LUF, keeping the transmission losses as close as possible to the equivalent case considering the original system settings.

To accomplish this objective the following metrics are defined:

$$LUF = \sum_{i=1}^{N_L} \frac{I_i}{I_i^{nom}} \tag{7.21}$$

where:

LUF is the line utilization factor of the system,

I_i is the current flowing in line i for present settings (potential solution),

I_i^{nom} is the nominal current in line i,

N_L is the number of lines in the system.

$$J_1 = LUF_0 \Big/ LUF \tag{7.22}$$

where:

J_1 is the line utilization factor metric,

LUF_0 is the LUF before the system parameters are optimized.

$$J_2 = P_{loss} \Big/ P_{loss0} \tag{7.23}$$

where:

J_2 is the transmission losses metric,

P_{loss} is the total transmission losses using present settings (potential solution),

P_{loss0} is the total transmission losses before the system parameters are optimized.

The power system stability constraints (no overloaded lines and no voltage violations) are also included in the main objective as penalty functions. In this case, the same security constraints as in the previous optimization stage (SCOPF) are used. The definition of these metrics corresponds to those presented in (7.5)-(7.8).

Therefore the overall objective function (J) is defined as:

$$J = \omega_1 \cdot J_1 + \omega_2 \cdot J_2 + \omega_{p1} \cdot J_3 + \omega_{p2} \cdot J_4 + \omega_{p3} \cdot J_5 + \omega_{p4} \cdot J_6 \qquad (7.24)$$

where:

J is the overall objective function,

ω_1, ω_2 are weights that reflex the relative importance of each objective (maximization of LUF and minimization of transmission losses),

ω_{p1}, ω_{p2}, ω_{p3}, ω_{p4} are penalty weights that penalize system violations.

The selection of weights and penalty factors, as well as the technical criteria that need to be satisfied, depend on the particular interest of the operator or utility. In this case, the values of $\omega_1 = \omega_2 = 1$, $\omega_{p1} = 5$, $\omega_{p2} = 1$, $\omega_{p3} = 0.25$, and $\omega_{p4} = 1$, are used.

This selection of weights gives equal importance to the improvement of LUF and transmission losses. However the highest priority is given to correcting the number of overloaded lines. If the lines continue operating above their thermal limits, cascade outages will lead the system to voltage collapse. To avoid this situation, the main purpose

of this stage is to reduce the number of overloaded lines (J_3) to zero if possible. A second metric that helps with this purpose is J_4, the maximum line loading.

Regarding the penalty weights for bus voltage violations, little penalty is given to low bus voltages since the next stage, which optimally allocates shunt compensation, will compensate these buses.

Particle definition

The PSO particle is defined as the vector containing the line reactances of the system. There are 177 transmission lines and therefore the particle vector has 177 components, $x_i \in \Re^{177}$.

$$x_i = \begin{bmatrix} X_{L1} & X_{L2} & \dots & X_{L177} \end{bmatrix} \tag{7.25}$$

where:

x_i is the PSO particle's vector, also called decision vector,

X_{Lk} is the line reactance of line k, $k \in \{1,2,...,177\}$.

Search space definition

The components of the PSO particle are limited by the maximum compensation that the DSSC units can provide, which in this case correspond to 20% of the value of the corresponding line reactance.

$$0.8 \cdot X_{Lk}^{0} \le X_{Lk} \le 1.2 \cdot X_{Lk}^{0}, \quad k \in \{1,2,...,177\} \tag{7.26}$$

where:

X_{Lk}^{0} is the original reactance of line k (i.e. without DSSC modules).

The values of all original line reactances are shown in Appendix C.

In the case of the system constraints (feasible region), they are included in the main objective function as the penalty functions in (7.5)-(7.8).

Besides the limits of each component of the decision vector and system constraint, the following criterion is applied to the candidate solutions:

$$J_i = \begin{cases} J_i & if \quad J_{3,i} \le J_3^o \\ \infty & if \quad J_{3,i} > J_3^o \end{cases} \tag{7.27}$$

where:

J_i is the objective function value of particle i using present settings (potential solution),

$J_{4,i}$ is the value of metric J_4 of particle i using present settings,

J_4^0 is the value of metric J_4 before the system parameters are optimized.

The metric defined in (7.27) strongly rejects all solutions that have more overloaded lines than the original case.

PSO parameters

The concept of fine tuning PSO, as described in section 7.3.1, is also utilized in this stage, to aid the search for optimal line reactance's values.

A summary of the PSO parameters is presented in Table 7.6.

Table 7.6: PSO parameters, series compensation stage

Parameter	Tested values
Inertia constant	Linearly decreased inertia weight
Individual acceleration constant (c_1)	2.5
Maximum velocity	10% of corresponding limits
Number of particles	15
Maximum number of iterations	100

Once the series compensation stage is performed, the obtained objective function value (J_{Series}) is compared with the one corresponding to the SCOPF stage (J_{SCOPF}). If this value results to be better than the one achieved in the previous stage ($J_{Series} < J_{SCOPF}$), then the next optimization stage is performed, otherwise a new trial of the series compensation routine is carried out.

7.3.3 Shunt compensation stage

The shunt compensation stage is the last step in the optimization process. Its objective is to find the optimal locations and sizes of shunt FACTS devices, in this case STATCOM units, such that the number of bus voltage violations is minimized both for the base case (where all elements of the system are in service) and under contingency

conditions. The STACOM units are selected as an illustrative example; but the same methodology can be applied to SVC devices or capacitor banks.

The overall progress towards the fully optimized system considering the shunt compensation stage is shown in Figure 7.6.

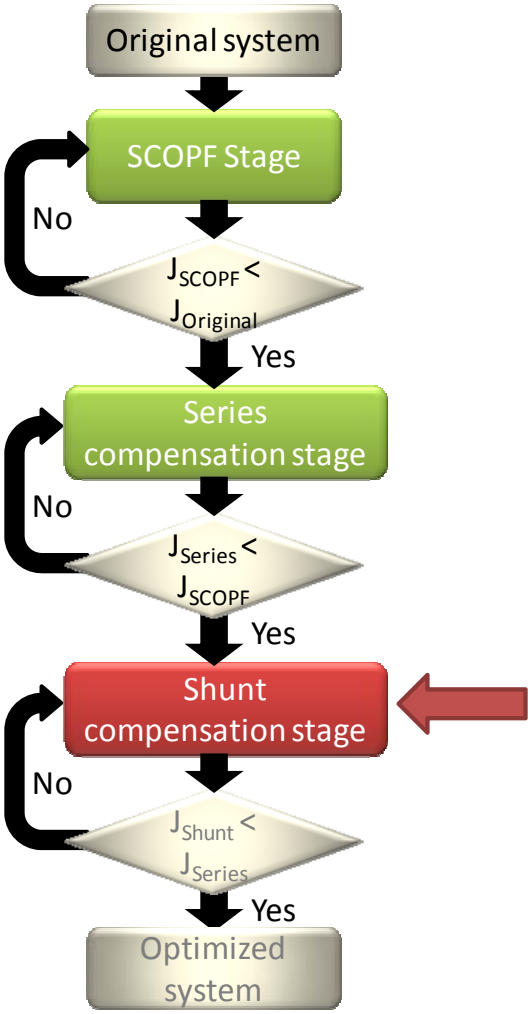

Figure 7.6: Flow chart, overall progress and shun compensation stage

The optimization objective considers the cost of installation of these units and, therefore, the number of units to be allocated in the system, must also be minimized.

In addition to the location and rating of these units, this stage also provides the operator with the information on which STATCOM units should be operating and the corresponding optimal settings for their voltage references, such that the power system performance is improved and the system remains stable under different contingencies.

Consequently this stage considers two independent optimization algorithms. The first corresponds to the optimal allocation algorithm (which finds location and sizes) while the second is the optimal settings algorithm (which finds optimal voltage references for each unit).

The interaction between the two algorithms is shown in Figure 7.7.

- Starting with the system in its base case (with all components in service), the optimal allocation algorithm finds promising locations and sizes for a number STATCOM units. The number of STATCOM units is minimized, by including a penalty function in the cost metric.
- Once promising locations and sizes are found, the optimal settings algorithm is carried out to find the optimal voltage reference of each STATCOM's controller, such that the minimum number of voltage violations occurs in the system. The global optimum value is obtained when there are no voltage violations.
- If the solution, with optimal settings, cannot satisfy a pre-defined level of performance, then the solution is rejected.
- If the performance is considered above the specified standards, after the optimal settings are obtained for the base case, the system is subjected to the effect of

different contingencies. For each contingency the optimal STATCOM settings are then calculated to find the best performance under the corresponding system topology.

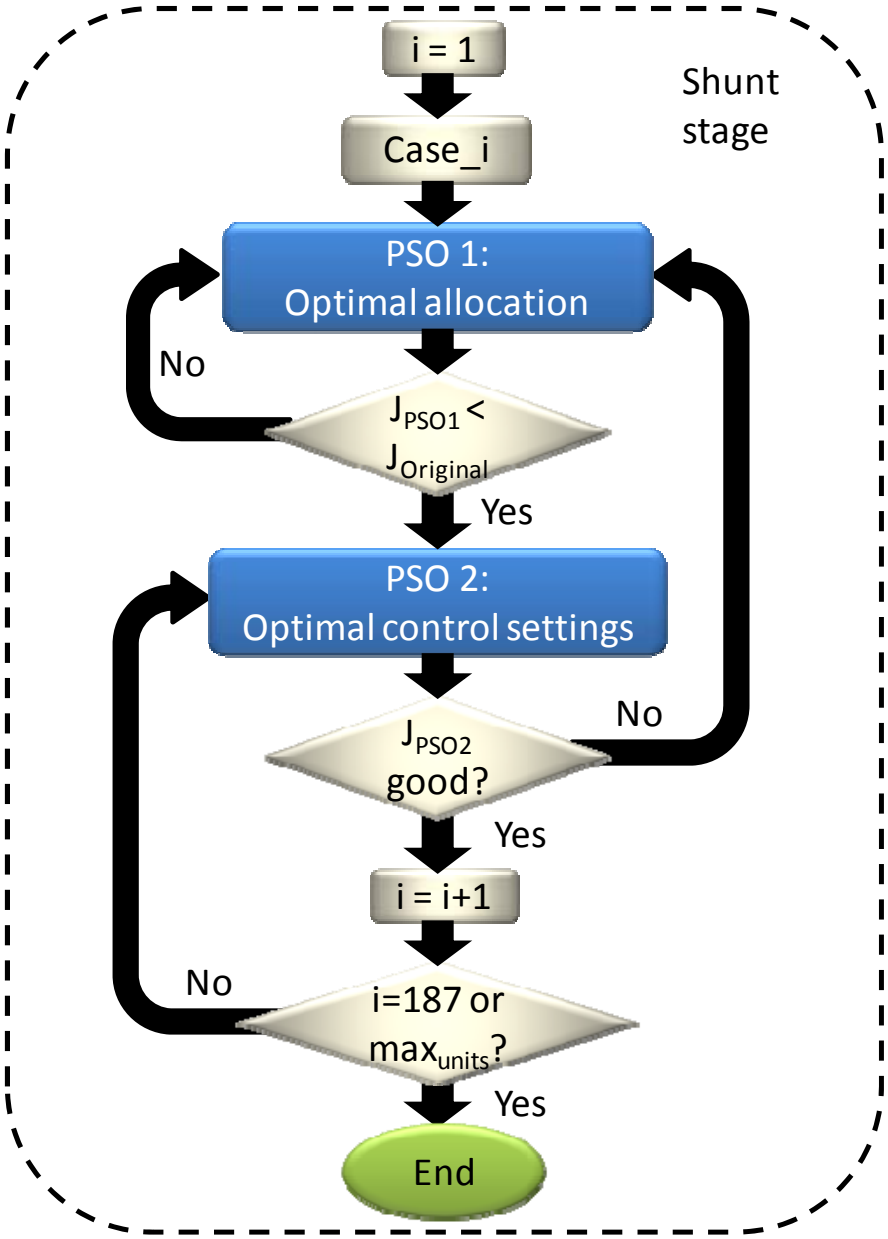

Figure 7.7: Flow chart, two step optimization process for shunt compensation stage

- If it is not possible to maintain the bus voltages within security limits, the optimal allocation algorithm is performed to find locations and sizes for new units. Later, optimal settings are found to improve the performance of the system.
- The process is repeated until the system operates in stable condition for the base case and all contingencies, or a maximum number of STATCOM units is reached.

7.3.3.1 Optimal allocation algorithm

Fitness function definition

Analogous to the series compensation stage, the objective function considers two goals as well as security constraints that are incorporated in the main objective as penalty functions.

The goal is to improve the voltage profile of the system, by minimizing the voltage deviations, with the minimum number and sizes of units.

To accomplish the previous goal the following cost metric is considered:

$$J_1 = \frac{1}{2} \cdot \left(\frac{N_{units}}{N_{units}^{\max}} + \sum_{i=1}^{Nunits} \frac{\eta_i}{N_{units}^{\max} \cdot \eta^{\max}} \right) \tag{7.28}$$

where:

J_1 is the STATCOM cost metric,

N_{units} is the number of units allocated in the present solution,

$N_{units}^{\max}$ is the maximum number of units that can be allocated in the system,

η_i is the size or rating of STATCOM unit i, $i \in \{1, 2, ..., N_{units}\}$,

η^{max} is the maximum STATCOM size or rating in MVA.

The cost metric in (7.28) has two components, the first component acts as a penalty factor when the number of units increases. In particular, if the number of units is greater that a predefined maximum number, $N_{units}^{\max}$, the value of this component in the objective function becomes greater than one. For this study, the maximum number of units is set to 15. From the economic perspective this first component can also be understood as a normalized value of the fixed costs associated with the installation of each STATCOM.

The second component of metric J_1 is related to the variable cost component of each device. In this case, this cost is assumed to be a linear function of the size of the unit. As a result, if the STATCOM has a larger rating then it also has a higher cost. The value of this component is normalized by the total MVA that can be allocated in the system, which is calculated as the product of the maximum number of STATCOM units and the maximum allowed size η^{max}. In this case, the maximum STATCOM size is set to 250 MVA.

Each component of the STATCOM cost metric (7.28) is normalized to have comparable values around one. Since the metric is defined as the summation of the two components, a factor of 0.5 is also added to make the overall value to be around one, and therefore be comparable with other metrics in the objective overall function.

Another metric used in this stage corresponds to the normalized voltage deviation metric (J_2) which has the same definition as in (7.4).

In addition, the system security constraints (related to overloaded lines and bus voltage violations) are included in the main objective function using the metrics, J_3 - J_6, defined in (7.5)-(7.8).

Finally, the overall objective function is defined as:

$$J = \omega_1 \cdot J_1 + \omega_2 \cdot J_2 + \omega_{p1} \cdot J_3 + \omega_{p2} \cdot J_4 + \omega_{p3} \cdot J_5 + \omega_{p4} \cdot J_6 \qquad (7.29)$$

where:

J is the overall objective function,

ω_1, ω_2 are weights that reflect the relative importance of the cost metric and the normalized voltage deviation metric,

ω_{p1}, ω_{p2}, ω_{p3}, ω_{p4} are penalty weights that penalize system violations.

As mentioned in previous stages, the values of the weights and penalty factors, as well as the definition of the technical and cost metrics, can be adjusted to reflect the particular interest of operators and utilities. Some metrics can be emphasized with respect to others depending on the particular power system and management policies. In this particular study, the following values are used: $\omega_1 = \omega_2 = 1$, $\omega_{p1} = \omega_{p2} = 25$, $\omega_{p3} = \omega_{p4} = 5$.

The selection of the weight values gives equal importance to the economic and the technical criteria. The penalty factors are adjusted so that there is a high penalty for

those solutions that improve the voltage profile but overload the transmission lines. This situation is extremely undesirable and needs to be avoided, in other words, the algorithm should preserve the results obtained from the previous optimization stage (series compensation stage).

The number of bus voltage violations has higher importance as compared with the original cost metric (7.28) and normalized voltage deviation metric (7.4). The reason for this particular rule corresponds to the overall purpose of improving the reliability of the system. In this way, maintaining the system within security limits becomes a priority.

Particle definition

The PSO particle definition (decision vector) is defined as:

$$x_i = \left[\lambda_1 \quad \eta_1 \quad \lambda_2 \quad \eta_2 \quad \ldots \quad \lambda_{Nunits} \quad \eta_{Nunits}\right] \tag{7.30}$$

where:

λ_h is the location of STATCOM unit h, $h \in \{1, 2, ..., N_{units}\}$,

η_h is the size of STATCOM unit h, $h \in \{1, 2, ..., N_{units}\}$.

Search space definition

The constraints used in this optimization stage are those described in (4.4)-(4.7).

PSO parameters

The PSO parameters are presented in Table 7.7.

Table 7.7: PSO parameters, shunt compensation stage, optimal allocation

Parameter	Tested values
Inertia constant	Linearly decreased inertia weight
Individual acceleration constant (c_1)	2.5
Maximum velocity for bus location	25
Maximum velocity for STATCOM size	50
Number of particles	25
Maximum number of iterations	300

7.3.3.2 Optimal settings algorithm

Fitness function definition

The objective of this PSO routine is to find the optimal voltage references of the STATCOM control units such that the best performance of the system is obtained. Since the reliability of the system is the main concern of this study, the fitness function corresponds to the total number of voltage violations. The global optimum value is when the STATCOM settings allow the system to have zero violations ($J=0$).

$$J = Vbus\_low + Vbus\_high \tag{7.31}$$

where:

J is the overall objective function,

Vbus_low is the number of buses with low voltage violation (below 0.95 p.u.),

Vbus_high is the number of buses with high voltage violation (above 1.05 p.u.).

Particle definition

The PSO particle definition is defined as:

$$x_i = \left[V_1^{ref} \quad V_2^{ref} \quad ... \quad V_{Nunits}^{ref} \right] \tag{7.32}$$

where:

V_h^{ref} is the voltage reference of STATCOM unit *h*, $h \in \{1, 2, ..., N_{units}\}$.

Search space definition

Only one constraint applies to this problem:

$$0.95 \le V_h^{ref} \le 1.05, \quad h \in \{1, 2, ..., N_{units}\} \tag{7.33}$$

The voltage reference cannot exceed the voltage limits of 0.95 and 1.05 p.u. If a particle solution leads to a voltage reference greater than 1.05 then this value is changed to the upper bound of 1.05. On the other hand, if the particle's solution proposes a voltage reference smaller than 0.95 then the unit is disconnected otherwise a detrimental effect to the voltage profile of the system will occur.

PSO parameters

The concept of fine tuning PSO, as described in section 4.3.1, is utilized in this stage to obtain the maximum efficiency in the search for optimal STATCOM settings.

A summary of the PSO parameters is presented in Table 7.8.

Table 7.8: PSO parameters, shunt compensation stage, optimal setting

Parameter	Tested values
Inertia constant	Linearly decreased inertia weight
Individual acceleration constant (c_1)	2.5
Maximum velocity	50% of corresponding limits
Number of particles	30
Maximum number of iterations	100

7.5 Summary

This chapter describes a proposed PSO-based optimization framework to solve the problem of improving the power system's reliability using FACTS devices.

In particular, a modified version of the IEEE 118 bus system is used to study the effect of optimizing present system infrastructure and new FACTS installations to make the system N-1 secure.

The optimization process is carried out considering three sequential stages: (i) SCOPF stage, (ii) series compensation stage, and (iii) shunt compensation stage.

The first stage, SCOPF, utilizes the concept of security constrained optimal power flow to optimize the settings of present equipment (transformer's tap ratios, generator's outputs, etc.) such that the generation cost and voltage profile are improved.

The optimization is performed for a base case (all components in service) and for the 186 branch outages that correspond to the N-1 contingency criteria. For this reason, special emphasis is given to satisfying security limits to avoid overloaded lines and bus voltage violations.

From the optimization perspective the concept of fine tuning PSO, which limits the maximum velocity to a small percentage of the variable's range of movement, is introduced to aid in the search mechanism. In addition, the system security constraints for overloaded lines and bus voltage violations are included in the main objective function as penalty factors. In general, this optimization framework has shown to be very efficient in avoiding solutions that lead to system instability.

The second stage, called the series compensation stage, is used to relieve transmission lines congestion using distributed FACTS devices, in particular DSSC modules. The system is assumed to be fully deployed, meaning that there is full controllability of all transmission lines. The DSSC is modeled as a lumped device with the capability of changing the value of the corresponding line reactance by 20% in either direction (increase or decrease).

The results of the optimization process are the optimal control settings for each DSSC module, such that the number of overloaded lines is minimized and the line utilization factor is improved with a minimum impact over the total transmission losses of the system. The control settings correspond to the control reference, in this case the desired value for the line reactance of each transmission line. It is important to note that the value of the reference provides optimal global control over the power system as

opposed to local control where only the close neighborhood of the transmission line experiences an improvement.

Finally, the shunt compensation stage uses a two step optimization process. The first step provides optimal allocation and rating for shunt FACTS devices, in this case STATCOM units, and the second step indicates whether the units have to be in service and, if so, what is the optimal control reference, in this case the voltage at the point of common coupling.

The technical criteria for the shunt stage correspond to the improvement of voltage profile (minimization of voltage deviations) at minimum cost. Analogous to the first two stages (SCOPF and series compensation), special attention is given to maintaining all system variables within security limits.

The multistage PSO-based optimization framework, discussed in this chapter, is then applied to the problem of optimizing the reliability of a modified version of the IEEE 118 bus system. The obtained results are reported and discussed in the next chapter.

CHAPTER 8

OPTIMIZATION OF POWER SYSTEM RELIABILITY

8.1 Introduction

Chapter 7 introduced a multistage PSO-based optimization framework to improve the reliability of the power system, where the objective is to enable the IEEE 118 bus system to satisfy the N-1 security criterion using the existing infrastructure and new FACTS installations, in particular DSSC and STATCOM units (models described in Appendix A).

The proposed optimization process considers three stages: (i) security constrained optimal power flow (SCOPF) stage, (ii) series compensation stage, and (iii) shunt compensation stage.

This chapter presents the analysis of the obtained simulation results. First the study focuses on the overall improved reliability once all three optimization stages are completed. The improvement is discussed considering the base case (all elements in service) and the first ten contingencies followed by a detailed analysis of three critical contingencies. Finally a summary of the system state for the base case and all 186 contingencies is presented and discussed.

Second, the specific results for each optimization stage are reported for two illustrative cases: the base case (case 1), where there is no contingency, and case 32, where the line that connects buses 25 and 27 is taken out of service.

8.2 Analysis of improved reliability

Due to the large amount of information (base case plus 186 contingencies), the simulation results to the problem of improving the reliability of the power system using FACTS devices are presented as follows:

- A general overview of the system state is presented in Table 8.1 for the base case and the first ten contingencies (section 8.2.1). This information is compared with the state of the system prior to the optimization process presented in Table 7.1.
- There are three critical contingencies that required a separate analysis, which are presented in Table 8.2. The comparison between the optimized system state and the original system state (in Table 7.2) is discussed (section 8.2.2).
- Then a summary, analogous to Table 7.3, is presented that considers the base case (all elements in service) and all contingencies (section 8.2.3).

8.2.1 Results for base case and first ten contingencies

Table 8.1 shows the system state after all three optimization stages are completed for case 1 (all elements in service) and the first ten contingencies. The columns of Table 8.1 show the voltage deviation metric (V_{dev}) as defined in (7.3), the total power losses (P_{loss}), the minimum and maximum bus voltages (V_{min} and V_{max} respectively), the number of overloaded lines (OVL) and the number of voltage violations ($V_{violations}$).

There are remarkable differences between the state of the system before the optimization process is performed (Table 7.1) and thereafter (Table 8.1). In order to

clearly visualize these differences, they are graphically illustrated in Figure 8.1 to Figure 8.4.

Table 8.1: Optimized system condition for base case and 10 contingencies

Case #	From Bus	To Bus	V_{dev}	P_{loss} [W]	V_{min} [p.u.]	V_{max} [p.u.]	OVL	$V_{violations}$
1	-	-	0.258	122.1	0.952	1.050	0	0
2	1	2	0.253	107.6	0.951	1.050	0	0
3	1	3	0.255	121.4	0.952	1.046	0	0
4	4	5	0.253	133.4	0.951	1.050	0	0
5	3	5	0.256	114.6	0.951	1.050	0	0
6	5	6	0.260	112.4	0.952	1.050	0	0
7	6	7	0.243	121.2	0.950	1.050	0	0
8	8	9	0.272	156.7	0.951	1.050	0	0
9	9	10	0.248	121.0	0.950	1.050	0	0
10	4	11	0.246	128.3	0.950	1.050	0	0
11	5	11	0.255	112.6	0.950	1.050	0	0

Figure 8.1 shows the values of the voltage deviation metric (V_{dev}), as defined in (7.3), for case 1 (all elements in service) and the first ten contingencies (cases 2 to 11). The red bar, labeled "Pre", shows the values of this metric with the original system settings (i.e. before the optimization process is performed); the green bar, labeled "Post", indicates the value of the metric for the optimized system (i.e. after all three optimization stages have been carried out).

A comparison of the heights of the red and green bars for each case shows that the voltage profile is substantially improved. In fact, there is an average of 25% decrement in the voltage deviation metric, and in some cases (number 8 and 9) the reduction is as much as a 50%.

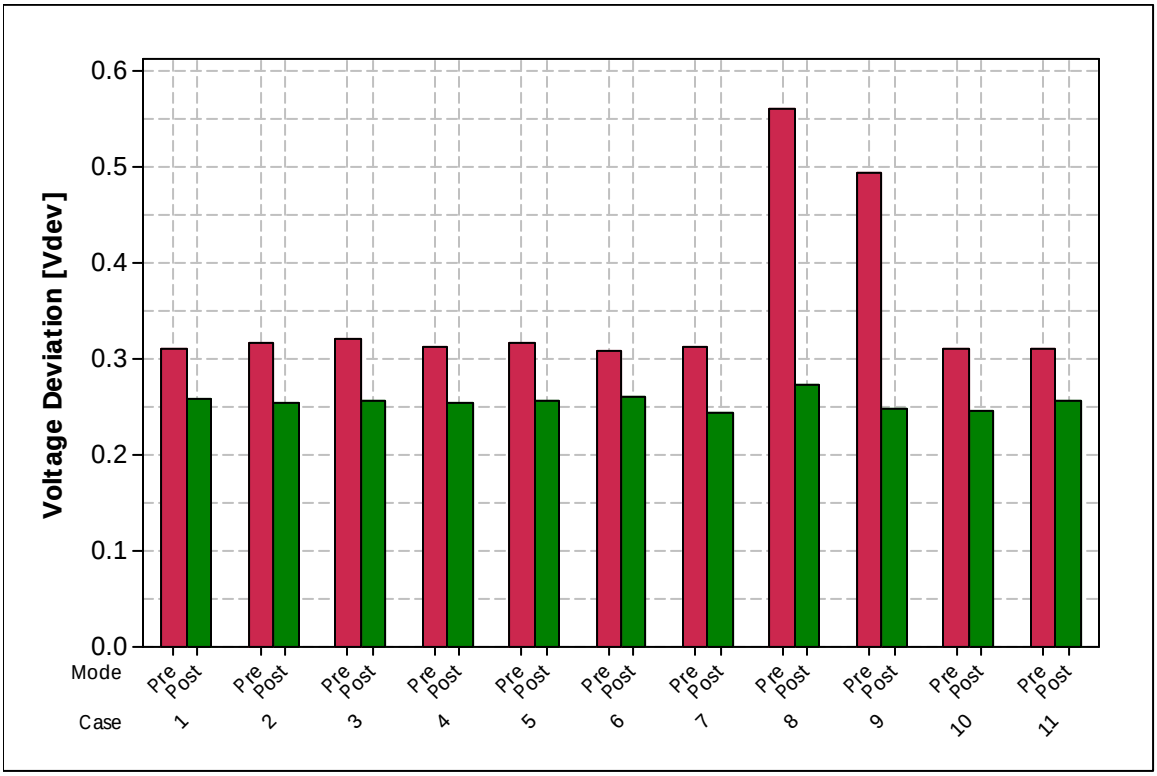

Figure 8.1: Results for voltage deviation metric, pre and post optimization.

Figure 8.2 shows the values of the total transmission losses (P_{loss}), for case 1 (all elements in service) and the first 10 contingencies (cases 2 to 11).

Analogous to the previous case, the red bar, labeled "Pre", shows the values prior to the optimization process and the green bar, labeled "Post", indicates the corresponding value after all three optimization stages have been performed.

Comparing the pre and post optimization values, it is possible to note that there is a mild effect on the transmission losses (green and red bars have similar heights in most cases), which specifically translate in an average reduction of 3.7%. This implies that the system can be fully optimized without significantly affecting the total transmission losses.

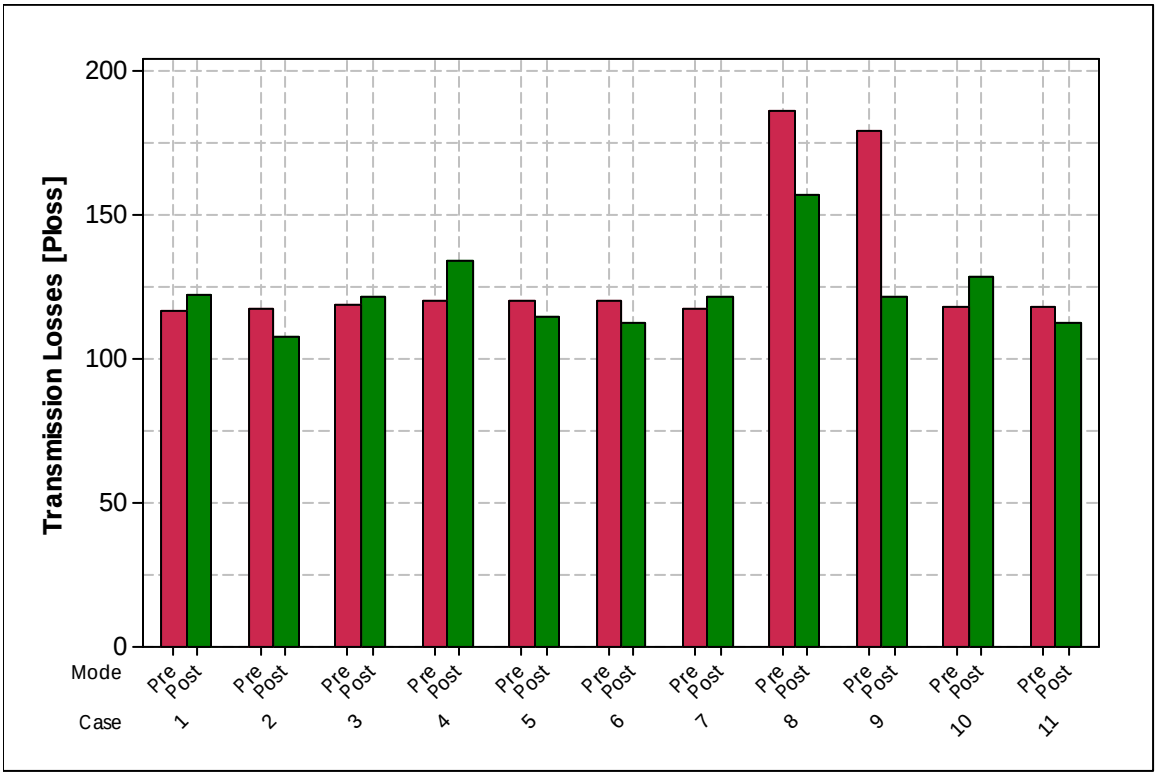

Figure 8.2: Results for total transmission losses, pre and post optimization

In particular, the DSSC modules operating only with local control tends to increase the transmission losses because they relieve congested lines by increasing the net impedance of particular lines to distribute the current to lines with lower LUF but higher impedances. In this case, after the series compensation stage is performed, the DSSC control references are capable of achieving a global optimal performance of the system, thus the total transmission losses are minimally affected.

Finally, Figure 8.3 and Figure 8.4 show the values of the number of overloaded lines and bus voltage violations respectively, for case 1 (all elements in service) and the first 10 contingencies (cases 2 to 11).

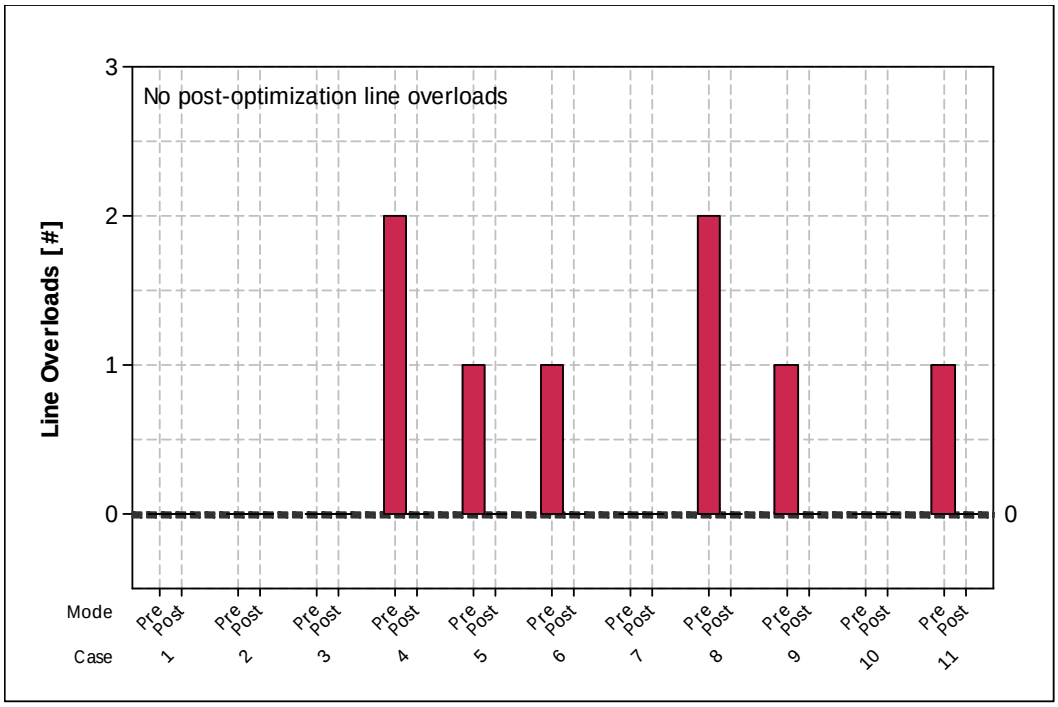

Figure 8.3: Results for number of overloaded lines, pre and post optimization

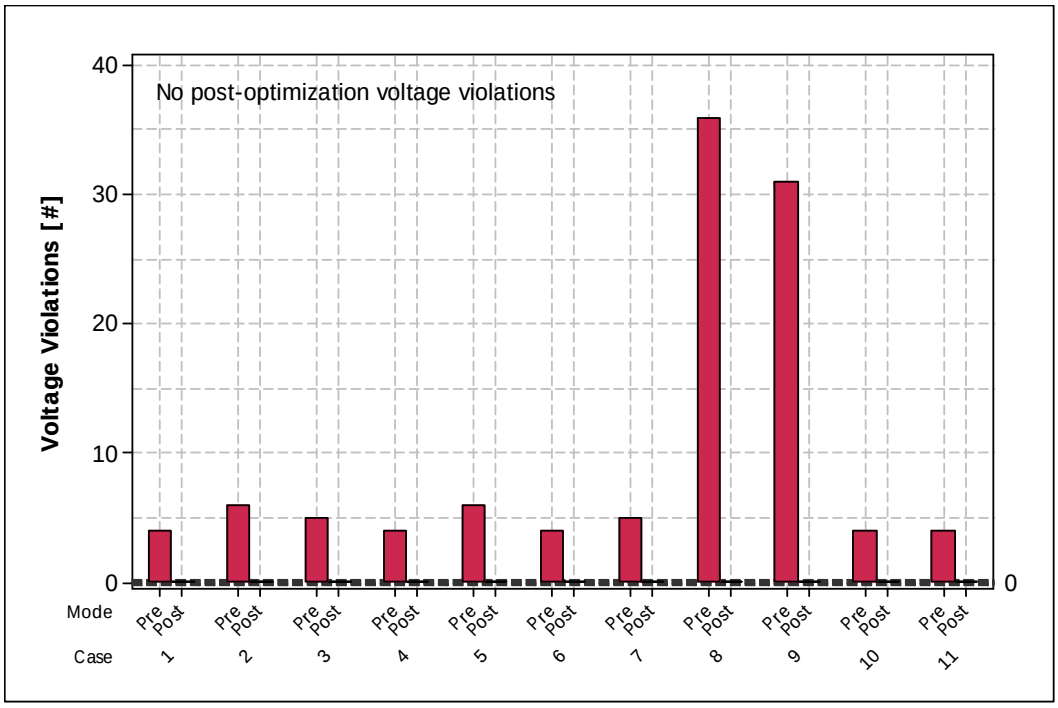

Figure 8.4: Results for bus voltage violations, pre and post optimization

Following the same format, the pre-optimization (red bars) and post-optimization (green bars) values are plotted. However, neither of the figures posses green bars because, after all three optimization stages are performed, there are no overloaded lines and no bus voltage violations. The system is therefore capable of maintaining the voltage within limits, and after each contingency there are no overloaded lines that can cause further outages.

8.2.2 Critical contingencies

There are three contingencies in the system that must be analyzed separately. The states of the original and the optimized systems (after all three optimization stages) for these contingencies are summarized in Table 8.2.

The columns of this table show the voltage deviation metric (V_{dev}) as defined in (7.3), the total power losses (P_{loss}), the minimum and maximum bus voltages (V_{min} and V_{max} respectively), the number of overloaded lines (OVL) and the number of voltage violations ($V_{violations}$).

Table 8.2: Critical contingencies, optimized system

System settings	#	From Bus	To Bus	V_{dev}	P_{loss} [W]	V_{min} [p.u.]	V_{max} [p.u.]	OVL	$V_{violations}$
Original	169	110	112	1.043	115.12	0	1.05	0	4
Optimized	169	110	112	0.259	114.91	0.96	1.05	0	0
Original	176	12	117	1.046	115.49	0	1.05	0	5
Optimized	176	12	117	1.022	100.25	0.95	1.05	0	0
Original	179	8	5	3.353	798.93	0	1.05	10	44
Optimized	179	8	5	0.299	130.83	0.91	1.06	0	0

For case 169, where the branch out of service corresponds to the line from bus 110 to bus 112, the load shedding at bus 112 is unavoidable because the line out of service is the only one that supplies this load. However, it is important to note that, prior to the optimization of the system settings, this outage leads to 4 voltage violations and once the optimization process is completed, there are no bus voltage violations.

A similar situation occurs with case 176. The outage corresponds to the line between buses 12 and 117, which is the only line that supplies the load at bus 117. After the load at bus 117 is shed, the optimized system has no limit violations and operates in stable conditions.

Finally, case 179 (transformer that connects buses 8 and 5 is out of service) that originally lead to catastrophic cascade events; it operates within security limits after the system is optimized.

In particular, all overloaded lines are relieved and the voltage profile is drastically improved as shown by the change in the value of the voltage deviation metric, defined in (7.3), from 3.353 to 0.229.

Considering the bus voltage violations, it is not possible to keep the system within the desirable ±5% voltage deviations. However, the system is capable of operating within the limits defined by the ITIC curve and, therefore, the system remains in a stable mode of operation after the contingency occurs.

8.2.3 Summary of the results

Based on all the contingencies considered, with the exception of only the three previous cases in Table 8.2, a summary of the system condition for the N-1 contingency analysis is presented in Table 8.3.

The rows of Table 8.3 show the original system (prior to any of the optimization stage), a summary of the system after the SCOPF stage is performed, then a summary of the system after the series compensation stage is carried out, and finally the overall results when the optimization process is complete (after the shunt compensation stage is completed).

The columns of Table 8.3 show the maximum voltage deviation metric (V_{dev}), maximum total power losses (P_{loss}), and the minimum and maximum bus voltages (V_{min} and V_{max} respectively). These values correspond to the extreme data points over the entire dataset that includes the base case (all components in service) and 183 contingencies. In other words, Max_V_{dev} is the maximum voltage deviation metric among the 184 cases considered in this study, V_{min} is the minimum bus voltage of all 184 cases and so on.

Table 8.3: Summary of system condition for N-1 contingency analysis

System settings	Max V_{dev}	Max P_{loss} [MW]	V_{min} [p.u.]	V_{max} [p.u.]	Total OVL	Total $V_{violations}$
Original	1.170	186.83	0.63	1.06	22	1145
SCOPF stage	0.361	156.66	0.87	1.06	18	61
Series Stage	0.363	156.66	0.84	1.06	0	63
Shunt stage (Optimized System)	**0.313**	**156.66**	**0.92**	**1.06**	**0**	**0**

Additionally, the total number of overloaded lines (OVL) and the total number of voltage violations ($V_{violations}$) are also shown in Table 8.3. These total numbers correspond to the summation over the 184 cases.

As Table 8.3 shows, the performance of the system has improved dramatically. The maximum voltage deviation metric V_{dev}, reduces by 73% from a value of 1.17 (original system settings) to 0.313 (optimized system settings), while the maximum power losses shows a moderate improvement of 16% from 186.83 to 156.66 MW. The most significant differences are found in the cases of the total number of overloaded lines (OVL) and total number of bus voltage violations ($V_{violations}$); the system with original settings has several overloaded lines and 1,145 bus voltages outside the desired limits. However, after the system settings are optimized, there are no overloaded lines and all the bus voltages are within desired limits.

8.3 Detailed analysis of selected cases

The previous section has shown the improvement of the power system reliability after all three optimizations stages have been performed. Including the specific results for each optimization stage involves an enormous amount of information that will make this document to be extremely lengthy. For this reason, the results for the individual optimizations stages are reported in this section for two cases only: base case, where all elements of the system are in service and case 32 that corresponds to the outage of the line between buses 25 and 27. The two cases are selected in order to illustrate the full capability and benefits of the proposed PSO-based optimization framework.

8.3.1 Base case

SCOPF stage

The results for the objective function value in (7.9) and objective functions metrics, as in (7.2), (7.4), (7.5)-(7.8), are shown in Table 8.4.

Table 8.4: Objective function value and metrics for SCOPF stage, base case

J	J_0	J_1	J_2	J_3	J_4	J_5	J_6
1.8345	5.000	0.9996	0.8348	0	0	0	0

Table 8.4 shows that the overall objective function value improves by 83%, from an original value of 5 (J_0) to an optimized value of 1.834 (J). Most importantly, the metrics related to maintaining the security of the system within security margins, J_3-J_4, are equal to zero in the optimized system. This indicates that there are no overloaded lines or bus voltage violations.

Considering the generation cost metric (J_1), there is a negligible difference of less than 0.1% ((1-J_1), percentagewise) as compared to the original system. The normalized voltage deviation metric (J_2) indicates that the voltage deviation metric in the optimized system is 17% less ((1-J_2), percentagewise) than the value for the original system.

A comparison between the state of the original system and optimized system is shown in Table 8.5. The columns of Table 8.5 present the information of the generation cost (ED), as defined in (7.1), the value of the voltage deviation metric (V_{dev}), defined in (7.3) , the total transmission power losses (P_{loss}), line utilization factor (LUF), as in (7.21), maximum line loading (Max_L), minimum and maximum bus voltages.

Table 8.5: Original and optimized system state, SCOPF stage, base case

	ED [$]	V_{dev}	P_{loss} [MW]	LUF [%]	Max_L [p.u.]	V_{min} [p.u.]	V_{max} [p.u.]
Original system	1651	0.31	116	29	0.90	0.93	1.05
System_SCOPF	1651	0.26	122	31	0.93	0.95	1.05

The information in Table 8.5, shows the numerical values of some variables analyzed above. The conclusions from this data are consistent with the ones drawn from the metric and objective function analysis. In addition, Table 8.5 shows an improvement in the line utilization factor of 2% and a change of the maximum loading of transmission lines from 90% to 93%.

The optimal system settings are shown in Table 8.6 to Table 8.9.

Table 8.6: Optimal generator settings, base case

Gen #	Bus	P_g [p.u.]	V_{ref} [p.u.]
1	10	4.03	1.041
2	12	1.20	0.993
3	25	2.00	1.050
4	26	3.31	1.050
5	49	2.49	1.050
6	61	1.87	1.023
7	65	3.34	1.019
8	66	3.71	1.050
9	69	4.54	1.033
10	80	4.22	1.050
11	87	0.03	1.008
12	89	6.89	1.005
13	100	2.23	1.029
14	103	0.25	1.019
15	111	0.44	0.995

Table 8.6 presents the optimal generator settings: optimal power output (P_g) and the voltage reference (V_{ref}) for all 15 generator units in Figure 7.1. The p.u. values of the

active power output (P_g) are calculated considering the overall base power of the system, which is 100 MVA (as opposed to the rating of each machine); this fact explains why most of these values are greater than one.

Table 8.7 gives the operator the information about the optimal tap ratio in all the variable tap transformers in the system. Table 8.8 shows the optimal setting for the phase shifter transformer, its optimal tap ratio and optimal phase angle.

Table 8.7: Optimal transformer tap settings, base case

Tranf #	From bus	To bus	Tap setting
1	8	5	0.974
2	26	25	0.978
3	30	17	0.897
4	38	37	0.906
5	63	59	0.927
6	64	61	1.008
7	65	66	0.975
8	68	69	0.895

Table 8.8: Optimal phase shifter transformer settings, base case

From bus	To bus	Tap setting	Angle [º]
81	80	0.981	8.52

Table 8.9 shows the optimal settings for the capacitor banks. The settings presented in this table correspond to the reactive power injection in p.u. For this particular study it is assumed that the reactive compensation can be adjusted from zero (disconnected) to the maximum rating in steps of 5 MVAr. Additionally, positive values

indicate reactive power injection (capacitors) and negative values correspond to reactive power consumption (reactors).

These per unit quantities can be converted into actual values in MVAr by multiplying the p.u. value by the system base power which in this case is 100 MVA.

Table 8.9: Optimal capacitor banks settings, base case

Unit #	Bus	Q_c [p.u.]
1	5	-0.50
2	34	0.15
3	37	-0.30
4	44	0.05
5	45	0.10
6	46	0.15
7	48	0.10
8	74	0.10
9	79	0.25
10	82	0.15
11	83	0.10
12	105	0.15
13	107	0.05
14	110	0.05

Series compensation stage

After the SCOPF stage is completed, there are no overloaded lines and it is not necessary to perform any series compensation.

Shunt compensation stage

The SCOPF stage is capable of adjusting the settings of the existing equipment such that the there are no bus voltage violations, thus it is not necessary to incur any expenses of additional shunt compensators.

8.3.2 Case 32

Case 32, which corresponds to the outage of the line between buses 25 and 27, is selected to illustrate all three optimization stages: SCOPF stage, series compensation stage, and shunt stage.

SCOPF stage

The results for the objective function value, as in (7.9), and objective functions metrics ((7.2), (7.4),(7.5)-(7.8)) are shown in Table 8.10.

Table 8.10: Objective function value and metrics for SCOPF stage, case 32

J	**J_0**	**J_1**	**J_2**	**J_3**	**J_4**	**J_5**	**J_6**
6.782	9.000	1.001	0.594	1	0.927	0.444	0

These values indicate that the overall objective function value (J) has an improvement of 25%, from a pre-optimization value of 9 (J_0) to an optimized value of 6.782 (J).

The metrics J_3 and J_4, which are related to the line loading, are nonzero. In particular, J_4 is 0.927 which indicates that there is a reduction in the maximum line loading. However the value of J_3 is 1 which means that the number of overloaded lines did not change as compared with the pre-optimization system settings. In other words, the optimization of existing equipment settings improve the line loading and relieve congestion but not by sufficient amounts to correct overloaded lines.

In the case of metrics J_5 and J_6, their values show that the number of low bus violations is reduced by 56% ((1-J_5), percentagewise) and there are no high voltage violations ($J_6 = 0$), neither in the original nor in the optimized system.

The metric associated with generation cost (J_1) changes by a negligible amount, indicating that the optimization of the system performance in this stage does not incur economic penalties. The normalized voltage deviation metric (J_2), as defined in (7.4), improves considerably as it is reduced by 41% ((1-J_2), percentagewise) with respect to its pre-optimization value.

A comparison between the state of the pre-optimization system and the optimized system (after the SCOPF stage) is shown in Table 8.11.

The columns of Table 8.11 present information on the generation cost (ED) defined in (7.1), the actual value of the voltage deviation metric (V_{dev}), as in (7.3), the total power losses (P_{loss}), line utilization factor (LUF), defined in (7.21), maximum line loading (Max_L), minimum and maximum bus voltages.

Table 8.11: Original and optimized system state, SCOPF stage, case 32

	ED [$]	**V_{dev}**	**P_{loss} [MW]**	**LUF [%]**	**Max_L [p.u.]**	**V_{min} [p.u.]**	**V_{max} [p.u.]**
Original system	1652	0.49	132.0	32.0	1.11	0.86	1.05
System_SCOPF	1653	0.29	133.3	32.1	1.03	0.93	1.05

The information in Table 8.11, gives the actual values of the variables of interest. An analysis of these actual values support the conclusions presented above. In other words, after the SCOPF optimization is performed: (i) the voltage deviation metric (V_{dev}),

as defined in (7.3), is considerably reduced, (ii) the transmission losses are not affected, (iii) the maximum loading in transmission lines is improved (however not enough to avoid overloaded lines), and (iv) the minimum voltage is substantially improved. All these benefits are obtained without increasing the generation costs (ED).

The optimal system settings, resulting from the SCOPF stage, are shown in Table 8.12 to Table 8.15.

Table 8.12 presents the optimal power output (P_g) and voltage reference (V_{ref}) settings for each generator.

Table 8.12: Optimal generator settings, case 32

Gen #	Bus	P_g [p.u.]	V_{ref} [p.u.]
1	10	3.45	1.050
2	12	1.16	1.026
3	25	1.81	1.050
4	26	3.16	1.050
5	49	1.57	1.037
6	61	1.29	0.993
7	65	4.20	0.998
8	66	4.20	1.050
9	69	5.80	1.050
10	80	5.00	1.050
11	87	0.03	1.011
12	89	6.44	1.036
13	100	2.44	1.002
14	103	0.88	1.026
15	111	0.32	1.000

Table 8.13 provides the information about the optimal tap ratio in all eight variable tap transformers in the system and Table 8.14 shows the optimal setting for the phase shifter transformer, its optimal tap ratio and optimal phase angle.

Finally, Table 8.15 shows the optimal settings for capacitor banks. In the same fashion as the previous case (base case), the settings presented in this table correspond to the reactive power injection in p.u.

Table 8.13: Optimal tap transformers settings, case 32

Unit #	From bus	To bus	Tap setting
1	8	5	1.001
2	26	25	1.015
3	30	17	0.859
4	38	37	0.898
5	63	59	0.878
6	64	61	1.136
7	65	66	1.007
8	68	69	0.954

Table 8.14: Optimal phase shifter transformer settings, case 32

From bus	To bus	Tap setting	Angle [º]
81	80	0.900	10.02

Table 8.15: Optimal capacitor banks settings, case 32

Unit #	Bus	Q_c [p.u.]
1	5	-0.50
2	34	0.10
3	37	-0.20
4	44	0.10
5	45	0.10
6	46	0.05
7	48	0.10
8	74	0.15
9	79	0.20
10	82	0.15
11	83	0.10
12	105	0.30
13	107	0.05
14	110	0.05

Series compensation stage

After the SCOPF optimization stage is performed (with results presented in Table 8.11) the maximum loading of transmission lines is reduced from 1.11 p.u. to 1.03 p.u. This last value indicates the presence of overloaded lines in the system and therefore it is necessary to perform the series compensation stage.

The results for the overall objective function, in (7.24), and objective functions metrics ((7.22), (7.23), (7.5)-(7.8)) are shown in Table 8.16.

Table 8.16: Objective metrics, series compensation stage, case 32

J	**J_0**	**J_1**	**J_2**	**J_3**	**J_4**	**J_5**	**J_6**
2.198	8.250	0.985	0.994	0	0	0.875	0

The results in Table 8.16 indicate a significant improvement in the overall objective function, the original value of 8.25 (J_0) is reduced by 75% to 2.198 (J).

The technical metrics J_1 and J_2 are related with the LUF and the transmission losses respectively. Both of them have a slight improvement as compared with the system state prior to this optimization stage.

The bus violation metrics (J_5 and J_6) indicate that there is an improvement of one fewer low voltage violation and no high voltage violations. This conclusion is drawn considering the definitions of both metrics presented in (7.7) and (7.8).

While metrics J_1, J_2, J_5 and J_6 do not change significantly, the main impact on the reduction of the objective function value is given by the metrics associated with the

overloaded lines, J_3 and J_4. The values of these two metrics are zero reflecting that, after the optimization process is completed, there are no overloaded lines in the system.

A comparison between the states of the system after the SCOPF stage and after the series compensation stage is shown in Table 8.17.

The columns of Table 8.17 present the information of the generation cost (ED), as defined in (7.1), the actual value of the voltage deviation metric (V_{dev}), as in (7.3), the total power losses (P_{loss}), line utilization factor (LUF), defined in (7.21), maximum line loading (Max_L), minimum and maximum voltages.

Table 8.17: System state, pre and post series compensation stage, case 32

	ED [$]	**V_{dev}**	**P_{loss} [MW]**	**LUF [%]**	**Max_L [p.u.]**	**V_{min} [p.u.]**	**V_{max} [p.u.]**
System_SCOPF	1653	0.293	133.3	32.1	1.03	0.93	1.05
System_Series_comp	1653	0.289	132.5	32.6	0.91	0.93	1.05

The optimal DSSC settings obtained at the end of this optimization stage are shown in Table 8.18. These values correspond to the control reference of the DSSC modules in the form of the value of the line reactance, in p.u., that needs to be achieved.

Table 8.18: Optimal DSSC settings, series compensation stage

#	**Bus From**	**Bus To**	**X_L [p.u.]**	**#**	**Bus From**	**Bus To**	**X_L [p.u.]**	**#**	**Bus From**	**Bus To**	**X_L [p.u.]**
1	1	2	0.0836	**60**	46	48	0.1686	**119**	77	82	0.0982
2	1	3	0.0389	**61**	47	49	0.0701	**120**	82	83	0.0295
3	4	5	0.0066	**62**	42	49	0.2905	**121**	83	84	0.1069

Table 8.19 continued

#	Bus From	Bus To	X_L [p.u.]	#	Bus From	Bus To	X_L [p.u.]	#	Bus From	Bus To	X_L [p.u.]
4	3	5	0.1033	**63**	42	49	0.2673	**122**	83	85	0.1358
5	5	6	0.0517	**64**	45	49	0.2066	**123**	84	85	0.0760
6	6	7	0.0170	**65**	48	49	0.0497	**124**	85	86	0.1042
7	8	9	0.0288	**66**	49	50	0.0848	**125**	86	87	0.1822
8	9	10	0.0290	**67**	49	51	0.1463	**126**	85	88	0.1031
9	4	11	0.0665	**68**	51	52	0.0474	**127**	85	89	0.1585
10	5	11	0.0749	**69**	52	53	0.1855	**128**	88	89	0.0789
11	11	12	0.0167	**70**	53	54	0.1149	**129**	89	90	0.1831
12	2	12	0.0637	**71**	49	54	0.2627	**130**	89	90	0.0861
13	3	12	0.1652	**72**	49	54	0.2502	**131**	90	91	0.0765
14	7	12	0.0307	**73**	54	55	0.0620	**132**	89	92	0.0478
15	11	13	0.0670	**74**	54	56	0.0099	**133**	89	92	0.1652
16	12	14	0.0835	**75**	55	56	0.0126	**134**	91	92	0.1127
17	13	15	0.2914	**76**	56	57	0.1111	**135**	92	93	0.0752
18	14	15	0.2043	**77**	50	57	0.1092	**136**	92	94	0.1778
19	12	16	0.0822	**78**	56	58	0.1039	**137**	93	94	0.0796
20	15	17	0.0489	**79**	51	58	0.0583	**138**	94	95	0.0370
21	16	17	0.1928	**80**	54	59	0.2648	**139**	80	96	0.1655
22	17	18	0.0483	**81**	56	59	0.2718	**140**	82	96	0.0613
23	18	19	0.0454	**82**	56	59	0.2822	**141**	94	96	0.0882
24	19	20	0.1092	**83**	55	59	0.1889	**142**	80	97	0.0824
25	15	19	0.0462	**84**	59	60	0.1500	**143**	80	98	0.1214
26	20	21	0.0911	**85**	59	61	0.1413	**144**	80	99	0.1967
27	21	22	0.0797	**86**	60	61	0.0109	**145**	92	100	0.2888
28	22	23	0.1609	**87**	60	62	0.0588	**146**	94	100	0.0568
29	23	24	0.0484	**88**	61	62	0.0410	**147**	95	96	0.0486
30	23	25	0.0931	**89**	63	64	0.0217	**148**	96	97	0.0977
31	25	27	0.1833	**90**	38	65	0.1043	**149**	98	100	0.1489
32	27	28	0.0821	**91**	64	65	0.0285	**150**	99	100	0.0758
33	28	29	0.1098	**92**	49	66	0.0874	**151**	100	101	0.1112
34	8	30	0.0410	**93**	49	66	0.0995	**152**	92	102	0.0615

Table 8.20 continued

#	Bus From	Bus To	X_L [p.u.]	#	Bus From	Bus To	X_L [p.u.]	#	Bus From	Bus To	X_L [p.u.]
35	26	30	0.0733	**94**	62	66	0.2340	**153**	101	102	0.1173
36	17	31	0.1822	**95**	62	67	0.0993	**154**	100	103	0.0594
37	29	31	0.0325	**96**	66	67	0.0862	**155**	100	104	0.1753
38	23	32	0.1323	**97**	65	68	0.0135	**156**	103	104	0.1271
39	31	32	0.0982	**98**	47	69	0.2946	**157**	103	105	0.1431
40	27	32	0.0807	**99**	49	69	0.3584	**158**	100	106	0.2636
41	15	33	0.1042	**100**	69	70	0.1315	**159**	104	105	0.0389
42	19	34	0.2416	**101**	24	70	0.4673	**160**	105	106	0.0650
43	35	36	0.0095	**102**	70	71	0.0422	**161**	105	107	0.2081
44	35	37	0.0554	**103**	24	72	0.2043	**162**	105	108	0.0623
45	33	37	0.1147	**104**	71	72	0.1772	**163**	106	107	0.1940
46	34	36	0.0309	**105**	71	73	0.0527	**164**	108	109	0.0321
47	34	37	0.0091	**106**	70	74	0.1523	**165**	103	110	0.1650
48	37	39	0.0864	**107**	70	75	0.1363	**166**	109	110	0.0727
49	37	40	0.1860	**108**	69	75	0.1302	**167**	110	111	0.0691
50	30	38	0.0498	**109**	74	75	0.0463	**168**	110	112	0.0594
51	39	40	0.0514	**110**	76	77	0.1654	**169**	17	113	0.0244
52	40	41	0.0526	**111**	69	77	0.1151	**170**	32	113	0.1682
53	40	42	0.1556	**112**	75	77	0.1730	**171**	32	114	0.0612
54	41	42	0.1269	**113**	77	78	0.0132	**172**	27	115	0.0875
55	43	44	0.2628	**114**	78	79	0.0251	**173**	114	115	0.0113
56	34	43	0.1389	**115**	77	80	0.0400	**174**	68	116	0.0045
57	44	45	0.0806	**116**	77	80	0.1092	**175**	12	117	0.1224
58	45	46	0.1440	**117**	79	80	0.0838	**176**	75	118	0.0508
59	46	47	0.1456	**118**	68	81	0.0166	**177**	76	118	0.0448

Shunt compensation stage

Considering the base case and all contingencies, the shunt compensation stage finds that the optimal solution is the placement of eight STATCOM units in the system. The optimal location and sizes are shown in Table 8.21.

Table 8.21: STATCOM units, optimal location and sizes

#	Bus	Rating [MVA]
1	3	15
2	28	30
3	37	250
4	38	100
5	41	25
6	76	24
7	112	16
8	118	240

In particular, for case 32 (outage of line 25 to 27), the objective function value and metrics are shown in Table 8.22. The overall objective function value shows a dramatic improvement of 84%, from a value of 6 (J_0) to a value of 0.985 (J), mainly because the security constraints metrics, J_3-J_6, are all equal to zero, implying that there are no overloaded lines or bus voltage violations.

Table 8.22: Objective metrics for shunt compensation stage, case 32

J	J_0	J_1	J_2	J_3	J_4	J_5	J_6
0.985	6	0.892	0.093	0	0	0	0

In addition, the normalized voltage deviation metric, as defined in (7.4), reduces its value by 11% ($(1-J_1)$, percentagewise) from that of the system prior to this optimization stage.

The STATCOM cost metric J_2 has a small value because, for this particular contingency, the best performance is obtained with only one STATCOM unit in service which corresponds to unit number two, with 30 MVA.

Table 8.23 shows the actual values of the variables that describe the system state: generation cost (ED), as defined in (7.1), voltage deviation metric (V_{dev}), as in (7.3), total transmission losses (P_{loss}), line utilization factor (LUF), defined in (7.21), minimum and maximum bus voltages, and compares the results of the series compensation stage with the shunt compensation stage.

Table 8.23: System state, pre and post shunt compensation stage, case 32

	ED [$]	**V_{dev}**	**P_{loss} [MW]**	**LUF [%]**	**Max_L [p.u.]**	**V_{min} [p.u.]**	**V_{max} [p.u.]**
System_Series_comp	1653	0.289	132.5	32.6	0.91	0.93	1.05
System_Shunt_comp	1653	0.255	130.9	32.6	0.903	0.955	1.05

As compared with the results obtained in the series compensation stage, it is possible to note the following differences:

- The minimum voltage increases to the desired range of ±5% voltage deviation.
- The maximum loading of the transmission lines reduces to 90.3% as compared to the case with the original system settings (pre-optimization).

As a second optimization process, the optimal settings for the STATCOM units are found and shown in Table 8.24. The settings correspond to whether a certain unit should be in service or not and, if in service, what is the desired voltage reference at the point of common coupling.

It is important to note that the solution found in Table 8.21 considers the base case

and all 186 contingencies, for this reason not all STATCOM units are required to be in operation at all times. To minimize the control effort of these devices, this optimization process optimally decides which units should be in operation for each different case.

The columns in Table 8.24, show the state of the STATCOM units for this particular case (case 32). The value of 0 indicates that the corresponding unit is disconnected and the value of 1 implies that the device is in service. In addition, the optimal voltage reference in p.u. is also included. As mentioned above, the optimal solution corresponds to only one STATCOM unit in service, unit 2, with a voltage reference of 0.9758 p.u.

Table 8.24: STATCOM units, optimal settings, case 32

#	Bus	On/off [0,1]	V_{ref} [p.u.]
1	3	0	-
2	28	1	0.9758
3	37	0	-
4	38	0	-
5	41	0	-
6	76	0	-
7	112	0	-
8	118	0	-

8.4 Summary

This chapter has shown the application of the proposed PSO method to solve the problem of improving the power system reliability using FACTS devices.

In particular, a modified version of the IEEE 118 bus system is used to study the effect of optimizing present system infrastructure and new FACTS installations to make the system N-1 secure.

The optimization process is carried out considering three sequential stages: (i) SCOPF stage, (ii) series compensation stage, and (iii) shunt compensation stage.

The first stage, SCOPF, optimizes the settings of present equipment. Optimal generator active power outputs, AVR voltage references, transformer tap ratios and phase shifts, and capacitor bank settings are provided by the proposed optimization framework. These optimal settings are provided for the base case (all components in service) and for the 186 branch outages that correspond to the N-1 contingency criteria so that the system can operate within its security margins, avoiding overloaded lines and bus voltage violations.

The second stage (series compensation stage) relieves the transmission lines' congestion that cannot be resolved by the previous SCOPF optimization stage. It uses DSSC modules that can change the reactance of the corresponding transmission lines between 0.8 p.u. and 1.2 p.u. The results of this optimization stage provide the operator of the power system with the optimal control reference settings (desired reactance values) for each DSSC module, such that the number of overloaded lines is minimized and the line utilization factor is improved with a minimum impact over the total transmission losses of the system. These results are available for the base case and all 186 contingencies.

Finally, the third optimization stage (shunt compensation stage) provides optimal allocation and rating for STATCOM devices such that the voltage profile (minimization

of voltage deviations) is improved at minimum cost. Analogous to the first two stages (SCOPF and series compensation), special attention is given to maintaining all system variables within their security limits. In addition, this optimization indicates whether the STATCOM units have to be in service and, if so, what is the optimal control reference, in this case the voltage at the point of common coupling.

The overall results of all three optimization stages are very significant, considering the base case and all 186 contingencies. The original system has 22 overloaded lines, 1145 bus voltage violations and three critical contingencies leading to voltage collapse (Table 7.2 and Table 7.3). After the optimization is performed, there are no overloaded lines, all bus voltages are within limits, and the critical contingencies are mitigated, thus the system satisfies the N-1 security criterion (Table 8.3). These results are obtained with minimum impact on the generation costs and with the minimum cost of new FACTS installations.

PART IV: OPTIMIZATION OF POWER SYSTEM PERFORMANCE USING PSO

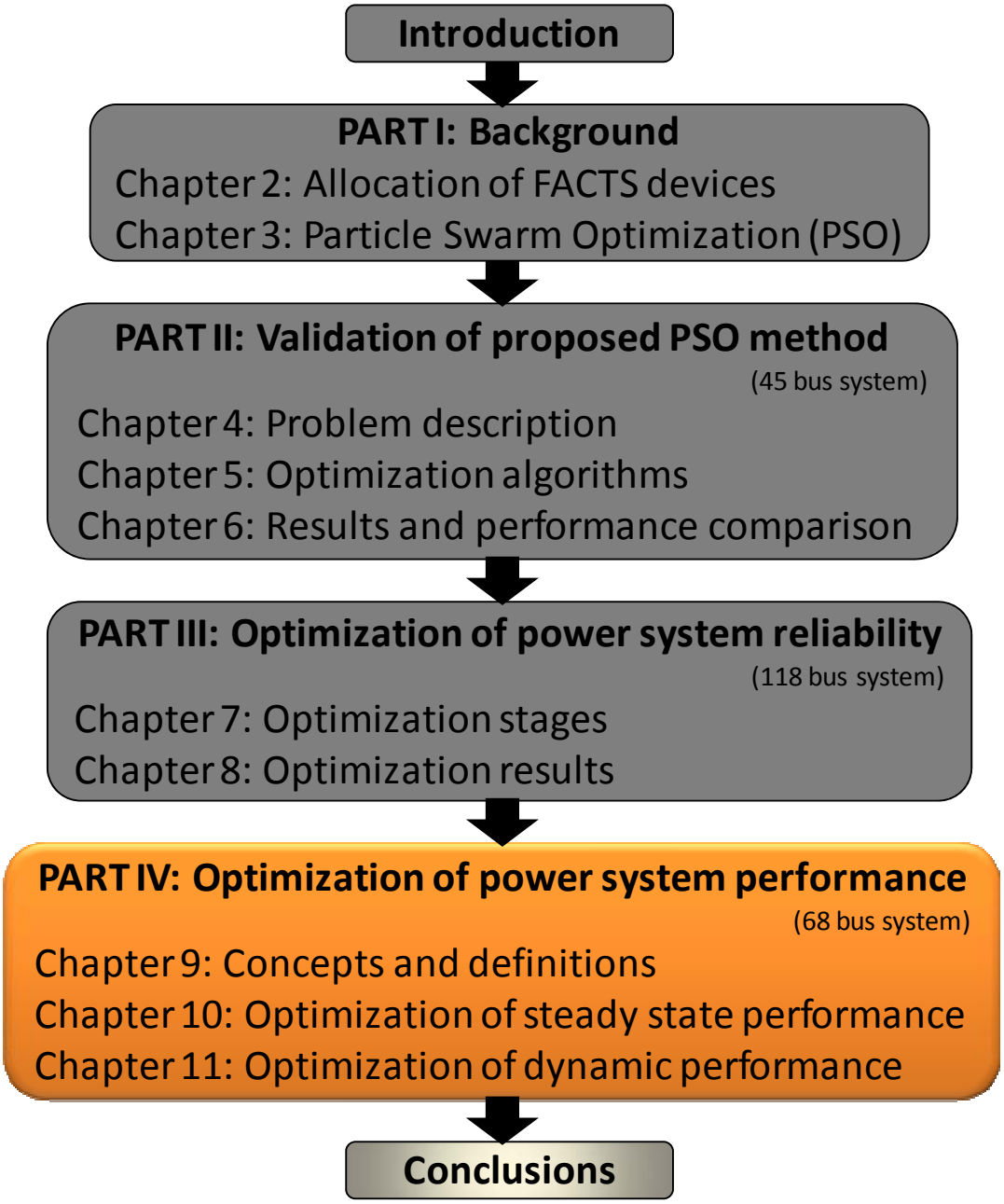

CHAPTER 9

PERFORMANCE DEFINITION AND CONCEPTS

9.1 Introduction

Part IV, optimization of power system performance using PSO, proposes a two-stage PSO-based optimization framework to improve the performance of the power system using FACTS devices. The improvement in the response of the power system is evaluated considering steady state conditions as well as during small and large perturbations.

This chapter introduces concepts, associated to the evaluation of the power system performance, that are used in this study.

In particular, the concept of linearization of the power system around its operating point, bifurcation analysis and continuation power flow, which are used in the optimization of steady state performance, is presented in section 9.2.

Section 9.3 introduces the background necessary to understand how the performance of the power system is evaluated under small and large perturbations. Specifically, this section explains the concepts of small signal stability analysis (sssa) and the methodology for selecting large perturbations (critical faults) in the power system.

Finally, section 9.4 describes a 16 machine - 68 bus system which is used to illustrate the capabilities of the optimization framework in finding the optimal performance of the system considering both technical and economical criteria. In addition

to the description of the system, an assessment of the performance of the system is carried out, using the concept described in 9.2 and 9.3, to evaluate its pre-optimization state.

9.2 Steady state performance

9.2.1 Linearization of the power system

The representation of a dynamic system, such as a power system, can be described by a series of differential and algebraic equations (DAE) of the form [100]-[102]:

$$\begin{aligned} \dot{x} &= f(x, y, u) \\ 0 &= g(x, y, u) \end{aligned} \tag{9.1}$$

Where x is a state vector, which generally includes the generator's angle and speed, transient voltages, excitation system voltages, etc. The algebraic vector, y, contains bus voltage magnitudes, angles, stator currents, etc. and the control vector, u, represents exciter voltage references, mechanical inputs, etc.

The dynamic system representation in (9.1) can be linearized around a stable operating point (x_0,y_0,u_0), giving the following state-space description [100]-[102]:

$$\Delta\dot{x} = A \cdot \Delta x + B \cdot \Delta u \tag{9.2}$$

where:

$$A = \nabla_x f - \nabla_y f \cdot \left(\nabla_y g\right)^{-1} \cdot \nabla_x g \tag{9.3}$$

and

$$B = \nabla_u f - \nabla_y f \cdot \left(\nabla_y g\right)^{-1} \cdot \nabla_u g \tag{9.4}$$

where:

A: is the state matrix of the system,

∇: is the partial derivative operator, nabla,

$\nabla_y g$ is the complete power flow Jacobian matrix (J_{LFV}).

9.2.2 Bifurcation analysis and continuation power flow

In order to perform a steady state analysis of the power system under increasing load conditions, (9.1) can be re-written, to also consider the loadability level of the system, by dropping the control vector, *u,* and adding the loading parameter (λ_L) [100], [103]-[105]:

$$\begin{aligned} 0 = \dot{x} &= f(x, y, \lambda_L) \\ 0 &= g(x, y, \lambda_L) \end{aligned} \tag{9.5}$$

The loading parameter, λ_L, is a scalar that multiplies generation and load as follows ((9.6) assumes that there is a slack bus as opposed to distributed slack bus) [100]:

$$
\begin{aligned}
P_G &= \lambda_L \cdot P_{G0} \\
Q_G &= \lambda_L \cdot Q_{G0} \\
P_L &= \lambda_L \cdot P_{L0} \\
Q_L &= \lambda_L \cdot Q_{L0}
\end{aligned}
\tag{9.6}
$$

where:

P_G is the vector of generator active powers with increased loading,

P_{Go} is the vector of generator active powers in the base case,

Q_G is the vector of generator reactive powers with increased loading,

Q_{Go} is the vector of generator reactive powers in the base case,

P_L is the active power load vector with increased loading,

P_{L0} is active power load vector in the base case,

P_Q is the reactive power load vector with increased loading,

P_{Q0} is the reactive power load vector in the base case.

The linear analysis of the power system represented by (9.5) allows the identification of the critical point before the system collapses from the voltage stability point of view. This critical point can be either a saddle-node bifurcation point (SNB) or a limit-induced bifurcation (LIB) [103].

The mathematical conditions for a SNB point are either (9.7) or (9.8) [100]:

$$
\begin{aligned}
g(x, y, \lambda_L) &= 0 \\
\nabla_y g(x, y, \lambda_L) v &= 0 \\
|v| &= 1
\end{aligned}
\tag{9.7}
$$

or

$$g(x, y, \lambda) = 0$$
$$\nabla_y g(x, y, \lambda)^T w = 0 \tag{9.8}$$
$$|w| = 1$$

where:

v is the right eigenvector of the complete power flow Jacobian matrix (J_{LFV}),

w is the left eigenvector of the complete power flow Jacobian matrix (J_{LFV}).

On the other hand, the mathematical conditions for a LIB point are [100]:

$$g(x, y, \lambda) = 0$$
$$\rho(y) = 0 \tag{9.9}$$

where $\rho(y)$ represents additional constraints such as reactive power generator limits, bus voltage limits, or transmission line limits (maximum current or maximum apparent power).

In practice, whether the system collapses by a SNB or a LIB point, the Jacobian matrix (J_{LFV}) tends to be either singular (SNB) or rather close to singularity (LIB) at the collapse point [103].

The continuation power flow (CPF) is a useful tool to assess the steady state voltage stability of a power system [104]. In the CPF, a predictor and corrector scheme can be used to avoid the illness of power flow solution at the vicinity of the voltage collapse point (Figure 9.1).

In the predictor step, a tangent vector is calculated from a generic equilibrium point, to estimate a subsequent solution corresponding to a different value of the load parameter, then this estimate is corrected using a corrector step which can generally be obtained either by means of a local parametrization or a perpendicular intersection [100], [104].

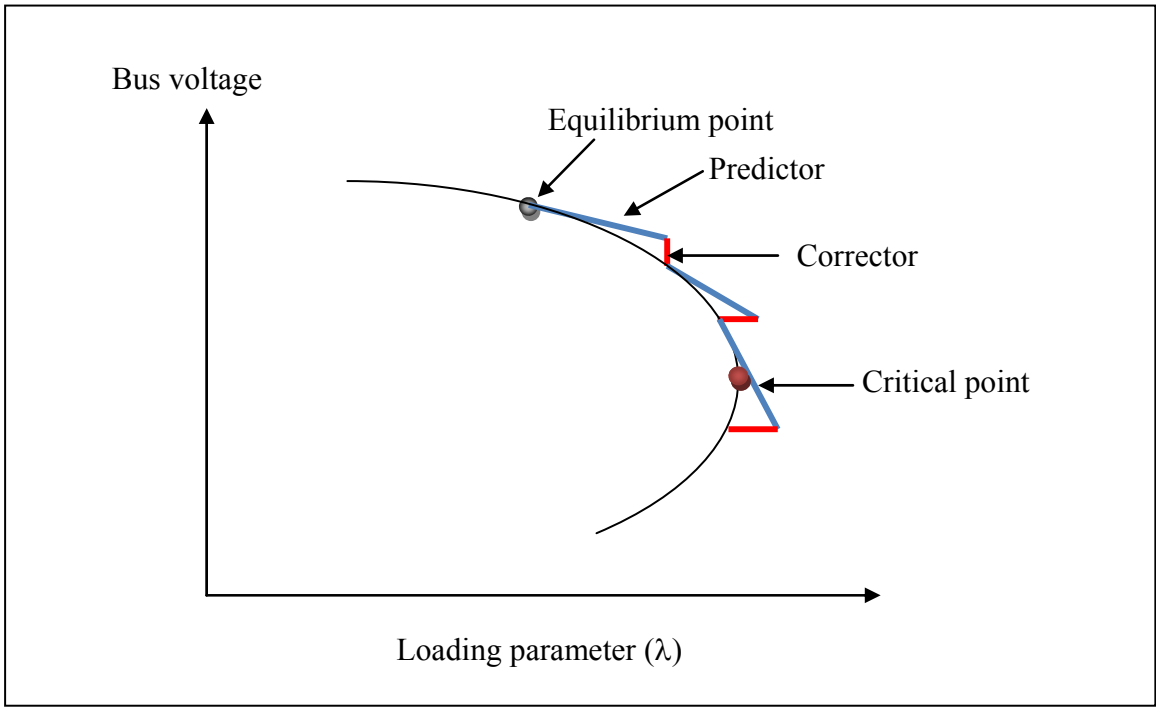

Figure 9.1: Continuation power flow visualization

The CPF routine can stop either when a SNB or a LIB point is encountered or when the nose curve is completed, in both cases the result of the CPF is the maximum loading parameter (i.e. the values of the loading parameter at the critical point), which

represents the maximum load that the system can tolerate without falling into a voltage collapse [100]-[104], [105].

9.3 Performance under small and large perturbations

9.3.1 Small signal stability analysis

The concept of small signal stability analysis (sssa) is related to the analysis of the stability of the power system when the system is subject to a small perturbation around its operational point. These small disturbances are very common and they mainly come from random fluctuations in the load due to weather conditions and suchlike [101].

Studies of the behavior of the system, under perturbations of small magnitude, indicate that the electromechanical oscillations in the post-fault recovery stage are linear in nature, and therefore a linear system model of the power system can be used to analyze and predict its behavior under such circumstances [101].

In general, there are two types of electromechanical oscillations [102]: (i) local modes, typically in the 1 to 3 Hz range between a remotely located power station and the rest of the system, and (ii) inter-area modes in the range of less than 1 Hz, where clusters of generators oscillate against each other.

A multimachine linearized analysis computes the eigenvalues of the system and finds those machines that contribute to a particular eigenvalue (either local or inter-area modes) by calculating the corresponding participation factors.

The eigenvalues of the state matrix of the system, A, are the roots of the characteristic equation [101], [102]:

$$det(\lambda I - A) = 0 \tag{9.10}$$

where:

λ are the eigenvalues of the system,

I is the identity matrix.

The eigenvalues resulting from solving (9.10) can be real, zero, or pairs of complex conjugates. These complex conjugate eigenvalues are due to the fact that the state matrix, A, is real and therefore the characteristical polynomial has real coefficients.

Every pair of complex conjugate eigenvalues can be written as [101]:

$$\lambda_i = \sigma_i \pm j\omega_i \tag{9.11}$$

where:

σ_i is the real part of eigenvalue i,

ω_i is the imaginary part of eigenvalue i.

Then the corresponding damping ratio (ρ_i) and the natural frequency (f_n) can be computed as [101], [102]:

$$\rho_i = -\frac{\sigma_i}{\sqrt{\sigma_i^2 + \omega_i^2}} \tag{9.12}$$

$$\omega_n = \frac{\omega_i}{\sqrt{1-\rho_i}}\,, \qquad f_n = \frac{\omega_n}{2\pi} \tag{9.13}$$

The dynamic voltage stability is analyzed by monitoring the eigenvalues of the linearized system as a power system is progressively loaded. Oscillatory instability occurs when a pair of complex conjugate eigenvalues crosses to the right-half plane. This is referred to as dynamic voltage instability or Hopf bifurcation [102], [105].

In general, the s-plane where the eigenvalues are plotted can be divided in several areas. The area where it is desired to have all the system eigenvalues it has a D-shape as it is shown in Figure 9.2 [34]. This area is limited by the line of minimum damping (ρ^*), which can be any desired value typically over 5%, and the overshoot coefficient, σ^*, that is typically set to -3 [34].

9.3.2 Selection of large system perturbations

The perturbation of a power system can broadly be classified in two groups: small (that can be analyzed using sssa) and large. Perturbations such as generator tripping, faults in transmission lines and loss of load have a severe impact on the dynamic behavior of the power system and often stability conditions are affected. Therefore, these types of disturbances must be carefully studied using transient stability analysis, where the system is modeled as a non-linear dynamic process [101].

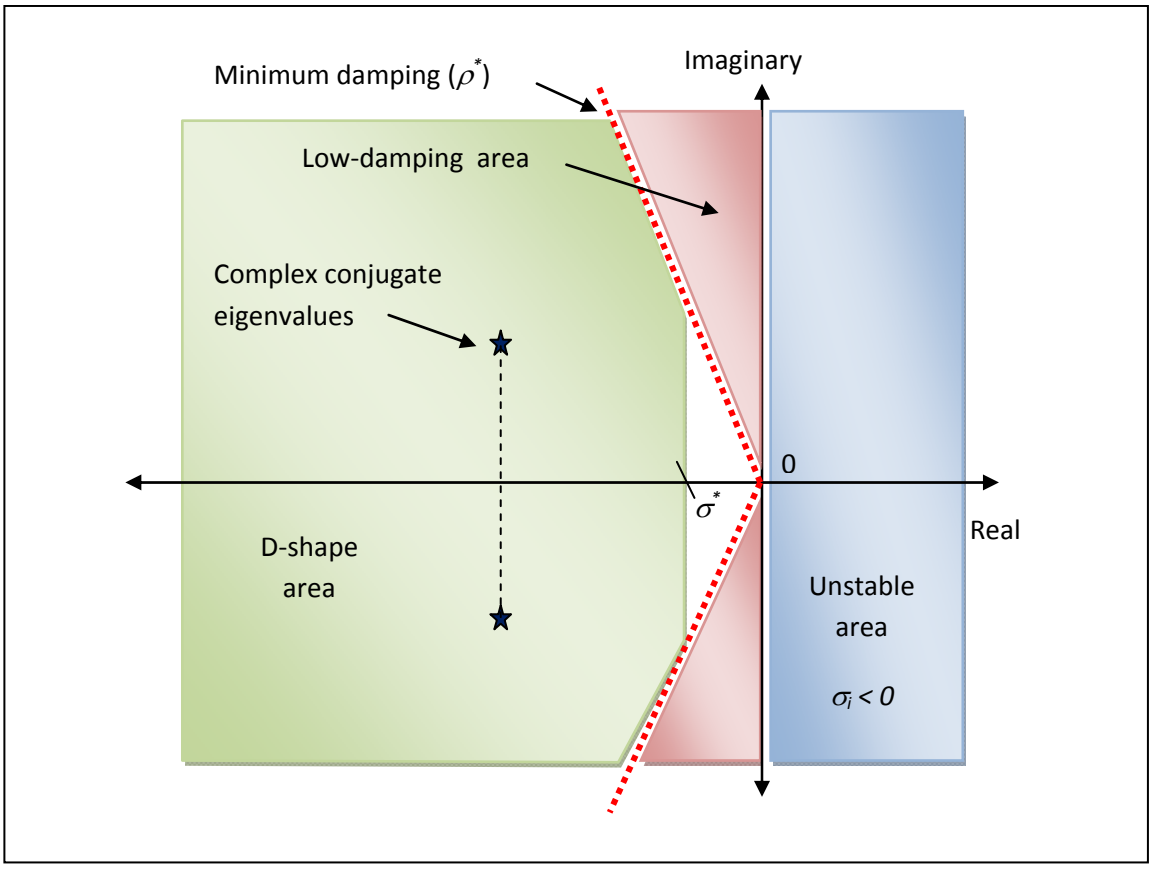

Figure 9.2: D-shape area in s-plane

To be able to assess the transient performance of the power system, a set of representative and credible contingencies have to be selected. There are several methodologies that have proposed to aid the selection of critical contingencies. In this study, the critical contingencies are selected on the basis of the relative values of the real power performance index (P.I.) proposed in [18].

The definition of this index is presented in (9.15).

$$P.I. = \sum_{i=1}^{N_L} \frac{w_i}{2 \cdot a} \cdot \left(\frac{P_{Li}}{P_{Li}^{max}} \right)^{2 \cdot a} \tag{9.15}$$

where:

N_L is the total number of lines,

w_i is a weight factor to represent the importance of different transmission lines,

a is the exponent,

P_{Li} is the active power flowing through line i,

P_{Li}^{max} is the maximum active power that can flow through line i (rated capacity)

The value of the index P.I. is small if all the line flows are within their limits, but it is large when the transmission lines are overloaded [26].

Other methods for contingency utilize a second-order performance index, which in general, may suffer from a so-called masking effect [26]. In the case of the P.I. index, this masking effect, can be avoided by using higher order performance indices, $a > 1$, typically $a=2$ [18], [26].

9.4 Problem description

In this study, a modified version of the 68 bus system is used. It is a reduced order model of the New England and New York interconnected power systems published in 1970 [106]. Generators 1 to 9 represent the New England Test System (NETS) and

generators 10 to 13 correspond to the New York Power System (NYPS). The last three generators (14, 15 and 16) are three interconnected areas in the NYPS.

The one line diagram of the system is shown in Figure 9.3. The corresponding detailed data is presented in Appendix D.

All generators are represented by a sixth order model which is obtained assuming the existence of a field circuit plus an additional rotor circuit along the d-axis and two additional rotor circuits along the q-axis [100]. There are nine generators equipped with automatic voltage regulators (AVRs), in particular standard IEEE model 1 [100] (Appendix D), the other 7 machines the field voltage is calculated considering a simple oscillation stabilizer, which includes a feedback of the rotor speed and the active power produced by the machine [100]. In this study no power system stabilizers PSS are used.

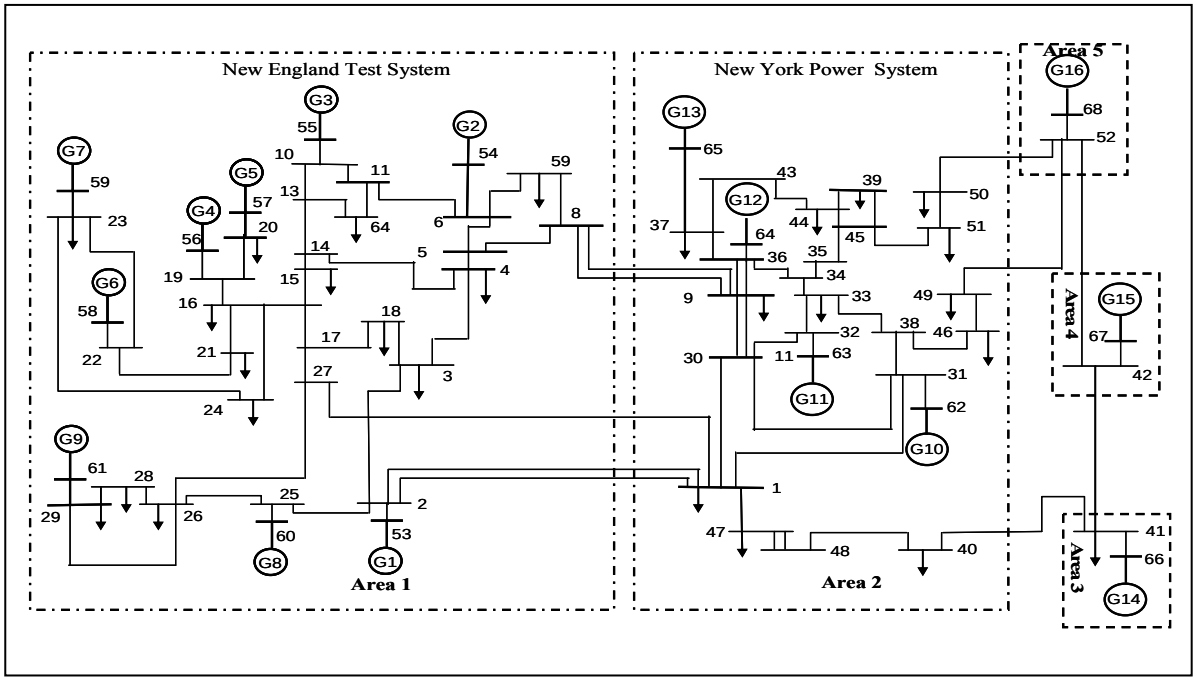

Figure 9.3: One line diagram of the modified 68 bus system

9.4.1 Steady state condition of the system

For the 68 bus system in Figure 9.3, the generators, loads, and imports from other neighboring areas are representative of the operating conditions in the early 1970s. Under these conditions, the voltage profile of the system is shown in Figure 9.4, and the loading of the 66 transmission lines in the system is shown in Figure 9.5.

Figure 9.4 indicates that there are no buses with bus voltages below 0.9 p.u., in fact, all bus voltages are within 0.9 p.u. and 1.1 p.u. Therefore, with the system sustaining a loadability factor of 1.0 p.u., no voltage compensation is needed.

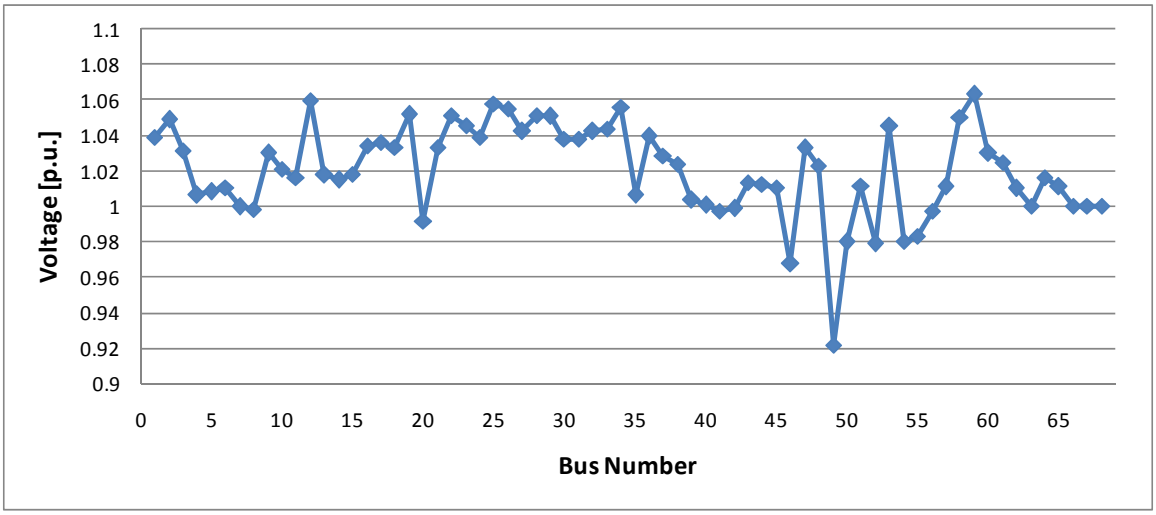

Figure 9.4: Voltage profile of the 68 bus system.

Figure 9.5 shows that the loading of transmission lines are between 0.15 p.u. and 0.8 p.u. and consequently there are no overloaded lines.

A summary of the state of the system is presented in Table 9.1. The columns of the table corresponds to the maximum loadability of the system (λ_L), total voltage

deviation (V_{dev}) as defined in (7.3), transmission power losses (P_{loss}), LUF as defined in (7.21), number of overloaded lines (OVL), and minimum and maximum voltage, V_{min} and V_{max} respectively. It is important to note that, under the above conditions, the result of the CPF indicates that the maximum loading parameter, λ_L, is only 1.076 p.u.

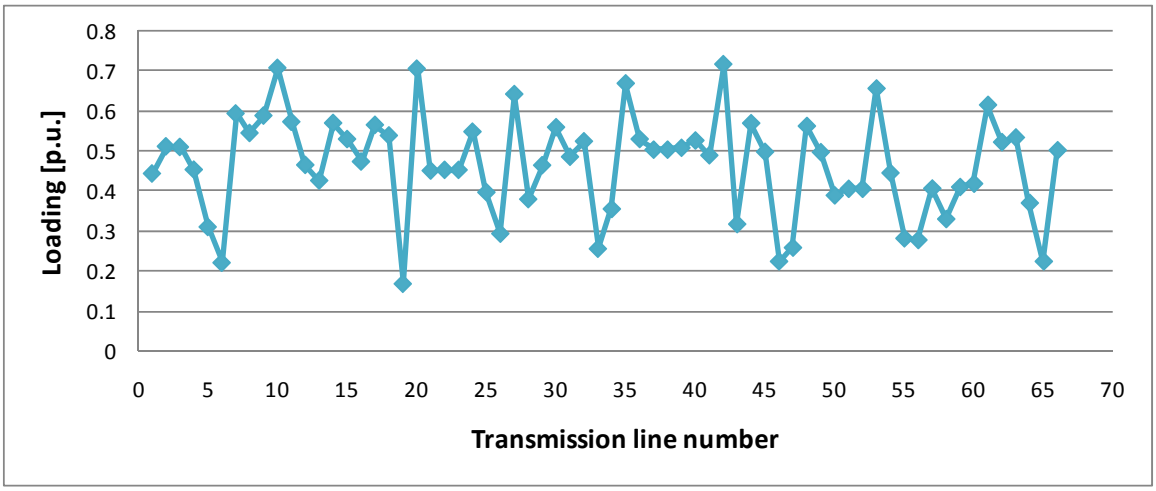

Figure 9.5: Transmission Line loading

Table 9.1: State of the 68 bus system at 1.0 p.u. load

λ_L [p.u.]	V_{dev}	P_{loss} [W]	LUF [%]	OVL	V_{min} [p.u.]	V_{max} [p.u.]
1.076	0.269	205.9	46.5	0	0.921	1.063

As shown in Table 9.1, in this pre-optimization state there are buses above 1.05 p.u. value, therefore the acceptable limits for bus voltages are defined along this particular case study as: 0.95 p.u. and 1.10 p.u. as the minimum and maximum bus voltage respectively.

9.4.2 Small signal stability analysis

The eigenvalue analysis of this system indicates that there are four pairs of eigenvalues that presents low damping. Figure 9.6 shows the plot of the system's eigenvalues, and shows the information of those that presents low damping ratio.

The dynamic order of the system is 132. From these eigenvalues, 130 correspond to real negative eigenvalues, 30 of them are pairs of complex conjugates and 2 are zero eigenvalues.

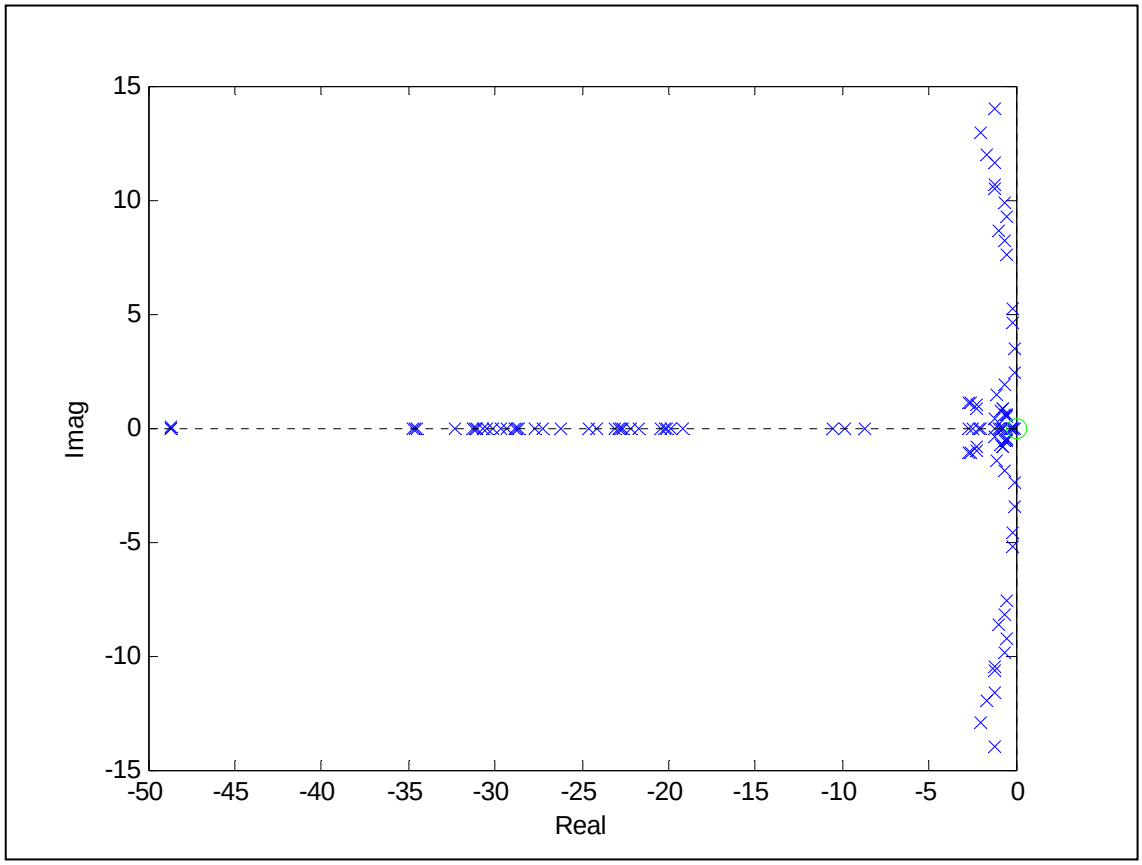

Figure 9.6: System eigenvalues, 68 bus system

The existence of the two zero eigenvalues is explained because of the redundancy in the state variables and do not represent any detrimental effect to the power system performance, in other words, they are not associated to an unstable operating point.

In fact, the first zero eigenvalue occurs because all machine speeds and angles are expressed in absolute terms and it can be avoided if one machine is taken as a reference [101]. The existence of the second zero eigenvalue is justified because the governor actions are not represented. If turbine-governor models are used, then the second zero eigenvalue does not exist [101].

Further analysis of the system eigenvalues indicates that there are four eigenvalues with natural frequencies less than 1 Hz, which have low damping (Table 9.2).

Table 9.2: Inter-area modes- 68 bus system

Eigenvalue #	Real Part	Imaginary Part	Damping Ratio [%]	Frequency [Hz]	Associated Machine
76, 77	-0.20317	±5.1187	4.0	0.81	Generator 15
78, 79	-0.15682	±4.4973	3.6	0.71	Generator 13
80, 81	-0.07053	±3.141	2.5	0.50	Generator 14
82, 83	-0.07833	±2.3162	3.4	0.37	Generator 13

Table 9.2 shows the corresponding eigenvalues, damping ratios and natural frequencies. In addition, the last column Table 9.2 shows the most associated machines for each eigenvalue, considering the analysis of the participation factors.

9.4.3 Large perturbation analysis

This section presents the criteria for selecting critical contingencies that later on are going to be used to evaluate the performance of the power system under large perturbations.

The selection for a critical contingency in a transmission line based on the criteria presented in section 9.3.2. Figure 9.7 shows the values of the P.I. index for each contingency. There are 66 transmission lines in the system that corresponds to the case number of the x-axis of Figure 9.7. Among these 66 cases, cases number 50 and number 66 present the highest P.I. values (148.6 and 108.3 respectively), however case 66 (corresponding to the outage of the line that connects buses 40 and 41) is selected because it presents a higher number of overloaded lines (Table 9.3).

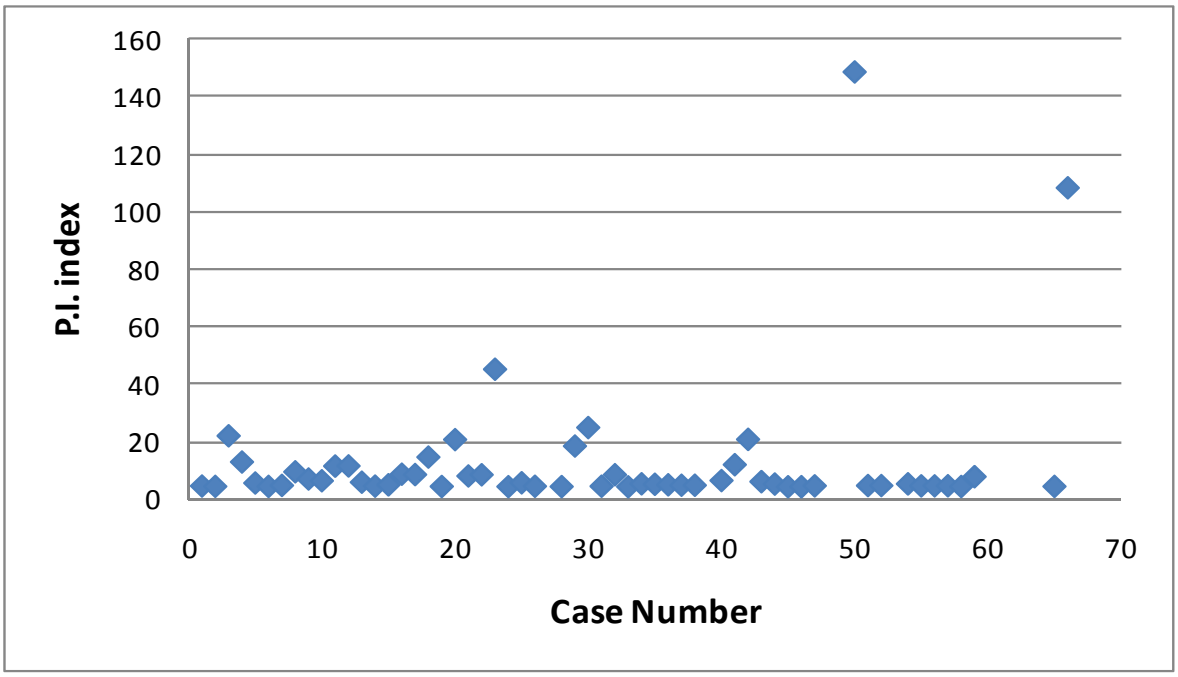

Figure 9.7: P.I. indexes for all line outages in the 68 bus system

Table 9.3: P.I. index for critical contingencies in 68 bus system

Case #	From Bus	To Bus	Transmission loses	Overloaded lines	Voltage Violations	P.I. index
66	41	40	635.2053	11	18	108.3
50	1	47	600.1842	9	16	148.6

Considering the information above, for this study, three contingencies are selected to investigate the transient performance of the 68 bus system:

- Fault 1: a 3-phase (L-L-L) short circuit is placed at the terminals of generator 15. The duration of the fault is 100 milliseconds and the fault resistance is 25 [mΩ]. Generator 15 is one of the critical generator units since, according to the sssa performed in section 9.4.1, it oscillates against generator 14 and the cluster consisting of generators 10 to13. A fault of these characteristics makes the power system become unstable.

- Fault 2: a 3-phase (L-L-L) short circuit is applied in the middle of the transmission line that connects buses 40 and 41. The duration of the fault is 100 milliseconds and the fault resistance has an almost negligible value. After the fault occurs, the system is capable of returning to a stable operating point, however this particular fault has one of the highest P.I. index (as defined in (9.15)) among all other lines outages (Figure 9.7).

- Fault 3: a 3-phase (L-L-L) short circuit is placed at bus 37. The duration of the fault is 100 milliseconds and the fault resistance has an almost negligible value. The load center located at bus 37 is the largest in the system, its proximity to generator 13

exacerbates the impact in the behavior of the system when a fault occurs. A fault in this load center makes the power system become unstable.

9.5 Summary

This chapter presents fundamental concepts to understand the assessment of the power system performance for steady state and the behavior under small and large perturbations in the system.

In particular, for the steady state performance, the basics of the linearized analysis of the power system are explained together with the bifurcation analysis and continuation power flow (CPF).

Considering the dynamic response of the system, the small signal stability analysis is introduced to study the behavior of the system in the presence of small disturbances. When the system is subject to large perturbations, transient analysis, using a non-linear model is the system, is required together with a careful selection of critical contingencies. The P.I. index is described in this chapter to aid the selection of the critical faults in transmission lines.

The previous concepts have been applied to the specific study of a 16 machine - 68 bus system, which is a reduced order model of the New England and New York interconnected power systems published in 1970s.

The steady state analysis reveals that (i) the system does not require voltage support while operating at nominal conditions (1 p.u. load), (ii) there are no overloaded

lines and the LUF is equal to 46.5%, and (iii) the CPF indicates that the maximum loading of the system corresponds to 1.076 p.u.

The results of the sssa show that the system posses four inter area modes with undesired low damping (below 5%) mainly associated with generator 14 and 15 swinging against a cluster of generators 10 to 13.

Finally, the selection of critical contingencies corresponds to (i), a 3-phase short circuit at the terminals of generator 15, (ii) a 3-phase short circuit at the largest load center (located at bus 37), and (iii) a 3-phase short circuit at the middle of the transmission line that connects buses 40 and 41.

All this information provides the fundamental concepts to understand the analysis and the mathematical tools that are used the following two chapters, and illustrate the results of this analysis for the 16 machine – 68 bus system prior to the optimization process.

CHAPTER 10

OPTIMIZATION OF STEADY STATE PERFORMANCE

10.1 Introduction

Part IV, optimization of power system performance using PSO, proposes a two-stage PSO-based optimization framework to improve the performance of the power system using FACTS devices. The improvement in the response of the power system is evaluated considering steady state conditions as well as during small and large perturbations.

Chapter 9 presents a description of the concept utilized in this study to assess the steady state performance of the power system, in particular, a linearized analysis of the power system, bifurcation analysis, and CPF. Additionally, a full description of the system under study, a 16 machine - 68 bus system, is presented.

This chapter focuses on the first stage of the optimization process which is related to the improvement of the steady state performance of the system.

This first stage considers a double-loop optimization algorithm for optimal allocation and control settings of series and shunt compensation, particularly, distributed static series compensator (DSSC) modules and capacitor banks (DSSC device model is described in Appendix A).

As for the series FACTS devices, in this study the DSSC modules are represented as lumped devices with the capability of changing the corresponding line reactances by up to 20% in both directions (increase or decrease). The system is assumed to be fully

deployed, meaning that the operator has the capability of controlling a compensator on very line of the system. The purpose of the first optimization loop is to find optimal control references for each DSSC module, such that the maximum loadability of the system is achieved.

In addition, the second optimization loop is capable of finding optimal locations and sizes of capacitor banks that are used to improve the voltage profile under critical load conditions. The objective function of this stage is to increase the loadability of the system at minimum cost, keeping the system operating under stable conditions.

Both optimization loops for series and shunt compensation, utilize the CPF to compute the maximum loadability of the system. All the algorithms are implemented using PSAT software.

It is important to note that the overall algorithm, considering series and shunt compensation loops, improves the performance of the system under present conditions, but it is designed so that it can be used as a planning tool considering future scenarios with increased demand. This feature is achieved by repeatedly executing the double loop (series-shunt) algorithm. Then, for a given load level, the optimal FACTS installations and control references are found such that the demand can be satisfied at minimum cost while the power system is stably operating.

10.2 Double loop optimization algorithm

The optimization of the power system performance under steady state conditions is carried out considering a double loop optimization algorithm as shown in Figure 10.1.

The interaction between the two optimization loops is as follows:

- First the steady state performance of the system is evaluated to determine what kind of compensation, series or shunt, is required.
  - If the system has low bus voltages and no overloaded lines then the shunt compensation is required first.
  - If the system has overloaded lines but no bus voltage violations then the series compensation stage is performed first.
  - If the system has both overloaded lines and bus voltage violations, then the series compensation loop is performed first since the adjustment of the DSSC modules may have a detrimental effect over the voltage profile (if the total compensation is inductive).
  - If there are no overloaded lines and no bus voltage violations, then CPF is performed to determine maximum loadability of the system and to verify if the limit induced bifurcation (LIB) point corresponds to a bus voltage violation or a maximum line flow. The selection of which compensations loop to perform first is decided according to the results of the CPF. If a saddle node bifurcation (SNB) point is encountered then perform series compensation loop first, to avoid the cost of installing additional capacitor banks.

- Second, assuming without loss of generality that the series compensation loop is carried out first, the algorithm finds the maximum loadability of the system using DSSC modules. The result of the CPF indicates the nature of the stopping criteria, if a LIB point is found due to low bus voltage, then the shunt compensation loop is

executed, otherwise series compensation loop is repeated to find an alternative solution.

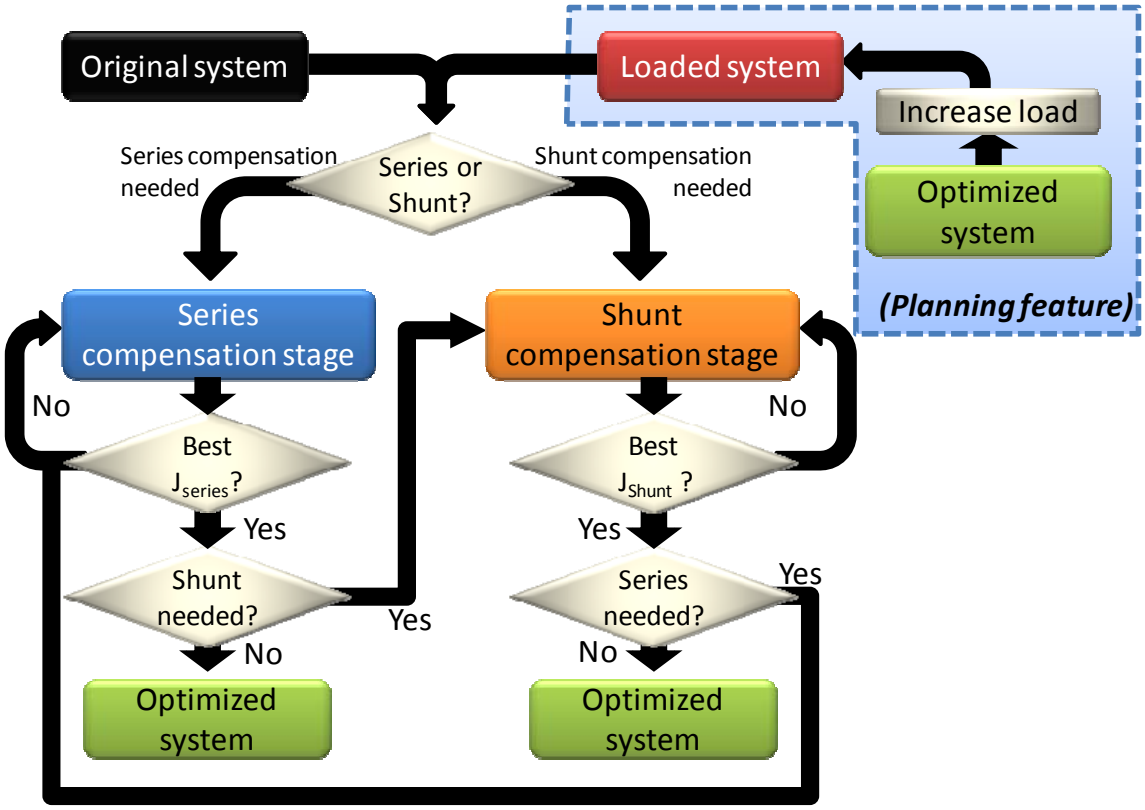

Figure 10.1: Flow chart of double loop optimization algorithm for steady state performance

- Third, the shunt compensation loop is performed to find optimal installation of new capacitor banks. The optimal location and sizes are found such that the maximum loadability of the system is achieved at minimum cost. At the point of maximum loadability, the nature of the stopping criteria is verified, if a LIB point is found due to line a limit violation, then the series compensation loop is carried out. If the LIB is

due to low voltage, then the operator should revise the economical criteria in the objective function, because adjustments may be necessary for either the maximum number of capacitor banks or relevance of the economic metric in the overall objective function.

The interaction between series and shunt compensation loops can be repeated until the global optimal solution is found for the system. At this point, the global optimal steady state performance of the power system will be achieved, the DSSC modules will be operating at their maximum controllability level, and the maximum number of capacitor banks, defined by the economical criteria, will be in service.

As mentioned before, the double-loop optimization process proposed in this study is capable of finding the optimal steady state performance of the power system under present load conditions, however it can also be utilized as a planning tool to find optimal power system performance under different scenarios of increasing demand. For example, if it is foreseen that the demand will increase by 20% in ten years and by 35% in twenty years, then the double loop optimization algorithm can be executed starting with the system loaded at 1.2 p.u. and 1.35 p.u. respectively. This planning analysis can be done considering an even increase of the demand (all loads of the system are increased by the same percentage) or under non-homogeneous demand growth (different load centers increase their demand at different rates).

The following subsections provide the details of each optimization loop (series and shunt compensation loop): objective function, particle definition and system constraints are discussed in each case.

10.2.1 Series compensation loop

The purpose of this PSO-based optimization stage is to find the optimal reference settings for DSSC modules such that the loadability of the system is maximized keeping the system operating in a stable region (within security limits). In addition to the loadability of the system, the line utilization factor (LUF) (defined in (7.21)) and the total transmission losses are considered as part of the optimization criteria

As mentioned before, in this study the DSSC modules are represented as lumped devices with the capability of changing the line reactance by up to 20% in both directions (increase or decrease). The interaction between turbine-generators and the capacitive compensation of DSSC modules is not part of this study, and therefore the phenomenon sub synchronous resonance (SSR) is neglected in the optimization objectives. However, the requirement of avoiding sub-synchronous oscillations (SSO) can be added in the optimization problem (either as an optimization objective or as a constraint) when turbine-governors and electromagnetic flux dynamics are modeled in the system.

Fitness function definition

The objective function considers three goals (multiobjective function) as well as security constraints that are incorporated into the main objective function as penalty functions.

The main goal of this optimization loop is to maximize the loadability of the system. Since in this study the optimization problems are defined by default as a

minimization problem, then the following metric is defined:

$$J_1 = \lambda_{L0} / \lambda_L \tag{10.1}$$

where:

J_1 is the loadability metric (obtained by means of the CPF),

λ_{L0} is the loadability of the uncompensated system,

λ_L is the loadability of the compensated system (potential solution).

A second goal is to improve the LUF of the system, as defined in (7.21), keeping the transmission losses as close as possible to the original uncompensated case. To accomplish this objective the following metrics (10.2) and (10.3) are defined:

$$J_2 = LUF_0 / LUF \tag{10.2}$$

where:

J_2 is the line utilization factor metric,

LUF_0 is the LUF of the uncompensated system,

LUF is the total LUF of the compensated system (potential solution).

$$J_3 = P_{loss} / P_{loss0} \tag{10.3}$$

where:

J_3 is the transmission losses metric,

P_{loss} is the total transmission losses of the compensated system (potential solution).

P_{loss0} is the total transmission losses of the uncompensated system.

The system security constrains are incorporated using penalty functions when a violation, either a bus voltage or a line overload, occurs. In this way, three metrics are proposed that consider (i) the violations in line loading (10.4), (ii) low voltage violations (10.5), and (ii) high voltage violations (10.6).

$$J_4 = \begin{cases} OVL / OVL_0 & if\ OVL_0 > 0 \\ OVL & if\ OVL_0 = 0 \end{cases} \tag{10.4}$$

where:

J_4 is the overloaded lines metric,

OVL is the number of overloaded lines of the compensated system (potential solution).

OVL_0 is the number of overloaded lines of the uncompensated system.

$$J_5 = \begin{cases} Vbus\_low / Vbus\_low_0 & if\ Vbus\_low_0 > 0 \\ Vbus\_low & if\ Vbus\_low_0 = 0 \end{cases} \tag{10.5}$$

where:

J_5 is low voltage violation metric,

Vbus_low is the number of buses with low voltage violation of the compensated system (potential solution).

$Vbus\_low_0$ is the number of buses with low voltage violation of the uncompensated system.

The value to determine a low voltage violation corresponds to 0.90 p.u. This value is lower than the value of 0.95 p.u. presented in section 9.4.1 to give more flexibility to the DSSC modules in controlling the power flow in various transmission lines. It is important to note that the relaxation of this value is possible since the voltage profile is improved later on in the shunt compensation loop.

$$J_6 = \begin{cases} Vbus\_high \Big/ Vbus\_high_0 & if\ Vbus\_high_0 > 0 \\ Vbus\_high & if\ Vbus\_high_0 = 0 \end{cases} \tag{10.6}$$

where:

J_6 is high voltage violation metric,

Vbus_high is the number of buses with high voltage violation (above 1.1 p.u.) of the compensated system (potential solution).

$Vbus\_high_0$ is the number of buses with high voltage violation of the uncompensated system.

Therefore the overall objective function (J) is defined as:

$$J = \omega_1 \cdot J_1 + \omega_2 \cdot J_2 + \omega_3 \cdot J_3 + \omega_p \cdot (J_4 + J_5 + J_6) \tag{10.7}$$

where:

J is the overall objective function,

ω_1, ω_2 *and* ω_3 are weights that reflect the relative importance of each objective (maximization of loadability, maximization of LUF and minimization of transmission losses),

ω_p is penalty weight that penalize system violations.

The selection of weights and penalty factors, as well as the technical criteria that need to be satisfied, depend on the particular interest of the operator or utility. In this case, the values of $\omega_1 = 3$, $\omega_2 = 1$, $\omega_3 = 0.25$, $\omega_p = 5$, are used.

This selection of weights gives equal more relevance to the improvement of the loadability of the system, followed by the improvement of LUF and giving less importance to the transmission losses.

Particle definition

The PSO particle is defined as the vector containing the line reactances of the system. There are 66 transmission lines and therefore the particle vector has 66 components, $x_i \in \Re^{66}$.

$$x_i = \begin{bmatrix} X_{L1} & X_{L2} & \dots & X_{L66} \end{bmatrix} \tag{10.8}$$

where:

x_i is the PSO particle's vector, also called decision vector,

X_{Lk} is the line reactance of line k, $k \in \{1, 2, ..., 66\}$.

Search space definition

The components of the PSO particle are limited by the maximum compensation that the DSSC units can provide, which in this case correspond to 20% of the value of the corresponding line reactance.

$$0.8 \cdot X_{Lk}^{0} \le X_{Lk} \le 1.2 \cdot X_{Lk}^{0}, \quad k \in \{1, 2, ..., 66\} \tag{10.9}$$

where:

X_{Lk}^{0} is the original reactance of line k (i.e. without DSSC modules).

The values of all original line reactances are shown in Appendix D.

In the case of the system constraints (feasible region), they are included in the main objective function as the penalty functions in (10.4)-(10.6).

Additionally to the previous constrains, the following criterion is applied to the candidate solutions:

$$J_i = \begin{cases} J_i & if \quad J_i \le J_i^o \\ \infty & if \quad J_i > J_i^o \end{cases} \tag{10.10}$$

where:

J_i is the objective function value of particle i using present DSSC settings (potential solution),

J_i^0 is the value of metric J of the original system (no DSSC).

This last rule rejects all solutions that have a worse objective function value than the original case (no DSSC).

PSO parameters

The concept of fine tuning PSO, described in section 7.3.1, is utilized in this optimization loop. A summary of the PSO parameters is presented in Table 10.1.

Table 10.1: PSO parameters, series compensation loop

Parameter	Tested values
Inertia constant	Linearly decreased inertia weight
Individual acceleration constant (c_1)	2.5
Maximum velocity	5% of corresponding limits
Number of particles	15
Maximum number of iterations	100

10.2.2 Shunt compensation loop

The shunt compensation loop consists of optimizing the steady state performance of the power system. Its objective is to find the optimal locations and sizes of capacitor banks, so that loadability of the system is maximized while the number of bus voltage violations, at a given load level, is minimized.

The optimization objective considers the improvement of the system loadability and the cost of installation of the capacitor banks, and therefore, to minimize the number of banks to be allocated in the system.

Fitness function definition

Analogous to the series compensation loop, the objective function considers three goals as well as security constraints which are integrated in the main objective function as penalty functions.

The main goal is to improve the loadability of the system and improve the voltage profile of the system, with a minimum number of capacitor banks and minimum size for

each one of them.

To accomplish this goal, the loadability metric defined in (10.1) is used together with the normalized voltage deviation metric defined in (7.3) and (7.4) and the cost metric described in (10.11).

$$J_3 = \frac{1}{2} \cdot \left(\frac{N_{units}}{N_{units}^{\max}} + \sum_{i=1}^{Nunits} \frac{\eta_i}{N_{units}^{\max} \cdot \eta^{\max}} \right) \tag{10.11}$$

where:

J_3 is the capacitor banks' cost metric,

N_{units} is the number of capacitor banks allocated in the present solution,

$N_{units}^{\max}$ is the maximum number of capacitor banks that can be allocated in the system and is limited to 5 capacitor banks in this particular study,

η_i is the size or rating of capacitor bank i, $i \in \{1, 2, ..., N_{units}\}$ in MVAr,

η^{max} is the maximum size or rating of any capacitor bank and is equal 250 MVAr in this particular study.

The cost metric in (10.11) is analogous to the one defined in (7.28) for the case of STATCOM units. It has two components, the first component acts as a penalty factor when the number of units increases and therefore it can be understood as a normalized value of the fixed costs associated with the installation of each capacitor bank.

The second component of metric J_3 is related to the variable cost component of each capacitor bank, which is assumed to be a linear function of the size of the capacitor bank.

Each component of J_3 is normalized to have comparable values around one. Since this metric is defined as the summation of the two components, a scaling factor of 0.5 is used to make the overall value to be around one, and therefore be comparable with other metrics in the objective overall function.

In addition to the previous three metrics, the system security constraints (related to overloaded lines and bus voltage violations) are included in the main objective function using the metrics, J_4 - J_6, as defined before in (10.4)-(10.6).

Finally, the overall objective function is defined as:

$$J = \omega_1 \cdot J_1 + \omega_2 \cdot J_2 + \omega_3 \cdot J_3 + \omega_p \cdot (J_4 + J_5 + J_6) \tag{10.12}$$

where:

J is the overall objective function,

ω_1, ω_2 and ω_3 are weights that reflect the relative importance of the loadability metric, the normalized voltage deviation metric, and the cost metric respectively.

ω_p is a penalty weight that penalizes system violations.

The values of the weights, penalty factors, and the definition of the technical and cost metrics, can be adjusted according to the interest of operators and utilities. In this particular study, the following values are used: $\omega_1 = 3$, $\omega_2 = 1$, $\omega_3 = 0.75$, and $\omega_p = 5$.

This selection of the weight values gives more relevance to the maximization of the loadability of the system followed by the improvement of the voltage profile. The weight value ω_3, associated to the cost metric, is set in 0.75; however, since the sensitivity of the results with respect to this variable is high, different values of the weight ω_3 are investigated as part of this research.

Particle definition

The PSO particle definition (decision vector) is defined as:

$$x_i = [\lambda_1 \quad \eta_1 \quad \lambda_2 \quad \eta_2 \quad \ldots \quad \lambda_{Nunits} \quad \eta_{Nunits}] \tag{10.13}$$

where:

λ_h is the location of capacitor bank h, $h \in \{1, 2, ..., N_{units}\}$,

η_h is the size of capacitor bank h, $h \in \{1, 2, ..., N_{units}\}$.

Search space definition

The constraints used in this optimization stage are those described in (10.14)-

(10.17). In other words, the bus location cannot be greater that the total number of buses in the system (10.14), it is not possible to locate two capacitor banks at the same bus (10.15), the voltage profile of the system must be kept between 0.95 p.u. and 1.1 p.u. (10.16), and finally the size of the capacitor bank cannot exceed a maximum value of 250 MVAr (10.17).

$$1 \le \lambda_h \le N_{bus}, \quad h \in \{1, 2, ..., N_{units}\} \tag{10.14}$$

$$\lambda_i \ne \lambda_j \qquad \forall i, j \tag{10.15}$$

$$0.95 \le V_i \le 1.10 \ , \quad i \in \{1, 2, ..., N_{bus}\} \tag{10.16}$$

$$0 \le \eta_h \le 250 \ , \quad h \in \{1, 2, ..., N_{units}\} \tag{10.17}$$

In addition to the above constraints, the following criterion is applied to the candidate solutions:

$$J_i = \begin{cases} J_i & if \ \left(J_1^i + J_2^i \right) \le \left(J_1^0 + J_2^0 \right) \\ \infty & otherwise \end{cases} \tag{10.18}$$

where:

J_i is the objective function value of particle i using present capacitor bank allocation (potential solution),

J_1^i is the value of metric J_1 of particle i using present capacitor bank allocation (potential solution),

J_2^i is the value of metric J_2 of particle i using present capacitor bank allocation (potential solution),

J_1^0 is the value of metric J_1 of the system with no capacitor banks allocated,

J_2^0 is the value of metric J_1 of the system with no capacitor banks allocated.

This last rule rejects all solutions that have a worse objective function value than the original case (no capacitor banks).

PSO parameters

The PSO parameters are presented in Table 10.2.

Table 10.2: PSO parameters, shunt compensation loop

Parameter	Tested values
Inertia constant	Linearly decreased inertia weight
Individual acceleration constant (c_1)	2.5
Maximum velocity for bus location	17
Maximum velocity for STATCOM size	50
Number of particles	40
Maximum number of iterations	100

10.3 Simulation results and technical discussion

10.3.1 Series compensation loop

The results for the overall objective function, in (10.7), and objective function metrics ((10.1)-(10.6) are shown in Table 10.3.

Table 10.3: Objective function value and metrics for series compensation loop

J	J_0	J_1	J_2	J_3	J_4	J_5	J_6
3.75	4.25	0.84	0.98	0.95	0	0	0

The results in Table 10.3 indicate that the overall objective function value is reduced by 12%, from an original value of 4.25 (J_0) to an optimized value of 3.75 (J).

All three technical metrics J_1, J_2 and J_3, which are related to the maximum loadability of the system (10.1), LUF (10.2) and transmission losses (10.3) respectively, present some degree of improvement, while all three penalty functions associated with the system security constraints (J_4 -J_6, as defined in (10.4)-(10.6)) are zero, implying that there a no overloaded lines and no bus voltage violations.

The main goal of this optimization loop is the improvement of the loadability of the system, which is related to metric J_1 defined in (10.1). The value of $J_1 = 0.84$ indicates that the loadability of the system is improved by 19% (($1/J_1$-1), percentagewise) because of the action of the DSSC modules.

The results of the series compensation loop also indicate that the 19% improvement in the loadability of the system cannot be increased any further using DSSC modules because the results of the CPF indicate that the maximum loadability is found

due to a LIB point associated to low bus voltages. For this reason, to keep improving the loadability of the system, shunt compensation is required.

A summary of the system state before and after the series compensation loop is presented in Table 10.4.

Table 10.4: System state, pre and post series compensation loop

	λ_L	V_{dev}	P_{loss} [MW]	LUF [%]	Max_L [p.u.]	V_{min} [p.u.]	V_{max} [p.u.]
Original System	1.07	0.269	205.9	46.5	0.71	0.92	1.063
System_Series_comp	1.28	0.299	195.4	47.3	0.74	0.98	1.068

The columns of Table 10.4 present the information of the maximum loadability of the system (λ_L), the value of the voltage deviation metric (V_{dev}), as in (7.3), the total power losses (P_{loss}), line utilization factor (LUF), as defined in (7.21), maximum line loading (Max_L), minimum and maximum bus voltages. The values corresponding to these parameters are obtained with the system operating at 1 p.u loading.

Table 10.4 confirms the conclusion obtained from Table 10.3 by showing the improvement of the loadability of the system from an original value of 1.07 p.u. to 1.28 p.u. Additionally, when the system is operating at 1 p.u. load, there is a slight detrimental effect on the voltage profile (V_{dev}) because of the action of the DSSC modules, however the transmission losses and LUF are improved. Finally, the last three columns of Table 10.4 show that there are no overloaded lines or bus voltage violations in the series compensated system.

The optimal DSSC settings obtained at the end of this optimization loop are shown in Table 10.5. These values correspond to the control reference of the DSSC modules in the form of the value of the line reactance, in p.u., that needs to be achieved.

Table 10.5: Optimal DSSC settings, series compensation loop

#	Bus From	Bus To	X_L [p.u.]	#	Bus From	Bus To	X_L [p.u.]	#	Bus From	Bus To	X_L [p.u.]
1	1	2	0.033	**23**	16	21	0.011	**45**	1	31	0.013
2	1	30	0.006	**24**	16	24	0.005	**46**	31	38	0.012
3	2	3	0.012	**25**	17	18	0.007	**47**	33	38	0.053
4	2	25	0.010	**26**	17	27	0.014	**48**	38	46	0.023
5	3	4	0.017	**27**	21	22	0.017	**49**	46	49	0.022
6	3	18	0.011	**28**	22	23	0.009	**50**	1	47	0.015
7	4	5	0.010	**29**	23	24	0.028	**51**	47	48	0.021
8	4	14	0.010	**30**	23	59	0.033	**52**	47	48	0.021
9	5	6	0.003	**31**	25	26	0.039	**53**	48	40	0.018
10	5	8	0.013	**32**	26	27	0.012	**54**	35	45	0.014
11	6	7	0.011	**33**	26	28	0.038	**55**	37	43	0.022
12	6	11	0.007	**34**	26	29	0.059	**56**	43	44	0.001
13	7	8	0.004	**35**	28	29	0.012	**57**	44	45	0.058
14	8	9	0.044	**36**	9	30	0.015	**58**	39	44	0.049
15	9	30	0.022	**37**	9	36	0.016	**59**	39	45	0.101
16	10	11	0.005	**38**	9	36	0.016	**60**	45	51	0.008
17	10	13	0.003	**39**	36	37	0.004	**61**	50	52	0.069
18	13	14	0.008	**40**	34	36	0.009	**62**	50	51	0.018
19	14	15	0.017	**41**	33	34	0.013	**63**	49	52	0.091
20	15	16	0.011	**42**	32	33	0.008	**64**	52	42	0.048
21	16	17	0.007	**43**	30	31	0.022	**65**	42	41	0.072
22	16	19	0.023	**44**	30	32	0.023	**66**	41	40	0.067

Finally, the control effort of the DSSC modules is calculated as follows:

$$C.E. = \sum_{i=1}^{N_{Lines}} \left|\Delta X_{Li}\right| \cdot I_{Li}^2 \tag{10.19}$$

where:

C.E. is the total control effort of the DSSC modules,

N_{Lines} is the total number of transmission lines in the system,

ΔX_{Li} is the p.u. difference in the line reactance of transmission line *i* (i.e. the value of original line reactance minus the value of the optimized line reactance, both in p.u.),

I_{Li} is the current of transmission line *i* in p.u.

On the one hand, the total control effort of the DSSC modules, calculated as in (10.19), is equal to 580.4 MVAr. On the other hand, the benefit provided by the DSSC modules, as mentioned before, is to increase the loadability factor by 19%. This translates, considering the system data presented in Appendix D, into 3,477 MVA more load that the system can carry when the DSSC modules are operating.

10.3.2 Shunt compensation loop

As mentioned in the previous section, the DSSC modules are capable of increasing the loadability of the system from a value of 1.07 p.u to 1.28 p.u. After the series compensation loop, the results of the CPF indicate that the loadability of the system cannot be increased any further because of the presence of bus voltage violation in the system. Figure 10.2 shows the voltage profiles of the system under 1.0 p.u. and 1.28 p.u. load. This figure shows that three buses go below to the acceptable voltage

limits, and particularly one of them reach the value of 0.8 p.u. which is the lowest value that the CPF considers before declaring a LIB point.

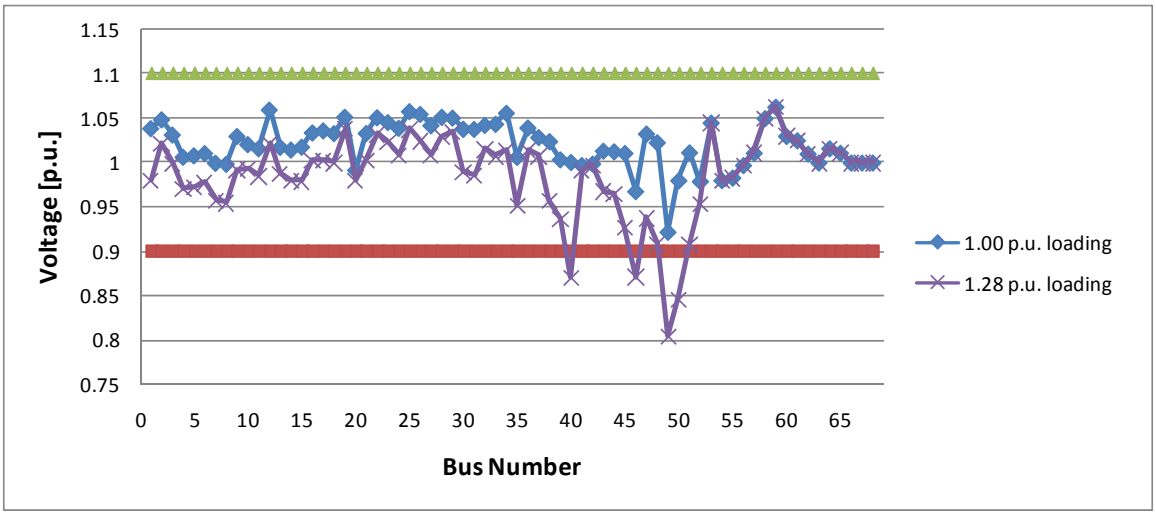

Figure 10.2: Voltage profile, 68 bus system, at 1.0 p.u. and 1.28 p.u. load.

The shunt compensation loop is therefore executed, starting with the system loaded at 1.28 p.u., with series compensation. The results are presented in Table 10.6.

Table 10.6: Objective function value and metrics for shunt compensation loop

J	J_1	J_2	J_3	J_4	J_5	J_6
4.13	0.9425	0.587	0.90	0	0	0

The results in Table 10.6 show that all three technical metrics J_1, J_2 and J_3, that are respectively associated to the maximum loadability of the system (10.1), normalized voltage deviation metric (7.4) and total cost (10.11), are improved with respect to the

values of the system with no shunt compensation. The penalty functions associated with the system security constraints (J_4 -J_6, as defined in (10.4)-(10.6)) are zero, implying that there are no overloaded lines and no bus voltage violations.

Analogous to the series compensation loop, the main goal is to maximize the loadability of the system. The value of $J_1 = 0.9425$ indicates that the loadability of the system is improved by 5.75% (($1/J_1-1$), percentagewise) with respect to the system with no shunt compensation and load equal to 1.28 p.u. This percentage of 5.75% translates into a 35.3% (($1/J_1 \cdot 1.28$), percentagewise) total improvement considering the combined effect of the capacitor banks and the DSSC modules.

The results of the shunt compensation loop also indicate that the voltage deviation metric is improved by 41% (($1-J_3$), percentagewise) as compared with the uncompensated system.

The results of the CPF indicate that the maximum loadability is found due to a LIB point associated with a line flow limit; therefore to keep improving the loadability of the system, it is necessary to execute the series compensation loop. In this fashion, the proposed double loop optimization process can be repeated iteratively to the system to find optimal series and shunt compensation at different load levels.

A summary of the system state before and after the shunt compensation loop is presented in Table 10.7. The columns of this table contains the information of the maximum loadability of the system (λ_L), the value of the voltage deviation metric (V_{dev}), as in (7.3), the total power losses (P_{loss}), line utilization factor (LUF), as defined in (7.21), maximum line loading (Max_L), minimum and maximum bus voltages.

Table 10.7: System state, pre and post shunt compensation loop

	λ_L	V_{dev}	P_{loss} [MW]	LUF [%]	Max_L [p.u.]	V_{min} [p.u.]	V_{max} [p.u.]
System_Series_comp	1.28	0.299	195.4	47.3	0.74	0.98	1.068
System_Shunt_comp	1.35	0.207	342.9	59.8	0.92	0.95	1.063

The values corresponding to V_{dev}, P_{loss}, LUF, Max_L, V_{min}, and V_{max} are obtained with the system operating at 1.28 p.u loading in the case of the shunt compensated system and at 1.0 p.u. for the series compensated system. This fact explains the large differences between some of the variables, in particular the transmission power losses, LUF, and maximum line loading.

Considering the loadability of the system, Table 10.7 shows that the maximum λ_L, combining series and shunt compensation, is 1.35 p.u. which is in agreement with the value derived from Table 10.6.

Regarding the actual solution of the capacitor banks allocation problem, the shunt compensation loop finds that the optimal solution is the placement of three capacitor banks in the system. The optimal location and sizes are shown in Table 10.8.

Table 10.8: Capacitor banks, optimal location and sizes

#	Bus	Rating [MVA]
1	48	50
2	49	174
3	50	76

The solution in Table 8.21 considers a weighting factor $w_3 = 0.75$ for the cost metric J_3, defined in (10.11). As part of this study, different values for this weighting

factor as well as different numbers of capacitor banks are tried with the results shown in Figure 10.3-Figure 10.5. The reason for this investigation is to evaluate how the technical criteria can be limited by economical constraints.

Figure 10.3 shows the value of the maximum loadability of the system (λ_L) that can be obtained for different values of the cost metric weight (w_3) and different numbers of capacitor banks.

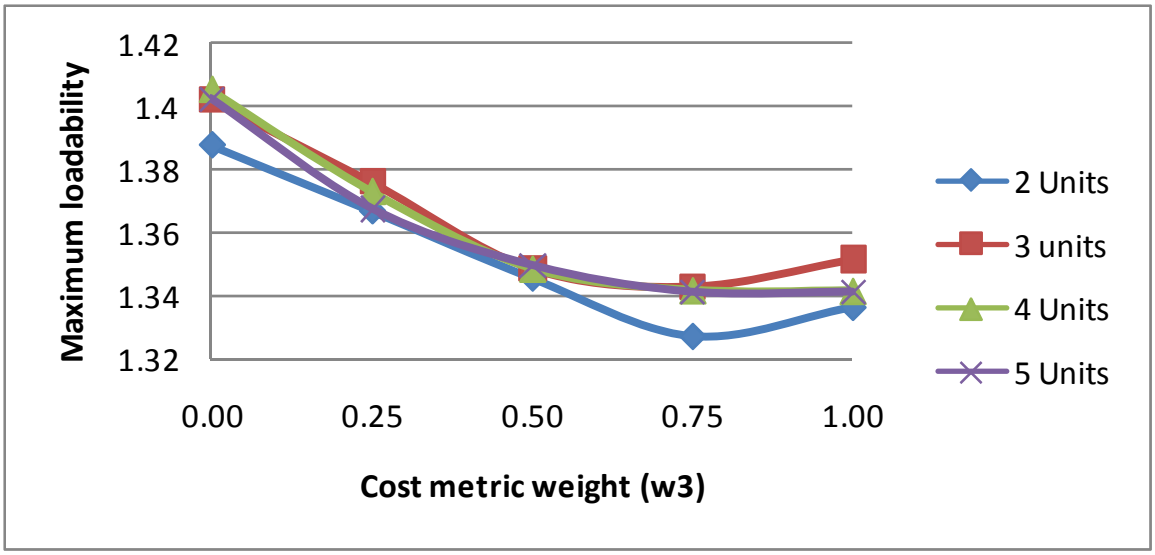

Figure 10.3: Maximum loadability at different importance levels of the cost metric

Five different values of cost metric weight (w_3) are considered: 0, 0.25, 0.5, 0.75 and 1.0. The value of $w_3 = 0$ implies that the cost of installing the capacitor banks is not taken into account as an optimization objective, while $w_3=1.0$ gives maximum importance to the cost metric.

Figure 10.3 shows that the value of $w_3=0.75$ gives the most conservative scenario for the capacitor banks' allocation, because it leads to the lowest loadability of the

system. For instance, with 3 capacitor banks the maximum loadability that can be achieved is 1.4 p.u. when there are no economical constraints ($w_3 = 0$) but it is reduced to 1.345 p.u. when the cost metric is emphasized ($w_3 = 0.75$).

These results are explained by the fact that by giving more priority to the cost metric the total amount of allocated MVAs is reduced (Figure 10.4).

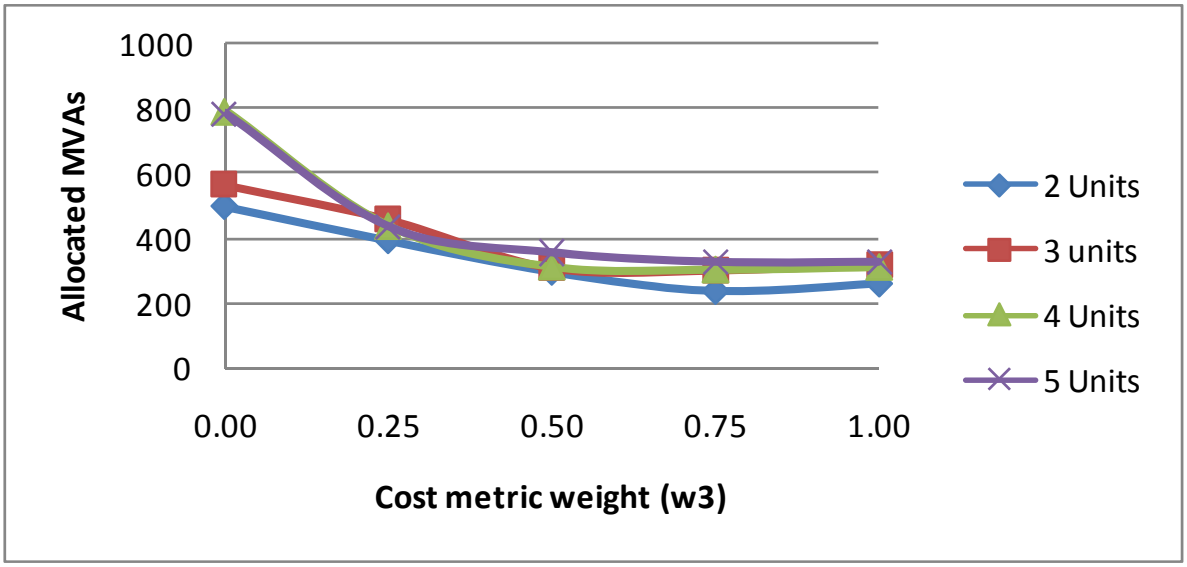

Figure 10.4: Total number of allocated MVAs at different importance levels of the cost metric

Figure 10.5 shows the loadability of the system that can be achieved by different numbers of capacitor banks. It is possible to note that, independently of the relative importance given to the cost metric (i.e. for all five values of w_3), there is noticeable improvement when the number of units is increased from 2 to 3, but not much change when the number of capacitor banks is further increased (saturation effect). This result

confirms that the optimal number of capacitor banks to be placed in the system corresponds to 3.

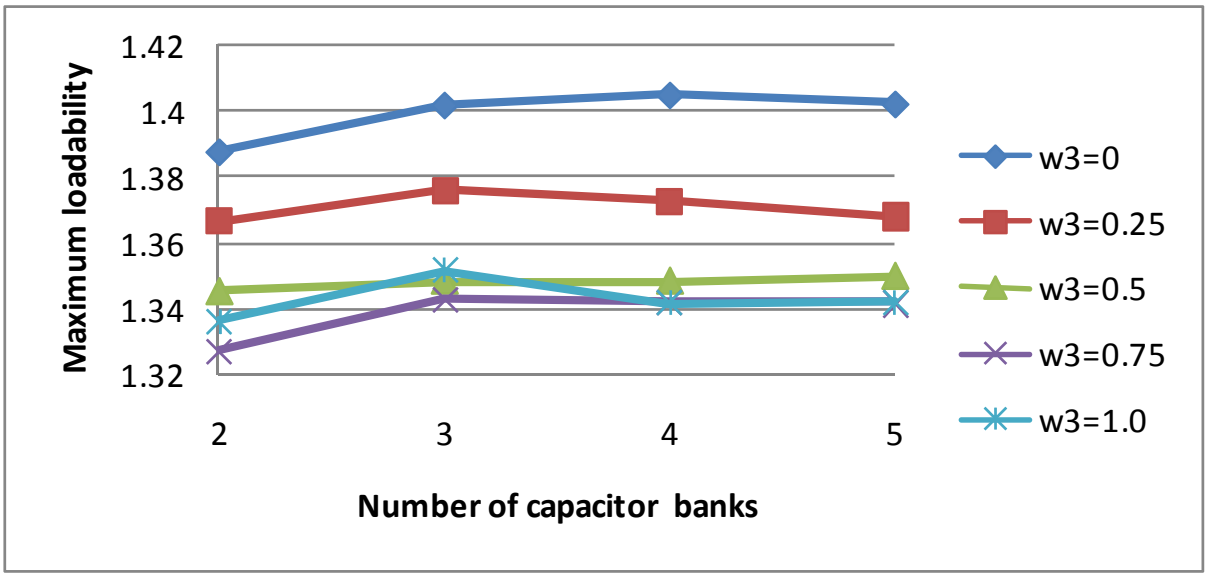

Figure 10.5: Maximum loadability considering different number of capacitor banks

10.3.3 Overall results

Table 10.9 presents an overall summary of the results obtained by the double loop optimization process proposed in this chapter.

Table 10.9: System state, pre and post series-shunt compensation loop

	λ_L	V_{dev}	P_{loss} [MW]	LUF [%]	Max_L [p.u.]	V_{min} [p.u.]	V_{max} [p.u.]
Original System	1.07	0.269	205.9	46.5	0.71	0.92	1.063
Compensated System	1.35	0.207	342.9	59.8	0.92	0.95	1.063

The columns of this table are the maximum loadability of the system (λ_L), the value of the voltage deviation metric (V_{dev}), as in (7.3), the total power losses (P_{loss}), line utilization factor (LUF), as defined in (7.21), maximum line loading (Max_L), minimum and maximum bus voltages.

It is important to note that the values corresponding to V_{dev}, P_{loss}, LUF, Max_L, V_{min}, and V_{max} are obtained with the system operating at 1.28 p.u loading in the case of the shunt compensated system and at 1.0 p.u. for the original system (without shunt compensation). This fact explains the large differences between some of the variables, in particular the transmission power losses, LUF, and maximum line loading.

The most relevant result in Table 10.9 is the improvement of the loadability of the system (λ_L) form a value of 1.07 p.u. to 1.35 p.u. due to the combined actions of series and shunt devices (DSSC modules and capacitor banks respectively) . The improvement of the loadability factor is carried out imposing a stable system operation at every step of the optimization process. As a consequence the system can operate at 1.35 p.u. loading maintaining the line flows and bus voltages within desired limits.

10.4 Summary

This chapter proposes a double loop PSO-based optimization framework to improve the steady state performance of the power system using series and shunt compensation, in particular DSSC modules and capacitor banks.

The optimization process consists of two optimization loops: (i) a series compensation loop and (ii) a shunt compensation loop. These two loops can be repeatedly executed to maximize the loadability of the system without violating the system security constraints (i.e. keeping the line flows and bus voltages within limits).

The first optimization loop, called series compensation loop, is used to relieve transmission lines congestion using distributed FACTS devices, in particular DSSC modules. The system is assumed to be fully deployed, meaning that there is full controllability of all transmission lines. The DSSC is modeled as a lumped device with the capability of changing the value of the corresponding line reactance by 20% in either direction (increase or decrease).

The result of the optimization process is the optimal control settings (desired value for the line reactances) for each DSSC module, such that the loadability of the system is maximized without incurring any overloaded lines Additionally, the line utilization factor is improved with a minimum impact over the total transmission losses of the system.

The second optimization loop, named shunt compensation loop, provides optimal allocation and rating for capacitor banks such that the loadability of the system (found by the means of the CPF) is a maximum. In addition to the loadability of the system, the voltage profile (minimization of voltage deviations) is improved at minimum cost.

The results of the proposed double loop PSO-based optimization framework applied to a 16 machine - 68 bus system (described in section 9.4) shows that system loadability can be improved from 1.07 p.u. to 1.28 p.u. when the DSSC modules are optimally tuned. At this point, the results of the series compensation loop also confirm

that the system loadability cannot be increased any further with series compensation only because the CPF stopping criteria indicate the presence of a LIB point associated with low bus voltages.

As a consequence a shunt compensation loop is executed increasing the loadability of the system to 1.35 p.u. At this loading level, that considers the action of both DSSC modules and capacitor banks, the system is capable of operating with all variables within security limits.

In this case, the results of the CPF indicates that a LIB point due to a line flow limit is encountered and therefore a new cycle of series-shunt compensation can be performed starting with the system at 1.35 p.u. loading level.

In this fashion, the proposed double loop PSO-based optimization framework can be used as a planning tool providing optimal control references for the DSSC modules and optimal location and sizes of capacitor banks with the system under different scenarios of future demand.

This chapter has address the improvement of the power system performance using steady state criteria, next chapter focuses on the improvement of the behavior of the power system subject to small and large disturbances.

CHAPTER 11

OPTIMIZATION OF DYNAMIC AND TRANSIENT PERFORMANCE

11.1 Introduction

Part IV, optimization of power system performance using PSO, proposes a two-stage PSO-based optimization framework to improve the performance of the power system using FACTS devices. The improvement in the response of the power system is evaluated considering steady state conditions as well as during small and large perturbations.

Chapter 9 presents a description of some fundamental concepts that are utilized in this study to evaluate the performance of the power system: linearized analysis of the power system, small signal analysis for small disturbances, and an assessment of critical faults for large perturbation analysis. Chapter 9 also provides a complete description of the 16 machine - 68 bus system used in this study.

The first stage of the proposed two-stage PSO-based optimization framework, related with the improvement of the steady state performance of the power system, is described in detail in chapter 10. This chapter focuses on the second stage of the optimization process which is related to the improvement of the performance of the system under small and large disturbances.

This second stage considers a two-sequential-stage, PSO-based, optimization algorithm for optimal allocation and control of shunt FACTS devices, in particular STATCOM units (model described in Appendix A).

The main objective is to find optimal locations, sizes and control parameters (for both internal and external controllers) of the STATCOM devices, such that a maximum benefit is obtained over the entire power system, instead of focusing on local neighborhoods. In particular, this study focuses on increasing the damping of the system to mitigate large perturbations and inter-area modes.

Once the optimization process is complete, the inter-area modes are mitigated and the response of the system for large perturbations is significantly improved. Faults that could make the system unstable are rapidly mitigated due to the effect of the optimally placed and controlled STATCOM devices.

11.2 Two-stage optimization algorithm

A two-stage, PSO based, optimization algorithm is proposed to solve the optimization of the dynamic and transient performance of the power system. The proposed flow chart is shown in Figure 11.1.

The optimization process starts with the steady state optimized system (procedure described in chapter 10), and then two optimization stages are carried out sequentially. First, the number of STATCOM units, their optimal locations and sizes are determined considering the improvement of the power system performance subject to large perturbations. In particular, the main objective is to maximize the system damping at minimum cost (minimum number of units and minimum sizes).

Additionally, in this first stage, the optimal control settings for each STATCOM internal controller are found. The internal controller of each STATCOM corresponds to a

simple voltage regulator presented in Appendix A. The novelty in this scheme for control parameter setting is that the overall response of the system is taken into account, as opposed to traditional methods for tuning control parameters that only focus on the behavior of the voltage at the point of common coupling.

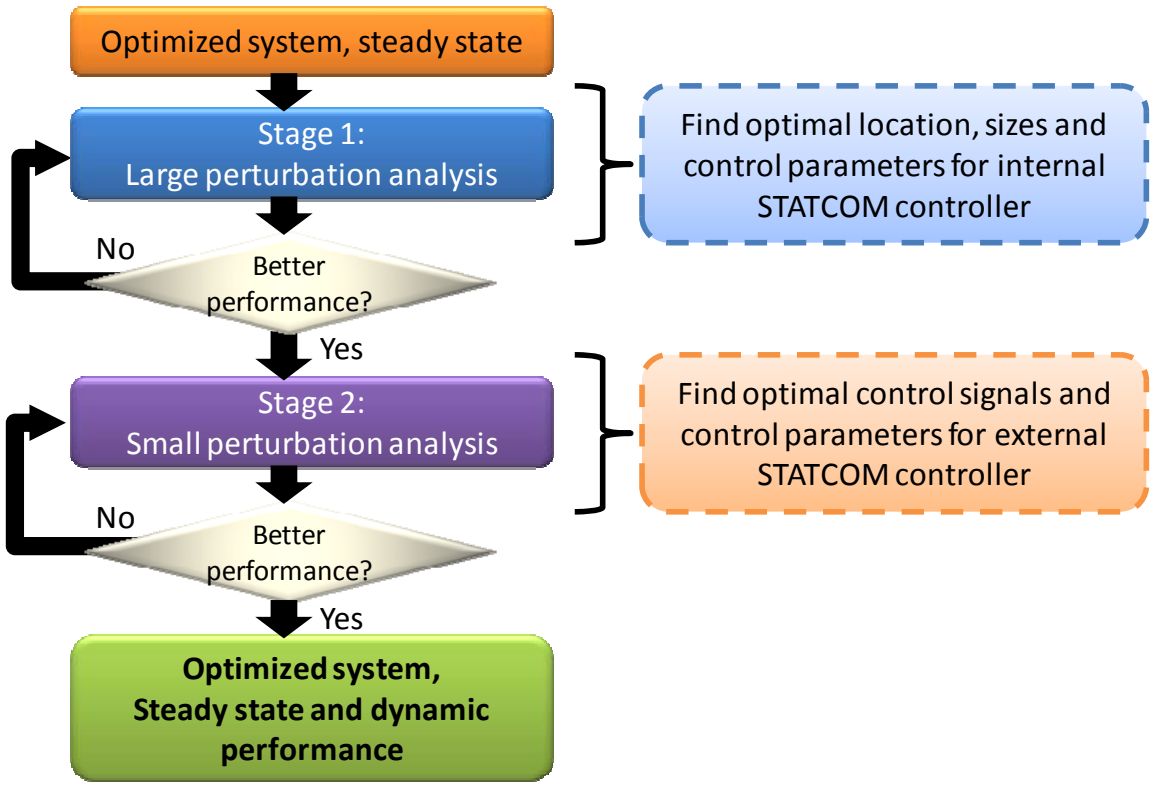

Figure 11.1: Flow chart of the two-stage optimization algorithm for power system dynamic performance

The internal controllers of the STATCOM units provide fast damping during fault conditions, however their steady state outputs do not appreciably improve the damping of inter area modes [101], [107]. This implies that the STATCOM units require an external

control, known as supplementary power oscillation damping (POD), to improve the response of the system considering small signal stability.

Therefore, the second optimization stage considers the number of units, location, sizes and internal controller parameters computed by the previous optimization stage and finds the optimal number of external controllers, their control signal and their control parameters such that the response of the system under small disturbances is optimized. The detailed model of the STATCOM external controller (power oscillation damper) is presented in Appendix A

The following subsections provide the details of each optimization stage: objective function, particle definition and system constraints are discussed in each case.

11.2.1 Large perturbation analysis

The purpose of this optimization stage is to find the optimal number of STATCOM units, their location, sizes and internal controller parameters, such that the damping of the power system, under fault conditions, is improved.

The STATCOM model and the details of its internal controller are presented in Appendix A.

The simulation of the performance of the power system is carried out in the time domain considering three critical faults:

- Fault 1: 100 ms, temporary 3-phase, short circuit at the terminals of generator 15,
- Fault 2: 100 ms, temporary 3-phase short circuit in the middle of the transmission line that connects buses 40 and 41,

- Fault 3: 100 ms, temporary 3-phase short circuit at largest load center (bus 37).

The selection of this last fault is based on the analysis based on the P.I. index, defined in (9.15), which is explained in chapter 9, section 9.4.3.

Fitness function definition

The main objective of this optimization stage is to minimize the voltage oscillations in the power system under fault conditions at minimum cost.

This minimum cost is related to minimize the number of STATCOM units to be allocated as well as their sizes. In this study, the cost metric defined in (7.28) is utilized. The maximum number of STATCOM units to be allocated is 5 and the maximum size of each device corresponds to 250 MVA.

As technical criteria, for each of the three critical faults considered in this study the following performance metric is defined:

$$J_{h+1} = \sum_{i=1}^{N_{bus}} w_i \cdot V_{i,h} \tag{11.1}$$

where:

J_{h+1} is the performance metric corresponding to fault h, $h \in \{1,2,3\}$

N_{bus} is the total number of buses in the system,

w_i is a weighting factor,

$V_{i,h}$ is the total voltage deviation, defined as:

$$V_{i,h} = \sum_{t=0}^{t_f} \left(\left| V_{i,h}(t) - \overline{V_{i,h}} \right| \right) \tag{11.2}$$

where:

t_f is the total simulation time,

$V_{i,h}(t)$ is the value of the p.u. voltage at bus i and time t, during fault h,

$\overline{V_{i,h}}$ is the average value of the p.u. voltage at bus i, during fault h.

Equation (11.1) corresponds to the weighted sum of the voltage deviations in the system, where the weighting factor w_i is defined as:

$$w_i = \begin{cases} 0.25 & if\ V_{i,0} \in [R_0, R_1) \\ 0.50 & if\ V_{i,0} \in [R_1, R_2) \\ 0.75 & if\ V_{i,0} \in [R_2, R_3) \\ 1.00 & if\ V_{i,0} \in [R_3, R_4] \end{cases} \tag{11.3}$$

where:

$V_{i,0}$ is the total voltage deviation, as in (11.2), in the original system (no STATCOM units allocated).

Additionally,

$$R_0 = \min_i \{V_{i,0}\},\ i \in \{1, 2, ..., N_{bus}\} \tag{11.4}$$

$$R_4 = \max_i \{V_{i,0}\},\ i \in \{1, 2, ..., N_{bus}\} \tag{11.5}$$

$$R_1 = R_0 + 0.25 \cdot (R_4 - R_0) \tag{11.6}$$

$$R_2 = R_0 + 0.50 \cdot (R_4 - R_0) \tag{11.7}$$

$$R_3 = R_0 + 0.75 \cdot (R_4 - R_0) \tag{11.8}$$

The weighting factor scheme in (11.3), implies that more importance is given to the minimization of voltage deviations at those buses that are mostly impacted by the corresponding fault h, $h \in \{1,2,3\}$.

Considering the weights in (11.3), the maximum weight value of 1 is given to that 25% of the buses that have the largest total voltage deviation; then the weight is reduced to 0.75 for those buses where the total voltage deviation is larger than half of the buses but less than the first quartile. A weight of 0.5 is assigned to the buses where the total voltage deviation is larger than the lower 25% but less that the second quartile, and finally, a weight of 0.25 is assigned to the lowest quartile (25% of the buses that are less affected by the corresponding system fault).

The objective function in (11.1) considers weighted voltage deviations for all the buses in the system, providing a global scheme for parameter setting as opposed to traditional methods for tuning control parameters that only focus in the behavior on the voltage at the point of common coupling.

The overall objective function of this stage is then:

$$J = \omega_1 \cdot J_1 + \omega_2 \cdot J_2 + \omega_3 \cdot J_3 + \omega_4 \cdot J_4 \tag{11.9}$$

where:

J is the overall objective function,

ω_1, is weight that reflect the relative importance of the cost metric,

ω_2, ω_3 and ω_4 are weights that reflect the relative importance of each fault.

In this study, $\omega_2 = \omega_3 = \omega_4 = 1.0$, indicating that all faults are equally important. The values of ω_2, ω_3, and ω_4 can be adjusted differently, if among the selected contingency set some faults are more severe than others, or incur in larger economical penalties or have a greater probability of occurrence.

Additionally, since the technical metrics J_2-J_4 are not normalized, the weight associated with the cost metric, ω_1, is set to a value of 500 to make it comparable in magnitude with the technical metrics.

Particle definition

The PSO particle definition (decision vector) has two components as defined in (11.10) and (11.11):

$$x_i^{loc} = \begin{bmatrix} \lambda_1 & \eta_1 & \lambda_2 & \eta_2 & \dots & \lambda_{Nunits} & \eta_{Nunits} \end{bmatrix} \tag{11.10}$$

where:

x_i^{loc} is the vector containing STATCOM location and sizes,

λ_h is the location of STATCOM unit *h*, $h \in \{1,2,...,N_{units}\}$,

η_h is the size of STATCOM unit *h*, $h \in \{1,2,...,N_{units}\}$.

$$x_i^{cont} = \left[Kr_1 \quad Tr_1 \quad Kr_2 \quad Tr_2 \quad ... \quad Kr_{Nunits} \quad Tr_{Nunits} \right] \tag{11.11}$$

where:

x_i^{cont} is the vector containing STATCOM internal controller parameters,

Kr_h is the regulator gain of STATCOM *h*, $h \in \{1,2,...,N_{units}\}$,

Tr_h is the regulator time constant size of STATCOM *h*, $h \in \{1,2,...,N_{units}\}$.

Finally, the overall PSO particle is given by (11.12).

$$x_i = \left[x_i^{loc} \quad x_i^{cont} \right] \tag{11.12}$$

Search space definition

The constraints used in this optimization stage are described in (10.14)-(10.17).

They are related to: (i) the bus location cannot be greater that the total number of buses in the system (10.14), (ii) two STATCOM units cannot be located at the same bus (10.15), (iii) the desired limits for bus voltages are 0.95 p.u. and 1.1 p.u. (as explained in 9.4.1) (10.16), and finally (iv) the size of any STATCOM unit cannot exceed a maximum value of 250 MVAr (10.17).

In addition to the system constrains previously presented, there some constraints related to the particle limits, particularly to the vector containing the STATCOM controller internal parameters, x_i^{cont}, (11.13), (11.14).

$$10 \le Kr_h \le 250, \quad h \in \{1, 2, ..., N_{units}\} \tag{11.13}$$

$$0.01 \le Tr_h \le 1, \quad h \in \{1, 2, ..., N_{units}\} \tag{11.14}$$

The selection of the lower and upper limits for these two parameters corresponds to a rather wide range around typical values of $Kr_1 = 50$ and $Tr_1 = 0.1$.

Finally, two restrictions apply to the overall objective function (J): (i) if the particle currently evaluated (potential solution) leads to an unstable operation of the system, causing the time domain simulation to diverge, then the objective function value, J, is set to infinity, and (ii) if the voltage deviations, resulting from the fitness evaluation of the current particle, are worse than the original case (without STATCOM) for any of the faults under study, then the objective function value, J, is also set to infinity, (11.15).

$$J = \begin{cases} \inf & if\ J_{2,k} > J_{2,0} \\ \inf & if\ J_{3,k} > J_{3,0} \\ \inf & if\ J_{4,k} > J_{4,0} \\ J & otherwise \end{cases} \tag{11.15}$$

where:

$J_{h+1,k}$ is the value of metric J_{h+1}, corresponding to fault h, $h \in \{1,2,3\}$, for current particle k (potential solution),

$J_{h+1,0}$ is the value of metric J_{h+1}, corresponding to fault h, $h \in \{1,2,3\}$, of the original system (when there are no STATCOM units).

PSO parameters

The PSO parameters used in this study are presented in Table 11.1Table 10.2.

Table 11.1: PSO parameters, large perturbation analysis

Parameter	Tested values
Inertia constant	Linearly decreased inertia weight
Individual acceleration constant (c_1)	2.5
Maximum velocity for bus location	17
Maximum velocity for STATCOM size	50
Maximum velocity for control parameters	25% of corresponding limits
Number of particles	40
Maximum number of iterations	100

11.2.2 Small perturbation analysis

As mentioned before, the internal controllers of the STATCOM units do not improve appreciably the damping of inter area modes [101], and they may even have a detrimental effect on this damping [107]. Therefore, external controllers, POD (Appendix A), are applied to the STATCOM units allocated in the previous stage.

This second optimization stage finds the optimal number of external controllers, their control signals and their control parameters such that the response of the system under small disturbances is optimized.

The main objective is to improve the damping of the inter area modes of the system, which correspond to four modes as shown in Table 9.2. The evaluation of the power system performance is therefore carried out using sssa.

Since the sssa provides a solution only valid around the operating point where the power system model is linearized, once this second optimization stage is completed, the time domain response of the system under large perturbation is evaluated to verify the effect of adding the POD controllers. If the response of the system under large perturbations is satisfactory then the optimal solution of this second stage is adopted, otherwise this second optimization loop is repeated.

Fitness function definition

In this optimization stage the performance of the power system is evaluated using sssa. In particular, the objective is to change the eigenvalues of the system such that they

can be in the desired D-shape area of the s-plane (Figure 9.2 in section 9.3.1).

The objective function metrics are then given by (11.16) and (11.18).

$$J_1 = \left| \sum_{i=1}^{N} \omega_i \cdot \left(\frac{\mathrm{Re}\{Eig_{cc}(i)\} - \sigma_0}{\sigma_0} \right) \right| \tag{11.16}$$

where:

J_1 is the overshoot metric,

N is the total number of complex conjugate eigenvalues,

Eig_{cc} is a vector that contains the complex conjugate eigenvalues of the system,

σ_0 is the minimum acceptable real part, equal to -3,

ω_i is a weighting factor which is equal to:

$$\omega_i = \begin{cases} 1 & if \quad \mathrm{Re}\{Eig_{cc}(i)\} > \sigma_0 \\ 0 & otherwise \end{cases} \tag{11.17}$$

This metric penalizes the eigenvalues with real parts larger that the desired value of σ_0. These eigenvalues lie closer to the imaginary axis, and therefore closer to the right-half of the s-plane, making the system more susceptible to unstable operation. Additionally, values of $\mathrm{Re}\{Eig_{cc}(i)\}$, $i \in \{1,2,...,N\}$ that are closer to the origin imply a worse overshoot in the system variables (bus voltages, machine speeds) when the system

is subjected to any perturbation (large or small).

$$J_2 = \sum_{i=1}^{N} \omega_i \cdot \left(\frac{Damping(Eig_{cc}(i)) - dr_0}{dr_0} \right) \tag{11.18}$$

where:

J_2 is the damping metric,

dr_0 is the minimum acceptable damping equal to 5%.

And,

$$Damping(Eig_{cc}(i)) = \left(\sqrt{\left(\frac{\sigma_i}{w_i} \right)^2 + 1} \right)^{-1} \tag{11.19}$$

where:

σ_i is the real part of $Eig_{cc}(i),\ i \in \{1,2,\ldots,N\}$

w_i is the imaginary part of $Eig_{cc}(i),\ i \in \{1,2,\ldots,N\}$

Additionally,

$$\omega_i = \begin{cases} 10 & if \quad Damping(Eig_{cc}(i)) < dr_0 \quad and \quad f < 1Hz \\ 1 & if \quad Damping(Eig_{cc}(i)) < dr_0 \quad and \quad f > 1Hz \\ 0 & otherwise \end{cases} \tag{11.20}$$

The damping metric, J_2, strongly penalizes the low damping in the inter area modes (eigenvalues whose corresponding frequencies are less than 1 Hz). It also penalizes any eigenvalue with an associated damping less than the desired value of 5%.

In addition to the technical metrics, J_1 and J_2, three penalty functions are included (11.21)-(11.23):

$$J_3 = N_{low\_damping} \Big/ 2 \tag{11.21}$$

where:

$N_{low\_damping}$ is the number of inter area modes with damping less than 5%.

$$J_4 = N_{pos\_eig} \tag{11.22}$$

where:

N_{pos_eig} is the number of positive eigenvalues.

$$J_5 = \frac{N_{POD}}{N_{units}} \tag{11.23}$$

where:

N_{POD} is the number of PODs being allocated,

N_{units} is the number of STATCOM units allocated after the first optimization stage.

Penalty function J_3, penalizes the number of inter area modes that have low damping, while penalty function J_4 deals with possible positive eigenvalues that may appear as the result of adding POD controllers. These positive eigenvalues are extremely undesirable since they represent an unstable operation of the system, and they should be avoided. Finally, penalty function J_5, is related to minimize the number of PODs installed in the system.

The overall objective function for this optimization stage is:

$$J = \omega_1 \cdot J_1 + \omega_2 \cdot J_2 + \omega_{p1} \cdot J_3 + \omega_{p2} \cdot J_4 + \omega_{p3} \cdot J_5 \qquad (11.24)$$

where:

J is the overall objective function,

ω_1 and ω_2 are weights that reflect the relative importance of the technical metrics,

ω_{p1}, ω_{p2} and ω_{p3} are penalty weights associated with metrics J_3-J_5.

The selection of weights and penalty factors depend on the particular interest of the operator or utility. In this case, the values of $\omega_1 = 1$, $\omega_2 = 5$, $\omega_{p1} = 5$, $\omega_{p2} = 1000$, and $\omega_{p3} = 1$, are used.

This selection of weights gives more importance to the mitigation of the inter area oscillations in the system, followed by the improvement of the overshoot metric. The penalty weight for the number of low damping inter area modes ω_{p1} is set to a value equal

to the corresponding weight of the damping metric, ω_2. In this way the dual effect of J_2 and J_3, emphasizes the main objective of this optimization stage.

Regarding the penalty given to metric J_4, ω_{p2}, this value is very high, since the situation of having positive eigenvalues is extremely undesired.

Finally, the weight associated with the number of PODs, ω_{p3}, is relatively low to provide more emphasis to satisfy the technical criteria.

Particle definition

The PSO particle definition (decision vector) contains ten elements per each POD that is allocated in the system. The decision variables for each POD are defined in (11.25), and a detailed model is presented in Appendix A.

$$x_k^{POD} = \left[L_{cs} \quad K_w \quad T_w \quad T_1 \quad T_2 \quad T_3 \quad T_4 \quad T_\varepsilon \quad V_s^{\max} \quad V_s^{\min} \right] \tag{11.25}$$

where:

x_k^{POD} is the vector containing parameters of POD unit k, $k \in \{1,2,\ldots, N_{units}\}$

L_{cs} is the location of the POD control signal,

K_w is the POD stabilizer gain,

T_w is the washout time constant for output signal,

T_1, T_2, T_3 and T_4, are the POD lead-lag constants,

T_ε is the low pass time constant for output signal,

V_s^{min} and V_s^{max} are the POD upper and lower bound for the output signal.

Then the particle vector is given by (11.26).

$$x_i = \left[x_1^{POD} \quad x_2^{POD} \quad \ldots \quad x_{Nunits}^{POD} \right] \tag{11.26}$$

Search space definition

In this stage, the location of the control signal is constrained by (10.14), which implies that the location is limited to the number of buses in the system.

In addition, each element of the POD external controller is limited by an upper and lower bound. In particular:

$$0.01 \le K_w \le 50 \tag{11.27}$$

$$1 \le T_w \le 20 \tag{11.28}$$

$$0.04 \le T_1, T_3 \le 4 \tag{11.29}$$

$$0.02 \le T_2, T_4 \le 2 \tag{11.30}$$

$$0.0001 \le T_\varepsilon \le 0.01 \tag{11.31}$$

$$-0.5 \le V_s^{\min} \le -0.1 \tag{11.32}$$

$$0.1 \le V_s^{\max} \le 0.5 \tag{11.33}$$

The selection of the lower and upper limits for these parameters corresponds to traditional ranges that have been applied to PSSs that have the same control structure and transfer function as the POD. Several references are taken into account in determining the ranges per each variable [100], [102], [108]-[111], nevertheless the final values highly depend on the characteristic of the system and the nature of the control signal (speed deviation, bus voltage, power output, etc).

Finally, if the overall objective function (J), resulting from the sssa evaluation of the current particle, is worse than the original case (without PODs) then the objective function value, J, is also set to infinity, (11.33).

$$J = \begin{cases} \inf & if \;\; J_{1-4} > J_0 \\ J & otherwise \end{cases} \tag{11.33}$$

where:

$J_{1\text{-}4}$ is the overall objective function value without metric J_5 that penalizes the number of POD controllers allocated in the system (i.e. considering $\omega_{p3} = 0$ in (11.24)), also equivalent to the weighted sum of J_1, J_2, J_3 and J_4.

J_0 is the value of overall objective function J of the original system (when there are no POD controllers installed in the system).

PSO parameters

The PSO parameters used in this stage are presented in Table 11.2.

Table 11.2: PSO parameters, small signal stability analysis

Parameter	Tested values
Inertia constant	Linearly decreased inertia weight
Individual acceleration constant (c_1)	2.5
Maximum velocity for control signal location	17
Maximum velocity for control parameters	25% of corresponding limits
Number of particles	50
Maximum number of iterations	500

11.3 Simulation results and technical discussion

11.3.1 Large perturbation analysis

The results for the overall objective function, in (11.9), and objective functions metrics (11.1) are shown in Table 11.3.

Table 11.3: Objective function value and metrics large perturbation analysis

J	J_1	J_2	J_3	J_4	$J_{2,0}$	$J_{3,0}$	$J_{4,0}$
445.26	258	115.13	43.15	28.97	380.12	193.99	38.86

Table 11.3 shows that the technical metrics associated to faults 1 (short circuit at generator 15) and 2 (short circuit at largest load center) have a substantial improvement. In particular, J_2, reduces its value to 30% of the original metric, $J_{2,0}$, (when no STATCOM is connected in the system) and J_3, decreases its value to 22% of the original metric, $J_{3,0}$. The third technical metric, J_4, associated with fault 3 (short circuit in

transmission line between buses 40 and 41), decreases to 26% as compared of its original value $J_{4,0}$.

The overall results indicate that there is a significant improvement in the dynamic performance of the system, which is quantified by an average reduction (considering all three faults) of 70% in the voltage deviations. This value of 70% is calculated considering the overall objective function value, J, minus the cost metric, J_1 (i.e. J-J_1) and compared with the overall objective function value of the original system with no STATCOM units connected ($J_{2,0}$+$J_{3,0}$+$J_{4,0}$).

The solution found by this optimization stage is to allocate three STATCOM units, with location, sizes and internal controller parameters presented in Table 11.4.

Table 11.4: Solution for large perturbation analysis

Unit	Location [Bus]	Size [MVA]	Regulator gain (Kr)	Regulator Time constant (Tr)
1	31	91	149.36	0.489
2	48	115	93.72	0.518
3	51	118	143.83	0.0516

11.3.2 Small signal stability analysis

As mentioned in earlier sections of this chapter, the mitigation of inter area modes cannot be achieved with the STATCOM internal controller only. The impact in the eigenvalues of the system, of the three STATCOM units found in the previous optimization stage is shown Table 11.5.

Comparing the damping of the inter area modes with and without the STATCOM units, it can be seen that the addition of the three STATCOM units has a detrimental effect in those eigenvalues of the system. This result is expected, since it has been reported in literature that the STATCOM DC voltage regulator contributes negative damping to a power system, while the AC voltage control has little influence on the system damping [107].

Table 11.5: System eigenvalues, STATCOM internal controller only

Frequency	Damping without STATCOM	Damping with STATCOM
0.82	4.0 %	3.7 %
0.73	3.6 %	3.0 %
0.55	2.5 %	1.8 %
0.39	3.4 %	2.1 %

In order to improve the response of the system from the perspective of the small signal stability, the second optimization stage of the proposed PSO-based optimization framework is executed and gives the results shown in Table 11.6.

Table 11.6: Objective metrics for small signal stability analysis

J	J_{1-4}	J_0	J_1	J_2	J_3	J_4	J_5
44.026	43.36	244.88	43.36	0	0	0	0.66

Table 11.6 shows that the objective function value (without penalties for the number of POD controllers allocated in the system), J_{1-4} (defined (11.33)), is 82% smaller than the value without the POD controller, J_0, thus representing a significant improvement in the system eigenvalues.

This improvement is corroborated by considering the penalty functions J_3 and J_4 (defined in (11.21) and (11.22)) that indicate that, after the two POD controllers are allocated and tuned, there are no inter area modes with low damping ($J_3 = 0$) and there are no positive eigenvalues in the system ($J_4 = 0$). Finally, the value of J_5 (as in (11.23)) indicates that two out of the three STATCOM units are equipped with a POD controller.

The critical modes and their respective damping, before and after the allocation of the POD controllers, are shown in Table 11.7.

Table 11.7: System eigenvalues, STATCOM internal-external controller

Frequency	Damping without STATCOMs	Damping with STATCOMs and PODs
0.82	4.0 %	5.0%
0.73	3.6 %	5.1%
0.55	2.5 %	5.7%
0.39	3.4 %	5.0%

The solution found by this optimization stage is presented in Table 11.8.

Table 11.8: Solution for small perturbation analysis

Parameter	POD STATCOM 1	POD STATCOM 2
Control signal [Bus]	37	63
Stabilizer gain [K_w]	16.52	20.04
Washout time constant, T_w, [sec]	11.40	10.03
Lead-Lag block 1, (T_1,T_2), [sec]	(2.310, 0.420)	(2.370, 0.02)
Lead-Lag block 2, (T_3,T_4), [sec]	(0.777, 0.659)	(2.518, 1.120)
Low-pass time constant, T_ε, [sec]	0.0059	0.01
Stabilizer upper limit, V_s^{max}, [p.u.]	0.35	0.35
Stabilizer lower limit, V_s^{min}, [p.u.]	-0.35	-0.35

The solution in Table 11.8 is verified considering their control blocks: (i) washout filter, (ii) first lead-lag block, (iii) second lead-lag block, and (iv) stabilizer low-pass filter. Special attention is given to the first block and the fourth block.

The washout filter is a high pass filter that removes the steady state component of the control signal, the filter is such that the very low frequencies are removed but the inter area modes in the range of 0.3 to 1 Hz cannot be attenuated.

The washout filter corresponding to the POD controller at STATCOM 1 has a cut-off frequency of 0.014 Hz, meaning that any frequency below this value is attenuated by more than 3 dB. Additionally, the range of frequencies corresponding to the inter area modes have no attenuation (0 dB). The washout filter corresponding to the POD controller at STATCOM 2 has a cut-off frequency of 0.016 Hz and the frequencies in the range of the inter area modes have no attenuation. Therefore both washout filters satisfy the design criteria.

Considering the stabilizer low pass filter, its main function is to remove high frequency components that may be associated with undesired noise in the control signal. The corresponding cut-off frequencies are 26.5 Hz and 15.9 Hz, for the POD controllers at STATCOM unit 1 and 2 respectively, which completely satisfy the design criteria.

11.3.3 Overall results

The following sections present the overall dynamic performance of the 68 bus power system under selected faults (section 9.4.3 of chapter 9), considering the results from the two optimization loops described in sections 11.2.1 and 11.2.2.

For each case, the performance of the system is illustrated using the time domain response of the bus voltages where the STATCOM units are located (buses 31, 48, and 51). Additionally, some other buses that are mainly affected by the corresponding fault are also shown.

Fault 1: 100 ms 3 phase short circuit at generator 15

For this particular fault, the main affected buses in the system correspond to those in the neighboring areas of the buses where the STATCOM units are located, thus only the response of buses 31, 48 and 51 are presented. Figure 11.2 - Figure 11.4. In addition, the plot of the speed deviations of generator 15 is presented in Figure 11.5.

Figure 11.2 shows the voltage deviations in p.u. value of bus 31 where the first STACOM units is connected. The graph shows three responses: (i) the system without STATCOM units (original system), (ii) the system with three STATCOM units allocated in the system with their corresponding internal controllers (optimal solution found by the first optimization stage), and (iii) the system with all three STATCOM units and POD controllers in the first two STATCOMs, located at buses 31 and 48 respectively (optimal solution of second optimization stage).

Figure 11.2 indicate that there is a substantial improvement in the system response and damping when the STATCOM units are allocated. The original system has a negative damping and the oscillations keep growing; but when the STATCOM units with their internal controller are added to the system the amplitude of the oscillations reduces drastically although there is still a long settling time. Once the POD controllers

are installed in the first two STATCOM units, the damping improves further and the settling time becomes much shorter, taking only a few cycles to mitigate the oscillations.

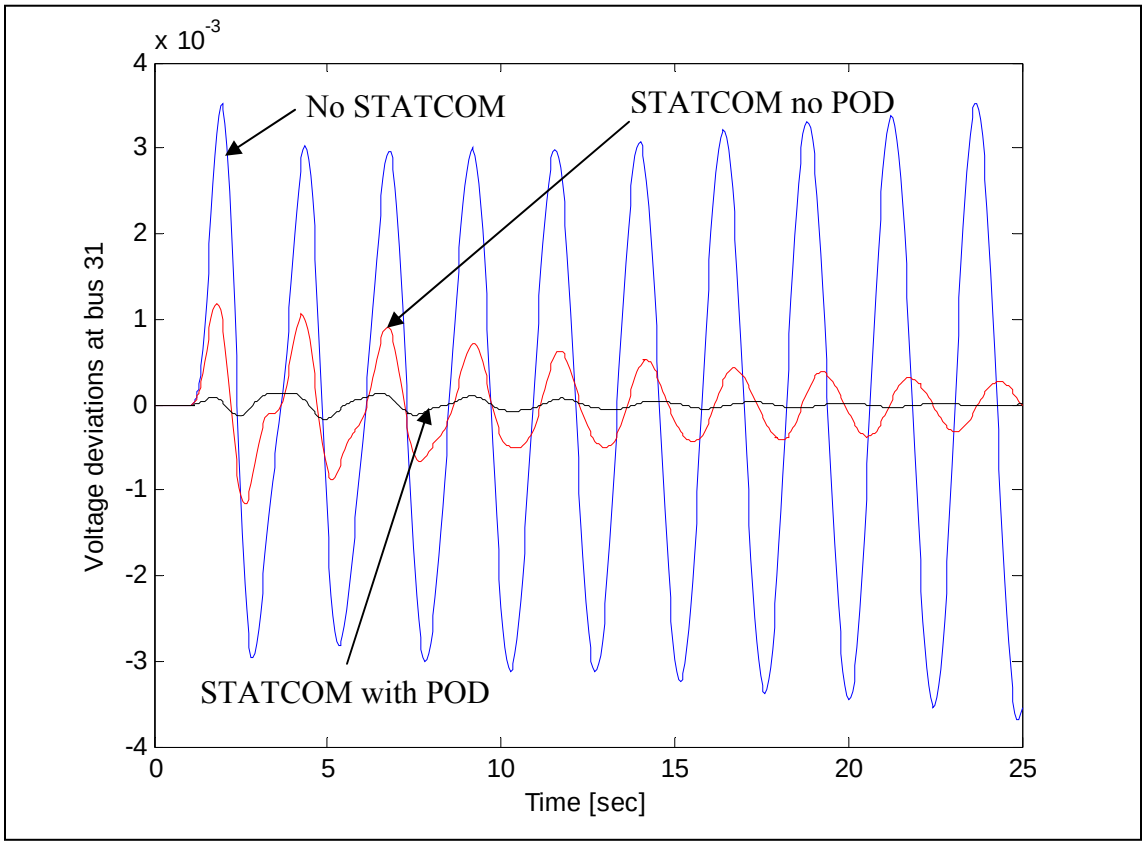

Figure 11.2: Voltage deviations [p.u.] at bus 31, fault 1

A similar response can be noted in Figure 11.3 that shows the voltage deviations at the point of common coupling of the second STATCOM unit. The system response improves by adding the STATCOM units and the POD controllers considering both the

amplitude of the oscillations and the settling time.

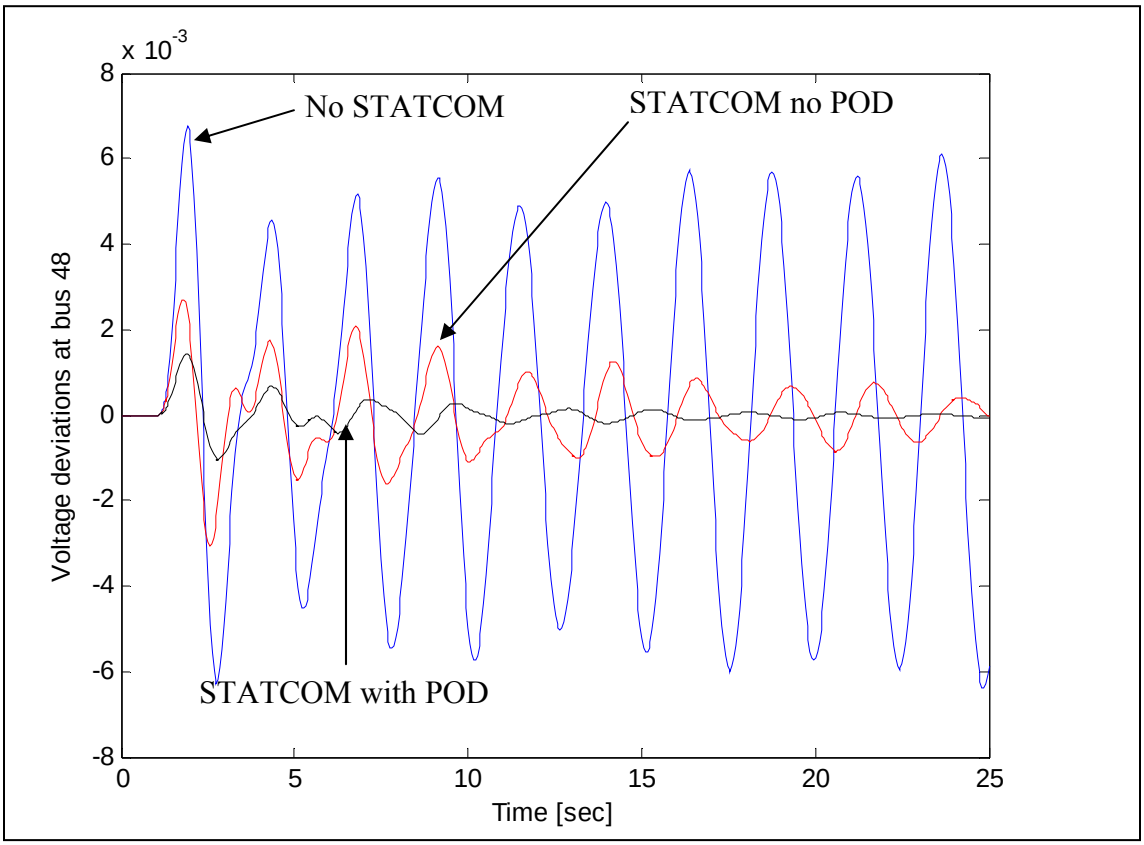

Figure 11.3: Voltage deviations [p.u.] at bus 48, fault 1

The response at the point of connection of the third STATCOM unit shown in Figure 11.4 corroborates the previous analysis. Additionally, as mentioned before, the three buses, 31, 48 and 51, are among the buses where this particular fault has the worst impact. Neighboring buses, 47, 49 and 50, present similar responses to those shown in

Figure 11.2 - Figure 11.4.

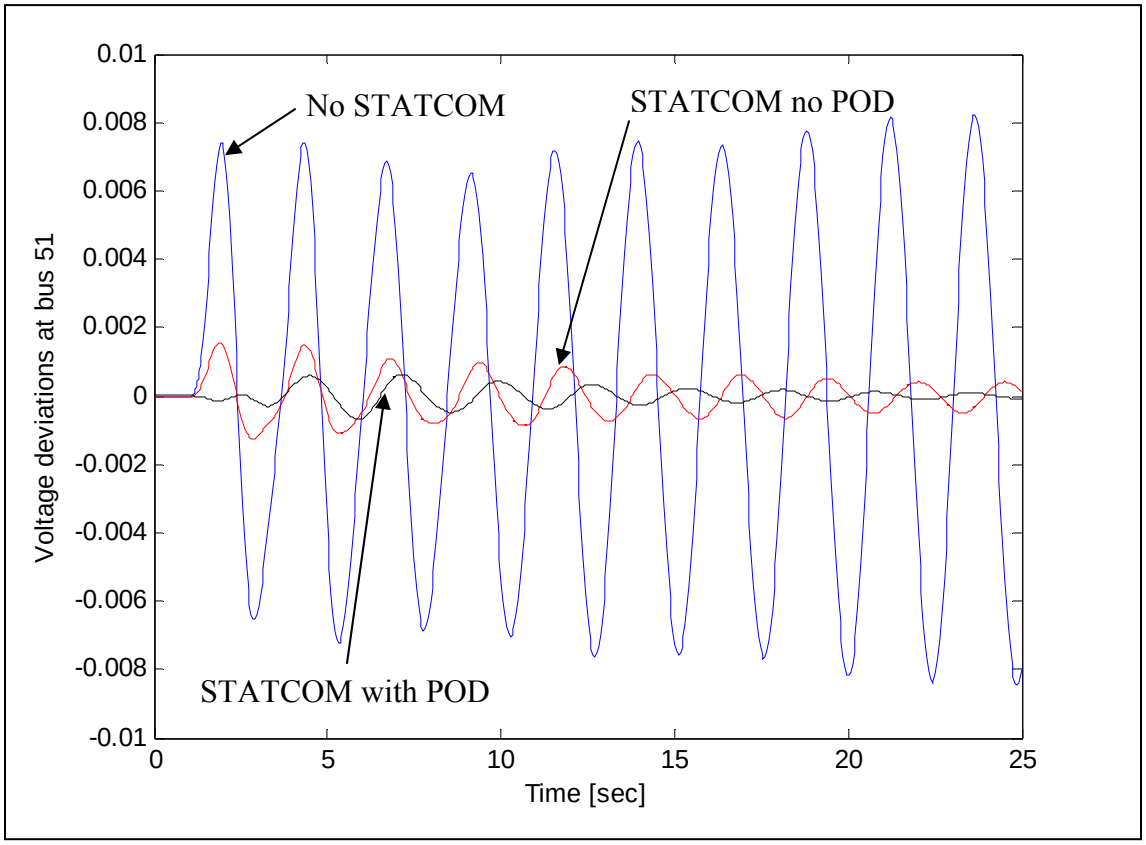

Figure 11.4: Voltage deviations [p.u.] at bus 51, fault 1

Since this particular fault corresponds to a short circuit at the terminal of generator 15, Figure 11.5 shows the speed deviations, in p.u. value, of this generator. The figure presents the response of the system when no STATCOM devices are allocated, which is corrected when the STATCOM and their internal controllers are in place, and further improved with the effect of the external controllers (PODs).

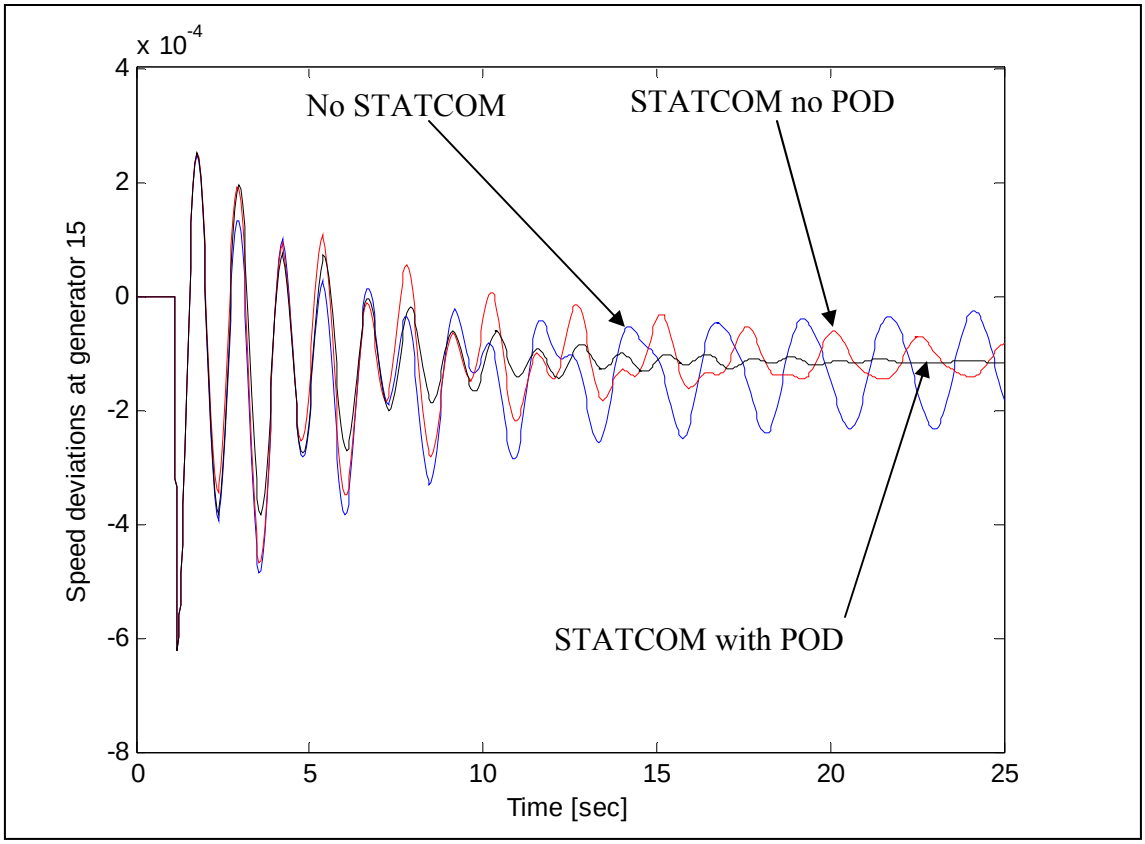

Figure 11.5: Speed deviation [p.u.] generator 15, fault 1

As an overall observation, the STATCOM installation helps the system to improve the damping under transient conditions and the POD controllers improve the system response significantly by decreasing the settling time.

Fault 2: 100 ms 3 phase short circuit along a transmission line (buses 40-41)

For this particular fault the buses mainly affected are buses 40, 41, 47, and 48. Bus 48 corresponds to the point of connection of the second STATCOM unit, and

therefore is chosen to illustrate the performance of the system under transient conditions (Figure 11.17). In addition the buses where the other two STATCOMS are connected, buses 31 and 51, are presented in Figure 11.6 and Figure 11.8 respectively.

Finally, the voltage deviations at bus 40 (one of the extremes of the faulted transmission line) are shown in Figure 11.9.

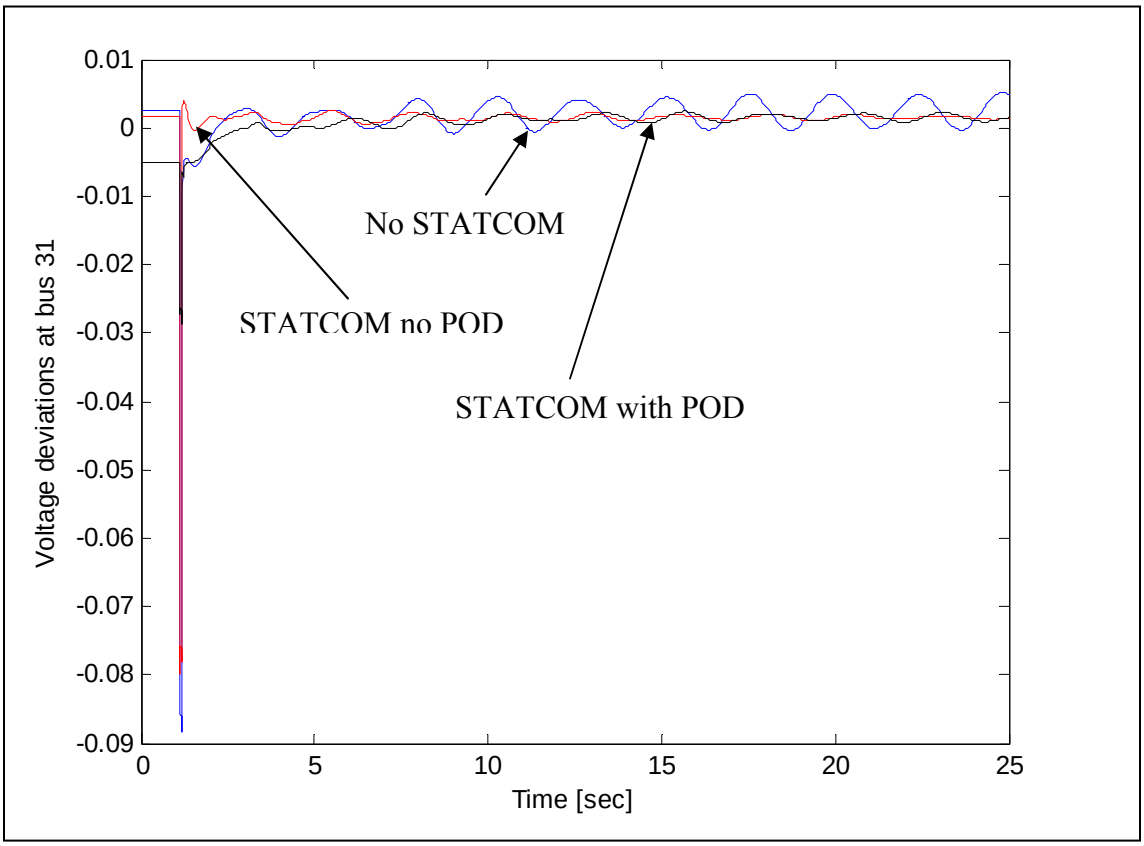

Figure 11.6: Voltage deviations [p.u.] at bus 31, fault 2

The results for the voltages at the point of common coupling of each STATCOM unit (Figure 11.6 - Figure 11.8) show that the transient response of the system is

improved by the installation of the STATCOM units. Moreover, there is also an improvement when the POD controllers of the first and second STATCOM units (at buses 31 and 48 respectively), are added to the system (parameters of both POD controllers are shown in Table 11.8). In all three cases (buses 31, 48, and 51), the oscillation magnitudes rapidly decrease.

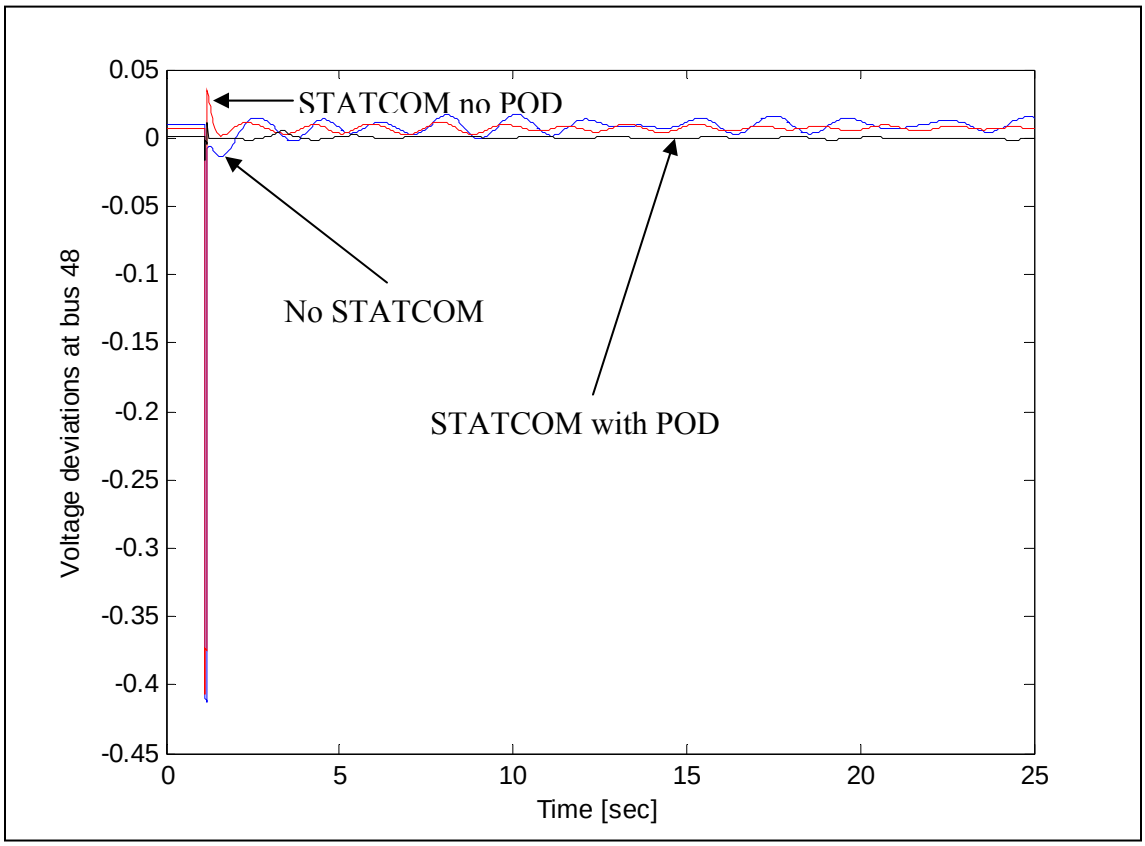

Figure 11.7: Voltage deviations [p.u.] at bus 48, fault 2

Figure 11.9, shows the voltage deviations at one end of the faulted transmission line (bus 40). In this case, it is possible to corroborate the previous observations: (i) the

transient performance of the system is improved by the addition of the STATCOM units and their internal controllers and (ii) there is an improvement when the external, POD, controllers are added to the system.

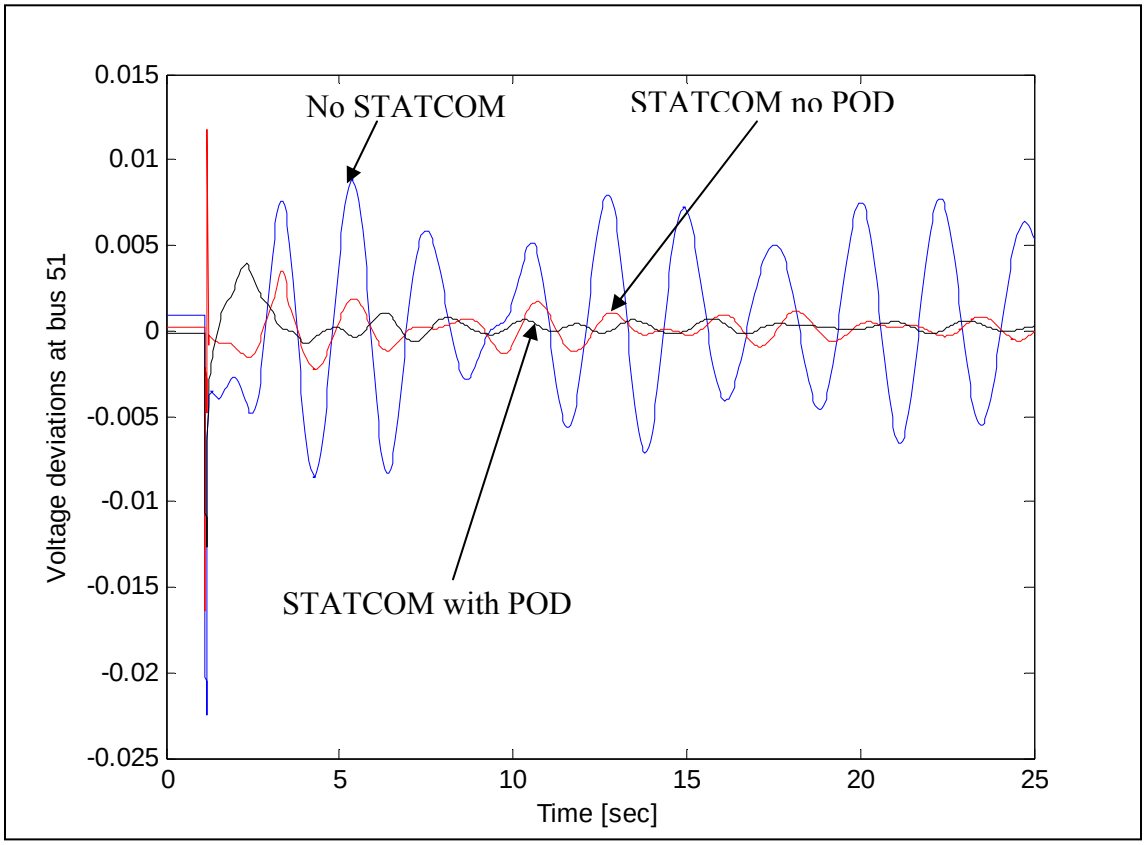

Figure 11.8: Voltage deviations [p.u.] at bus 51, fault 2

The effect of damping the oscillation of the system produced by this particular fault may appear mild from observing Figure 11.6 - Figure 11.9, however there is an additional benefit that can be also appreciated and that is the voltage support provided by the STATCOM units during the initial voltage sag, when the fault occurs.

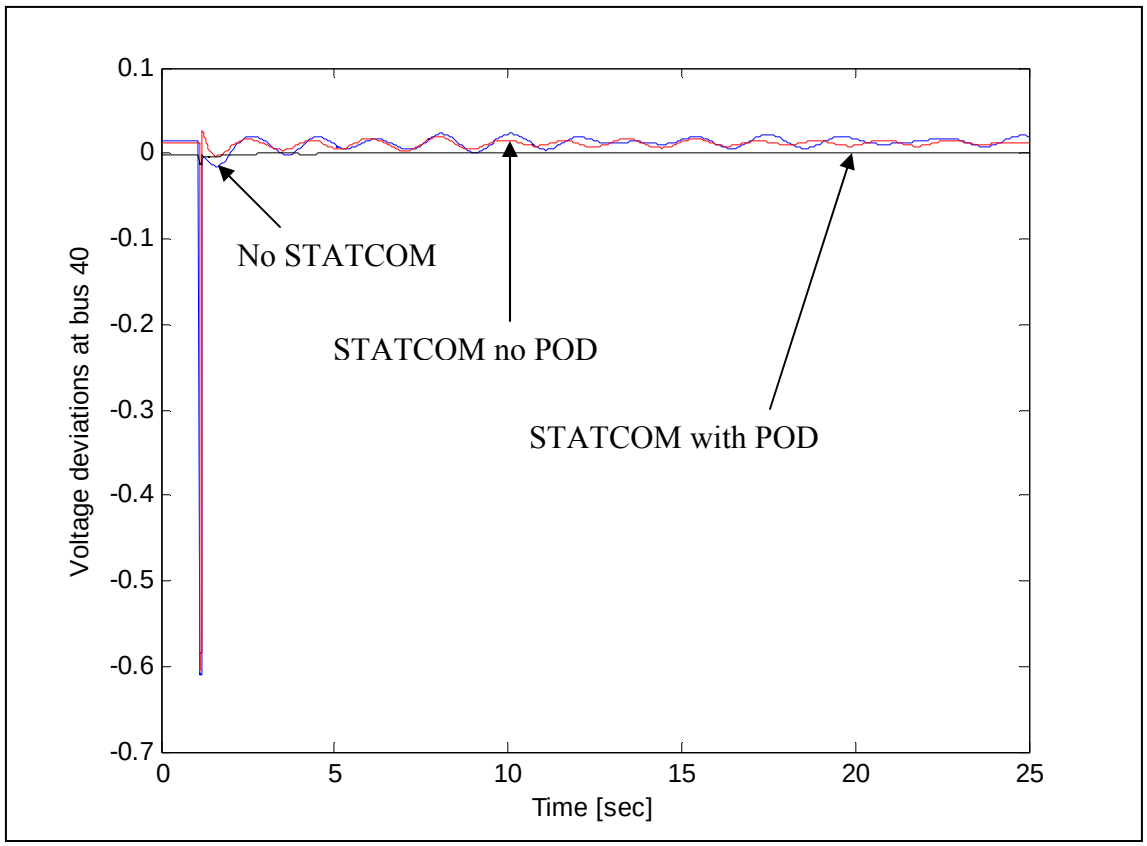

Figure 11.9: Voltage deviations [p.u.] at bus 40, fault 2

Figure 11.10 shows a close-up of Figure 11.9, particularly at the moment when the fault occurs and immediately thereafter (time frame between 1 to 1.5 seconds, with the fault being applied at $t = 1.1$ seconds).

This close-up shows that the STATCOM units with internal control only are not capable of providing significant support during the initial voltage sag since the reference of the internal controllers is only local (bus at the point of common coupling for each device).

By adding the external control signals properly processed by the STATCOM external controllers (PODs) the response at the time when the fault is taking place is considerably improved and the initial voltage sag becomes almost insignificant.

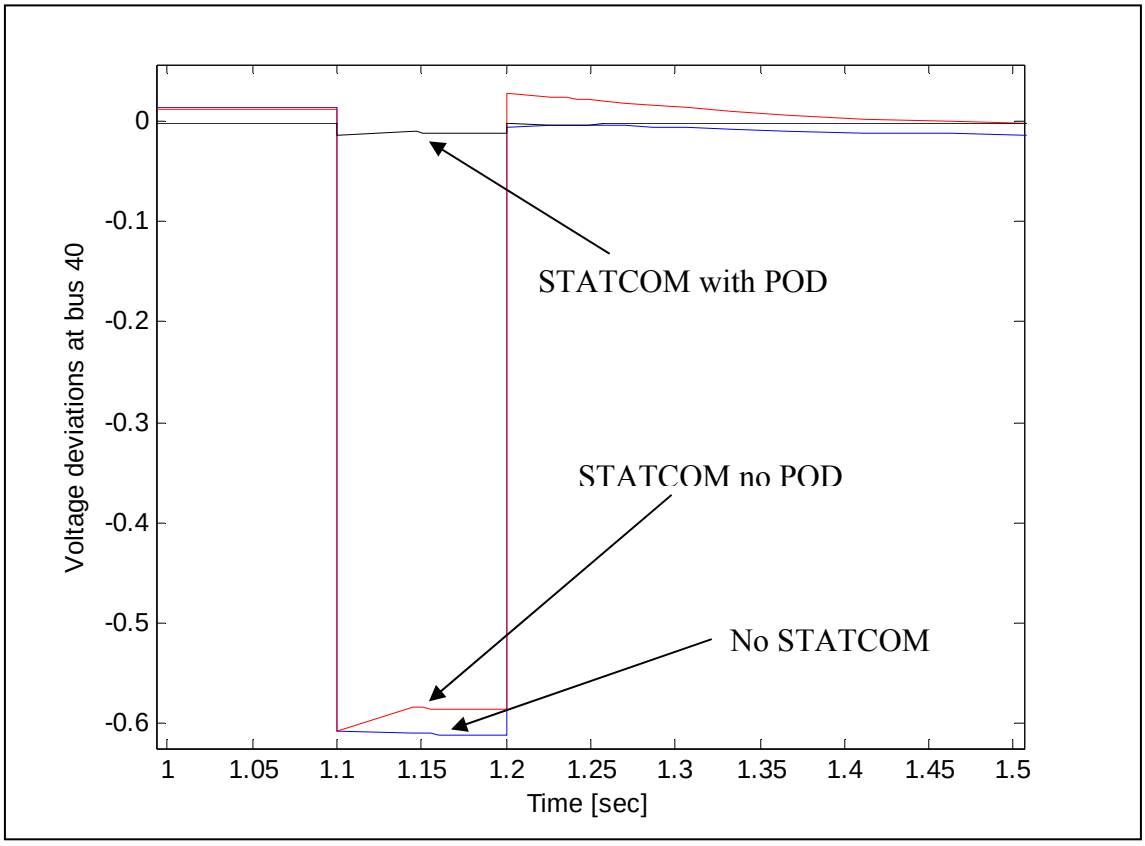

Figure 11.10: Voltage deviations [p.u.] at bus 40 (close-up), fault 2

Fault 3: 100 ms 3 phase short circuit at largest load center (bus 37)

For this particular case, Figure 11.11 shows the voltage deviations of bus 50 which is one of the most affected buses in the system. Figure 11.12 and Figure 11.13 present the voltage deviations at the point of common coupling of the first two

STATCOM units allocated in the system. The third STATCOM unit located at bus 51 is not shown because of its similarities with the response at bus 50 (Figure 11.11). Finally, the voltage deviations at the load center where the fault occurs (bus 37) are plotted in Figure 11.14.

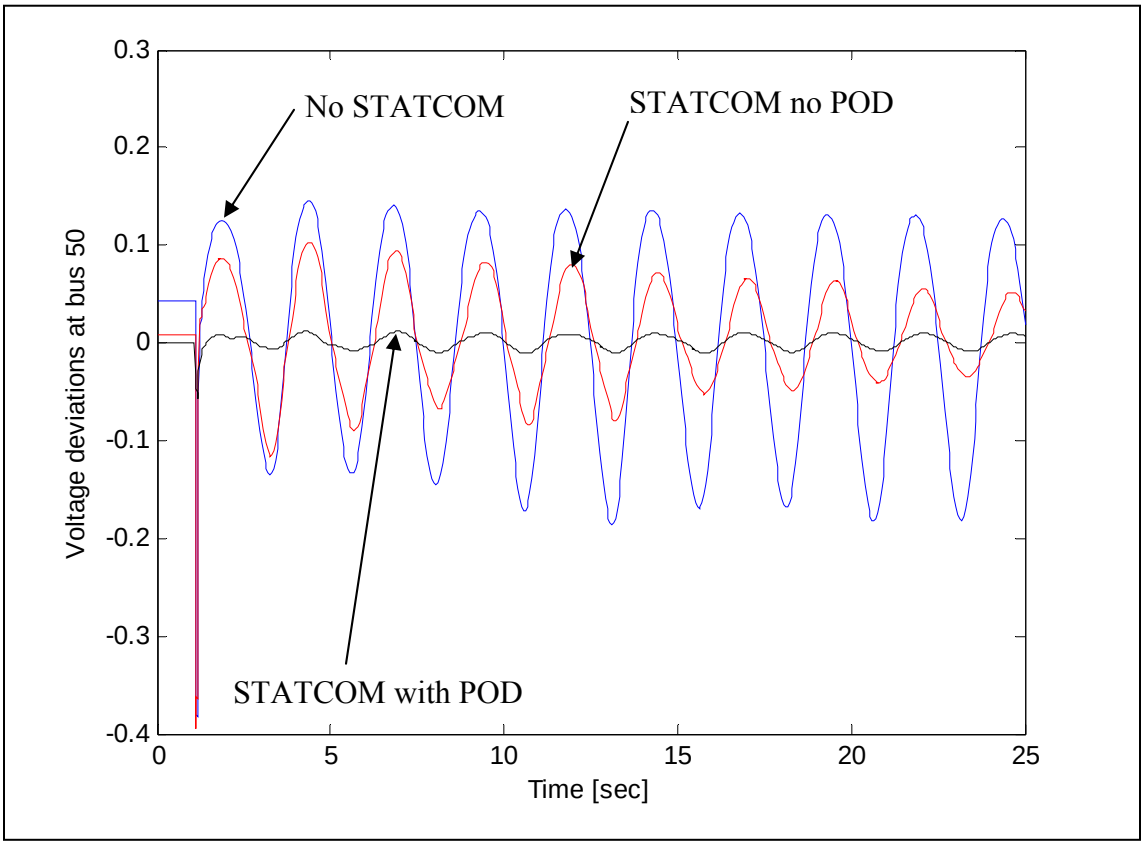

Figure 11.11: Voltage deviations [p.u.] at bus 50, fault 3

Figure 11.11 shows the voltage deviations in p.u. value of bus 50, which is severely affected by this fault. The reason of this high impact at bus 50 is because the inter-area mode, between the cluster of generators 10-13 and generator 16, is excited and

therefore an increase in the magnitude of oscillations is observed at the point where these two areas are bonded together.

For this particular case (bus 50), the response of the system during transient conditions is improved by the STATCOM units and their internal controllers; however the most significant improvement it is observed when the POD controllers are added to the system. In this last response the amplitude of the oscillations are reduced to a minimum value almost instantly after the fault occurs.

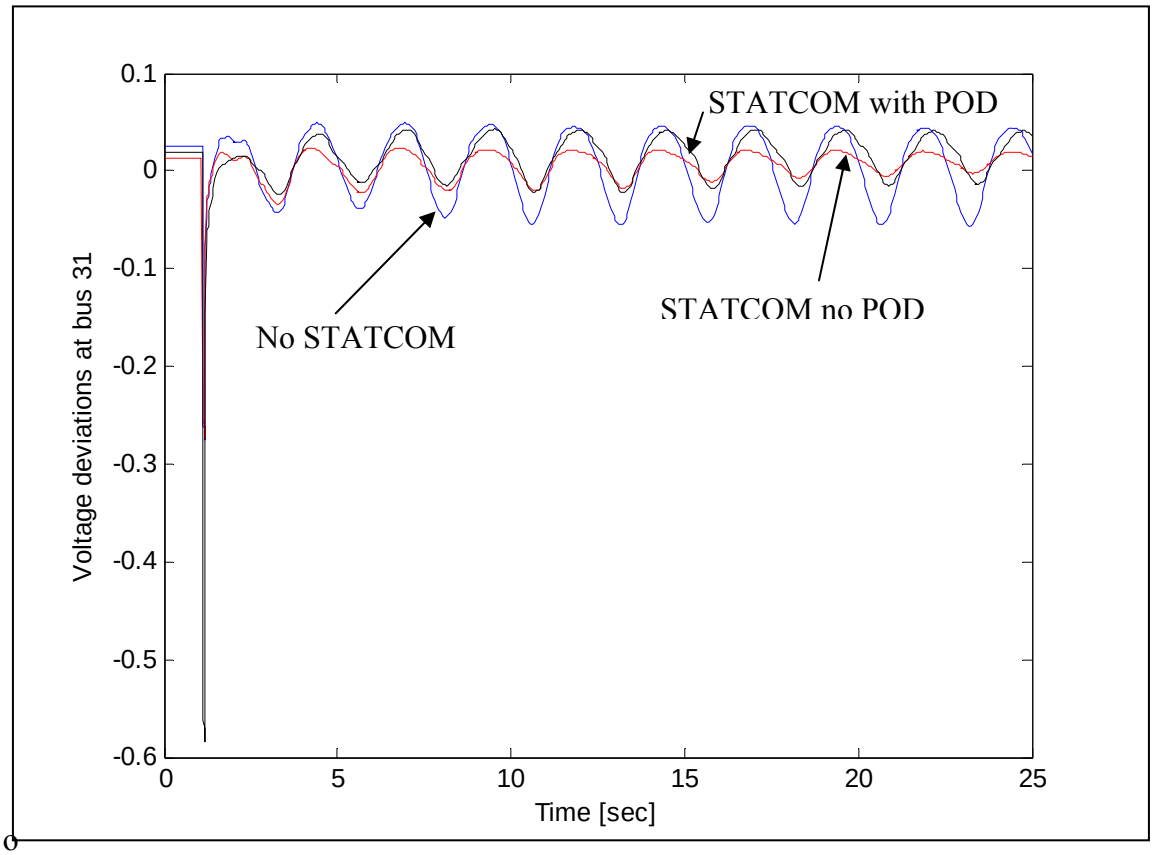

Figure 11.12: Voltage deviations [p.u.] at bus 31, fault 3

A different situation is observed in the case of Figure 11.12 -Figure 11.14, that show the voltage deviations and bus 31, where the first STATCOM is connected, bus 48, corresponding to the point of connection of the second STATCOM, and the load center at bus 37 where the fault occurs.

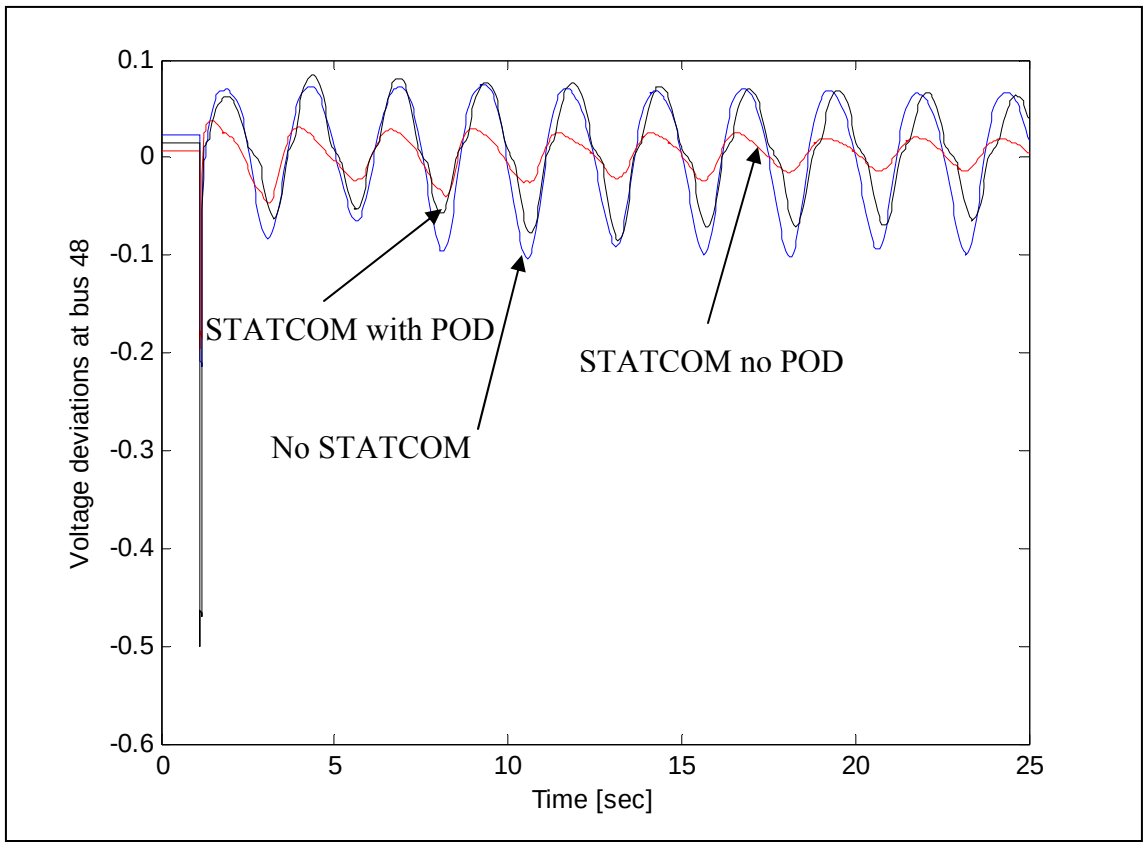

Figure 11.13: Voltage deviations [p.u.] at bus 48, fault 3

In all three figures, the response of the original system is improved by the STATCOM units and their internal controllers; however the addition of the POD

controllers, that focus on mitigating the inter-area oscillations between area 2 and area 5 (buses 50 and 51), have a detrimental effect on the response in area 2 of the system (buses 31 and 37) and in the connection of area 2 and area 4 (buses 40, 47, and 48 for which the behavior is illustrated using bus 48 in Figure 11.13).

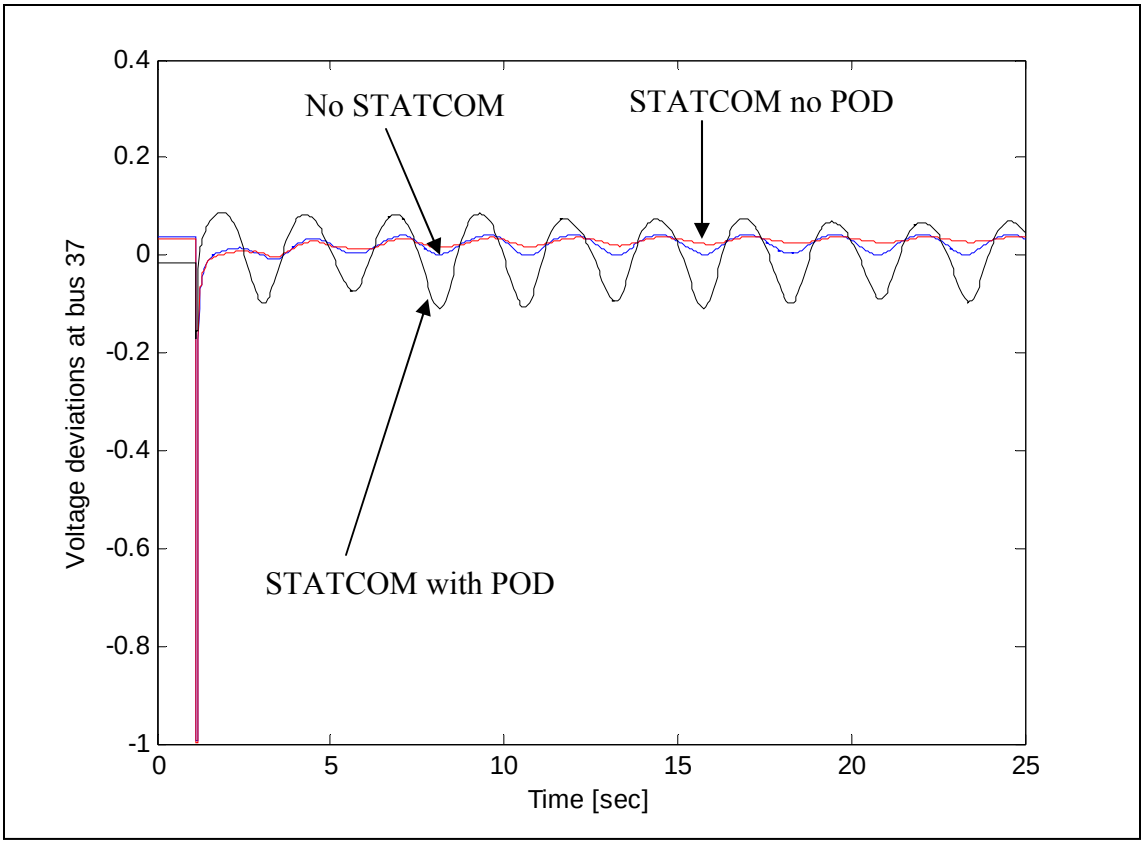

Figure 11.14: Voltage deviations [p.u.] at bus 37, fault 3

This type of response (Figure 11.12 - Figure 11.14) are not uncommon if it is considered that the POD controllers are tuned to provide damping at specific modes that may or may not be substantially excited by the corresponding fault. Inversely, a particular

fault may excite modes for which the POD controllers are not specifically tuned to provide additional damping.

The discussion of this problematic raises the topic of the wide area control (WAC) and the advantages of having a supervisory level that may change the control parameters of various devices in the system to improve the response under different fault scenarios [112]. Having this supervisory level may have a sacrifice in time (delays due to communication systems), but it can substantially improve the dynamic response of the power system [112].

To illustrate this concept, an exercise is included in this study where only one POD controller is allocated in the system. The parameters of this one POD controller (POD at STATCOM unit located in bus 31) are tuned to specifically improve the response of the system for fault 3, a short circuit at the largest load area of the system (located in bus 37), using the optimization stage described in section 11.2.2.

The results of this example are shown in Figure 11.15 - Figure 11.18, and the specific parameters for the POD controller are presented in Table 11.9.

Table 11.9: Solution for POD controller at STATCOM unit 1, fault 3

Parameter	POD STATCOM 1
Control signal [Bus]	65
Stabilizer gain [K_w]	0.20
Washout time constant, T_w, [sec]	9.87
Lead-Lag block 1, (T_1,T_2), [sec]	(1.80, 0.47)
Lead-Lag block 2, (T_3,T_4), [sec]	(2.30, 1.12)
Low-pass time constant, T_ε, [sec]	0.0019
Stabilizer upper limit, V_s^{max}, [p.u.]	0.5
Stabilizer lower limit, V_s^{min}, [p.u.]	-0.5

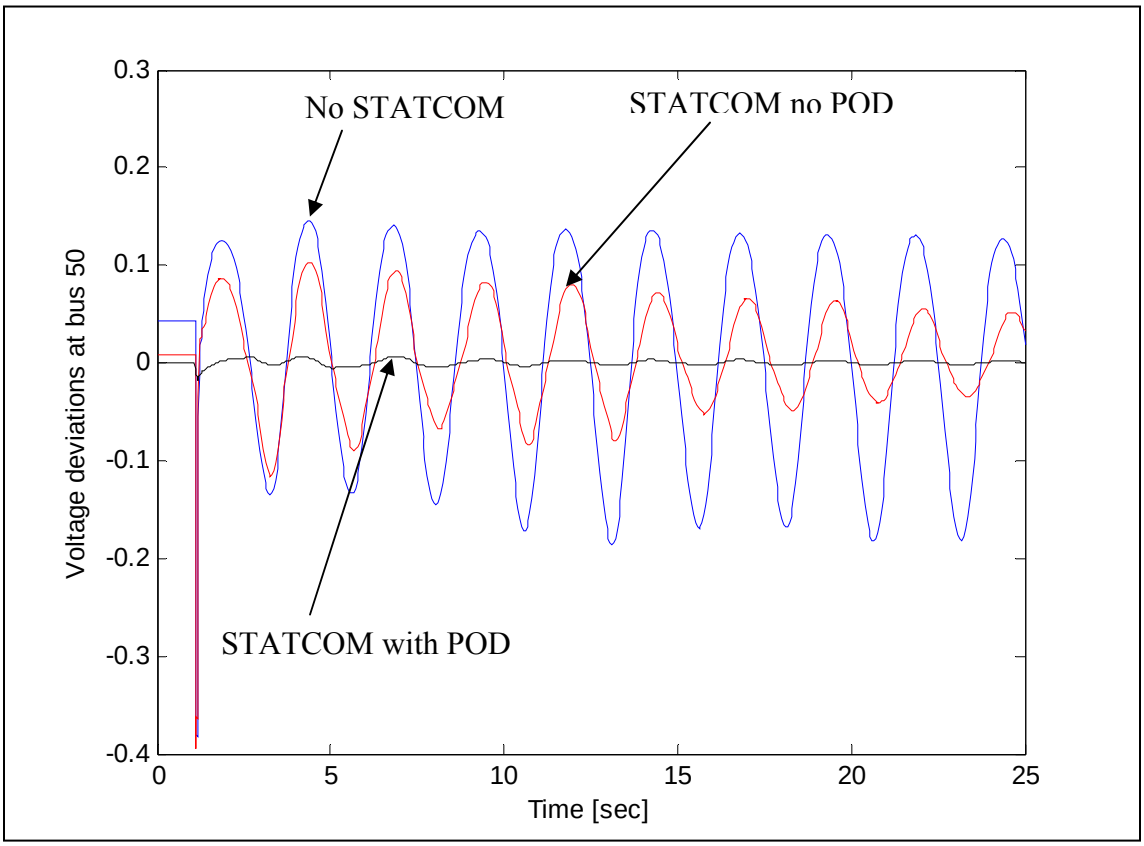

Figure 11.15: Voltage deviations [p.u.] at bus 50, fault 3 (WAC)

Figure 11.15 shows the three responses of the system: (i) without STATCOM units (original system), (ii) with three STATCOM units and their corresponding internal controllers (optimal solution found by the first optimization stage), and (iii) with all three STATCOM units and only one POD controller in the first STATCOM unit located in bus 31. In this figure, the response of the system is substantially improved when the POD controller of the first STATCOM is now specifically tuned to provide damping for this particular fault. The comparison between Figure 11.11 and Figure 11.15, indicate that the

results in the second case (Figure 11.15) are better than the previous results (Figure 11.11).

The previous two PODs (with control signal coming from buses 37 and 63) decreased the damping at buses 31, 48 and 37 (Figure 11.12-Figure 11.14). However, this negative effect is not observed in Figure 11.16 - Figure 11.18 that illustrate the results at the same buses, but now with a specially tuned POD at bus 31 to give optimal results for fault 3 disturbance.

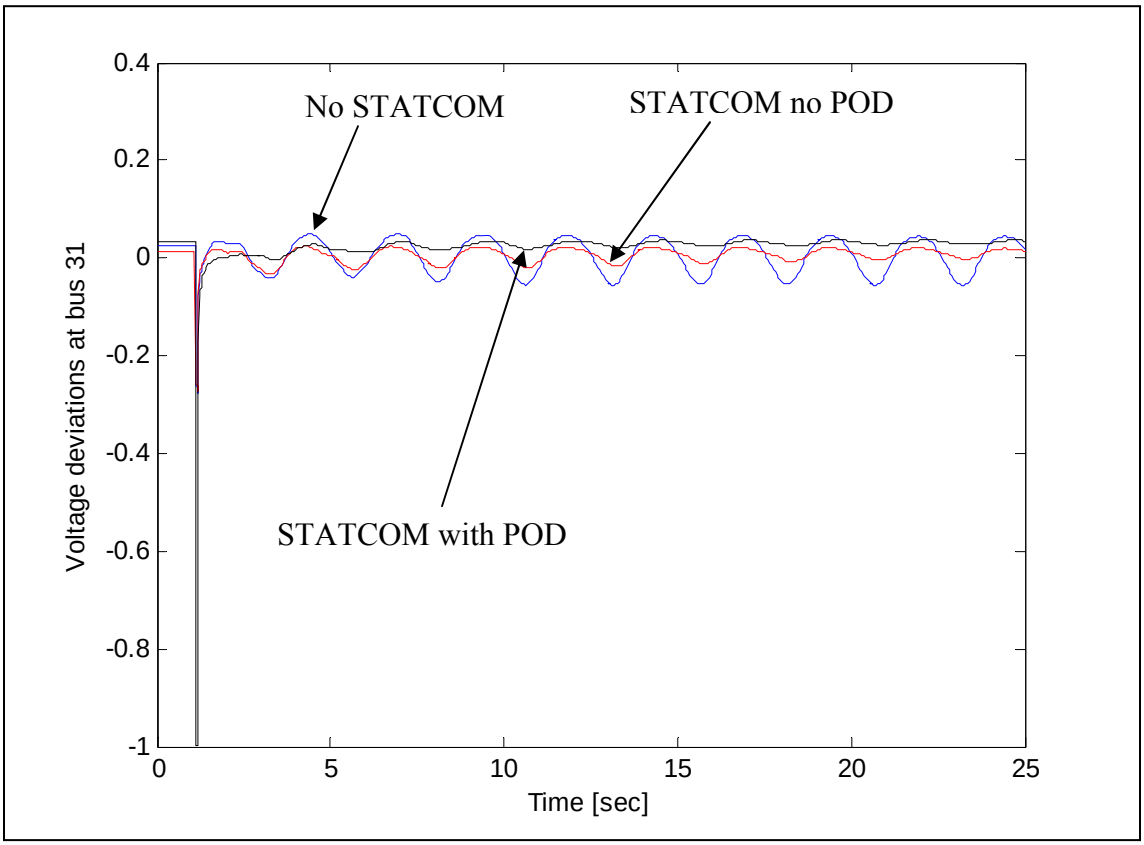

Figure 11.16: Voltage deviations [p.u.] at bus 31, fault 3 (WAC)

In all three buses, bus 31 in Figure 11.16, bus 48 in Figure 11.17, and bus 37 in Figure 11.18, there is an improvement in the damping of the oscillations generated by this fault, particularly in the point of common coupling of the first and second STATCOM units (buses 31 and 48 respectively).

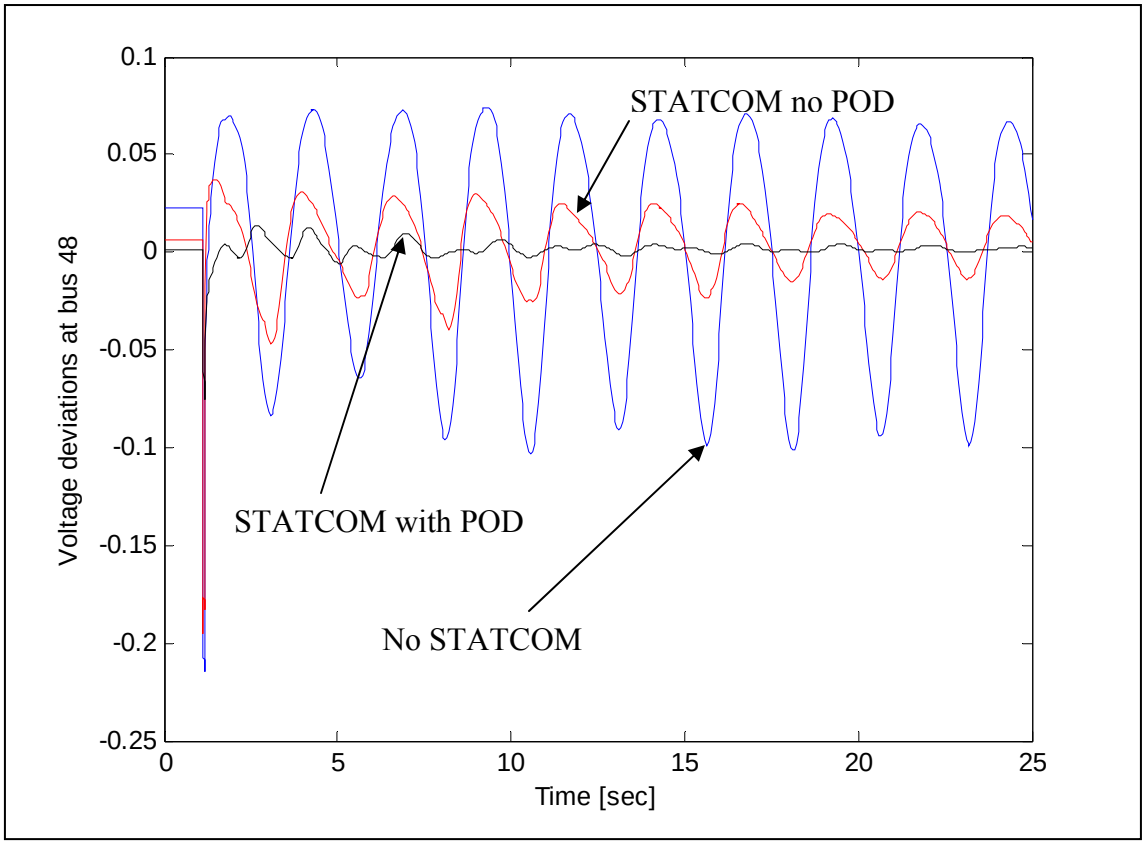

Figure 11.17: Voltage deviations [p.u.] at bus 48, fault 3 (WAC)

This proves the benefits of considering WAC in a power system: a supervisory level can adjust the parameters of the POD controllers over time, depending on different operating conditions and contingencies, to achieve optimal power system performance.

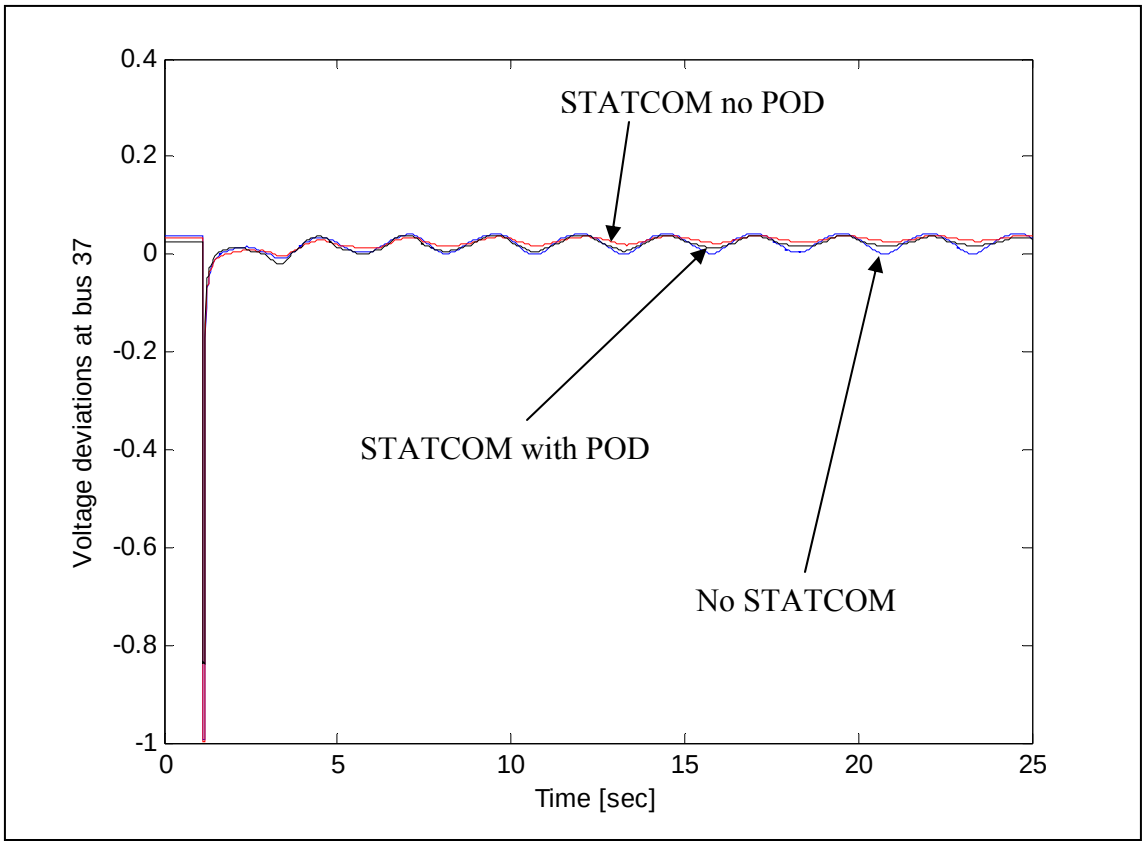

Figure 11.18: Voltage deviations at bus 37, fault 3 (WAC)

11.4 Summary

This chapter proposes a two stage PSO-based optimization framework to improve the dynamic performance of the power system using FACTS devices. For illustrative purposes, STATCOM devices are chosen in this study, however the methodology can be applied to any single or multiple type of FACTS devices. The proposed optimization process consists in two optimization loops that are carried out sequentially.

First, the transient performance of the system is optimized by means of the STATCOM units and their internal controllers using a large perturbation analysis. In particular, this stage provides the optimal number of STATCOM units, locations, sizes and parameters for the STATCOM internal controllers (model in Appendix A) such that the voltage deviations in the system are minimized under various faults described in chapter 9, section 9.4.3.

The novelty in this scheme for tuning control parameters is the overall response of the system is taken into account in the objective function to be minimized, and therefore it provides a global optimality rather than focusing on only the buses where each device is respectively connected and on its immediate neighboring buses.

After this first optimization stage is performed, a second optimization stage takes place where the performance of the system is further improved by adding STATCOM external controllers, properly tuned considering small signal stability analysis.

The optimization algorithm provides the optimal location for the control signal and the optimal parameters of the STATCOM external controller (POD) such that the inter-area modes of the system are mitigated (POD controller's model is presented in Appendix A).

Results of this proposed PSO-based optimization framework, for improving the dynamic performance of the power system, in a 16 machine – 68 bus system indicate that the dynamic response under various contingencies is considerably improved by the STATCOM devices and their internal controllers. An additional improvement can be obtained if the external controllers (POD) of selected STATCOM unit are added to the system.

The overall results obtained for both optimization stages illustrate the advantages of the proposed method: once the optimization process is completed, the damping of the inter-area modes are within the desired range and the response of the system for large perturbations is significantly improved. Faults that could potentially make the system unstable are rapidly mitigated due to the control effort of the optimally placed and controlled STATCOM devices.

Finally, the results obtained in this chapter also point out the necessity of incorporating wide area control schemes in modern power systems, such that the improvement of the system can be maximized by customizing the control parameters of various devices according to different fault conditions. A particular example is shown to illustrate this by optimizing the control parameters of one POD controller (in STATCOM unit connected to bus 31) to improve the dynamic performance of the system for a short circuit in the largest load center of the system (bus 37). The obtained results prove that the proposed control scheme can be applied to consider WAC and control schemes at supervisory level.

CHAPTER 12

CONCLUSION, CONTRIBUTIONS AND RECOMMENDATIONS

12.1 Conclusions

The objective of this research has been to create a PSO-based optimization framework to solve the problem of improving the power system reliability and performance using FACTS device s (Figure 12.1).

Part I of this research focuses on theoretical background. Different optimization techniques, currently applied to solve this problem, are explored together with their advantages and disadvantages. Additionally, the concepts behind the PSO and the proposed Enhanced-PSO methods are discussed in detail.

Part II of this study consists of validating the proposed Enhanced PSO method as a suitable algorithm to solve this type of problem. The optimal allocation of multiple STATCOM units in a 45 bus system part of the Brazilian power network is used as an illustrative example to analyze the advantages of the proposed method as compared to other optimization techniques. The results of this Part II, clearly validates the superior performance of the proposed Enhanced-PSO method.

Part III of this investigation is related to applying the Enhanced-PSO method to create a PSO-based multistage optimization framework to improve the power system reliability using FACTS devices. In particular, the IEEE 118 bus system is used as an illustrative example to show the effectiveness of the optimization framework. The results

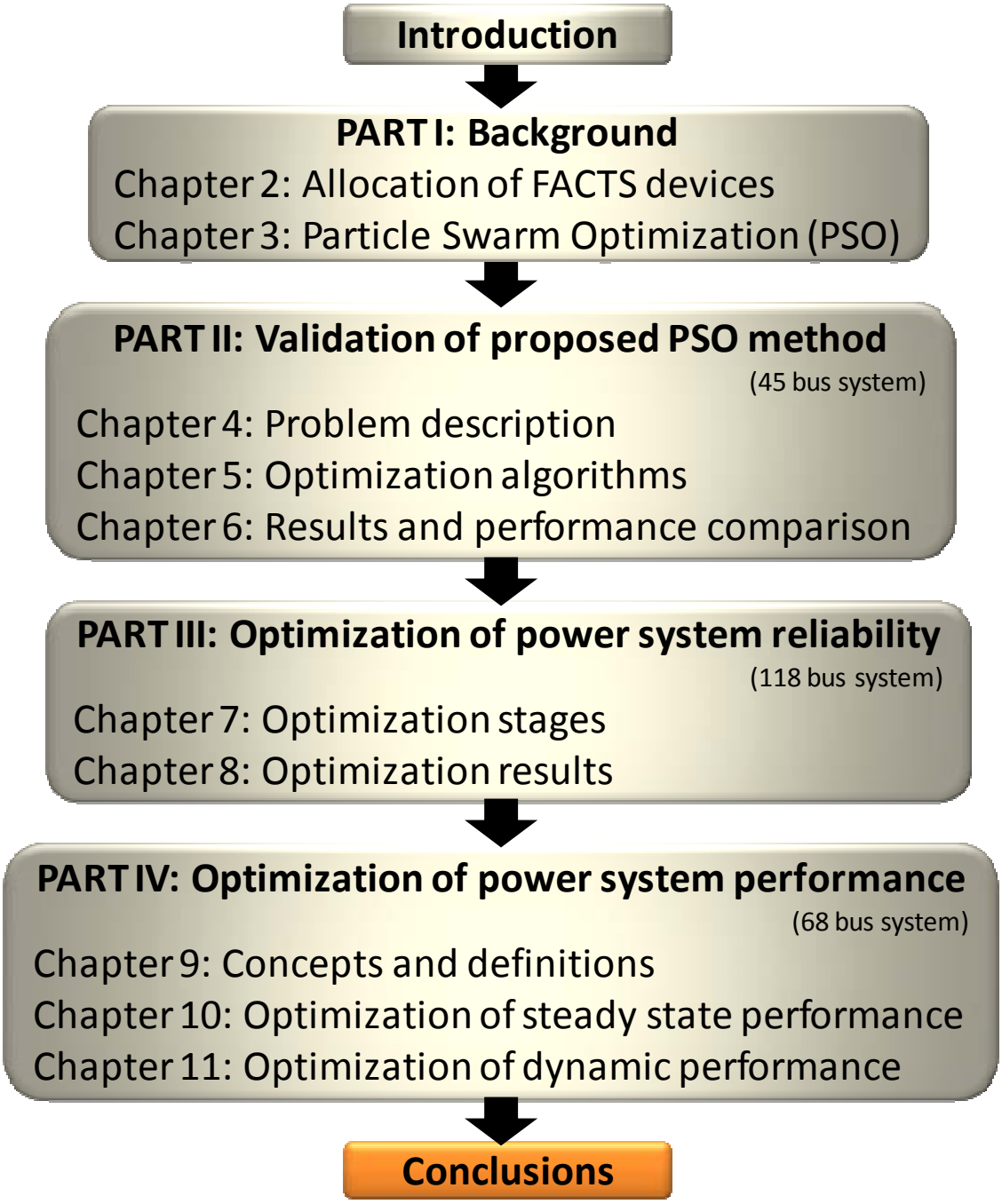

Figure 12.1: Optimization performed in this research

obtained after the optimization process is completed reveal a significant improvement in the reliability of the system with minimum economical impact.

The last part of this work, Part IV, again uses the proposed Enhanced-PSO method to create a two-stage optimization process that allows the performance of the system to be improved in both steady state and under small and large perturbation. The results obtained for a 16-machine, 68 bus system prove that the proposed method is very effective in finding solutions to the problem of optimally allocating and controlling FACTS devices, that significantly improve the power system performance considering both technical and economical criteria.

The following sections present specific concluding remarks of each of the four parts of this investigation.

12.1.1 Part I summary and conclusions

This part presents some general background on optimization theory and the existing optimization methods to solve the problem of optimal allocation of FACTS devices in the power system, particularly classical optimization methods, allocation based on technical criteria, and evolutionary computation techniques.

The following conclusions can be drawn from the analysis of present literature:

- The use of classical optimization methods (mixed integer linear programming (MILP), mixed integer non-linear programming (MINLP), Bender's decomposition, Branch-and-bound (B&B), etc) is limited by the size of the system and non-convexity problems. If the size of the power system increases, then computational effort

becomes too large; additionally, the behavior of the system is highly non-linear and therefore it is not recommended to rely on convexity assumptions on which these methods are typically based.

- Considering those methods based on technical criteria (sensitivity analysis and modal analysis), only the technical feasibility is considered, and regardless of the improvement in the power system performance, it is not possible to evaluate the degree of optimality of the solution provided by these methods.

- Finally, evolutionary computation techniques (genetic (GA), particle swarm optimization (PSO), bacterial foraging algorithm (BFA), tabu search (TS), evolutionary programming (EP), etc.) have recently gained interest from many researchers because they are simple to implement, capable of handling highly non-linear systems, and finding optimal solutions with a reasonable computational effort. The results obtained up to date are promising; however, the scalability of these techniques to large power systems and their application to power system dynamic performance is still under investigation.

For this study, an enhanced particle swarm optimizer is developed to overcome the disadvantages of the optimization techniques presented above. This Enhanced-PSO technique represents the core of a PSO-based, multistage, optimization framework proposed in this study to improve the reliability and the performance of the power system using FACTS devices.

12.1.2 Part II summary and conclusions

Part II focuses on the validation of the superior performance of the proposed Enhanced-PSO formulation in solving the problem of optimal allocation of FACTS devices in a power system. This validation is done by comparing the performance of the proposed Enhanced- PSO with other optimization techniques, in particular three evolutionary computation techniques: canonical PSO formulation, GA and BFA and two classical optimization techniques: Bender's decomposition and B&B.

The problem to be solved corresponds to the optimal allocation of multiple STATCOM units in a 45 bus system, part of the Brazilian power network. The objective is to improve the voltage profile of the entire system at minimum cost (minimum STATCOM sizes), and the system constraints include keeping all bus voltage deviations between ±5% of the corresponding nominal voltage, limiting the size of each STATCOM device to a maximum of 250 MVA, excluding the generator buses from the search and avoiding multiple units connected to the same bus.

The comparison between methods is done based on three critical aspects: (i) convergence into feasible regions, (ii) analysis of global optimality, and (iii) scalability of the algorithm to address large power systems.

The following conclusions can be derived from this study:

- An exhaustive search, performed to identify the global optimum of the problem (section 4.3), indicates that only 1.12% of the total possible solutions lead to feasible conditions (all system constraints are satisfied). This small percentage of solutions is scattered among the entire problem hyperspace which makes it difficult for an optimization algorithm to converge to a feasible region. Additionally, the

computational effort, involved in exhaustively evaluating all possible solutions and finding the global optimum, is 37,187,500 power flow solutions.

- In the case of the canonical and Enhanced-PSO, the optimal settings of the PSO parameters are investigated using statistical analysis (section 5.2.2). The results of this optimal parameter selection suggest the following guidelines to set the PSO parameters:
  - ✓ Implement a linearly decreasing inertia constant that provides a wide range of movement in the early search and has less influence in the later stages where the search has narrowed into promising areas. A suitable scheme is proposed in (5.2).
  - ✓ Give more emphasis to the self knowledge as compared to the social information channels. An individual acceleration constant of 2.5 is proposed in this study.
  - ✓ A maximum velocity for the FACTS location equal to 25% of the total domain (total number of buses for shunt units or total number of line for series devices).
  - ✓ A maximum velocity for the FACTS unit size equal to 20% of the maximum device's rating.

- The convergence into feasible regions is analyzed by comparing the performance of the Enhanced-PSO algorithm with the canonical PSO formulation, GA, and BFA using Weibull analysis (section 6.2). The characteristic times to find the first feasible solution, obtained from this analysis, indicate that the Enhanced-PSO substantially outperforms all other techniques. Additionally, considering the physical meaning of

the Weibull parameters, α and β, the Enhanced-PSO method shows an increasing ability to locate feasible solutions as the number of iterations increases.

- The capability of the proposed approach in finding the global optimal solution is evaluated for two classical optimization techniques (Bender's decomposition and B&B) and three evolutionary computation techniques (the proposed Enhanced-PSO method, GA, and BFA). The parameters used to evaluate the performance of each technique include the ability of finding the global optimal solution and the computational effort (section 6.3).
  - ✓ The Enhanced-PSO, GA, and Bender's decomposition are able to find the global optimum, however BFA and B&B algorithm are trapped in a local minimum.
  - ✓ Considering the computational effort, the Enhanced-PSO and GA have almost identical computational times since the maximum number of power flow computations is set to the same value of 2,000 power flows. Benders' decomposition method is also able to find the correct solution, however it requires excessive computational effort compared to the Enhanced-PSO and GA (31.5 times more power flow evaluations).
  - ✓ The proposed Enhanced-PSO method is more accurate in finding the global optimal solution than the GA (smaller standard deviation). In addition, it has 100% convergence rate while GA only delivers a modest 32%.

- The scalability of the Enhanced-PSO is studied by analyzing the performance of the algorithm in solving the optimal allocation of multiple STATCOM units for the IEEE

118 bus system (section 6.4). The following guidelines are proposed for setting the number of particles and maximum number of iterations:

- ✓ Set the number of particles to approximately 25% of the total number of possible locations multiplied by the number of units that need to be allocated.
- ✓ Use the following stopping criteria: if the value of the *gbest* has not change in a certain number of iterations or if it is changing by less that 5% with respect to its previous value, then stop the algorithm. An alternative stopping criterion, that limits the computation effort to a fixed amount, is to keep the maximum number of iterations to a value of 100.

These proposed guidelines are used for the IEEE 118 bus system, and the obtained results are compared with the 45 bus system. Using statistical analysis it is shown that the performance of the algorithm is not affected by the size of the power system, since it maintains similar properties for converging into feasible regions and accuracy in finding optimal solutions.

In summary, the proposed Enhanced-PSO method has been validated as a suitable algorithm for the problem of optimization of power system performance using FACTS devices. In particular, the proposed method converges faster into feasible regions and is more accurate in finding optimal solutions than any other algorithm investigated, including classical optimization methods and evolutionary computation techniques. Moreover, the algorithm maintains its advantages when the power system size is increased.

12.1.3. Part III summary and conclusions

Part III introduces a multistage PSO-based optimization framework to improve the reliability of the power system using FACTS devices. The objective is to enable a modified version of the IEEE 118 bus system to satisfy the N-1 security criterion using the existing infrastructure and new FACTS installations, in particular distributed static series compensator (DSSC) and static compensator (STATCOM) units (models in Appendix A).

The optimization process considers three stages (sections 7.3.1 to 7.3.3):

(iv) Security Constrained Optimal Power Flow (SCOPF) stage: it provides the optimal settings for the present power system infrastructure. Optimal generator, transformer, and capacitor bank settings are found considering the economic dispatch and power system security constraints. From the optimization perspective, the concept of fine tuning PSO, which limits the maximum velocity to a small percentage of the variable's range of movement, is introduced to aid in the search mechanism. In addition, the system's security constraints for overloaded lines and bus voltage violations are included in the main objective function as penalty factors. In general, this optimization framework has shown to be very efficient in avoiding solutions that lead to system instability.

(v) Series compensation stage: assuming the system to be fully deployed with DSSC units (full controllability of all transmission lines) this stage provides the optimal control reference settings for each DSSC module. The DSSC is modeled as a lumped device with the capability of changing the value of the corresponding line reactance

by 20% in either direction (increase or decrease). The value of the DSSC control reference, in this case the desired value for the line reactance of each transmission line, is provided by the algorithm, considering global system controllability instead of traditional local control. The optimization objective is to maximize the line utilization factor (LUF) while minimizing the impact on transmission losses and voltage profile. Emphasis is given to security constraints related to the number of overloaded lines and maximum line loading.

(vi) Shunt compensation stage: this stage uses a two step optimization process, the first step provides the optimal number, locations and ratings for shunt FACTS devices, in this case STATCOM units, and the second step indicates whether the units have to be in service and, if so, what is the corresponding optimal control reference, in this case the voltage at the point of common coupling. Analogous to the series FACTS devices, the STATCOM control references are provided considering global control, such that the maximum benefit is obtained over the entire power system, instead of focusing on immediate neighborhoods. The objective of this stage is to improve the voltage profile at minimum cost while giving special attention to the mitigation of undesired voltage violations.

The optimization is performed for a base case (all components in service) and for the 186 branch outages that correspond to the N-1 contingency criteria. The overall results of all three optimization stages are significant: the original system has 22 overloaded lines, 1145 bus voltage violations and three critical contingencies leading to

voltage collapse (Table 7.2 and Table 7.3). After the optimization is performed, there are no overloaded lines, all bus voltages are within limits, and the critical contingencies are mitigated, thus the system satisfies the N-1 security criterion (Table 8.3). These results are obtained with minimum impact on the generation costs and with the minimum cost of new FACTS installations.

12.1.4. Part IV summary and conclusions

Part IV, optimization of power system performance using PSO, proposes a two-stage PSO-based optimization framework to improve the performance of the power system considering both steady state conditions and the system behavior under small and large perturbations.

A 16 machine - 68 bus system is used to illustrate the capabilities of the optimization framework in finding an optimal solution considering both technical and economical criteria.

First optimization stage

The first optimization stage, optimization of steady state performance, considers a double-loop optimization algorithm for optimal allocation and control settings of series and shunt compensation (DSSC modules and capacitor banks). These two loops can be repeatedly executed to maximize the loadability of the system without violating the system security constraints (i.e. keeping the line flows and bus voltages within limits). In addition, it can be used as a planning tool providing optimal control references for the

DSSC modules and optimal location and sizes of capacitor banks with the system under different scenarios of future demand.

- The first optimization loop, called series compensation loop, is used to relieve transmission lines congestion using DSSC modules. The system is assumed to be fully deployed, meaning that there is full controllability of all transmission lines. The DSSC is modeled as a lumped device with the capability of changing the value of the corresponding line reactance by 20% in either direction (increase or decrease).
- The result of the optimization process is the optimal control settings (desired value for the line reactances) for each DSSC module, such that the loadability of the system is maximized without incurring any overloaded lines Additionally, the line utilization factor is improved with a minimum impact on the total transmission losses of the system (section 10.2.1).
- The second optimization loop, named shunt compensation loop, provides optimal allocation and rating for capacitor banks such that the loadability of the system is maximum. In addition to the loadability of the system, the voltage profile (minimization of voltage deviations) is improved at minimum cost (section 10.2.2).

The results of the proposed double loop PSO-based optimization framework applied to a 16 machine - 68 bus system shows that system loadability can be improved from 1.07 p.u. to 1.35 p.u. considering the action of DSSC modules and the installation of three capacitor banks (section 10.3). At this loading level the system is capable of operating with all variables within security limits.

After the optimization process is completed, the results of the continuation power flow (CPF) indicates that a limit induced bifurcation (LIB) point due to line flow limit is encountered and therefore a new cycle of series-shunt compensation can be performed starting with the system at 1.35 p.u. loading level (thus the optimization framework can be used as a planning tool).

Second optimization stage

The second optimization stage, optimizes the dynamic and transient performance of the power network, considering a two-sequential-stage, PSO-based, optimization algorithm for optimal allocation and control of shunt FACTS devices, in particular STATCOM units (model described in Appendix A).

The performance is analyzed considering the system subjected to large perturbations (various faults) and also subjected to small changes around its operational point (small signal stability analysis (sssa)). The main objective is to find optimal locations, sizes and control parameters (for both internal and external controllers) of the STATCOM devices, such that a maximum benefit is obtained over the entire power system, instead of focusing on local neighborhoods. In particular, this study focuses on increasing the damping of the system to damp large perturbations and inter-area modes.

The proposed optimization process consists of two optimization loops that are carried out sequentially:

- First, the transient performance of the system is optimized by means of the STATCOM units and their internal controllers using large perturbation analysis. This

stage provides the optimal number of units, locations, sizes and parameters for STATCOM internal controllers such that the voltage deviations in the system are minimized under various faults described in section 9.4.3.

The novelty in this scheme for tuning control parameters is the overall response of the system is taken into account providing global optimality rather than focusing in only the buses where each device is respectively connected (section 11.2.1).

- Second, the dynamic performance of the system is further improved by STATCOM external controller, properly tuned considering sssa. In this case, the optimization algorithm provides the optimal location for the control signal and the optimal parameters of the STATCOM external controller (POD) such that the inter-area modes of the system are mitigated (section 11.2.2).

Results of this proposed PSO-based optimization framework, for improving the dynamic performance of the power system, in a 16 machine – 68 bus system, indicate that once the optimization process is complete, the damping of the inter-area modes are within the desired range (section 11.3.2) and the response of the system for large perturbations is significantly improved (section 11.3.1). Faults that could make the system unstable are rapidly mitigated due to the effect of the optimally placed and controlled STATCOM devices (11.3.3).

Additionally, the results show the need of incorporating wide area control schemes in modern power systems, so that the improvement of the system can be maximized by customizing the control parameter of various devices according to different operating points and/or fault conditions. Particularly, an example is shown in

this study to prove the feasibility of adapting this optimization framework to include wide area control criteria (section 11.3.3).

12.2 Contributions

The main contributions of this research are: (i) the development of a comprehensive and complete formulation of the problem of optimizing the power system's performance using FACTS devices and (ii) the development of a mathematical algorithm, called Enhanced-PSO, capable of pursuing global minimization, with a desired accuracy and a reasonable computational time.

Based on this two goals, the following are the specific contributions to the field:

- A theoretical study and comparison of various optimization methods including classical approaches and evolutionary computation techniques. The problem of improving the voltage profile using shunt compensation is used as an illustrative example of a power system problem. The efficiency of each optimization technique is evaluated based on its capability of achieving global optimality and the corresponding computational effort. Statistical analyses are used to assess the performance of stochastic based search algorithms, in particular their capability of converging into feasible regions and the accuracy in finding the global optimum of the problem.
- Development of a comprehensive problem formulation and optimization framework for improving power system reliability using distributed series compensation and shunt compensation. The improvement of the power system reliability is approached

from the perspective of satisfying the N-1 contingency criterion using existing network resources and new FACTS installations. The optimization framework is a multistage process, which considers security constrained optimal power flow, optimal global control settings of distributed static series compensators (DSSC) and optimal global control settings of static compensator (STATCOM).

- Development of a comprehensive problem formulation and an optimization framework for optimization of power system performance under steady state and transient conditions using series and shunt FACTS devices. The technical parameters to optimize, in steady state conditions, are the voltage profile, system loadability, transmission losses, and line utilization factor of the system. In the case of transient behavior, system damping and eigenvalue analysis are considered.

Some of the contributions described above are evidenced by the following papers:

- **Y.** del Valle, M. Digman, A. Gray, J. Perkel, G. K. Venayagamoorthy, R. G. Harley, "Enhanced particle swarm optimizer for power system applications" Proceedings of the IEEE Swarm Intelligence Symposium (SIS'08), St Louis, Missouri, USA, September 21-23, 2008, pp. 1-7.
- **Y. del Valle**, G.K. Venayagamoorthy, S. Mohagheghi,, J. C. Hernandez, and R.G. Harley, "Particle Swarm Optimization: basic concepts, variants and applications in power system". IEEE Transactions on Evolutionary Computation, Vol. 12, No.2 pp. 171-195, April, 2008.
- S. Mohagheghi, **Y. del Valle**, G.K. Venayagamoorthy and R.G. Harley, "A Proportional-Integrator Type Adaptive Critic Design Based Neurocontroller for a

Static Compensator in a Multimachine Power System". IEEE Transactions on Industrial Electronics. Vol. 54, No.1, February 2007, pp. 86-96.

- **Y. del Valle**, J.C. Hernandez, G.K. Venayagamoorthy and R.G. Harley, "Multiple STATCOM allocation and sizing using particle swarm optimization", Proceedings of the IEEE Power Systems Conference and Exposition (PSCE) 2006, Atlanta, Georgia, USA, October 29 – November 30, 2006, pp. 1884 - 1891.

- **Y. del Valle**, J. C. Hernandez, G.K. Venayagamoorthy, and R.G. Harley, "Optimal STATCOM sizing and placement using particle swarm optimization", Proceedings of the IEEE Transmission and Distribution Conference and Exposition Latin America 2006, Caracas, Venezuela, August 15 - 18, 2006.
- J. C. Hernandez, **Y. del Valle**, G.K. Venayagamoorthy, and R.G. Harley, "Optimal allocation of a STATCOM in a 45 bus section of the Brazilian power system using particle swarm optimization", Proceedings of the IEEE Swarm Intelligence Symposium (SIS'06), Indianapolis, Indiana, USA, May 12-14, 2006, pp. 69-75.
- G.K. Venayagamoorthy, **Y. del Valle**, S. Mohagheghi, W. Qiao, S. Ray, R.G. Harley, D.M. Falcao, G.N. Taranto, T.M.L. Assis, "Effects of a STATCOM, a SCRC and a UPFC on the dynamic behavior of a 45 bus section of the Brazilian power system", Proceedings of the Inaugural IEEE PES 2005 Conference and Exposition in Africa, Durban, South Africa, July 11-15, 2005, pp. 305-312.
- S. Mohagheghi, **Y. del Valle**, G.K. Venayagamoorthy, and R.G. Harley, "A comparison of PSO and back-propagation for training RBF neural networks for identification of a power system with STATCOM", Proceedings of the IEEE Swarm

Intelligence Symposium (SIS'05), Pasadena, California, USA, June 8–10, 2005, pp 381-384.

- **Y. del Valle**, S. Mohagheghi, G.K. Venayagamoorthy and R.G. Harley, "Training MLP neural networks for identification of a small power system: comparison of PSO and backpropagation". Proceedings of the 6th International Conference on Power System Operation and Planning (ICPSOP), Praia, Cape Verde, May 22 – 26, 2005, pp. 153-157.

Three more journal papers, based on the research presented in part III and part IV of this thesis, are being prepared.

In addition, the poster titled "Optimal STATCOM allocation using particle swarm optimization (PSO)" presented at the IEEE Power Engineering Society (PES) General Meeting (June 2006, Montreal), was awarded with the second place in the IEEE-PES Student Poster Contest.

The poster "Optimal allocation and sizing of multiple STATCOM units: a comparison between classical methods and evolutionary computation techniques" presented at the IEEE Power Engineering Society (PES) General Meeting (June 2007, Tampa), was awarded with the third place in the IEEE-PES Student Poster Contest.

12.3 Recommendations

Future work in this field can be developed in the following areas:

- The improvement of the power system reliability can be approached considering also N-2 or N-3 security criterion. The proposed multi-stage, PSO-based, optimization

framework can be modified to continue improving the reliability of the system when *N-x* elements of the system are under contingency.

- The cost metrics for installation of FACTS devices can be modified to consider more sophisticated functions for both, fixed and variable costs. Moreover, the cost of operation and maintenance can be added to the objective functions.
- The series compensation stage for the improvement of the power system's reliability and steady state performance can be respectively modified to relax the assumption of a power system fully deployed with distributed series FACTS devices (DSSC). In that case the objective function value can be adapted to find the optimal locations of the DSSC modules (critical transmission lines) and the minimum amount of series compensation needed, such that the system obtains a maximum benefit from these devices at minimum cost.
- Additionally, in the case of the large perturbation analysis of the power system, a more detailed study can be performed to include the dynamics of the DSSC modules, and to evaluate the impact of bypassing these modules in the case of a faulted transmission line equipped with DSSC modules.
- For improvement of the transient performance of the system, a probabilistic approach can be applied to the selection of critical faults. Additionally, the probability of occurrence can be added to the objective function to emphasize those faults that occur more often. As a supplementary criterion, economical penalties (due to load disconnection or suchlike) can also be added to the objective function.
- Other control schemes and intelligent controllers can be considered for STATCOM or other FACTS devices.

- The two-stage, PSO-based, optimization framework for improvement of power system dynamic performance can also be adapted to consider a supervisory level (wide area control).
- Finally, the PSO-based optimization frameworks can be adapted to consider unbalanced system conditions and faults.

APPENDIX A

FACTS DEVICES AND CONTROL MODELS

A.1 Distributed Static Series Compensator (DSSC) [95]

The concept of DSSC, whose basic schematic is shown in Figure A.1, corresponds to the family of distributed FACTS devices, in this case based on the static series compensator (SSSC).

"A single-turn transformer is used to magnetically couple and mechanically attach the DSSC module to the line. The required quadrature voltage is injected into the line through this coaxial transformer. The module is powered from the line to generate a regulated DC power supply for the controls and electronics. An additional current transformer is attached to the line to give feedback signals for the controls. A communication device is provided to receive instructions using wiresless or power-line communication technique, allowing the module to adjust according to changing operating conditions." [95]

Laboratory demonstrations performed by [95] demonstrated the capability of the DSSC modules in controlling the power flow between transmission lines. In a simple exercise, a system consisting of two transmission lines was used a testing setup where one DSSC module was attached to Line 1 and Line 2 was left uncompensated.

The results of this test indicate that when a DSSC module injects an inductive voltage on Line 1, the effective impedance of this line increases and therefore the current

is redirected to Line 2. On the contrary, when a capacitive voltage is injected on Line 1, its impedance reduces and the current flowing in this line increases, relieving Line 2.

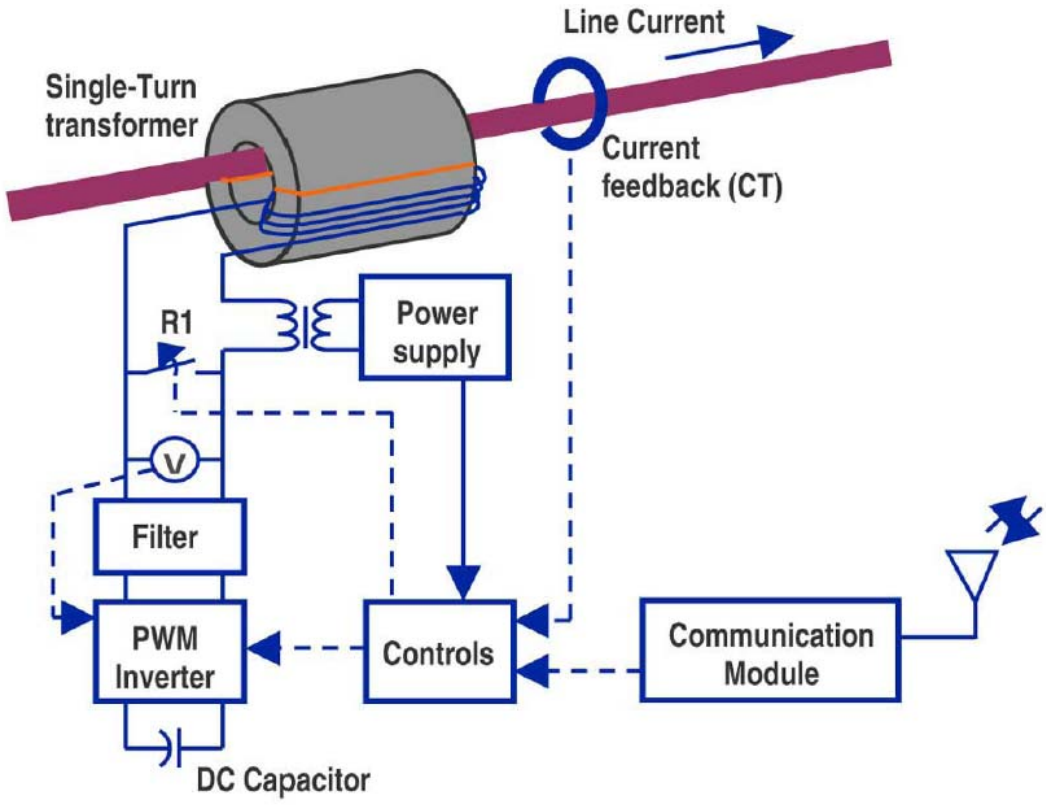

Figure A.1: Schematic of DSSC module [95]

"The current steering property of the technology opens the possibility of controlling the power-flow in a meshed network. On a under-utilized line, the modules can be controlled to inject a lagging voltage, so as to reduce the effective impedance of the line and to pull additional current into it. In congested areas, the control objective

would be to increase line impedance with leading voltage injection so as to push excess current into other parallel paths. This can have significant increase in system capacity and line utilization, and can be used as a simple scalable tool to improve network capacity." [95]

A.2 Static Compensator (STATCOM) [100]

A.2.1 STATCOM model and internal controller

The implemented STATCOM model corresponds to a current injection model, where the STATCOM current is always kept in quadrature in relation to the bus voltage so that only reactive power is exchanged between the ac system and the STATCOM. The dynamic model is shown in Figure A.2.

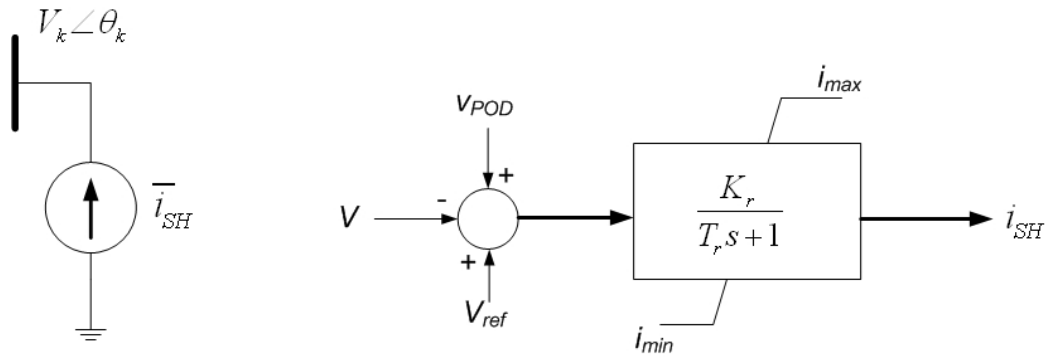

Figure A.2: STATCOM circuit and control block diagram [100].

The differential equation and the reactive power injected at the STATCOM bus are given, respectively, by [100]:

$$\dot{i}_{SH} = \frac{K_r \left(V_{ref} + v_{POD} - V \right) - i_{SH}}{T_r} \tag{A.1}$$

$$Q = -i_{SH} V \tag{A.2}$$

where:

K_r is Regulator gain,

T_r is the regulator time constant,

V_{ref} is the voltage reference,

V_{POD} is the voltage signal from the power oscillation damper,

V is the voltage at the point of common coupling,

i_{SH} is the current injected by the STATCOM.

A.2.2 STATCOM external controller (POD)

The block diagram of the STATCOM external controller, also called power oscillation damper (POD), is shown in Figure A.3.

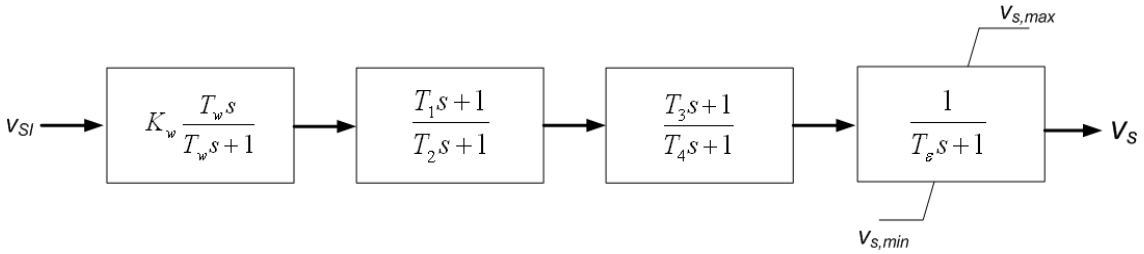

Figure A.3: Power oscillation damper [100]

The differential equations that determine the output of each block in Figure A.3 is given by [100]:

$$\dot{v}_1 = -\frac{K_w v_{SI} + v_1}{T_w} \tag{A.3}$$

$$\dot{v}_2 = \frac{\left(1-\frac{T_1}{T_2}\right)\left(K_w v_{SI} + v_1\right) - v_2}{T_2} \tag{A.4}$$

$$\dot{v}_3 = \frac{\left(1-\frac{T_3}{T_4}\right)\left(v_2 + \frac{T_1}{T_2}\left(K_w v_{SI} + v_1\right)\right) - v_3}{T_4} \tag{A.5}$$

$$\dot{v}_s = \frac{v3 + \frac{T_3}{T_4}\left(v_2 + \frac{T_1}{T_2}\left(K_w v_{SI} + v_1\right)\right) - v_s}{T_\varepsilon} \tag{A.6}$$

where:

$v_{s_{\max}}$	is the maximum stabilizer output signal in p.u.,
$v_{s_{\min}}$	is the minimum stabilizer output signal in p.u.,
K_w	Stabilizer gain,
T_w	Wash-out time constant in seconds,
T_1	First stabilizer time constant in seconds,
T_2	Second stabilizer time constant in seconds,
T_3	Third stabilizer time constant in seconds,
T_4	Fourth stabilizer time constant in seconds,
T_r	Low pass time constant for output signal in seconds.

APPENDIX B

45 BUS SYSTEM DATA

Table B.1: Generator data

Bus	S_{base}	V_{base}	P_g	V_{pu}
4	1860.0	13.8	0.565	1.02
7	260.0	13.8	0.827	1.04
11	1020.0	13.8	0.902	1.02
19	1860.0	13.8	0.677	1.022
28	1402.0	13.8	0.802	1.018
30	111.0	13.8	0.811	1.03
32	156.3	13.8	0.768	1.03
33	312.6	13.8	0.771	1.03
35	1402.0	13.8	0.795	1.02
39	556.0	13.8	0.881	1.00

Table B.2: Line data.

From	To	S_{base}	V_{base}	T_{ratio}	R_{pu}	X_{pu}	B_{pu}
29	36	100	525	0.0000	0.0005	0.0070	0.8392
29	2	100	525	0.0000	0.0014	0.0204	2.4475
22	21	100	525	0.0000	0.0005	0.0069	0.8216
20	21	100	525	0.0000	0.0019	0.0280	3.3576
21	23	100	525	0.0000	0.0012	0.0175	2.0970
24	25	100	525	0.0000	0.0021	0.0309	3.7183
15	16	100	230	0.0000	0.0182	0.0935	0.1595
15	16	100	230	0.0000	0.0182	0.0935	0.1595
17	16	100	230	0.0000	0.0154	0.0776	0.1350
17	16	100	230	0.0000	0.0154	0.0776	0.1350
17	18	100	230	0.0000	0.0216	0.1105	0.1863
17	18	100	230	0.0000	0.0216	0.1105	0.1863
29	27	100	525	0.0000	0.0014	0.0195	2.3970
18	34	100	230	0.0000	0.0180	0.0920	0.1553
18	34	100	230	0.0000	0.0180	0.0920	0.1553
34	46	100	230	0.0000	0.0129	0.0657	0.1128
46	5	100	230	0.0000	0.0033	0.0167	0.2859
34	5	100	230	0.0000	0.0096	0.0491	0.0842
5	6	100	230	0.0000	0.0386	0.1985	0.3400
38	37	100	230	0.0000	0.0019	0.0101	0.0204
38	37	100	230	0.0000	0.0022	0.0111	0.0232
38	37	100	230	0.0000	0.0022	0.0111	0.0232
37	6	100	230	0.0000	0.0177	0.0910	0.1585
27	26	100	525	0.0000	0.0022	0.0300	3.8300

Table B.2 continued

From	To	S_{base}	V_{base}	T_{ratio}	R_{pu}	X_{pu}	B_{pu}
37	6	100	230	0.0000	0.0177	0.0910	0.1585
37	41	100	230	0.0000	0.0207	0.0933	0.1718
37	41	100	230	0.0000	0.0168	0.0930	0.1720
37	41	100	230	0.0000	0.0176	0.0984	0.1798
41	40	100	230	0.0000	0.0202	0.1129	0.2062
40	8	100	230	0.0000	0.0250	0.1548	0.4690
6	8	100	230	0.0000	0.0463	0.2378	0.4084
6	8	100	230	0.0000	0.0463	0.2378	0.4084
8	9	100	230	0.0000	0.0163	0.0835	0.1440
8	9	100	230	0.0000	0.0163	0.0835	0.1440
2	3	100	525	0.0000	0.0007	0.0145	1.6610
9	10	100	230	0.0000	0.0163	0.0835	0.1440
9	12	100	230	0.0000	0.0316	0.1621	0.2784
10	12	100	230	0.0000	0.0153	0.0861	0.1344
43	42	100	230	0.0000	0.0125	0.0641	0.1109
43	42	100	230	0.0000	0.0089	0.0461	0.0796
43	44	100	230	0.0000	0.0172	0.0884	0.1434
43	44	100	230	0.0000	0.0172	0.0884	0.1434
42	44	100	230	0.0000	0.0110	0.1184	0.2027
44	45	100	230	0.0000	0.0181	0.0929	0.1607
42	45	100	230	0.0000	0.0229	0.1174	0.2027
2	3	100	525	0.0000	0.0007	0.0145	1.6610
12	45	100	230	0.0000	0.0344	0.1760	0.3040
12	45	100	230	0.0000	0.0344	0.1760	0.3040
12	13	100	230	0.0000	0.0306	0.1523	0.2702
13	14	100	230	0.0000	0.0245	0.1256	0.2041
14	15	100	230	0.0000	0.0088	0.0415	0.5211
36	20	100	525	0.0000	0.0005	0.0070	0.8392
2	20	100	525	0.0000	0.0018	0.0227	2.2721
20	24	100	525	0.0000	0.0014	0.0195	2.3968
20	22	100	525	0.0000	0.0019	0.0274	3.2867
28	29	100	13.8	0.0263	0.0000	0.0114	0.0000
33	34	100	13.8	0.0600	0.0000	0.0450	0.0000
25	38	100	525	2.2826	0.0000	0.0062	0.0000
26	41	100	525	2.2826	0.0000	0.0062	0.0000
39	40	100	13.8	0.0600	0.0000	0.0236	0.0000
7	8	100	13.8	0.0600	0.0000	0.0460	0.0000
11	12	100	13.8	0.0600	0.0000	0.0114	0.0000
3	43	100	525	2.2826	0.0000	0.0063	0.0000
13	20	100	230	0.4381	0.0000	0.0300	0.0000
35	36	100	13.8	0.0263	0.0000	0.0068	0.0000
19	20	100	13.8	0.0263	0.0000	0.0067	0.0000
4	24	100	13.8	0.0263	0.0000	0.0136	0.0000
21	15	100	525	2.2826	0.0000	0.0062	0.0000
23	17	100	525	2.2826	0.0000	0.0062	0.0000
31	34	100	138	0.6000	0.0000	0.0590	0.0000
30	31	100	13.8	0.1000	0.0000	0.0871	0.0000
32	34	100	13.8	0.0600	0.0000	0.0701	0.0000

Table B.3: Load Data.

Bus	S_{base}	V_{base}	P_{Lpu}	Q_{Lpu}
24	100	525	1.740	0.918
15	100	230	4.270	-0.250
37	100	230	8.130	1.100
41	100	230	3.930	-1.110
40	100	230	4.040	1.350
8	100	230	1.710	0.185
9	100	230	1.260	0.470
10	100	230	0.460	0.147
12	100	230	2.810	2.565
44	100	230	1.840	0.602
43	100	230	2.290	1.830
42	100	230	2.620	0.132
17	100	230	4.240	0.906
45	100	230	1.390	0.537
13	100	230	2.790	0.607
14	100	230	1.300	0.294
22	100	525	3.680	2.196
2	100	525	0.000	2.000
27	100	525	0.000	1.500
26	100	525	0.000	1.750
25	100	525	0.000	1.750
21	100	525	0.000	1.500
16	100	230	3.100	1.410
18	100	230	1.170	0.531
31	100	138	1.260	0.398
46	100	230	0.901	0.553
5	100	230	1.770	0.680
6	100	230	1.910	0.420
38	100	230	6.120	-4.550

APPENDIX C

118 BUS SYSTEM DATA

All values are in per unit system with base power equal to 100 MVA.

Table C.1: Generator data

Bus	S_{base}	V_{base}	P_g	V_{pu}	Q_{max}	Q_{min}
10	100	345	4.50	1.050	2.00	-1.47
12	100	138	0.85	0.990	1.20	-0.35
25	100	138	2.20	1.050	1.40	-0.47
26	100	345	3.14	1.015	10.00	-10.00
49	100	138	2.04	1.025	2.10	-0.85
61	100	138	1.60	0.995	3.00	-1.00
65	100	345	3.91	1.005	2.00	-0.67
66	100	138	3.92	1.050	2.00	-0.67
69	100	138	5.16	1.035	3.00	-3.00
80	100	138	4.77	1.040	2.80	-1.65
87	100	138	0.04	1.015	10.00	-1.00
89	100	138	6.07	1.005	3.00	-2.10
100	100	138	2.52	1.017	1.55	-0.50
103	100	138	0.40	1.001	0.40	-0.15
111	100	138	0.36	0.980	10.00	-1.00

Table C.2: Capacitor bank data.

Bus	V_{base}	G	B	Q_{min}	Q_{max}
5	138	0	-0.4	-50	0
34	138	0	0.14	0	20
37	138	0	-0.25	-30	0
44	138	0	0.1	0	20
45	138	0	0.1	0	20
46	138	0	0.1	0	20
48	138	0	0.15	0	20
74	138	0	0.12	0	20
79	138	0	0.2	0	30
82	138	0	0.2	0	30
83	138	0	0.1	0	20
105	138	0	0.2	0	30
107	138	0	0.06	0	10
110	138	0	0.06	0	10

Table C.3: Line data.

From	To	V_{base}	R_{pu}	X_{pu}	B_{pu}	S_{max}
1	2	138	0.0303	0.0999	0.0254	100
1	3	138	0.0129	0.0424	0.0108	100
4	5	138	0.0018	0.0080	0.0021	500
3	5	138	0.0241	0.1080	0.0284	100
5	6	138	0.0119	0.0540	0.0143	100
6	7	138	0.0046	0.0208	0.0055	100
8	9	345	0.0024	0.0305	1.1620	500
9	10	345	0.0026	0.0322	1.2300	500
4	11	138	0.0209	0.0688	0.0175	100
5	11	138	0.0203	0.0682	0.0174	125
11	12	138	0.0060	0.0196	0.0050	100
2	12	138	0.0187	0.0616	0.0157	100
3	12	138	0.0484	0.1600	0.0406	100
7	12	138	0.0086	0.0340	0.0087	100
11	13	138	0.0223	0.0731	0.0188	100
12	14	138	0.0215	0.0707	0.0182	100
13	15	138	0.0744	0.2444	0.0627	100
14	15	138	0.0595	0.1950	0.0502	100
12	16	138	0.0212	0.0834	0.0214	100
15	17	138	0.0132	0.0437	0.0444	500
16	17	138	0.0454	0.1801	0.0466	100
17	18	138	0.0123	0.0505	0.0130	125
18	19	138	0.0112	0.0493	0.0114	100
19	20	138	0.0252	0.1170	0.0298	100
15	19	138	0.0120	0.0394	0.0101	100
20	21	138	0.0183	0.0849	0.0216	100
21	22	138	0.0209	0.0970	0.0246	100
22	23	138	0.0342	0.1590	0.0404	100
23	24	138	0.0135	0.0492	0.0498	100
23	25	138	0.0156	0.0800	0.0864	500
25	27	138	0.0318	0.1630	0.1764	500
27	28	138	0.0191	0.0855	0.0216	100
28	29	138	0.0237	0.0943	0.0238	100
8	30	345	0.0043	0.0504	0.5140	200
26	30	345	0.0080	0.0860	0.9080	500
17	31	138	0.0474	0.1563	0.0399	100
29	31	138	0.0108	0.0331	0.0083	100
23	32	138	0.0317	0.1153	0.1173	150
31	32	138	0.0298	0.0985	0.0251	100
27	32	138	0.0229	0.0755	0.0193	100
15	33	138	0.0380	0.1244	0.0319	100
19	34	138	0.0752	0.2470	0.0632	100
35	36	138	0.0022	0.0102	0.0027	100
35	37	138	0.0110	0.0497	0.0132	100
33	37	138	0.0415	0.1420	0.0366	100
34	36	138	0.0087	0.0268	0.0057	100
34	37	138	0.0026	0.0094	0.0098	500
37	39	138	0.0321	0.1060	0.0270	100
37	40	138	0.0593	0.1680	0.0420	100

Table C.3 continued

From	To	V_{base}	R_{pu}	X_{pu}	B_{pu}	S_{max}
30	38	345	0.0046	0.0540	0.4220	150
39	40	138	0.0184	0.0605	0.0155	100
40	41	138	0.0145	0.0487	0.0122	100
40	42	138	0.0555	0.1830	0.0466	100
41	42	138	0.0410	0.1350	0.0344	100
43	44	138	0.0608	0.2454	0.0607	100
34	43	138	0.0413	0.1681	0.0423	100
44	45	138	0.0224	0.0901	0.0224	100
45	46	138	0.0400	0.1356	0.0332	100
46	47	138	0.0380	0.1270	0.0316	100
46	48	138	0.0601	0.1890	0.0472	100
47	49	138	0.0191	0.0625	0.0160	100
42	49	138	0.0715	0.3230	0.0860	100
42	49	138	0.0715	0.3230	0.0860	100
45	49	138	0.0684	0.1860	0.0444	100
48	49	138	0.0179	0.0505	0.0126	100
49	50	138	0.0267	0.0752	0.0187	100
49	51	138	0.0486	0.1370	0.0342	100
51	52	138	0.0203	0.0588	0.0140	100
52	53	138	0.0405	0.1635	0.0406	100
53	54	138	0.0263	0.1220	0.0310	100
49	54	138	0.0730	0.2890	0.0738	100
49	54	138	0.0869	0.2910	0.0730	100
54	55	138	0.0169	0.0707	0.0202	100
54	56	138	0.0028	0.0096	0.0073	100
55	56	138	0.0049	0.0151	0.0037	100
56	57	138	0.0343	0.0966	0.0242	100
50	57	138	0.0474	0.1340	0.0332	100
56	58	138	0.0343	0.0966	0.0242	100
51	58	138	0.0255	0.0719	0.0179	100
54	59	138	0.0503	0.2293	0.0598	100
56	59	138	0.0825	0.2510	0.0569	100
56	59	138	0.0803	0.2390	0.0536	100
55	59	138	0.0474	0.2158	0.0565	100
59	60	138	0.0317	0.1450	0.0376	100
59	61	138	0.0328	0.1500	0.0388	100
60	61	138	0.0026	0.0135	0.0146	500
60	62	138	0.0123	0.0561	0.0147	100
61	62	138	0.0082	0.0376	0.0098	100
63	64	345	0.0017	0.0200	0.2160	500
38	65	345	0.0090	0.0986	1.0460	500
64	65	345	0.0027	0.0302	0.3800	500
49	66	138	0.0180	0.0919	0.0248	500
49	66	138	0.0180	0.0919	0.0248	500
62	66	138	0.0482	0.2180	0.0578	100
62	67	138	0.0258	0.1170	0.0310	100
66	67	138	0.0224	0.1015	0.0268	100
65	68	345	0.0014	0.0160	0.6380	500
47	69	138	0.0844	0.2778	0.0709	100
49	69	138	0.0985	0.3240	0.0828	100

Table C.3 continued

From	To	V_{base}	R_{pu}	X_{pu}	B_{pu}	S_{max}
69	70	138	0.0300	0.1270	0.1220	500
24	70	138	0.0022	0.4115	0.1020	100
70	71	138	0.0088	0.0355	0.0088	100
24	72	138	0.0488	0.1960	0.0488	100
71	72	138	0.0446	0.1800	0.0444	100
71	73	138	0.0087	0.0454	0.0118	100
70	74	138	0.0401	0.1323	0.0337	100
70	75	138	0.0428	0.1410	0.0360	100
69	75	138	0.0405	0.1220	0.1240	500
74	75	138	0.0123	0.0406	0.0103	100
76	77	138	0.0444	0.1480	0.0368	100
69	77	138	0.0309	0.1010	0.1038	100
75	77	138	0.0601	0.1999	0.0498	100
77	78	138	0.0038	0.0124	0.0126	100
78	79	138	0.0055	0.0244	0.0065	100
77	80	138	0.0170	0.0485	0.0472	500
77	80	138	0.0294	0.1050	0.0228	500
79	80	138	0.0156	0.0704	0.0187	100
68	81	345	0.0018	0.0202	0.8080	500
77	82	138	0.0298	0.0853	0.0817	100
82	83	138	0.0112	0.0367	0.0380	100
83	84	138	0.0625	0.1320	0.0258	100
83	85	138	0.0430	0.1480	0.0348	100
84	85	138	0.0302	0.0641	0.0123	100
85	86	138	0.0350	0.1230	0.0276	500
86	87	138	0.0283	0.2074	0.0445	500
85	88	138	0.0200	0.1020	0.0276	100
85	89	138	0.0239	0.1730	0.0470	150
88	89	138	0.0139	0.0712	0.0193	500
89	90	138	0.0518	0.1880	0.0528	500
89	90	138	0.0238	0.0997	0.1060	500
90	91	138	0.0254	0.0836	0.0214	100
89	92	138	0.0099	0.0505	0.0548	500
89	92	138	0.0393	0.1581	0.0414	500
91	92	138	0.0387	0.1272	0.0327	100
92	93	138	0.0258	0.0848	0.0218	100
92	94	138	0.0481	0.1580	0.0406	100
93	94	138	0.0223	0.0732	0.0188	100
94	95	138	0.0132	0.0434	0.0111	100
80	96	138	0.0356	0.1820	0.0494	100
82	96	138	0.0162	0.0530	0.0544	100
94	96	138	0.0269	0.0869	0.0230	100
80	97	138	0.0183	0.0934	0.0254	100
80	98	138	0.0238	0.1080	0.0286	100
80	99	138	0.0454	0.2060	0.0546	100
92	100	138	0.0648	0.2950	0.0472	100
94	100	138	0.0178	0.0580	0.0604	100
95	96	138	0.0171	0.0547	0.0147	100
96	97	138	0.0173	0.0885	0.0240	100
98	100	138	0.0397	0.1790	0.0476	100

Table C.3 continued

From	To	V_{base}	R_{pu}	X_{pu}	B_{pu}	S_{max}
99	100	138	0.0180	0.0813	0.0216	100
100	101	138	0.0277	0.1262	0.0328	100
92	102	138	0.0123	0.0559	0.0146	100
101	102	138	0.0246	0.1120	0.0294	100
100	103	138	0.0160	0.0525	0.0536	500
100	104	138	0.0451	0.2040	0.0541	100
103	104	138	0.0466	0.1584	0.0407	100
103	105	138	0.0535	0.1625	0.0408	100
100	106	138	0.0605	0.2290	0.0620	100
104	105	138	0.0099	0.0378	0.0099	100
105	106	138	0.0140	0.0547	0.0143	100
105	107	138	0.0530	0.1830	0.0472	100
105	108	138	0.0261	0.0703	0.0184	100
106	107	138	0.0530	0.1830	0.0472	100
108	109	138	0.0105	0.0288	0.0076	100
103	110	138	0.0391	0.1813	0.0461	100
109	110	138	0.0278	0.0762	0.0202	100
110	111	138	0.0220	0.0755	0.0200	100
110	112	138	0.0247	0.0640	0.0620	100
17	113	138	0.0091	0.0301	0.0077	100
32	113	138	0.0615	0.2030	0.0518	500
32	114	138	0.0135	0.0612	0.0163	100
27	115	138	0.0164	0.0741	0.0197	100
114	115	138	0.0023	0.0104	0.0028	100
68	116	345	0.0003	0.0041	0.1640	500
12	117	138	0.0329	0.1400	0.0358	100
75	118	138	0.0145	0.0481	0.0120	100
76	118	138	0.0164	0.0544	0.0136	100
8	5	345	0.0000	0.0267	0.0000	500
26	25	345	0.0000	0.0382	0.0000	500
30	17	345	0.0000	0.0388	0.0000	500
38	37	345	0.0000	0.0375	0.0000	500
63	59	345	0.0000	0.0386	0.0000	500
64	61	345	0.0000	0.0268	0.0000	500
65	66	345	0.0000	0.0370	0.0000	500
68	69	345	0.0000	0.0370	0.0000	500
81	80	345	0.0000	0.0370	0.0000	500

Table C.4: Load data.

Bus	V_{base}	P_{Lpu}	Q_{Lpu}	Bus	V_{base}	P_{Lpu}	Q_{Lpu}
1	138	0.487	0.258	19	138	0.430	0.239
2	138	0.191	0.086	20	138	0.172	0.029
3	138	0.373	0.096	21	138	0.134	0.076
4	138	0.368	0.115	22	138	0.096	0.048
6	138	0.497	0.210	23	138	0.067	0.029
7	138	0.182	0.019	24	138	0.117	0.000

Table C.4 continued

Bus	V_{base}	P_{Lpu}	Q_{Lpu}	Bus	V_{base}	P_{Lpu}	Q_{Lpu}
8	345	0.252	0.000	27	138	0.673	0.124
11	138	0.669	0.220	28	138	0.162	0.067
12	138	0.449	0.096	29	138	0.229	0.038
13	138	0.325	0.153	31	138	0.348	0.258
14	138	0.134	0.010	32	138	0.564	0.220
15	138	0.860	0.287	33	138	0.220	0.086
16	138	0.239	0.096	34	138	0.564	0.248
17	138	0.105	0.029	35	138	0.315	0.086
18	138	0.573	0.325	36	138	0.296	0.162
39	138	0.243	0.099	82	138	0.486	0.243
40	138	0.594	0.207	83	138	0.180	0.090
41	138	0.333	0.090	84	138	0.099	0.063
42	138	0.864	0.207	85	138	0.216	0.135
43	138	0.162	0.063	86	138	0.189	0.090
44	138	0.144	0.072	88	138	0.432	0.090
45	138	0.477	0.198	90	138	1.467	0.378
46	138	0.081	0.090	91	138	0.090	0.000
47	138	0.306	0.000	92	138	0.585	0.090
48	138	0.180	0.099	93	138	0.108	0.063
49	138	0.783	0.270	94	138	0.270	0.144
50	138	0.153	0.036	95	138	0.378	0.279
51	138	0.153	0.072	96	138	0.342	0.135
52	138	0.162	0.045	97	138	0.135	0.081
53	138	0.207	0.099	98	138	0.306	0.072
54	138	0.585	0.288	99	138	0.378	0.000
55	138	0.567	0.198	100	138	0.333	0.162
56	138	0.756	0.162	101	138	0.198	0.135
57	138	0.108	0.027	102	138	0.045	0.027
58	138	0.108	0.027	103	138	0.207	0.144
59	138	1.098	1.017	104	138	0.342	0.225
60	138	0.702	0.027	105	138	0.279	0.234
62	138	0.693	0.126	106	138	0.387	0.144
66	138	0.351	0.162	107	138	0.450	0.108
67	138	0.252	0.063	108	138	0.018	0.009
70	138	0.594	0.180	109	138	0.072	0.027
72	138	0.108	0.000	110	138	0.351	0.270
73	138	0.054	0.000	112	138	0.612	0.117
74	138	0.612	0.243	113	138	0.054	0.000
75	138	0.423	0.099	114	138	0.076	0.029
76	138	0.612	0.324	115	138	0.210	0.067
77	138	0.549	0.252	116	138	1.656	0.000
78	138	0.639	0.234	117	138	0.191	0.076
79	138	0.351	0.288	118	138	0.297	0.135
80	138	1.170	0.234				

APPENDIX D

68 BUS SYSTEM DATA

All values are in per unit system with a base power of 100 MVA. All controller time constants are in seconds.

Table D.1: Generator data

Gen	Bus	S_{base}	V_{base}	P_g	V_{pu}
1	53	100	13.8	2.50	1.045
2	54	100	13.8	5.45	0.980
3	55	100	13.8	6.50	0.983
4	56	100	13.8	6.32	0.997
5	57	100	13.8	5.05	1.011
6	58	100	13.8	7.00	1.050
7	59	100	13.8	5.60	1.063
8	60	100	13.8	5.40	1.030
9	61	100	13.8	8.00	1.025
10	62	100	13.8	5.00	1.010
11	63	100	13.8	10.00	1.000
12	64	100	13.8	13.50	1.016
13	65	100	13.8	35.91	1.011
14	66	100	13.8	17.85	1.000
15	67	100	13.8	10.00	1.000
16	68	100	13.8	40.00	1.000

Table D.2: Generator excitation data.

Gen	$V_{r,max}$	$V_{r,min}$	K_a	T_a	K_f	T_f	T_e	A_e	B_e
1	10	-10	30	0.02	0	1	0.785	0	0.9
2	10	-10	30	0.02	0	1	0.785	0	0.9
3	10	-10	30	0.02	0	1	0.785	0	0.9
4	10	-10	30	0.02	0	1	0.785	0	0.9
5	10	-10	30	0.02	0	1	0.785	0	0.9
6	10	-10	30	0.02	0	1	0.785	0	0.9
7	10	-10	30	0.02	0	1	0.785	0	0.9
8	10	-10	30	0.02	0	1	0.785	0	0.9
9	10	-10	30	0.02	0	1	0.785	0	0.9

Table D.3: Generator machine data.

Bus	S_{base}	V_{base}	X_l	R_a	X_d	X'_d	X''_d	T'_{d0}	T''_{d0}	X_q	X'_q	X''_q	T'_{q0}	T''_{q0}	M=2H	D
53	100	13.8	0.01	0	0.10	0.031	0.03	10.20	0.05	0.07	0.03	0.03	1.50	0.04	84.0	4.0
54	100	13.8	0.04	0	0.30	0.070	0.05	6.56	0.05	0.28	0.06	0.05	1.50	0.04	60.4	9.8
55	100	13.8	0.03	0	0.25	0.053	0.05	5.70	0.05	0.24	0.05	0.05	1.50	0.04	71.6	10.0
56	100	13.8	0.03	0	0.26	0.044	0.04	5.69	0.05	0.26	0.04	0.04	1.50	0.04	57.2	10.0
57	100	13.8	0.03	0	0.33	0.066	0.05	5.40	0.05	0.31	0.06	0.05	0.44	0.04	52.0	3.0
58	100	13.8	0.02	0	0.25	0.050	0.04	7.30	0.05	0.24	0.05	0.04	0.40	0.04	69.6	10.0
59	100	13.8	0.03	0	0.30	0.049	0.04	5.66	0.05	0.29	0.05	0.04	1.50	0.04	52.8	8.0
60	100	13.8	0.03	0	0.29	0.057	0.05	6.70	0.05	0.28	0.05	0.05	0.41	0.04	48.6	9.0
61	100	13.8	0.03	0	0.21	0.057	0.05	4.79	0.05	0.21	0.05	0.05	1.96	0.04	69.0	14.0
62	100	13.8	0.02	0	0.17	0.046	0.04	9.37	0.05	0.12	0.05	0.04	1.50	0.04	62.0	5.6
63	100	13.8	0.01	0	0.13	0.018	0.01	4.10	0.05	0.12	0.02	0.01	1.50	0.04	56.4	13.6
64	100	13.8	0.02	0	0.10	0.031	0.03	7.40	0.05	0.10	0.03	0.03	1.50	0.04	184.6	13.5
65	200	13.8	0.00	0	0.03	0.006	0.00	5.90	0.05	0.03	0.01	0.00	1.50	0.04	496.0	33.0
66	100	13.8	0.00	0	0.02	0.003	0.00	4.10	0.05	0.02	0.00	0.00	1.50	0.04	600.0	100.0
67	100	13.8	0.00	0	0.02	0.003	0.00	4.10	0.05	0.02	0.00	0.00	1.50	0.04	600.0	100.0
68	200	13.8	0.00	0	0.04	0.007	0.01	7.80	0.05	0.03	0.01	0.01	1.50	0.04	450.0	50.0

Table D.4: Line data.

From	To	S_{base}	V_{base}	T_{ratio}	R_{pu}	X_{pu}	B_{pu}	Tap Ratio	S_{max}
1	2	100	138	0	0.0035	0.0411	0.6987	0.000	2
1	30	100	138	0	0.0008	0.0074	0.4800	0.000	5
2	3	100	138	0	0.0013	0.0151	0.2572	0.000	8
2	25	100	138	0	0.0070	0.0086	0.1460	0.000	5
3	4	100	138	0	0.0013	0.0213	0.2214	0.000	5
3	18	100	138	0	0.0011	0.0133	0.2138	0.000	2
4	5	100	138	0	0.0008	0.0128	0.1342	0.000	2
4	14	100	138	0	0.0008	0.0129	0.1382	0.000	5
5	6	100	138	0	0.0002	0.0026	0.0434	0.000	8
5	8	100	138	0	0.0008	0.0112	0.1476	0.000	5
6	7	100	138	0	0.0006	0.0092	0.1130	0.000	8
6	11	100	138	0	0.0007	0.0082	0.1389	0.000	8
7	8	100	138	0	0.0004	0.0046	0.0780	0.000	5
8	9	100	138	0	0.0023	0.0363	0.3804	0.000	2
9	30	100	138	0	0.0019	0.0183	0.2900	0.000	8
10	11	100	138	0	0.0004	0.0043	0.0729	0.000	8
10	13	100	138	0	0.0004	0.0043	0.0729	0.000	5
13	14	100	138	0	0.0009	0.0101	0.1723	0.000	5
14	15	100	138	0	0.0018	0.0217	0.3660	0.000	2
15	16	100	138	0	0.0009	0.0094	0.1710	0.000	5
16	17	100	138	0	0.0007	0.0089	0.1342	0.000	5
16	19	100	138	0	0.0016	0.0195	0.3040	0.000	10
16	21	100	138	0	0.0008	0.0135	0.2548	0.000	8
16	24	100	138	0	0.0003	0.0059	0.0680	0.000	2
17	18	100	138	0	0.0007	0.0082	0.1319	0.000	5
17	27	100	138	0	0.0013	0.0173	0.3216	0.000	2
21	22	100	138	0	0.0008	0.0140	0.2565	0.000	10
22	23	100	138	0	0.0006	0.0096	0.1846	0.000	2
23	24	100	138	0	0.0022	0.0350	0.3610	0.000	8
23	59	100	138	0	0.0005	0.0272	0.0000	0.000	10
25	26	100	138	0	0.0032	0.0323	0.5310	0.000	2
26	27	100	138	0	0.0014	0.0147	0.2396	0.000	5
26	28	100	138	0	0.0043	0.0474	0.7802	0.000	5
26	29	100	138	0	0.0057	0.0625	1.0290	0.000	5
28	29	100	138	0	0.0014	0.0151	0.2490	0.000	5
9	30	100	138	0	0.0019	0.0183	0.2900	0.000	8
9	36	100	138	0	0.0022	0.0196	0.3400	0.000	8
9	36	100	138	0	0.0022	0.0196	0.3400	0.000	8
36	37	100	138	0	0.0005	0.0045	0.3200	0.000	50
34	36	100	138	0	0.0033	0.0111	1.4500	0.000	10
33	34	100	138	0	0.0011	0.0157	0.2020	0.000	15
32	33	100	138	0	0.0008	0.0099	0.1680	0.000	10
30	31	100	138	0	0.0013	0.0187	0.3330	0.000	10
30	32	100	138	0	0.0024	0.0288	0.4880	0.000	5
1	31	100	138	0	0.0016	0.0163	0.2500	0.000	5
31	38	100	138	0	0.0011	0.0147	0.2470	0.000	5
33	38	100	138	0	0.0036	0.0444	0.6930	0.000	5
38	46	100	138	0	0.0022	0.0284	0.4300	0.000	5
46	49	100	138	0	0.0018	0.0274	0.2700	0.000	8

Table D.4 continued

From	To	S_{base}	V_{base}	T_{ratio}	R_{pu}	X_{pu}	B_{pu}	Tap Ratio	S_{max}
1	47	100	138	0	0.0013	0.0188	1.3100	0.000	5
47	48	100	138	0	0.0025	0.0268	0.4000	0.000	5
47	48	100	138	0	0.0025	0.0268	0.4000	0.000	5
48	40	100	138	0	0.0020	0.0220	1.2800	0.000	10
35	45	100	138	0	0.0007	0.0175	1.3900	0.000	5
37	43	100	138	0	0.0005	0.0276	0.0000	0.000	5
43	44	100	138	0	0.0001	0.0011	0.0000	0.000	5
44	45	100	138	0	0.0025	0.0730	0.0000	0.000	5
39	44	100	138	0	0.0000	0.0411	0.0000	0.000	2
39	45	100	138	0	0.0000	0.0839	0.0000	0.000	5
45	51	100	138	0	0.0004	0.0105	0.7200	0.000	10
50	52	100	138	0	0.0012	0.0288	2.0600	0.000	15
50	51	100	138	0	0.0009	0.0221	1.6200	0.000	15
49	52	100	138	0	0.0076	0.1141	1.1600	0.000	10
52	42	100	138	0	0.0040	0.0600	2.2500	0.000	5
42	41	100	138	0	0.0040	0.0600	2.2500	0.000	5
41	40	100	138	0	0.0060	0.0840	3.1500	0.000	15
41	66	100	138	0	0.0000	0.0015	0.0000	1.000	75
42	67	100	138	0	0.0000	0.0015	0.0000	1.000	75
52	68	100	138	0	0.0000	0.0030	0.0000	1.000	75
1	27	100	138	0	0.0320	0.3200	0.4100	1.000	75
2	53	100	138	0	0.0000	0.0181	0.0000	1.025	75
6	54	100	138	0	0.0000	0.0250	0.0000	1.070	75
10	55	100	138	0	0.0000	0.0200	0.0000	1.070	75
12	11	100	138	0	0.0016	0.0435	0.0000	1.060	75
12	13	100	138	0	0.0016	0.0435	0.0000	1.060	75
19	20	100	138	0	0.0007	0.0138	0.0000	1.060	75
19	56	100	138	0	0.0007	0.0142	0.0000	1.070	75
20	57	100	138	0	0.0009	0.0180	0.0000	1.009	75
22	58	100	138	0	0.0000	0.0143	0.0000	1.025	75
25	60	100	138	0	0.0006	0.0232	0.0000	1.025	75
29	61	100	138	0	0.0008	0.0156	0.0000	1.025	75
31	62	100	138	0	0.0000	0.0260	0.0000	1.040	75
32	63	100	138	0	0.0000	0.0130	0.0000	1.040	75
36	64	100	138	0	0.0000	0.0075	0.0000	1.040	75
37	65	100	138	0	0.0000	0.0033	0.0000	1.040	75
35	34	100	138	0	0.0001	0.0074	0.0000	0.946	75

Table D.5: Load Data.

Bus	S_{base}	V_{base}	P_{Lpu}	Q_{Lpu}
1	100	138	2.527	1.186
3	100	138	3.220	0.020
4	100	138	5.000	1.840
7	100	138	2.340	0.840
8	100	138	5.220	1.770
9	100	138	1.040	1.250
12	100	138	0.090	0.880
15	100	138	3.200	1.530
16	100	138	3.290	0.320
18	100	138	1.580	0.300
20	100	138	6.800	1.030
21	100	138	2.740	1.150
23	100	138	2.480	0.850
24	100	138	3.090	-0.920
25	100	138	2.240	0.470
26	100	138	1.390	0.170
27	100	138	2.810	0.760
28	100	138	2.060	0.280
29	100	138	2.840	0.270
33	100	138	1.120	0.000
36	100	138	1.020	-0.195
37	100	138	60.000	3.000
39	100	138	2.670	0.126
40	100	138	0.656	0.235
41	100	138	10.000	2.500
42	100	138	11.500	2.500
44	100	138	2.676	0.048
45	100	138	2.080	0.210
46	100	138	1.507	0.285
47	100	138	2.031	0.326
48	100	138	2.412	0.022
49	100	138	1.640	0.290
50	100	138	1.000	-1.470
51	100	138	3.370	-1.220
52	100	138	24.700	1.230

REFERENCES

[1] Y. del Valle, G. K. Venayagamoorthy, S. Mohagheghi,, J. C. Hernandez, and R. G. Harley, "Particle Swarm Optimization: Basic Concepts, Variants and Applications in Power System," *IEEE Transactions on Evolutionary Computation*, Vol. 12, No.2 pp. 171-195, April, 2008.

[2] A. Schrijver, *Theory of linear and integer programming*. John Wiley and Sons, New York, 1998. ISBN: 0471982326, 9780471982326.

[3] J. Nocedal and S. J. Wright, *Numerical optimization*, Springer, New York, 1999. ISBN: 0387987932, 9780387987934.

[4] A. Nemirovski, Lecture notes on optimization IIII (ISyE 6663): convex analysis, nonlinear programming theory and nonlinear programming algorithms, School of Industrial and Systems Engineering, Georgia Institute of Technology, 2006.

[5] D. Bertsimas and J. N. Tsitsiklis, *Introduction to linear optimization, Athena Scientific Series in Optimization and Neural Computation*, 1997. ISBN: 1886529191, 9781886529199.

[6] D. Bertsekas, *Dynamic programming and optimal control*, Athena Scientific, Boston, MA, 2000. ISBN: 1886529086, 9781886529083.

[7] T. Bäck, *Evolutionary algorithms in theory and practice: evolution strategies, evolutionary programming, genetic algorithms*, Oxford University Press, Oxford, 1996. ISBN: 0195099710, 9780195099713.

[8] A.E. Eiben and J.E. Smith, *Introduction to evolutionary computing*, Springer, 2003. ISBN: 3540401849, 9783540401841.

[9] D. B. Fogel, *Evolutionary computation: toward a new philosophy of machine intelligence*, IEEE Press, Piscataway, NJ, 1995. ISBN: 0471669512, 9780471669517.

[10] A. Sharma, S. Chanana, S. Parida, "Combined optimal location of FACTS controllers and loadability enhancement in competitive electricity markets using MILP," Proc. of the IEEE Power Engineering Society General Meeting, 2005. Vol. 1, Jun. 2005, pp. 670–677.

[11] F. Lima, F. Galiana, I. Kockar and, J. Munoz, "Phase shifter placement in large-scale systems via mixed integer linear programming," *IEEE Transactions on Power Systems*, Vol. 18, no. 3, Aug. 2003, pp. 1029-1034.

[12] D. Wanhong, T. Lie, "Optimal compensation of variable series capacitors for

improved economic dispatch in power systems," Proc. of the IEEE International Conference on Energy Management and Power Delivery (EMPD) 1995,Vol. 2, Nov. 1995, pp. 732-737.

[13] S. Chanana, A. Kumar, "Effect of optimally located FACTS devices on active and reactive power price in deregulated electricity markets," Proc. of the IEEE Power India Conference, 2006, Apr. 2006, pp.7-14.

[14] N. Yorino, E. El-Araby, H. Sasaki, S. Harada, "A new formulation for FACTS allocation for security enhancement against voltage collapse," *IEEE Transactions on Power Systems*, Vol. 18, no. 1, Feb. 2003, pp. 3-10.

[15] E. El-Araby, N. Yorino, H. Sasaki, "A comprehensive approach for FACTS devices optimal allocation to mitigate voltage collapse," Proc. of the IEEE Transmission and Distribution Conference and Exhibition 2002: Asia Pacific. Vol. 1, Oct. 2002, pp. 62-67.

[16] E. De Oliveira, J. Marangon Lima, K. De Almeida, "Allocation of FACTS devices in hydrothermal systems," *IEEE Transactions on Power Systems*, Vol. 15, no. 1, Feb. 2000, pp. 276-282.

[17] S. Singh, A. David, "Congestion management by optimising FACTS device location," Proc. of the IEEE International Conference on Electric Utility Deregulation and Restructuring and Power Technologies (DRPT), 2000. Proceedings. Apr. 2000, pp.23–28.

[18] S. Singh, A. David, "A new approach for placement of FACTS devices in open power markets," IEEE Power Engineering Review, Vol. 21, no. 9, Sept. 2001 pp. 58-60.

[19] Yunqiang Lu, A. Abur, "Static security enhancement via optimal utilization of thyristor-controlled series capacitors," *IEEE Transactions on Power Systems*, Vol. 17, no. 2, May 2002, pp. 324-329.

[20] R. Shizawa, K. Nishida, T. Ohtaka, S. Iwamoto, "Allocation of TCSC from transient stability viewpoint," Proc. of the IEEE International Conference on Power System Technology (PowerCon) 2004. Vol. 1, Nov. 2004, pp. 216-221.

[21] S. Singh, "Location of FACTS devices for enhancing power systems' security," Proc. of the IEEE 2001 Large Engineering Systems Conference on Power Engineering (LESCOPE '01), Jul. 2001, pp. 162-166.

[22] S. Singh, A. David, "Placement of FACTS devices in open power market," Proc. of the IEEE 2000 International Conference on Advances in Power System Control, Operation and Management (APSCOM-00), Vol. 1, Nov. 2000, pp. 173-177.

[23] J. Singh, S. Singh, S. Srivastava, "Enhancement of power system security through

optimal placement of TCSC and UPFC," Proc. of the IEEE Power Engineering Society General Meeting, 2007. Jun. 2007, pp. 1–6.

[24] T. Orfanogianni, R. Bacher, "Steady-state optimization in power systems with series FACTS devices," *IEEE Transactions on Power Systems*, Vol. 18, no. 1, Feb. 2003, pp.19–26.

[25] H. Wang, F. Swift, M. Li, "Selection of installing locations and feedback signals of FACTS-based stabilisers in multimachine power systems by reduced-order modal analysis," Proc. of the IEE Generation, Transmission and Distribution, Vol. 144, no. 3, May 1997, pp. 263-269.

[26] B. Kumar, S. Singh, S. Srivastava, "Placement of FACTS controllers using modal controllability indices to damp out power system oscillations," IET Generation, Transmission & Distribution, Vol. 1, no. 2, March 2007, pp. 209-217.

[27] S. Gerbex, R. Cherkaoui, A. Germond, "Optimal location of multi-type FACTS devices in a power system by means of genetic algorithms," *IEEE Transactions on Power Systems*, Vol. 16, no. 3, Aug. 2001, pp:537–544.

[28] L. Ippolito, P. Siano, "Selection of optimal number and location of thyristor-controlled phase shifters using genetic based algorithms," Proc. of the IEE Generation, Transmission and Distribution, Vol. 151, no. 5, Sept. 2004, pp: 630–637.

[29] D. Radu, Y. Besanger, "A multi-objective genetic algorithm approach to optimal allocation of multi-type FACTS devices for power systems security," Proc. of the IEEE Power Engineering Society General Meeting, 2006, Jun. 2006, pp: 8-16.

[30] F. Wang, G. Shrestha, "Allocation of TCSC devices to optimize total transmission capacity in a competitive power market," Proc. of the IEEE Power Engineering Society Winter Meeting, 2001, Vol. 2, Feb. 2001, pp: 587-593.

[31] D. Radu, Y. Besanger, "Blackout prevention by optimal insertion of FACTS devices in power systems," Proc. of the IEEE International Conference on Future Power Systems, 2005, Nov. 2005, pp: 1-6.

[32] L.Cai, I. Erlich, G. Stamtsis, "Optimal choice and allocation of FACTS devices in deregulated electricity market using genetic algorithms," Proc. of the IEEE PES Power Systems Conference and Exposition, Vol. 1, Oct. 2004, pp: 201-207.

[33] A. Alabduljabbar, J. Milanovic, "Genetic algorithm based optimization for allocation of static VAr compensators," Proc. of the 8th IEE International Conference on AC and DC Power Transmission, Mar. 2006, pp: 115-120.

[34] S. Kaewniyompanit, Y. Mitani, K. Tsuji, "A method of /spl mu/GA combined neighboring search for approaching to an optimal type selection and placement of a

FACTS device for power system stabilizing purpose in a multimachine power system," Proc. of the IEEE International Conference on Power System Technology (PowerCon), Vol. 2, Nov. 2004, pp: 1451-1456.

[35] S. Najafi, M. Abedi, S. Hosseinian, "A novel approach to optimal allocation of SVC using genetic algorithms and continuation power flow," Proc. of the IEEE International Power and Energy Conference (PECon '06), 2006. Nov. 2006, pp. 202–206.

[36] A. Kazemi, D. Arabkhabori, M. Yari, J. Aghaei, "Optimal location of UPFC in power systems for increasing loadability by genetic algorithm," Proc. of the 41st International Universities Power Engineering Conference (UPEC '06), 2006, Vol. 2, Sept. 2006, pp. 774–779.

[37] D. Arabkhaburi, A. Kazemi, M. Yari, J. Aghaei, "Optimal placement of UPFC in power systems using genetic algorithm," Proc. of the IEEE International Conference on Industrial Technology (ICIT), 2006, Dec. 2006, pp. 1694-1699.

[38] H. Shaheen, G. Rashed, S. Cheng, "Optimal location and parameters setting of unified power flow controller based on evolutionary optimization techniques," Proc. of the IEEE Power Engineering Society General Meeting, 2007. Jun. 2007, pp. 1-8.

[39] S. Gerbex, R. Cherkaoui, A. Germond, "Optimal location of FACTS devices to enhance power system security," Proc. of the IEEE Power Tech Conference Proceedings, 2003 Bologna, Vol. 3, Jun. 2003, pp: 7-14.

[40] M. Saravanan, S. Slochanal, P. Venkatesh, P. Abraham, "Application of PSO technique for optimal location of FACTS devices considering system loadability and cost of installation," Proc. of the IEEE 7th International Power Engineering Conference (IPEC) 2005. Vol. 2, Dec. 2005, pp. 716-721.

[41] H. Mori, Y. Maeda, "A hybrid method of EPSO and TS for FACTS optimal allocation in power systems," Proc. of the IEEE International Conference on Systems, Man and Cybernetics (ICSMC '06), 2006. Vol. 3, Oct. 2006, pp. 1831-1836.

[42] W. Ongsakul, P. Jirapong, "Optimal placement of multi-type FACTS devices by hybrid TS/SA approach," Proc. of the IEEE International Symposium on Circuits and Systems (ISCAS), Vol. 3, May 2003, pp: III-375 - III-378.

[43] H. Mori, Y. Goto, "A parallel tabu search based method for determining optimal allocation of FACTS in power systems," Proc. of the IEEE International Conference on Power System Technology (PowerCon), Vol. 2, Dec. 2000, pp: 1077-1082.

[44] H. Mori, Y. Maeda, "Application of two-layered tabu search to optimal allocation of UPFC for maximizing transmission capability," Proc. of the IEEE International Symposium on Circuits and Systems (ISCAS), 2006. May 2006, pp. 1699-1702.

[45] J. Hao, L. Shi, Ch. Chen, "Optimising location of unified power flow controllers by means of improved evolutionary programming," Proc. of the IEE Generation, Transmission and Distribution, Vol. 151, no. 6, Nov. 2004, pp:705–712.

[46] W. Ongsakul, P. Jirapong, "Optimal allocation of FACTS devices to enhance total transfer capability using evolutionary programming," Proc. of the IEEE International Symposium on Circuits and Systems (ISCAS), Vol. 5, May 2005, pp: 4175-4178.

[47] M. Santiago-Luna, J. Cedeno-Maldonado, "Optimal placement of FACTS controllers in power systems via evolution strategies," Proc. of the IEEE/PES Transmission & Distribution Conference and Exposition: Latin America, 2006, Aug. 2006, pp. 1-6.

[48] A. Karami, M. Rashidinejad, A. Gharaveisi, "Optimal location of STATCOM for voltage security enhancement via artificial intelligent," Proc. of the IEEE International Conference on Industrial Technology (ICIT), 2006, Dec. 2006, pp. 2704-2708.

[49] J. Ramirez, I. Coronado, "A frequency response technique to allocate FACTS devices," Proc. of the IEEE Power Engineering Society Summer Meeting, 2001. Vol. 3, Jul. 2001, pp. 1530-1535.

[50] B. Mahdad, T. Belkacem, K. Srairi, "Optimal location and control of FACTS device in unbalanced power systems using sequence component," Proc. of the IEEE International Conference on Industrial Technology (ICIT), 2006, Dec. 2006, pp. 2966-2971.

[51] A. Alabduljabbar, J. Milanovic, "Placement and tuning of SVCs for the improvement of techno-economic performance of the network based on sequential number theoretic optimization algorithm," Proc. of the IEEE PES Power Systems Conference and Exposition (PSCE'06), 2006. Oct. 29 2006-Nov. 1 2006, pp. 890-895.

[52] M. Ishimaru, R. Yokoyama, G. Shirai, K. Lee, "Allocation and design of robust TCSC controllers based on power system stability index," Proc. of the IEEE Power Engineering Society Winter Meeting, 2002. Vol. 1, Jan. 2002, pp. 573-578.

[53] N. Sharma, A. Ghosh, R. Varma, "A novel placement strategy for FACTS controllers," *IEEE Transactions on Power Delivery*, Vol. 18, no. 3, Jul. 2003, pp. 982-987.

[54] R. Eberhart, Y.Shi and J. Kennedy, *Swarm intelligence*. San Francisco, CA: Morgan Kaufmann, 2001. ISBN: 1558605959, 9781558605954.

[55] R. Eberhart and J. Kennedy, "A new optimizer using particle swarm theory," Proc. of the 6th Int. Symp. Micro Machine and Human Science (MHS), Oct. 1995, pp. 39-43.

[56] S. Yang, M. Wang, and L. Jiao, "A quantum particle swarm optimization," Proc. of the IEEE Congress on Evolutionary Computation (CEC), Vol. 1, pp. 320-324, Jun. 2004.

[57] J. Kennedy and R. Eberhart, "Particle swarm optimization," Proc. of the IEEE Int. Conf. Neural Networks (ICNN), Vol. 4, Nov. 1995, pp. 1942-1948.

[58] M. Millonas, Swarms, phase transitions, and collective intelligence. in C.G. Langton, Artificial Life III, Proc. Santa Fe Institute Studies in the Sciences of Complexity, New York, NY: Addison-Wesley Publishing Company, Vol. XVII, pp. 417-445, 1994.

[59] J. Kennedy, "The particle swarm: social adaptation of knowledge," Proc. of the IEEE Int. Conf. Evolutionary Computation (ICEC), pp. 303-308 Apr. 1997.

[60] D. Boeringer and D. Werner, "Particle swarm optimization versus genetic algorithms for phased array synthesis," *IEEE Transactions on Antennas and Propagation*, Vol. 52 , no. 3 , pp. 771-779, Mar. 2004.

[61] Y. Shi, "Feature article on particle swarm optimization," IEEE Neural Network Society, Feature article Feb. 2004, pp. 8-13.

[62] J. Kennedy, "Small worlds and mega-minds: effects of neighborhood topology on particle swarm performance," Proc. of the IEEE Congress on Evolutionary Computation (CEC), Vol. 3, Jul. 1999, pp. 1931-1938.

[63] J. Kennedy and R. Mendes "Population structure and particle swarm performance," Proc. of the IEEE Congress on Evolutionary Computation (CEC), Vol. 2, May 2002, pp. 1671 - 1676.

[64] J. Kennedy and R. Mendes, "Neighborhood topologies in fully-informed and best-of-neighborhood particle swarms," Proc. of the IEEE International Workshop on Soft Computing in Industrial Applications (SMCia/03), Jun. 2003, pp. 45-50.

[65] R. Eberhart and Y. Shi, "Particle swarm optimization: developments, applications and resources," Proc. of the IEEE Congress on Evolutionary Computation (CEC), May 2001, Vol. 1, pp. 81-86.

[66] X. Hu, Y. Shi, and R. Eberhart, "Recent advances in particle swarm," Proc. of the IEEE Congress on Evolutionary Computation (CEC), Vol. 1, Jun. 2004, pp. 90-97.

[67] E. Ozcan and C. Mohan, "Particle swarm optimization: surfing the waves," Proc. of the IEEE Congress Evolutionary Computation (CEC), Vol. 3, Jul. 1999, pp. 1939-1944.

[68] M. Clerc and J. Kennedy, "The particle swarm-explosion, stability, and convergence in a multidimensional complex space," *IEEE Transactions Evolutionary Computation*, Vol. 6, no. 1, pp. 58-73, Feb. 2002.

[69] R. Eberhart and Y. Shi, "Comparing inertia weights and constriction factors in particle swarm optimization," Proc. of the IEEE Congress Evolutionary Computation (CEC), Vol. 1, Jul. 2000, pp. 84-88.

[70] F. Bergh and A. Engelbrecht, "A Cooperative approach to particle swarm optimization," IEEE Trans. on Evolutionary Computation, Vol. 8, no. 3, pp. 225-239, Jun. 2004.

[71] Y. Shi and R. Eberhart, "A modified particle swarm optimizer," Proc. of the IEEE World Congress on Computational Intelligence, May 1998, pp. 69-73.

[72] Y. Shi and R. Eberhart, "Empirical study of particle swarm optimization," Proc. of the IEEE Congress on Evolutionary Computation (CEC), Vol. 3, Jul. 1999, pp. 1945-1950.

[73] A. Esmin, G. Torres, and A. Zambroni, "A hybrid particle swarm optimization applied to loss power minimization," IEEE Trans. on Power Systems, Vol. 20, no. 2, pp. 859-866, May 2005.

[74] Y. Shi and R. Eberhart, "Parameter selection in particle swarm optimization," Proc. of the 7th International Conference of Evolutionary Programming (EP), May 1998, pp. 591-600.

[75] Y. Shi and R. Eberhart, "Empirical study of particle swarm optimization," Proc. of the IEEE Congress on Evolutionary Computation (CEC), Vol. 3, Jul. 1999, pp. 1945-1950.

[76] K. Parsopoulos and M. Vrahatis, "Recent approaches to global optimization problems through particle swarm optimization," Natural Computing, Vol. 1, May 2002, pp. 235-306.

[77] E. Laskari, K. Parsopoulos, and M. Vrahatis, "Particle swarm optimization for integer programming," Proc. of the IEEE Congress on Evolutionary Computation (CEC), Vol. 2, May 2002, pp. 1582-1587.

[78] D. Goldberg, *Genetic algorithms in search, optimization and machine learning*. Addison-Wesley Pub. Co. 1989. ISBN: 0201157675, 9780201157673.

[79] L. Schmitt, "Theory of genetic algorithms," Theoretical Computer Science (259),

2001, pp: 1-61.

[80] L. Schmitt, "Theory of genetic algorithms II: models for genetic operators over the string-tensor representation of populations and convergence to global optima for arbitrary fitness function under scaling," Theoretical Computer Science (310), 2004, pp: 181-231.

[81] G. Syswerda, "Uniform crossover in genetic algorithms," Proc. of the Third International Conference on Genetic Algorithms and Their Applications, San Mateo, CA, Jun. 1989, pp: 2-9.

[82] M. Vose, *The simple genetic algorithm: foundations and theory*, MIT Press, Cambridge, MA, 1999. ISBN: 0585077606, 9780585077604.

[83] T.K. Das, G.K. Venayagamoorthy, "Bio-inspired Algorithms for the design of multiple optimal power system stabilizers: SPPSO and BFA", Conference Record of the 2006 IEEE Industry Applications Conference, 41st IAS Annual Meeting. Vol. 2, 8-12 Oct. 2006, pp: 635 – 641.

[84] K. M. Passino, "Biomimicry of bacterial foraging for distributed optimization and control," Control System Magazine, IEEE, vol. 22, Issue 3, pp. 52-67, June 2002.

[85] W.J. Tang, Q.H. Wu, J.R. Saunders, "Bacterial foraging algorithm for dynamic environments", IEEE Congress on Evolutionary Computation, 2006. CEC 2006. 16-21 July 2006, pp: 1324 – 1330.

[86] G.L. Nemhauser and L.A. Wolsey, *Integer and combinatorial optimization*, Wiley-Interscience, New York, 1999. ISBN: 0471359432, 9780471359432.

[87] K. G. Murty, *Operations research: deterministic optimization models*, Prentice Hall, 1995. ISBN: 0130565172, 9780130565174.

[88] G. E. P. Box, W. G. Hunter, J. S. Hunter, *Statistics for Experimenters*, New York, John Wiley & Sons, Inc, 1978. ISBN: 0471093157, 9780471093152.

[89] R. B. Abernethy, *The New Weibull Handbook*, North Palm Beach, FL, Robert B. Abernethy, 1993. ISBN: 0965306208, 9780965306201.

[90] The IEEE 118 Bus Test System. [Online].
http://www.ee.washington.edu/research/pstca

[91] J. Deuse, K. Karoui, A. Bihain, and J. Dubois, "Comprehensive approach of power system contingency analysis", Proc. Of the IEEE Bologna Power Tech Conference, Vol. 3, pp. 23-26 June 2003, pp. 6-12.

[92] H. Ren, I. Dobson, and B. A. Carreras, "Long-term effect of the n-1 criterion on cascading line outages in an evolving power transmission grid", *IEEE Transactions*

on Power Systems, Vol. 23, No. 3, pp. 1217-1225, August 2008.

[93] A. Kusko and M. T. Thompson, *Power quality in electrical systems*, McGraw-Hill Professional, 2007. ISBN: 0071470751, 9780071470759.

[94] H. Johal, "Distributed series reactance: a new approach to realize grid power flow control". P.h. D. thesis dissertation, Electrical and Computer Engineering Department, Georgia Institute of Technology, 2008.

[95] R.C. Degeneff, W. Neugebauer, C.H. Saylor, and S.L. Corey, "Security constrained optimization: an added dimension in utility systems optimal power flow", IEEE Computer Applications in Power, Vol. 1, No. 4, October 1988, pp. 26–30.

[96] F. Capitanescu, M. Glavic, D. Ernst, and L. Wehenkel, "Contingency filtering techniques for preventive security-constrained optimal power flow", *IEEE Transactions on Power Systems*, Vol. 22, No.4, pp. 1690-1697, November 2007.

[97] J. Weber, "Implementation of a Newton-based optimal power flow into a power system simulation environment", Master thesis dissertation, Electrical and Computer Engineering Department, University of Illinois at Urbana-Champaign, 1997.

[98] P. Venkatesh, R. Gnanadass, and N.P. Padhy, "Comparison and application of evolutionary programming techniques to combined economic emission dispatch with line flow constraints", *IEEE Transactions on Power Systems*, Vol.18, No.2, pp.688-697, May 2003.

[99] Subsynchronous Resonance Working Group of the System Dynamic Performance Subcommitee, ' Reader Guide to Subsynchronous Resonance', *IEEE Transactions on Power System*, Vol. 7, No. 1, February 1992.

[100] F. Milano, "Documentation for Power System Analysis Toolbox (PSAT) version 2.0.0 β", March 8, 2007

[101] X. Zhang, C. Rehtanz, and B. Pal, *Flexible AC transmission systems: modelling and control*, Birkhäuser, 2006. ISBN: 3540306064, 9783540306061.

[102] P. Sauer and M. Pai, *Power system dynamics and stability*, Stipes Publishing L.L.C., 2007. ISBN 1588746739, 9781588746733C.

[103] Canizares, W. Rosehart, A. Berizzi, C. Bovo, "Comparison of voltage security constrained optimal power flow techniques". Proc. Of the IEEE Power Engineering Society Summer Meeting, 2001. Vol. 3, 15-19 July 2001, pp. 1680 – 1685.

[104] V. Ajjarapu, C. Christy, "The continuation power flow: a tool for steady state voltage stability analysis", *IEEE Transactions on Power Systems*, Vol.7, No.1, pp.416-423, Feb 1992.

[105] M. Ilic and J. Zaborszky, *Dynamics and control of large electric power systems*, Wiley, 2000. ISBN 0471298581, 9780471298588.

[106] G. Rogers, *Power System Oscillations,* Norwell, M. A. Kluwer, 2000. ISBN: 0792377125, 9780792377122.

[107] H. Wang, "Philips-Heffron Model of Power Systems Installed with STATCOM and Applications", IEE Proceedings- Generation, Transmission, Distribution, vol. 146, no. 5, Sept 1999, pp. 521-527.

[108] P. Kundur, M. Klein, G. Rogers, M. Zywno, "Application of power system stabilizers for enhancement of overall system stability", *IEEE Transactions on Power Systems*, Vol.4, No.2, pp. 614-626, May 1989.

[109] P. Kundur, D. Lee, H. Zein El-Din, "Power system stabilizers for thermal units: analytical techiques and on-site validation", *IEEE Transactions on Power Apparatus and Systems*, Vol. PAS-100, No.1, pp. 81-95, Jan 1981.

[110] W. Levine, *Control system applications*, CRC Press, 2000 ISBN: 0849300541, 9780849300547.

[111] Mitsubishi Electric Corporation, "Power system stabilizer (PSS)". Brochure. Sept 2001.

[112] S. Mohagheghi, "Adaptive Critic designs based neurocontrollers for local and wide area control of a multimachine power system with a static compensator". P.h. D. thesis dissertation, Electrical and Computer Engineering Department, Georgia Institute of Technology, 2006.